

Integrated analysis of relationships between 3D-structure, leaf
photosynthesis, and branch transpiration of mature
Fagus sylvatica and *Quercus petraea* trees
in a mixed forest stand

**Dissertation zur Erlangung der Doktorwürde (Dr. rer. nat.)
der Fakultät für Biologie, Chemie und Geowissenschaften
der Universität Bayreuth**

vorgelegt von
Stefan Fleck
aus Hohensolms

Bayreuth, August 2001

1. Gutachter: Prof. Dr. J.D. Tenhunen

Danksagung

Herrn Prof. Dr. John D. Tenhunen danke ich für die Überlassung des interessanten Themas, für die Förderung und die Anregungen zu meiner Arbeit und die gelungene Koordination mit anderen Projekten.

Markus Schmidt spreche ich meinen herzlichen Dank aus für die intensive und freundschaftliche Zusammenarbeit im Steigerwald, Diskussionen und Unterstützung in allen Phasen des Projekts sowie die Überlassung von Messdaten.

Dr. Eva Falge, Dr. Barbara Köstner und Dr. Ülo Niinemets danke ich für die ständige Diskussionsbereitschaft, fördernde und kritische Anteilnahme in allen Phasen des Projekts.

Bei Wolfgang Faltin bedanke ich mich für seine langanhaltende Bereitschaft zur koordinierten Modellentwicklung und die Unterstützung bei Biomasseernten.

Dr. Alessandro Cescatti, Dr. Manfred Forstreuter, Prof. Dr. Yoshitaka Kakubari, Dr. Hideyuki Saito und Dr. Jörn Strassemeyer danke ich für die aktive Unterstützung in fachlichen Fragen und für die Überlassung von Messdaten

Meiner Frau Regina Dehmel danke ich herzlich für die weitreichende Unterstützung im Zuge der Freilandarbeiten, für die kritische Durchsicht von Manuskripten und Literaturliste und das Management unserer Familie.

Allen weiteren Mitarbeitern und Helfern bei Freiland- und Laborarbeiten danke ich für ihre Ausdauer und Bereitschaft zu meist langwierigen Tätigkeiten: Annett Börner, Liane Chamsai, Alexandra Hahn, Uta Lohwasser, Friederike Mayer, Silke Potthast und Marc Schroeter - Dr. Martina Alsheimer, Dr. Bärbel Heindl-Tenhunen, Dr. Ueli Joss, Friederike Rothe, Hans-Joachim Scharfenberg, Annette Suske und Dr. Reiner Zimmermann gebührt darüber hinaus mein Dank für die freundschaftliche Aufnahme in die Arbeitsgruppe.

Dr. Markus Reichstein danke ich für die intensive Durchsicht von Manuskripten und gemeinsam mit Jens-Arne Subke für inhaltliche Diskussionen.

Bei Ralph Geyer bedanke ich mich für die Lösung zeitraubender Hard- und Software-Probleme.

Dr. Pedro Gerstberger, Dr. Alois-Kastner Maresch, Dr. Holger Lange, Gerhard Müller und Iris Whelan danke ich für fachliche und praktische Unterstützung.

Die vorliegende Arbeit wurde am Lehrstuhl Pflanzenökologie der Universität Bayreuth im Rahmen des vom Bundesministerium für Forschung und Technologie geförderten Projekts PT BEO 51 - 0339476C "Entwicklung eines 3-D-Mischbestandesmodells des N-abhängigen CO₂- und Wasseraustausches von Buchen-Mischbeständen in Nordbayern" durchgeführt.

Contents

1	Introduction	10
1.1	Problems in assessment of gas-exchange of mixed forest stands	10
1.1.1	The relevance of gas-exchange of mixed forest stands	10
1.1.2	Structure dependence of mixed stand gas-exchange	11
1.1.3	Unexplored effects of patterns of space capture	12
1.1.4	The complexity of canopy structure formation	12
1.1.5	Canopy structure formation is altered under elevated CO ₂ and ozone	13
1.1.6	Patterns of space capture are the relevant structure information for light utilization	14
1.1.7	Necessity of simulation models for the explanation of altered growth patterns	14
1.2	Conclusions	15
1.2.1	The relevance of complexity of structure	15
1.2.2	Implications for actual studies on mixed stand gas-exchange	16
1.2.3	Scope and organisation of this study	17
2	Tree crown structures of mature <i>Fagus sylvatica</i> and <i>Quercus petraea</i> trees	18
2.1	Objectives	18
2.2	Materials and Methods	19
2.2.1	Stand descriptions	19
2.2.1.1	<i>Buchenallee</i>	19
2.2.1.2	<i>Großebene and Steinkreuz</i>	20
2.2.2	Soil pH and soil C/N ratio	24
2.2.3	Canopy structure determination	24
2.2.4	Geodetic location measurements	26
2.2.5	Description of branch connections	27
2.2.6	Leaf cloud oriented biomass harvest and leaf sampling	28
2.2.7	Error estimations	29
2.3	Results	30
2.3.1	Allometric relationships of the branch system	30
2.3.1.1	<i>Branch basal area versus estimated sapwood area</i>	30
2.3.1.2	<i>Allometric relationships of ramification</i>	31
2.3.1.3	<i>Allometric relationships between basal area and leaf area or leaf weight</i>	33
2.3.2	Discussion of allometric relationships of the branch system	37
2.3.3	Leaf arrangement in whole tree crowns	40
2.3.3.1	<i>3D-representation of leaf clumping</i>	40
2.3.3.2	<i>Tree Leaf Area Indices</i>	43
2.3.3.3	<i>Arrangement of leaf clouds</i>	43
2.3.4	Layer oriented description of leaf distribution in the crown	46
2.3.4.1	<i>Leaf area of height layers</i>	46
2.3.4.2	<i>Leaf area densities of height layers</i>	48
2.3.4.3	<i>Effect of gap correction of leaf area densities</i>	50
2.3.4.4	<i>Volume gap fractions</i>	51

2.3.5	Leaf cloud oriented evaluation of leaf arrangement	53
2.3.5.1	<i>Properties of the crown environment of each leaf cloud</i>	57
2.3.5.2	<i>Angles of the leaf cloud plane</i>	60
2.3.5.3	<i>Main growth directions of leaf clouds</i>	61
2.3.5.4	<i>Azimuth angles</i>	65
2.3.5.5	<i>Spatial extension of leaf clouds</i>	67
2.3.5.6	<i>Leaf area densities of leaf clouds</i>	69
2.3.5.7	<i>Wood area densities of leaf clouds</i>	75
2.4	Interpretation of investigations on leaf clumping and arrangement	75
3	Spatial distribution of leaf properties in tree crowns.....	77
3.1	Materials and methods.....	77
3.1.1	Structural leaf parameters	77
3.1.2	Relative irradiance.....	78
3.1.3	Gas-exchange Measurements.....	78
3.1.4	Evaluation of A/C _i -curves with RACCIA.....	80
3.1.4.1	<i>The HARLEY/TENHUNEN model of leaf photosynthesis</i>	81
3.1.4.2	<i>RACCIA routine for species-specific parameterisation</i>	83
3.2	Results.....	86
3.2.1	Light and height dependence of leaf properties	86
3.2.1.1	<i>Relative Irradiance</i>	86
3.2.1.2	<i>Leaf angles</i>	88
3.2.1.3	<i>Angles of neighbouring branches</i>	90
3.2.1.4	<i>Leaf Form</i>	90
3.2.1.5	<i>Leaf mass per area (LMA)</i>	91
3.2.1.6	<i>Leaf nitrogen and carbon contents</i>	94
3.2.2	Photosynthesis measurements	96
3.2.2.1	<i>Comparison of PAM-2000 and RACCIA estimates of J_{max}</i>	96
3.2.2.2	<i>Day respiration (R_d)</i>	99
3.2.2.3	<i>Carboxylation capacity V_{cmax} and electron transport capacity J_{max}</i>	101
3.2.2.4	<i>Nitrogen dependence of J_{max} and V_{cmax}</i>	104
3.2.2.5	<i>The shape of temperature dependence functions for J_{max} and V_{cmax}</i>	106
3.2.2.6	<i>Ball-Woodrow-Berry-coefficient of stomatal sensitivity (g_{fac})</i>	109
3.2.3	Nitrogen dependent model of leaf photosynthesis for beech	112
3.2.3.1	<i>Model description</i>	112
3.2.3.2	<i>Parameterisation</i>	113
3.2.3.3	<i>Validation Measurements</i>	114
3.2.3.4	<i>Model validation</i>	117
3.3	Summary and discussion.....	118
4	Application of a 3D-light model to the 3D-representation of beech Gr12 and its stand.....	122
4.1	Methods.....	122
4.1.1	STANDFLUX-SECTORS.....	122
4.1.2	Representation of 3D-data with CRISTO.....	123
4.1.2.1	<i>Representation of stand structure with crown approximating polyhedrons</i>	124
4.1.2.2	<i>Volume and leaf area density calculation of polyhedrons</i>	125
4.1.2.3	<i>Segmentation of polyhedrons</i>	125

4.1.3	Parameterisation of STANDFLUX-SECTORS	128
4.1.3.1	<i>Segmentation of leaf cloud enveloping polyhedrons</i>	128
4.1.3.2	<i>Segmentation of crown approximating polyhedrons in the stand Großebene</i>	128
4.1.3.3	<i>Parameter determination for single compartments</i>	132
4.1.4	Validation of STANDFLUX-SECTORS.....	132
4.1.4.1	<i>Light and LMA simulations</i>	132
4.1.5	Validation data.....	133
4.2	Results	134
4.2.1	Stand Structure.....	134
4.2.1.1	<i>Crown length and position of oak and beech trees in the Steigerwald stands</i>	134
4.2.2	LMA-calculations	135
4.2.2.1	<i>Validation of the light model with the LMA/irradiance relationship</i>	135
4.2.2.2	<i>Estimation of leaf cloud LMA</i>	135
4.2.3	Comparison of climate and transpiration data	136
4.2.3.1	<i>Daily courses</i>	136
4.2.3.2	<i>Dependence of leaf cloud transpiration on climate variables</i>	140
4.2.3.3	<i>Summarising concepts</i>	142
4.3	Summary and discussion	142
5	Integrating discussion	144
5.1	Characteristics of oak and beech in the stand Großebene.....	144
5.2	Application of Beer's law	146
5.3	Leaf mass per area (LMA)	147
5.4	Implications for gas-exchange modelling.....	148
6	Summary.....	151
7	Zusammenfassung.....	153
8	Appendix.....	156
8.1	Parameter derivation for chapter 2.3.5	156
8.2	Measured A/C_r -curves	156
8.2.1	Leaves of beech Gr12	157
8.2.2	Leaves of oak Gr13	158
8.3	Figures.....	162
9	Literature.....	169
10	Abbreviations.....	182

1 Introduction

1.1 Problems in assessment of gas-exchange of mixed forest stands

1.1.1 The relevance of gas-exchange of mixed forest stands

Forty-four percent of the forests in Germany are made up of stands with mixed tree composition (SMALTSCHINSKI 1990), but despite the growing importance of such stands in forestry (BML 1998), little is known about their ecological significance and environmental economy, due to the long-standing focus on the cultivation of pure stands in forestry since the second half of the nineteenth century (KENK 1992). It is generally accepted that genetic variation and variation in physiological response between species is larger than between individuals of the same species, which leads to the conclusion that greater variance in terms of shade tolerance, space capture strategies of crown and root system, and strategies of reproduction is to be found among individuals of mixed stands than trees of pure stands (LARSON 1992).

Several related and derivable properties of mixed stands have been reported and include:

- Improved utilisation of limited resources due to complementary light and nutrient requirements (COBB ET AL. 1993, JOSE & GILLESPIE 1997, KELTY 1992, MILLER ET AL. 1993).
- Greater stability and better regeneration after disturbances due to storm, inundation, or insect pests (BATTAGLIA ET AL. 1999, BURSCHEL ET AL. 1993, KELTY 1992).
- Greater total productivity, which increases the sink-strength for CO₂ of these stands (BURSCHEL ET AL. 1993), but does not necessarily lead to greater timber production (BURKHART & THAM 1992, SALES LUIS & DO LORETO MONTEIRO 1998).
- More diverse understorey flora and stand fauna as a consequence of greater variability in the habitat characteristics in available niches (CUMMING ET AL. 1994, GARCIA ET AL. 1998, NICOLAI 1993).
- More natural stand structure and regeneration (DOBROWOLSKA 1998, ELLENBERG 1996, RACKHAM 1992).

Additional to these general and qualitative properties, the high proportion of mixed stands requires their explicit consideration in quantitative assessments. This is strengthened by the durability of actual changes in forest structure, that are introduced through the wide and continuing reorganisation of forests towards mixed stands since 1980 (KENK 1992), and whose environmental effects are not yet defined.

- In the international discussion on greenhouse gases, we would like to know how large the sink-strength of forests for CO₂ could be (UNO 1998, UNO 2000, EU-COMMISSION 1998, BUNDESMINISTERIUM FÜR UMWELT 1994).
- The groundwater quality below forested areas is increasingly endangered due to the mobilisation of accumulated heavy metals in the humus layer by acidic deposition (BENS 1999, WEYER 1993). Thus, the effects of stand structure and species composition, which have an important influence on acidic deposition and amount of newly formed ground water (BRECHTEL 1989, DRAAIJERS 1993), must be established.
- The flooding of rivers is influenced by land cover on a regional or smaller scale, because water retention times and absolute losses due to transpiration and interception vary (DÜSTER 1994, GEES 1997, BORK 2000). While the proportion of forested area in Germany was remarkably stable during the last 400 years (around 30% of total area, BORK 2000), tree

species composition of forests may also have major impacts on transpiration and interception losses and groundwater storage (BRECHTEL 1989).

The impact of structural heterogeneity of mixed stands on ecosystem water- and CO₂-fluxes has not yet been quantified. The bewildering variety (KENK 1992) of 729 different formations of mixed stands in West-Germany (SMALTSCHINSKI 1990) and the difficulty to document structural differences leads in turn to extreme difficulties in carrying out a process-oriented analysis of the impact of structural heterogeneity. Nevertheless, the growing significance of mixed stands requires an assessment of their contribution to CO₂-fixation, groundwater protection, and flood prevention and, therefore, the quantification of their gas-exchange.

1.1.2 Structure dependence of mixed stand gas-exchange

Measurements of transpiration and CO₂-exchange of forest stands are often based on up-scaling of sapflow observations or eddy covariance measurements. Already the predominantly measured pure stands have been suggested to vary in water use over a wide range (109-358 mm/a, measured at 11 German spruce stands; ALSHEIMER 1997, PECK & MAYER 1996, PECK 1995). The same is true for CO₂-uptake (0.8-5.4 t C/ (ha*a)), measured at three German spruce stands (VALENTINI ET AL. 2000). This variation apart from many other factors (climate, nutrient availability, age of trees, altitude, exposition, vitality, understorey, soil conditions, or measurement errors) is also attributed to stand structural influence (ALSHEIMER 1997, PECK & MAYER 1996). Maximum canopy conductance as estimated by sapflow measurements on fifteen pure stands (twelve different species) has been shown to vary between 1 and 5 cm/s and leaf area index (LAI) as a structure dependent quantity had the main effect on this variation (GRANIER ET AL. 2000). The large spatial heterogeneity of water fluxes among trees in forest stands (KÖSTNER ET AL. 1998) is still not understood, which makes up-scaling of sapflow data uncertain, especially in mixed stands. The number of eddy covariance studies with mixed stands is inadequate to conclude general trends from them (VALENTINI ET AL. 2000),

Gas exchange calculations for mixed stands with models are more uncertain than those for pure stands, because the assumption of lateral homogeneity, which is included in virtually all conventional stand models due to their original adjustment to pure stands (1D-models and big leaf models; BALDOCCHI & HARLEY 1995, GOND ET AL. 1999, LEUNING ET AL. 1995, REYNOLDS ET AL. 1992, SALA & TENHUNEN 1996), is not valid in mixed stands. Moreover, the calculation of stand photosynthesis and transpiration in horizontally inhomogeneous canopies cannot be based on horizontally averaged structural quantities due to non-linear relationships between structure, light interception, and photosynthetic CO₂ -fixation (JARVIS 1995). Spatially explicit 3D-models can consider such structural heterogeneity (CESCATTI 1997, FALGE 1997, WANG & JARVIS 1990), but they have not yet been used in this sense due to the demanding requirements for spatially correct parameterisation and long calculation time.

Gas-exchange calculations for mixed stands may even not be reliable when calculated on the basis of the proportional addition of the species contributions to gas-exchange in hypothetical pure stands, because inter-specific competition and synergy effects are not considered in this case. HERTEL and LEUSCHNER (1998) showed for a mixed stand of oak and beech, that fine-root growth of beech is strongly increased relative to the pure stand, when growing in presence of oak fine-roots. This led to a four- to fivefold higher fine-root density of beech than that of oak, with probable implications for the water-balance of both species. Investigations of LEUSCHNER (2000) point out that beech may also be advantaged in the aboveground competition with oak,

because its costs for space capture and shadow casting are only half that of oaks. ROTHE and KREUTZER (1998) found in an 80-100 year old mixed stand of spruce and beech 10-20% higher growth rates than would be expected by extrapolation of the growth rates of neighbouring pure stands and attributed this effect to the more intensive light utilisation in the canopy.

1.1.3 Unexplored effects of patterns of space capture

Patterns of space capture can be seen as the main cause for more intensive light utilisation in mixed stands. They are the result of tree positions and adaptive growth and have an impact on light climate and assimilation through the distribution of sun and shade leaves of physiologically different species in zones of mutual interaction with respect to light climate. Beech trees can for example obtain a large proportion of their C-profit from the photosynthesis of shade leaves, thus profiting from zones in the half-shade of spruce (ELLENBERG ET AL. 1986). While the effect of tree positions on light climate alone may be estimated with 3D-models (FALGE ET AL. 2000, SMITH 1994, WILLIAMS 1996), patterns of space capture in mature stands have not yet been analysed, so that their quantitative effect on gas-exchange is unknown. This is mainly due to the complexity of the three-dimensional distribution of physiologically different leaves in the canopy of a mixed stand and the problem to record it. However, theoretical studies show that the total assimilation already of a single plant with optimally distributed sun and shade leaves in the plant canopy may be twice that of the same plant with uniform leaves of intermediate qualities (FIELD 1991, HIROSE & WERGER 1987).

1.1.4 The complexity of canopy structure formation

Patterns of space capture and their dynamics in a mixed stand are a result of the complex interaction of species-specific growth patterns, which lead via shading effects on neighbouring tree crowns and advantageous light use to a spatial separation between the trees but also to an expansion of the whole stand's canopy. These growth patterns may also be termed space capture strategies. They are realised via bud formation and its orientation, persistence and activation (STAFSTROM 1995), internode dimensions, via angles, schemes, and frequencies of ramification (GARTNER 1995, HALLÉ ET AL. 1978), via cladoptosis (BUCK-SORLIN & BELL 1998), foliage development and shedding (GRUBB 1998), via the physiological support of leaves (NEWTON & JOLIFFEE 1998), and via the mechanical support and secondary growth of woody organs (MATTHECK 1995). The dependence of these processes on light, position in the tree crown, physiological age of the organs (DE REFFYE 1995), hormonal regulation (LITTLE & PHARIS 1995), density stress (NEWTON & JOLIFFEE 1998), and further growth conditions (DELEUZE ET AL. 1996) causes space capture to be species-specifically directed. Space capture is restricted due to the limited availability of assimilates, thus a trade-off between C-investments in efficiency of assimilation, mechanical stability, stress resistance, and in competitive fitness exists (GIVNISH 1995). The effect of growth on light climate and assimilation depends on the environmental situation and leads via the attained assimilation rate to a feedback effect on growth, which is dependent on several species-specific properties. These properties and their cost and benefit relationship become decisive factors for competition, when different species interact via their strategies of space capture. Important competition factors with impact on this feedback effect include:

- The species-specific height growth rate (GIVNISH 1995, KÜPPERS 1994)

- The species-specific, form-dependent horizontal dimension of the canopy (Givnish 1995, Kuuluvainen 1992)
- The reactivity to light climate (Efficiency and determination of the ramification pattern; COLLET ET AL. 1997, LAURI & TEROUANNE 1998, MÄKINEN 1996)
- The ability to react to the spatial situation before shading effects become real (Phytochrome system; APHALO ET AL. 1999, GILBERT ET AL. 1995)
- Shade production and self-shading (KIKUZAWA ET AL. 1996, KÜPPERS 1994, LEUSCHNER 2000)
- The light use efficiency and adaptability of the photosynthetic system in the shade and under changing conditions (HIKOSAKA 1996, NIINEMETS & TENHUNEN 1997)
- The intensity of source-sink-relations of the C-household (SPRUGEL ET AL. 1991)
- The C-allocation pattern between root and shoot (functional balance; MÄKELÄ 1997, NAIDU ET AL. 1998)
- The timing of growth and storage of assimilates (KÜPPERS 1994)
- The ratio between investments in growth, physiology, and storage (KÜPPERS ET AL. 1993)
- The water storage capacity (HOLBROOK 1995)
- The interaction between growth and transpiration (KURTH 1998, DE REFFYE ET AL. 1995)
- The efficiency and costs of pest defence
- The reactivity to injuries (GILL 1995, MATTHECK & BETHGE 1998)
- The reactivity to mechanical stimuli due to tree sways (DELEUZE ET AL. 1996)
- Stability of woody organs (GRONINGER ET AL. 2000, MATTHECK 1995, ZIPSE ET AL. 1998)

1.1.5 Canopy structure formation is altered under elevated CO₂ and ozone

C-investments and growth on the level of leaves, branches or saplings were often reported to be altered under elevated CO₂ and ozone concentrations in a way that is influenced by and influences space capture strategies:

- Growth reductions were reported from many tree species under elevated ozone concentrations. They can be light-dependent (TJOELKER ET AL. 1993) or time-shifted to the second year of the experiment (MATYSSEK ET AL. 1993) and may be related to branch length (MATYSSEK ET AL. 1995), number of internodes of beech (PEARSON & MANSFIELD 1994), leaf area (TJOELKER ET AL. 1993), and root growth of beech (DAVIDSON ET AL. 1992). However, higher leaf mass per area (MATYSSEK ET AL. 1992) and higher relative amounts of needle biomass (MORTENSEN 1994) were also observed.
- Under elevated CO₂ the growth of nearly all investigated tree species is enhanced. Growth changes are related to height growth of the stem, ramification patterns, senescence of leaves, and insertion height of the lowest leaves (REEKIE 1996), leaf area, number of leaves, leaf size, branch length and diameter of beech (EL KOHEN ET AL. 1993), leaf longevity, LAI, branching frequency, lengths of shoot and root, and number and size of fruits (BOWES 1993, HÄTTENSCHWILER & KÖRNER 1998, SIONIT ET AL. 1985, WULLSCHLEGER ET AL. 1995). Growth changes may also be light- and N-dependent (BROWN & HIGGINBOTTAM 1986, SALLANON ET AL. 1995). Long-term studies showed that photosynthesis is down-regulated in many species (EGLI ET AL. 1998, GRAMS ET AL. 1999, IDSO & IDSO 1994, TURNBULL ET AL. 1998), and partly that leaf area may be reduced by 60% (HÄTTENSCHWILER 1997).

The consequence of such changes in growth and investment of resources is inevitably a change of the pattern of space capture, which is harder to document, but has major impacts on

light climate, competition, CO₂- and water-balance with increasing influence as altered growth continues. Possible indirect effects of CO₂ and ozone on growth and C-investments are indicated by the fact, that many growth changes occur only in long-term investigations over several years (HÄTTENSCHWILER ET AL. 1997).

1.1.6 Patterns of space capture are the relevant structure information for light utilization

Light interception in forests is decisive for transpiration and photosynthesis and varies between 70 and 100% (BALDOCCHI & COLLINEAU 1994). The magnitude of resulting CO₂- and water fluxes is dependent on weather (temperature, humidity) and canopy internal structure, but not directly on branch-related growth changes. Instead the magnitude of CO₂- and water-exchange is directly dependent on interception and use of the incoming radiation, which is determined by the pattern of space capture, i. e., how much light is absorbed by woody organs, what proportion of sun and shade leaves are sunlit or shaded, whether the light is direct, diffuse or reflected, in which angle the leaves are directed towards the light and what are the gas exchange capacities and reflectance of the sunlit and shaded leaves (FALGE 1997, HOLBROOK 1995, PARKER 1995).

1.1.7 Necessity of simulation models for the explanation of altered growth patterns

Altered patterns of space capture in forests have probably already occurred due to the long-term impacts of increased CO₂ and ozone which affect their growth, assimilation, and transpiration. Wide-spread, long-term, and species-specific changes in stand productivity have been repeatedly observed during the last decade (KAUPPI ET AL. 1992, MYNENI ET AL. 1997, PRETZSCH 1996, ZINGG 1996) and may be interpreted in terms of altered strategies of C-distribution (PRETZSCH 1998). But these changes can not yet be attributed to a specific cause – changes in forest management, climate change, altered CO₂ and ozone concentrations, N-deposition, pollutants, and acid rain are still discussed as potential reasons (PRETZSCH 1998, ZINGG 1996) – which is mainly due to the large scale of this phenomenon. Simulation studies are required to enable up-scaling and the evaluation at ecosystem level of experimental results obtained at smaller scales. Direct investigations of atmospheric impacts by experimental manipulation of gas concentrations may only be carried out on a few stands due to their size and the resulting high expenses. Possible relationships between observed growth changes on leaf or branch level are not yet traceable for two reasons:

- Branching oriented and partly fractal growth models (CHEN ET AL. 1994, KURTH 1994, LIST & KÜPPERS 1998, DE REFFYE ET AL. 1997), which may be used for up-scaling of small-scale experimental results, were developed on measurements on young trees. They are still not able to reproduce all mechanisms of structure formation on the level of branches (KURTH 1998) and may not be validated with structure measurements on adult trees due to the complexity of the measurements.
- Experiments on CO₂- and ozone-dependent growth changes yield often opposite results dependent on the experimental set-up (WEBER & GRUHLKE 1995). While the growth of branches of *Liriodendron tulipifera* was observed to increase in a 24-weeks experiment, no similar effect was observed in a 3-years experiment on the same species (NORBY ET AL. 1992, O'NEILL 1987). The reason for such partly time-dependent opposite results is not known.

It could be that not all observed CO₂- or ozone-induced growth reactions at the branch level are direct effects of elevated CO₂ or ozone – instead, they could be part of a growth reaction of the whole tree that aims to adjust the pattern of space capture in order to correct the changed CO₂, water, and energy balance.

1.2 Conclusions

1.2.1 The relevance of complexity of structure

The general problems of all methods used for the assessment of gas-exchange in mixed stands are diversity of existing stands and conditions, size of the measured object, and complexity of structure. Due to the size of forest stands, expenses for eddy measurements are high, and only some of the numerous species combinations of mixed stands will be measured by this method. The measured results are not transferable to other mixed stands due to the potential influences of actual stand structure. The size of forest stands also requires up-scaling of sapflow measurements, which is uncertain in mixed stands due to structural variation. While principal assumptions of 1D-models are not met, 3D-models require due to size of stands and complexity of structure enormous amounts of data and long calculation time. Fractal models cannot yet be used to provide the structure information for 3D-models, because complexity of structure formation is not fully understood. The gas-exchange of mixed stands under altered conditions (for example due to CO₂ or ozone) cannot be predicted by any of these methods as long as the effect of structure is not included, because structure shifts occur under these conditions.

The complexity found in forest ecosystems and the associated problems for their scientific description has already led to the conclusion, that the scientific approach is ineffective for practical use in forestry (HAUHS ET AL. 2001). Additional problems arise since forest ecosystems are even more variable than complex dynamical systems and may, thus, not be classified as complex systems in a strict sense: Evolutionary processes lead to extinction and innovation of variables, thereby changing the number of degrees of freedom that should be fixed in complex dynamic systems (LANGE 1999).

On the other hand, the actual rapid developments in information technology brought a new situation in providing the capacity to store and evaluate very large amounts of data. This enables for the first time in history the explicit consideration of light-climate relevant canopy structure in calculations of gas-exchange and in the estimation of other structure-related processes in canopies. Under the assumption that the processes in forests are mechanistically determined and that evolutionary processes occur relatively slowly, it is probable, that this new situation will on the long run lead to a more holistic understanding of relationships between structure and function in forest canopies, in which many of the different findings on different scales may be integrated. An integrated, holistic understanding of relationships between structure and function of forest canopies seems to be valuable not only by itself or because it may increase the profit from former studies, but also because it can still provide answers, when completely different environmental questions than now will be posed to plant ecologists.

Therefore, the explicit consideration of structural complexity is reasonable and necessary as a basis for a mechanistic description of mixed stand gas-exchange from the actual view point, though the full profit of its evaluation will probably be gained in the future.

1.2.2 Implications for actual studies on mixed stand gas-exchange

Given that no single study can yet provide a holistic synthesis, a stepwise long-term strategy is required to cope with the complexity of mixed stands, which starts with intensive fine-scale structural measurements and combined gas-exchange measurements and ends with their complete evaluation with fine-scale models for light and gas-exchange. Up-scaling of functional measurements along 3D-structures of tree crowns is inevitably necessary to achieve this aim and a complete evaluation requires in the first place a complete description of structure and related properties.

Unfortunately, methods of structural measurements in forest canopies did not develop as rapidly as data processing by computers, so that the documentation of 3D canopy structure of trees is still time consuming. Though some new measurement methods were established for the application on smaller plants (SINOQUET ET AL. 1991, HIROTA & NAKANO 2000) or for a rougher description of 3D canopy structure (KOCH & REIDELSTÜRZ 1998, LEFSKY ET AL. 2000, TANAKA ET AL. 1998), 3D structure measurements on mature trees are not accelerated by these techniques, when physiological investigations on specific parts of the canopy shall be referable to them. Therefore, function-related measurements of 3D structure are the bottleneck for the further development towards a holistic understanding of structure and function of tree canopies. While a growing number of spatially explicit 3D-models of forest canopy light climate and gas-exchange exists (CANHAM ET AL. 1999, CESCATTI 1997, FALGE 1997, KNYAZIKHIN ET AL. 1997, RÖHRIG ET AL. 1999, WANG & JARVIS 1990) and further refinements are under development (FALTIN 2001), their spatial parameterisation is mostly rough or general, i.e., tree crowns are not segmented or are partitioned into a small number of symmetrical compartments. Thus, their high potential for detailed up-scaling of leaf and branch level measurements to the canopy is not fully used, which is simply due to the time-consuming process of three-dimensional structure measurements and the just as time-consuming process to recalculate these measurements into a fine-scale parameterisation.

The following implications for the actual study were derived:

- Canopy structure measurements have to be organised such, that their usefulness for different approaches of structure representation in 3D-models is guaranteed.
- Canopy structure measurements need a resolution that is valuable for many different kinds of physiological measurements in tree crowns (which is mostly the branch scale; VALLADERES 1999) and which is appropriate for the description of light-climate (see 1.1.6).
- Functional (gas-exchange) measurements on different scales should be combined with structure measurements to enable the analysis of relations between function and structure on different spatial levels.
- Co-operation with other researchers in the same stand is necessary to bring the necessary information together.
- As much as possible additional information about factors influencing gas-exchange for the given stand should be gathered.
- The results and samples should be stored in a manner that enables their future evaluation in other fields of research.

- The complete description of all gathered data is important to avoid irretrievable losses of potentially significant information, even when the evaluation of all gathered data to a given evaluation level may be impossible.
- Methods of automation should be found and used to reduce complexity and to facilitate further studies on structure-function relationships in mixed stands.

1.2.3 Scope and organisation of this study

The aim of this study is to provide field methods, a database, up-scaling relationships, and model subroutines for a spatially explicit analysis of mixed stand gas-exchange. The species- and stand-specific results that were obtained by application of these methods shall indicate where gas-exchange relevant differences in structure and physiology of *Fagus sylvatica* and *Quercus petraea* trees can be expected and shall contribute to a spatially explicit consideration of patterns of space capture in the 3D light-model STANDFLUX-SECTORS (FALGE 1997, FALTIN 2001, FLECK ET AL. 2001).

This required:

1. The development of partially automated methods for the model-independent description of tree crown structures (leaf cloud oriented biomass harvest) and stand structure (tree crown oriented stand survey)
2. The detailed, light-climate oriented, and therefore leaf cloud oriented 3D-description of crown structures of the two tree species and description of stand structure
3. The intensive investigation of tree crown structures for spatial regularities that enable up-scaling or are important for light-climate (leaf cloud properties)
4. The analysis of easily measurable quantities for up-scaling of structure (allometric relationships between branch or trunk basal area and leaf area)
5. Photosynthesis measurements on leaves on the standing trees and characterisation of their light-climate (evaluation of fish-eye photos)
6. Development of an optically controllable routine for **A/C_r-curves'** automatic evaluation (RACCIA) for the parameterisation of Farquhar-type leaf models of gas-exchange.
7. Investigations on light-climate relevant properties of leaves (leaf-angles)
8. Investigation and establishment of relationships between light-climate, leaf mass per area, leaf nitrogen, and leaf photosynthetic capacities of the two species
9. The development of a leaf nitrogen dependent photosynthesis model based on the LEAVES model (HARLEY & TENHUNEN 1991)
10. The development of a program for optical control and recalculation of structural measurements into a 3D-parameterisation, that can be applied to different model representations of 3D-structure (**optically controlled crown internal structure representation, CRISTO**)
11. The fine-scale parameterisation of the 3D-light model STANDFLUX-SECTORS (FLECK ET AL. 2001), its evaluation for branches, whose sapflow was measured (M. SCHMIDT, Lehrstuhl Pflanzenökologie, Universität Bayreuth, unpublished), and its validation using relative light values from hemispherical pictures

The chapters report these steps summarising for different spatial levels:

Chapter 2: Tree crown structures of mature *Fagus sylvatica* and *Quercus petraea* trees

(level of boughs and branches / leaf clouds)

Chapter 3: Spatial distribution of leaf properties in tree crowns (leaf level)

Chapter 4: Representation of tree and stand structure with CRISTO and application of the spatially explicit 3D light-model STANDFLUX-SECTORS to three-dimensional patterns of space capture in a mixed stand (stand and tree level)

2 Tree crown structures of mature *Fagus sylvatica* and *Quercus petraea* trees

2.1 Objectives

Up-scaling of branch level investigations to whole canopies requires the identification of regularities in tree crown structure that can be expressed as mathematical functions and related to easily measured quantities. One fundamental assumption of structural regularity that is used in most canopy gas exchange models is homogeneity throughout the volume or throughout the height range of certain compartments (tree crowns, segments, or layers), which enables the up-scaling of leaf-level photosynthesis rates by multiplication with leaf area of the compartment. This assumption is only an approximation to the real situation, and has to be tested in each case for correctness and utility. Because observations of heterogeneity within single tree crowns reject this assumption, the following hypotheses were formulated:

H1: The leaf distribution in single tree canopies is not homogeneous.

H2: The 3D-arrangement of branches and associated leaf clouds in the tree crowns is regular and its regularity is responsive to and relevant for light interception.

H3: Differences in the regularity of tree crown structure are partly species-specific.

The hope behind hypotheses **H2** and **H3** is to find alternative regularities within tree crowns that are useful for up-scaling. Two major implications for the evaluation arise, when these hypotheses are to be tested under natural conditions:

- Structural regularity (**H2**, **H3**) can have many different forms, so that many different possibilities must be explored with a variety of approaches.
- The necessary high resolution of crown structure measurements required in the search for regularities limits the number of trees that can be investigated, thus preventing statistical evaluation among trees. The results, therefore, cannot initially be generalised to other oaks and beeches, and cannot immediately represent species-specific differences (**H3**). The results must be considered as examples of tree structural properties, that could similarly occur with other oaks and beeches.

Thus, the investigations with respect to **H2** are of an explorative nature, while **H3** can only be examined with respect to the tree crowns sampled.

Nevertheless, a full *in situ* characterisation of structural constraints in mature tree crowns of oak and beech is achieved, that is useful in future considerations of light and gas-exchange models for mixed forest stands.

2.2 Materials and Methods

2.2.1 Stand descriptions

Results presented in this thesis rely on measurements that have been performed on three beech dominated stands in two mountainous regions in northern Bavaria. In 1997, structure-oriented investigations were performed in the 120 year old pure beech stand “Buchenallee” in the Fichtelgebirge highlands (50°03'N, 11°52'E) at an elevation of 905m (Fig. 1).

Relationships between structure and function were investigated in 1998 in the 120 year old stand “Großebene” in the Steigerwald highlands (49° 52'N, 10°28'E) at an elevation of 450m. This stand is separated by 1.3 km from the main investigation site “Steinkreuz” (140 years) of the BITÖK (Bayreuth Institute of Terrestrial Ecosystem Research), where additional structural and LAI-measurements were taken. Großebene and Steinkreuz are mixed stands of *Fagus sylvatica* and *Quercus petraea*. The measurements were carried out at the stands Großebene and Buchenallee due to the availability of climate and other measurements at the nearby stands Steinkreuz and Waldstein (GERSTBERGER 1997), their species composition, sapflow measurements in other projects on the same trees (M. SCHMIDT, DEPT. OF PLANT ECOLOGY, UNIVERSITY OF BAYREUTH, UNPUBLISHED), and because tree height allowed access to dominant trees with the available highlift.

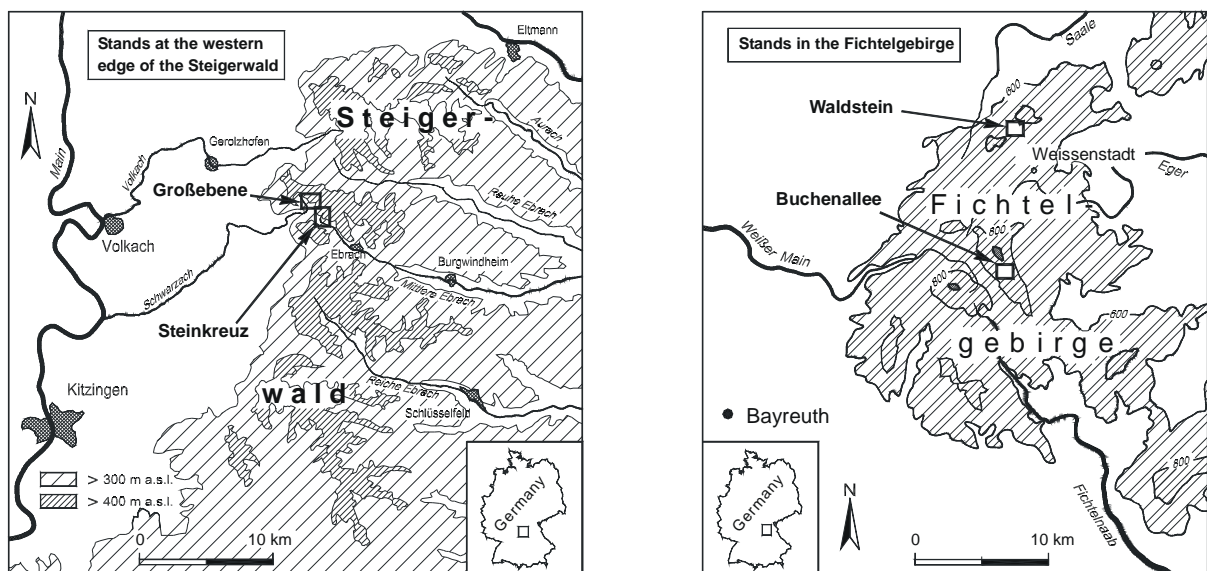


Fig. 1: Location of the investigated stands in the Steigerwald (left side) and in the Fichtelgebirge (BITÖK-maps created by P. GERSTBERGER)

2.2.1.1 Buchenallee

The Fichtelgebirge is a mountainous region created by volcanic activity during the Carboniferous and Permian and has a maximum elevation of 1051 m a.s.l. at the Schneeberg mountain, which is the highest elevation in Northern Bavaria. Low temperatures and high

precipitation are typical for the climate in the upper Fichtelgebirge. Climate measurements at the Waldstein mountain (765m a.s.l.) (unpublished data of the Chair of Microclimatology, BITÖK, University of Bayreuth) indicate an annual mean temperature of 6 °C. Mean annual precipitation at higher elevation in the Fichtelgebirge ranges from 1100 to 1300 mm and from 950 mm to 1100 mm in those parts below 900 m a.s.l. (BAYERISCHER KLIMAFORSCHUNGSVERBUND 1998). About 20% of precipitation is deposited from fog during 1160 h of foggy weather during the year (WRZESINSKY & KLEMM 2000).

Low soil-pH values on the mineral poor, silicate rich geological base material (granite) in combination with the cold and wet climate in the upper region promote podzolization of the soil, so that podzolised brown soils and podzolised leptosols ("Ranker") cover nearly the whole Schneeberg (FORSTAMT WEISSENSTADT 1989). The investigation area "Buchenallee" is located on the south slope of the Schneeberg with an inclination of 13.5° (measured with a Suunto inclinometer), ranging from 900 m to 915 m above sea level. The partly podzolised brown earth in this area has $pH_{(H_2O)}$ -values of around 4.75 in the upper 5 cm of the mineral soil. The C/N ratio of the 5.7 cm (on average) thick humus layer was found to be 17.6, which accounts for rather good nutrient availability.

The potential natural climax vegetation of the Fichtelgebirge should be a beech forest with natural admixture of coniferous trees such as spruce and fir (BOHN ET AL. 1999), although slow growth and a high occurrence of damage by pathogens suggest that beech is at its altitudinal limit at the Schneeberg: The oldest beeches at the Buchenallee are 120 years old, but are not higher than 26 m, thus belonging only to yield class 3 (FORSTAMT WEISSENSTADT 1989). Ten to 20 percent of the beeches are infected with different parasitic fungi, mostly *Fomes fomentarius*, *Nectria ditissima*, and *Fusarium avenaceum* (determination according to BUTIN 1983). Furthermore, the regions above 950 m a.s.l. of the comparable adjacent highlands in Thüringer Wald, Erzgebirge, Böhmerwald, and Bayerischer Wald have mountainous spruce forests as their potential natural vegetation [BOHN ET AL. 1999]. Pure spruce plantations were favoured in the past in the Fichtelgebirge for economic reasons, so that today around 90% of the forest is made up of uniform and even-aged Norway spruce stands (*Picea abies* (L.) Karst.).

2.2.1.2 Großebene and Steinkreuz

The Steigerwald is a hilly region between 200 and 490 m a.s.l., with highest elevations at its steep western edge which is 200m higher than the adjacent plain of the Main river (see Fig. 1). Altitude decreases continuously from the escarpment toward the east, where maximum altitudes of 300m a.s.l. are attained. Three valleys in east-west direction separate the Steigerwald into four chains of low mountains. Climatic conditions change in correspondence with the elevation gradient: 750 mm to 850 mm precipitation are reached in the uplands of the western part, while the lower and the eastern parts experience only 650 mm to 750 mm (BAYERISCHER KLIMAFORSCHUNGSVERBUND 1998). Precipitation is much lower and mean annual temperature (7 – 8 °C; WELSS 1985) is higher than in the Fichtelgebirge, which leads to arid periods during the summer that are indicated by less precipitation (in mm) than twice the temperature (in °C) according to the definition of WALTER & BRECKLE (1999). Arid periods occurred even in the relatively wet year 1998 (see Fig. 2).

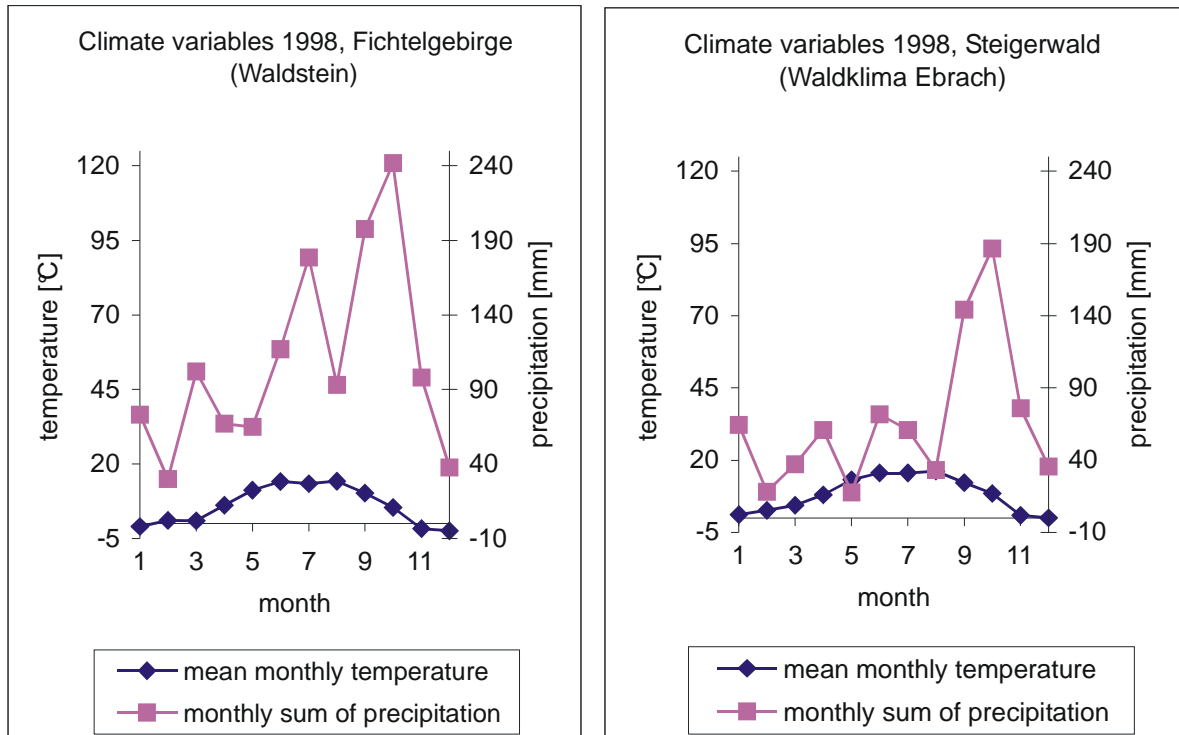


Fig. 2: Annual course of climate variables at the investigated sites in the year 1998. Arid periods are indicated by less precipitation (in mm) than twice the temperature (in °C) (W ALTER & BRECKLE 1999), i.e., when the temperature curve lies above the precipitation curve in this diagram.

The geological formations of the Steigerwald belong mainly to upper triassic sandstones (Sandsteinkeuper). Blasensandstein, Coburger Sandstein and Burgsandstein build 23-27 m, 5-9 m, and 30 m thick layers above the underlying, largely water-impermeable, and clayey-siltic Lehrberg-layer (30 m) (EMMERT 1985). The sandstone layers include multiple inter-bedding of clay and sandstone layers that are usually some dm in thickness (EMMERT 1985). Sandy brown earth soils develop mainly on Coburger Sandstein and Burgsandstein, while two-layer-soils with a stony phase and clayey pelosols occur mainly above Blasensandstein- and Lehrberg-layers (SEILER 1995, WELSS 1985). Pelosols are typically found on the plains, and two-layer-soils may develop on steeper slopes by solifluction of the Blasensandstein-layers.

The investigated stands are located on the south-east side of the Stollberg (max. altitude 475 m a.s.l.), 2-3 km east of the western edge of the Steigerwald. South slopes on the south-western side of this mountain are warm enough to belong to the most eastern areas of viticulture in Bavaria. The potential natural vegetation of this region belongs to the sessile oak / hornbeam forests in warm-dry areas with little or no occurrence of beech (BOHN ET AL. 1999). Both stands are found on strongly acidic brown earth ($\text{pH}_{\text{H}_2\text{O}} = 3.7$ in 0-5 cm depth, measured in November 2000), which was also found by CHANG (1999) for Steinkreuz. Nitrogen availability of both stands was found to be good (C/N-ratio of the humus layer was 15.2 in both stands). Humus layers were found to be 1.5 to 3.5 cm thick.

Großebene and Steinkreuz are mixed stands of *Fagus sylvatica* and *Quercus petraea* with a high proportion of beech, that were established by natural regrowth around 1880 (Großebene) and in the period of 1863 to 1872 (Steinkreuz) (FORSTAMT EBRACH 2000). The dominance of beech is still supported by natural regrowth of seedlings, and this may partly be due to the higher precipitation rates on the western edge of the Steigerwald, where drought resistance is not as important for competition as it is in the lower or eastern parts. High acidity is not necessarily a disadvantage for natural regrowth of beech seedlings (LEUSCHNER ET AL. 1993). Another reason may be found in the fact that oaks in this area are periodically infested by insects of the *Tortrix viridiana* community. The populations of these insects may increase enormously in some years and infested oaks in the Steigerwald may lose their entire leaf biomass (SCHÄFER 1997). While 1995 – 1997 was a period of high pest activity (HEAD FORESTER GEIZ, FORSTDIENTSTELLE OBERSCHWARZACH, PERS. COMMUNICATION), no obvious insect damage occurred to the oaks during the investigation year 1998. Forest management in the Steigerwald generally supports the growth of oaks by selective logging of the oak suppressing beeches (SCHÄFER 1997).

The main differences between two nearly even-aged stands in the Steigerwald are their height growth, their tree density, the vigour of oaks, and soil depth. Trees in Steinkreuz are approximately 10 m higher than in Großebene and tree density is much lower, causing greater light availability on the ground and greater cover by understorey vegetation and regrowing trees

Table 1: Main site factors of the three investigated stands of *Fagus sylvatica* and *Fagus sylvatica* mixed with *Quercus petraea*

Stand	Buchenallee	Großebene	Steinkreuz
Location			
Position	11°51'27-34" E, 50°02'30-32" N	10°26'43-52" E, 49°52'41-48" N	10°27'38-44" E, 49°52'15-19" N
Region	Fichtelgebirge	Steigerwald	
Mountain (maximum elevation)	Schneeberg (1051m a.s.l.)	Stollberg (475m a.s.l.)	
Altitude	910m a.s.l.	460m a.s.l.	440m a.s.l.
Area	2424m ² * ¹	3097m ² * ¹	12900m ² * ²
Inclination	13.5°	2°	5,5°
Exposition	SSW	SE	SSE

Climate			
Mean annual precipitation (long term; '97; '98)	1100mm - 1300mm 968mm* ³ 1299mm* ⁴	650mm - 800 mm 653mm 807mm	
Annual mean temperature (long term; '97; '98)	- 6.0 °C * ⁴ 5.9°C * ⁴	7.5°C; 7.1°C; 8.3°C	
Range of monthly mean temperatures (long term; '97; '98)	- -4.5°C – 17.1°C * ⁴ -2.5°C – 14.2°C * ⁴	-1.5°C - 16°C ; -3.7°C - 15.7°C; 0.0 °C - 16.2°C	
Days p.a. with mean temperature > 5°C (long term; '97; '98)	- 189 * ⁴ 199 * ⁴	215 185 249	

Soil			
Geology	Coarse-grained core-granite of the Fichtelgebirge	Middle Keuper (Upper Triassic), inter-bedding of coarse-grained sandstone ("Blasensandstein") and clayey layers	Middle Keuper (Upper Triassic), inter-bedding of coarse- or fine-grained sandstone ("Blasensandstein, Coburger Sandstein") and clayey layers
Soil type (FAO-Classification; SCHEFFER & SCHACHTSCHABEL 1998)	Loamy-sandy, partly podzolic brown soil (Dystric Cambisol)	Loamy-sandy brown soil with stony phase (Cambisol)	Sandy brown soil (Cambisol)
Soil-depth	30-100cm	5-40cm	50-80cm
Humus-layer	5.7 ± 0.8 cm	2.6 ± 0.9 cm	2.4 ± 0.9cm
Soil-pH _(H₂O) in 0-5cm	4.75 ± 0.13	3.72 ± 0.21	3.65 ± 0.29
C/N of humus layer	17.55 ± 0.45	15.16 ± 2.66	15.15 ± 2.25

Vegetation			
Tree Species composition	99% <i>Fagus sylvatica</i> , 1% <i>Pseudotsuga menziesii</i>	66% <i>Fagus sylvatica</i> , 34% <i>Quercus petraea</i>	75% <i>Fagus sylvatica</i> , 24% <i>Quercus petraea</i> , 1% <i>Carpinus betulus</i>
Stand age	120a	120a	140a
LAI* ⁷	8.1	6.1	6.2
Yield class	3	1	1
Trees per ha	524	526.3	358.1
Max. stand height	26m	30m	39m
Understorey cover	2%	<1%	5 -10%
Main understorey species	<i>Deschampsia flexuosa</i> , <i>Oxalis acetosella</i> , mosses	<i>Anemone nemorosa</i> , tree seedlings	<i>Luzula albida</i> , <i>Deschampsia flexuosa</i> , geophytes, mosses

Human Impact			
Forest management	Periodic thinning (up to 30% removal)	Single stem harvests, supporting growth of oaks	No management but ecological research since 1994
Ca ²⁺ -deposition	4.8 (1.6) kg/(ha*a) * ⁶	10.6 (2.8) kg/(ha*a) * ⁵	
Mg ²⁺ -deposition	2.0 (0.4) kg/(ha*a) * ⁶	2.8 (0.5) kg/(ha*a) * ⁵	
Na ⁺ -deposition	11.3 (4.5) kg/(ha*a) * ⁶	7.6 (3.8) kg/(ha*a) * ⁵	
K ⁺ -deposition	26.1 (2.9) kg/(ha*a) * ⁶	33.0 (3.1) kg/(ha*a) * ⁵	
Cl ⁻ -deposition	19.1 (6.8) kg/(ha*a) * ⁶	11.6 (5.1) kg/(ha*a) * ⁵	
SO ₄ ²⁺ -deposition	35.1 (9.2) kg/(ha*a) * ⁶	18.6 (7.6) kg/(ha*a) * ⁵	
NH ₄ ⁺ -deposition	16.7 (7.2) kg/(ha*a) * ⁶	12.5 (5.5) kg/(ha*a) * ⁵	
NO ₃ ⁻ -deposition	18.5 (6.2) kg/(ha*a) * ⁶	11.6 (4.8) kg/(ha*a) * ⁵	

*¹ horizontally projected area of measured tree crown extensions

*² fenced area

*³ Measurement at DWD-station Bischofsgrün (675m a.s.l.)

*⁴ Measurement at Waldstein investigation site (765m a.s.l.)

*⁵ Measurement in bulk precipitation (portion in brackets), canopy drip, and stemflow at the Steinkreuz investigation site 1996/1996 (LISCHEID & GERSTBERGER 1997)

*⁶ Measurement in bulk precipitation (portion in brackets) and canopy drip in the Norway spruce stand at the Waldstein investigation site 1993-1998 (MANDERSCHIED & ALEWELL 2000)

*⁷ calculated from tree diameters and allometric relationships (Fig. 14) that were adjusted with a constant factor based on leaf area determinations of the harvested trees from each stand

in a shrubby stage. Steinkreuz is of much lower density and this cannot be due solely to its slightly greater age. The retardation of growth and development of the Große Ebene stand is probably due to its restricted soil depth which is often less than 10 cm and around 30 cm on average. Thus, root growth at this site for younger as well as old trees appears limited, as observed from the root stock of wind-thrown beeches in the stand. Another difference in the stands concerns the vigour of oaks. While oaks in Große Ebene are healthy and greater in height than the beeches (height measured with the forest survey laser Criterion 400, Laser Technology Inc., Englewood, Colorado), Steinkreuz oaks appear out-competed by very tall beeches and they have much less dense crowns.

The investigation year 1997 was with 968 mm precipitation (DWD-Climate Station Bischofsgrün, 675 m a.s.l.) and a mean temperature of 6.0 °C (BIT ÖK investigation site Waldstein, 765 m a.s.l.) in the Fichtelgebirge, and 653 mm and 7.1 °C in the Steigerwald (LFW Forest Climate Station Ebrach) a relatively dry but not warm year with a relatively short summer season. The year 1998 (1299 mm precipitation and 5.9 °C at the Waldstein investigation site and 803 mm / 8.3 °C at the LFW Forest Climate Station Ebrach) was a very wet year with high temperatures and long summer season in the Steigerwald (see Fig. 2).

2.2.2 Soil pH and soil C/N ratio

Five soil cores per stand were removed in November and December 2000 and separated into humus layer and 5cm thick stratified samples of the mineral soil (0-5cm, 5-10cm, 10-15cm, 15-20cm). Thickness of the humus layer (including organic layer) was measured in the field, and samples were brought to the laboratory. Twenty gram of each sub-sample were mixed with 50ml deionized water for 4 – 24 hours and pH was measured with a pH-electrode. The remainder of the soil samples was sieved with a 2mm sieve and oven-dried at 90°C for at least 48 hours for C and N determination in a C/N-analyser (CHN-O-Rapid, Foss Heraeus GmbH, Hanau, Germany).

2.2.3 Canopy structure determination

Canopy structure of selected trees was determined in order to develop a “leaf cloud” oriented description of tree crowns of beech and oak. A quantitative description of foliage clustered in leaf clouds (see 2.2.4 for a definition) will allow testing of up-scaling methods for gas-exchange from leaves to canopies by including the intermediate level of organisation associated with branches. Thus, canopy structure is viewed from the perspective of gas-exchange as it is influenced by the spatial arrangement of physiologically distinguished tissues (sun leaves, shade leaves, respiring organs) and their impact on light-climate. Measurements included the geodetic location of branches and leaf clouds inside the crown, the description of the branch system, sampling of leaves for determination of leaf structure, and leaf cloud oriented biomass harvest. Geodetic measurements were mostly done in the leafless state in early spring, and leaves were sampled between June and August to reduce the effects of decreasing leaf mass per area (LMA) and nitrogen retranslocation on nitrogen tissue concentrations (DAY & MONK 1977, KLOEPEL ET AL. 1993, SCHULTE 1992). Biomass harvest started mid of August and was completed in the first days of September before yellowing of the leaves.

The necessarily high resolution of these measurements limited the number of trees investigated to three beeches and one oak, thus preventing statistical evaluation among trees. The findings,

therefore, cannot be generalised to other oaks and beeches, but must be considered as examples of tree structural properties, that could similarly occur with other oaks and beeches.

Two beech trees in the Buchenallee stand (Bu38, Bu45) and one beech and one oak at the Großebeene (Gr12, Gr13) were chosen for study (see Fig. 3). Their size and social position were selected to obtain leaves in all levels of light exposure. Thus, trees had to be tall enough to project above the uppermost leaf-layer of the stand, but small enough to reach with the available highlift. Oak and beech in the Großebeene stand were required to stand adjacent to each other. Atypical trees with gross anomalies, such as severe pathogen damage, or atypical crown architecture due to early ramification into two stems, or broken tops, or due to proximity to gaps or roads were excluded from consideration as objects for this study.

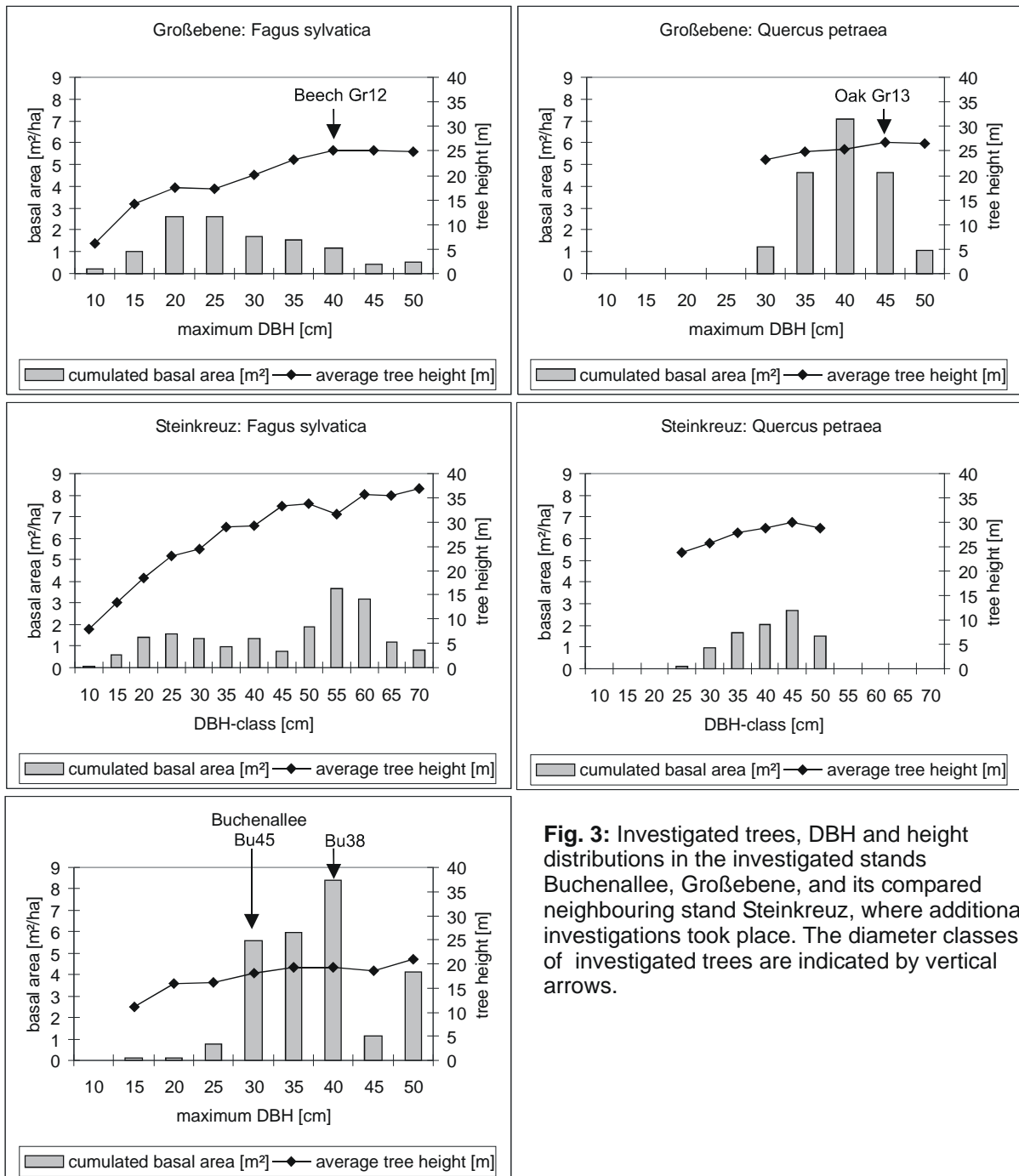


Fig. 3: Investigated trees, DBH and height distributions in the investigated stands Buchenallee, Großebeene, and its compared neighbouring stand Steinkreuz, where additional investigations took place. The diameter classes of investigated trees are indicated by vertical arrows.

2.2.4 Geodetic location measurements

Access to the crown was achieved with a highlift (Teupen Hylift, Gronau-Epe, Germany) with maximum vertical extension of 23 m. The 1 m by 0.8 m cabin of the highlift was carefully moved through the canopy so that nearly any point inside the crown could be reached without leaving the cabin. Positions in the crown were measured with an electronic theodolite on the ground aimed at an infrared reflector on a pole held by a person in the cabin. The theodolite (Wild Tachymat, Heerbrugg, Switzerland) measures azimuth angle and elevation angle with an accuracy of 3" and distance to the measuring point with an accuracy of $3 \text{ mm} \pm 2 \text{ ppm}$ (relative to the distance), so that relative co-ordinates of the reflector in relation to the location of the theodolite could be determined.

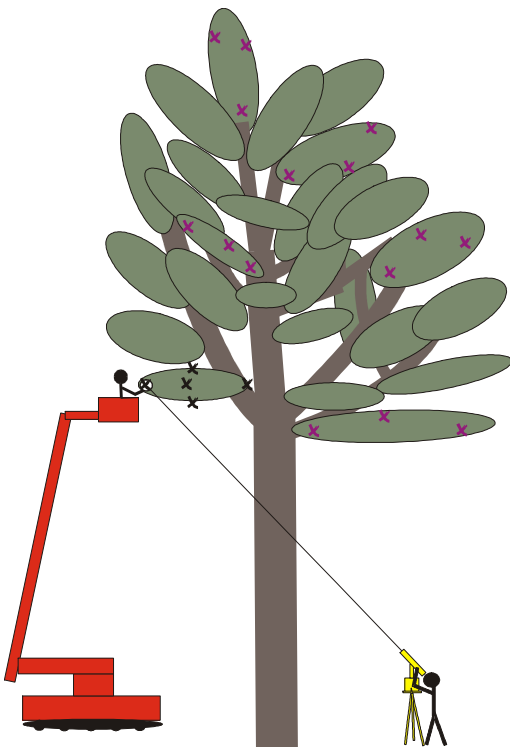


Fig. 4: Schematic illustration of the measurement procedure for determining locations within the canopy.

Each branch was labelled and characteristic points on the surface of its appending leaf cloud (see below) were determined by location measurement with an infrared theodolite. The theodolite measures angles and distance to the reflector and uses these data to calculate 3D co-ordinates. It had to stand at a distance of at least 30 m because it could not aim at angles above 40°.

Ramification points of the stem and of all branches larger than 3 cm in diameter (2 cm in the Buchenallee stand) were located to describe the structure of the woody parts of the crown. Positions on the surface of all leaf clouds of branches larger than 3 cm in diameter (2 cm in the Buchenallee stand) or with more than 50 leaves (20 leaves in the Buchenallee stand) were located to describe the leaf distribution in the crown.

A leaf cloud is considered here as the conglomeration of leaves attached to one branch. Its spatial extension is described by a leaf cloud enveloping polyhedron of the following form: Considering that any leaf cloud has a plane, which is the plane of the largest possible polygon that may be constructed in the 3-dimensional extension of the leaf cloud, that polygon is approximately described by four (or more, if necessary) corner points (see Fig. 5). The extension orthogonal to the plane of the leaf cloud is measured in both directions at each corner point with a meter-stick, so that four (or more) parallel axes are determined. Linking the endpoints of the parallel axes in the same order as the corner points of the original polygon leads to a ring of linked polygons. Then two roofs are set on both sides of the ring to complete

the polyhedron by linking the endpoints of the parallel axes with the endpoints of an additional central axis, which is measured in the same way. This axis is in the centre of the leaf cloud, where the extension orthogonal to the leaf cloud plane is longest.

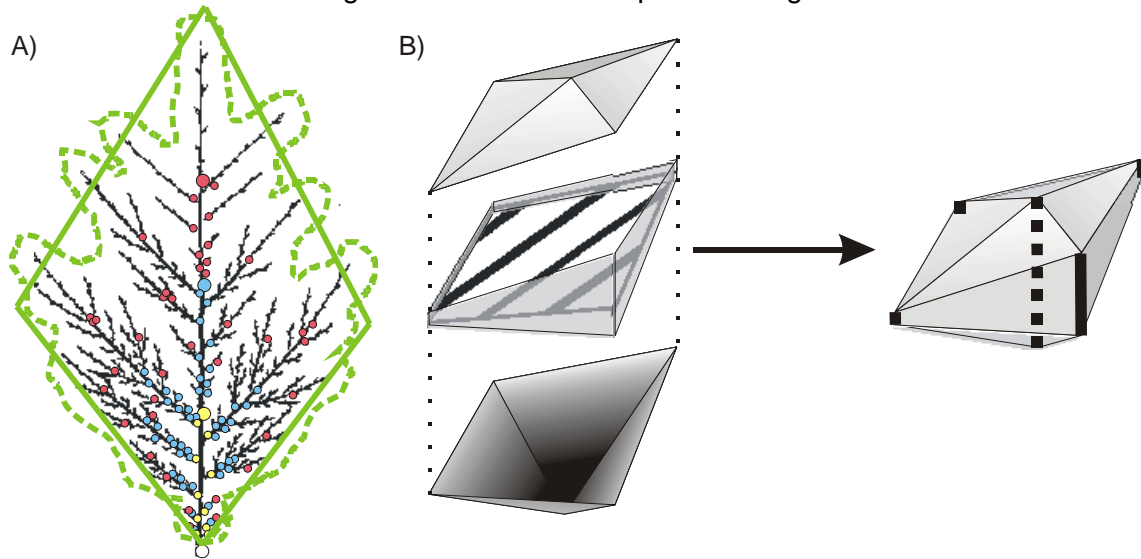


Fig. 5: a) Beech branch with maximum planar extension of its leaf cloud (leaf cloud plane, dotted line), which is approximately described by a quadrangle. The former leaf cloud planes can be reconstructed from bud-scars of past years (circles of same colour per year). **b)** Construction of leaf cloud enveloping polyhedrons on the basis of such a quadrangle (hatched area) and rectangular distance measurements at four corner points (fat lines) and 1 central point of the quadrangle (fat dotted line).

It is very unlikely that the field-measurement of polygon corner points itself yields co-ordinates that are exactly situated in a plane. Therefore, the plane of the leaf cloud was determined as that plane that is closest to all measured polygon corner points. Additionally, distance measurements along parallel axes are made such that they may integrate over a section of the leaf clouds' surface of maximum 40cm radius when this was necessary to get a reasonable approximation to the leaf cloud form. Optical control of the 3D-data (Visualisation with CRISTO, chapter 4) was used to identify misleading measurements due to measurement failures (reflection signal from the plant instead of the reflector) or due to false classification of the measurement, which would have had a strong influence on the whole description, although there were altogether not more than 15 points at which this occurred. These measurements were repeated or reasonably estimated from the optical impression and photos (in one case).

The problem of tree sway influencing accuracy of the resulting description of leaf clouds was not as large as expected, because it became apparent that the trees typically experience wind speeds that are too low to move leaf clouds. If leaf clouds are moved under high wind speeds, they mostly move in a manner that describes an arc around the stem rather than modification of leaf cloud form.

2.2.5 Description of branch connections

Main boughs were named with a letter in alphabetical order of the nodes along the stem, starting with the lowest bough. Nodes along the boughs were named with numbers (A1, A2, A3,...; B1, B2, B3...) starting from the stem node (A0, B0, C0, ...). Affiliated boughs were named with an additional letter in the order of the nodes along the main bough (AA, AB, AC,...) and nodes along the affiliated boughs were named again with numbers (AA1,AA2,...; AB1,AB2,...).

Finally the leaf cloud supporting branches were named after the node where they originate with an additional sign for their position relative to the superior bough (left or right side-branch, end-branch). Circumferences of main boughs were measured close to the main trunk.

2.2.6 Leaf cloud oriented biomass harvest and leaf sampling

All leaf clouds of two beeches in the Buchenallee stand (Bu38 and Bu45) and of the oak Gr13 (Großebene) as well as 18 leaf clouds of the beech Gr12 (Großebene) were harvested during August / beginning of September 1997 in Buchenallee and 1998 in Großebene with a saw from the highlift. The main branch of each leaf cloud was cut above the last ramification point of the branch system and directly under the first leaves, was transferred into the cabin and carefully brought to the forest floor. In Buchenallee, 5 leaves were sampled in advance on the sun-side and 5 leaves on the stem-side of a leaf cloud for area and dry weight determination. Oak and beech leaf clouds in the mixed stand Großebene were divided along the main branch into pieces of 1m length; 5 leaves of each piece were sampled for area and weight measurements. All leaves of each leaf cloud were detached, the samples of each leaf cloud or 1m-segment were oven-dried (80°C for at least 48 h) and dry weight was determined. The remaining wood of beech leaf clouds of the Buchenallee stand and some leaf clouds from the Großebene trees was put in bags, oven-dried for at least 144 h and weighed. Leaf area measurements were done with the portable CI-202 leaf area meter (CID, Idaho, USA) (Buchenallee) and with the stationary DIAS area meter (Delta-T, Cambridge, England). Leaf mass per area (LMA) was calculated for all sampled leaves. Leaf area of each leaf cloud was then calculated, assuming an average LMA-value for each segment and a linear change of LMA between stem-side and sun-side of the cloud. Leaf area density of leaf clouds was calculated based on total leaf area and the calculated volume of their leaf cloud enveloping polyhedrons (see chapter 4). Projected wood area of a sub-sample of 20 leaf clouds from beech Bu38 was determined with the DIAS area meter and area per dry weight was calculated.

Basal area of the cut branches was determined from the average diameter measurement with callipers in two directions from cambium to cambium. A pH-borderline between the outer rings of the branch cross-sectional area and the inner rings was determined by dyeing the cut surface immediately after cutting with a 0.5% solution of the pH-indicator Bromine Cresol Green in ethanol (KÖSTNER, DEP. OF PLANT ECOLOGY, UNIVERSITÄT BAYREUTH, PERS. COMMUNICATION 1997). The radius to the visible boundary-line was measured (average of four directions), as was the bark thickness. This borderline represents the change between heartwood and sapwood on oak cuttings and is used to determine the sapwood/heartwood border of *Abies sachalinensis* (BAMBER & FUKAZAWA 1985). It could not be proven that the observed abrupt change in pH-values on fresh beech cuttings similarly indicates the sapwood, e.g. the expected changes in wood water content and chemical composition of the wood associated with sapwood (SKAAR 1988, NAIR 1995). Though heartwood formation in beech in the sense of development of thyloises and storage of phenolic compounds does not start unless the tree is older than 80 or 100 years (HILLIS 1987), sapflow velocities in younger beech trunks decrease with distance from the bark and are correlated with a decrease in water content of the wood (CERMAK ET AL. 1992, GRANIER ET AL. 2000). Therefore, "sapwood area" of oak was calculated based on the observed pH-borderline, while for beech branches the "area of outer rings" was calculated from the specific borderline between high pH-values in the outer rings and low pH-values in the inner rings. Outer and inner boundaries were assumed to be circular for both species.

Leaf sampling for carbon and nitrogen content with a C/N-analyser (CHN-O-Rapid, Foss Heraeus GmbH, Hanau, Germany), leaf-angle determination with a protractor, and measurement of leaf-form parameters were done along four vertical lines in beech crowns of the Buchenallee, but randomly in co-ordination with photosynthesis measurements in the Große Ebene stand.

All trees recovered slowly after their complete defoliation. Oak Gr13 developed giant leaves (threefold size) in the following year, which may be due to its inability to form more leaves from the reduced number of buds. During its harvest, it was discovered that beech Bu45 was infected with a fungus that formed (like *Fusarium avenaceum*) longitudinal chaps in the bark, but could also be detected by growth of the fungus into bark tissue as evidenced in cross-sections of nearly each branch. This infection became more severe in the following years. Further investigations on most samples of the harvested trees will still be possible due to their storage in the BITÖK sample base.

2.2.7 Error estimations

While measurement errors in soil pH and C/N ratio due to calibration of the pH-electrode or the C/N analyser, or weighing errors may be assessed to be lower than 1%, spatial variation in the stand may fully be overlooked on the base of 5 samples per stand. Additional errors may be introduced due to locally high proportions of sand in the samples, but this was not observed. Thus, soil pH and C/N-ratio measurements characterise the stands on the base of spot-checks that are only valid for the location of the samples.

Methodical measurement errors in geodetic location measurements are rather small: The given measurement errors of the theodolite (angle and distance) result in a spatial deviation of ± 0.5 cm per dimension, when the distance to the measured object is 100m. 100m is more than the measurement distance to the very most measured points. An additional error of ± 1 cm per dimension may result from height tracking of points that were not visible from the position of the theodolite: These points were measured by holding the reflector up to 1 m above or below the object and measuring the vertical distance with a meter-stick for later correction of the height co-ordinate. ± 5 cm deviation per dimension result from the width of the reflector and another ± 5 cm from the movement of leaf clouds in the wind. Thus, all measured co-ordinates may deviate up to 11.5 cm per dimension from their original position.

About 2% of the total leaf area of each leaf cloud may potentially be not included in the leaf cloud enveloping polyhedron that approximates its distribution in space. Leaf area densities of height layers may additionally be erroneous due to inhomogeneous distribution of leaf area inside the volume or height range of polyhedrons – this error may principally reduce the calculated leaf area of a 10cm height layer in one polyhedron to 0% of the calculated value, thereby potentially doubling the leaf area densities of a neighbouring layer. This error is systematic due to the growth determined distribution of leaves in the leaf cloud, which may be assumed to be similar in any leaf cloud. Therefore, it is likely to decline when several leaf clouds with different height extension are considered in a horizontal layer. The potential error increases when the vertical layer extension decreases. The maximum error resulting from inhomogeneity of leaf clouds for 10cm height layers of the whole crown (considering about 10 leaf clouds) was estimated to be 20%, while that of 1m height layers of the whole crown should be lower than 5%.

2.3 Results

2.3.1 Allometric relationships of the branch system

Allometry in its most restrictive meaning is used to indicate any departure from a condition called geometric similitude, which results when geometry and shape are conservatively expressed among a series of objects differing in size (NIKLAS 1994). Allometric relationships in this sense describe the relationship between the size or growth of parts of an organism and size or growth of other parts of this organism and, therefore, may often be useful for scaling purposes. The objective of this part of the study is to provide species-specific up-scaling relationships to facilitate measurements of 3D-structure and to explore structural differences and common traits of the branch systems of oak and beech that might reflect ecological differences and potentially affect growth and assimilation rates of both species.

2.3.1.1 Branch basal area versus estimated sapwood area

Fagus sylvatica forms a diffuse porous wood with slow heartwood formation over several years, so that large parts of the stem cross section may in principal be water conducting [SCHWEINGRUBER 1978]. *Quercus petraea* on the other hand forms a ring-porous wood with annual heartwood formation, which causes almost all of the large vessels in the 1 year old growth ring to fail as conductive units [SCHWEINGRUBER 1978, CERMAK ET AL. 1992]. Though some of the smaller latewood vessels may be conductive for several years, no water flow was observed deeper than 2cm beneath the cambium in a dye injection experiment on two trunks (8 cm and 30 cm in diameter) of *Quercus robur* (CERMAK ET AL. 1992). Despite the differences in wood-anatomy between the stems of both species, no significant difference was observed in the basal area to sapwood area relationship of oak branches and the basal area to “area of outer rings” relationship of beech branches (Fig. 6). All investigated branches were 5 to 15 years old and smaller than 6cm in diameter. Approximately 90% of the basal area of all branches was included in the outer rings or sapwood and r^2 values higher than 0.99 show that this ratio is strictly conserved in branches of both species up to 6cm in diameter. The ratio between sapwood area and basal area does not decline with increasing branch basal area, indicating that the non-conducting part of the cross section grows in constant relation to the sapwood

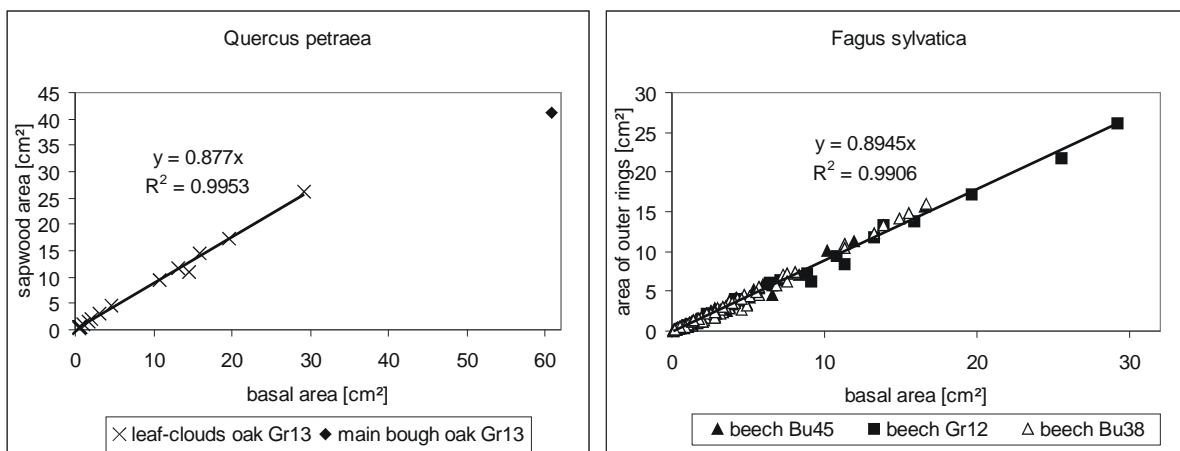


Fig. 6: Allometric relationship between branch basal area and sapwood area of leaf clouds of three beeches and one oak. Separate linear fits for each tree had slopes 0.91, 0.91, 0.87, and 0.88 for the trees Bu38, Bu45, Gr12, and Gr13, respectively. One investigated bough of oak Gr13 did not follow this relationship for leaf cloud supporting branches (left graph).

growth. One broken older bough of oak Gr13 deviated from the highly correlated regression line for smaller branches.

2.3.1.2 Allometric relationships of ramification

Constant relationships were also found between the basal area of wood-elements and the cumulated cross-sectional area of affiliated leaf cloud branches. The relationship between the summed basal area of appending main boughs and the basal area of the stem was 73,5% in oak Gr13, 67,8% in beech Gr12 and 71,9% in beech Bu45.

Main boughs of oak Gr13 differed in their basal area relationship to the leaf cloud supporting branches depending on the light situation of the branches: Those boughs, that did not reach the sun crown with their leaves (shade boughs, see Table 2) had a four- to five-fold greater basal area than their affiliated branches due to their high proportion of dead branches. The affiliated branch basal areas on sun main boughs on the other hand summed to 74% of the sun main boughs basal area (Fig. 7).

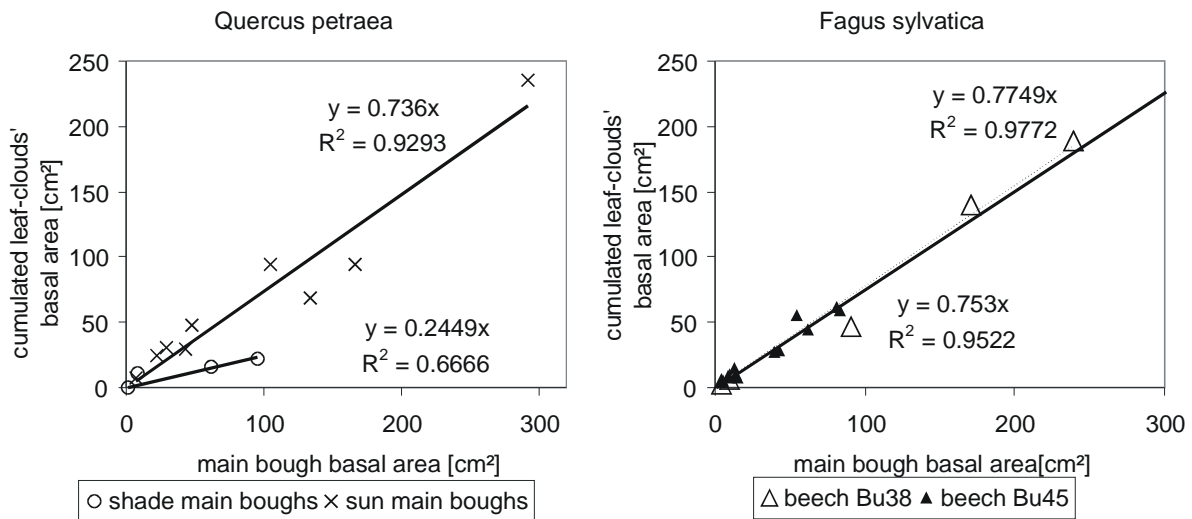


Fig. 7: Basal area relationship between main boughs and their affiliated branches. Shade boughs of oak were considered separately due to their high proportion of dead branches

No difference between sun and shade boughs was found in beech branches, where the basal area ratio between leaf cloud branches to boughs was 75% and 77%, respectively. A reason for the species-specific difference may be seen in different wood structure. Vessels of the shade boughs' xylem that became useless due to a dying branch cannot be reused in *Quercus petraea*, where annual heartwood formation prevents the reuse of vessels, while this is in principal possible through lateral intervessel pits (ZIMMERMANN 1983) in *Fagus sylvatica* boughs. Another reason might be the higher shade tolerance of beech branches (which can be derived from the longer crowns of beech in both mixed stands, see chapter 4 and Fig.19b), leading to a smaller proportion of dead branches in the shade crown of beech than in the shade crown of oak. Unlike the beeches, most oaks in the Großebene and in the Steinkreuz stand had several dead boughs below the living crown; oak Gr13 had four of them.

The classification of sun boughs and shade boughs was established according to their maximum height above the floor (see Table 2). The boughs that reached the upper 1-2m of the crown were classified as sun boughs. These boughs formed a distinct group with nearly the

same maximum height in oak Gr13, while its lower boughs were very different in maximum height. The beech trees showed a more continuous extension of boughs throughout their crown's height range. In the transition zone between the arbitrarily classified sun and shade boughs, higher boughs occurred with extreme south extension while lower boughs were oriented away from the south direction (Table 2). Because south-extended boughs are likely to experience more light than north extended boughs, these boughs were classified as sun boughs, while the lower, north oriented boughs were classified as shade boughs.

Table 2: Shade- and Sun-boughs of the investigated trees

<i>Quercus petraea</i>				<i>Fagus sylvatica</i>											
Gr13			Gr12			Bu38			Bu45						
B o u g h	Min. / Max. height [m]	Max. south [m]	B o u g h	Min. / Max. height [m]	Max. south [m]	B o u g h	Min. / Max. height [m]	Max. south [m]	B o u g h	Min. / Max. height [m]	Max. south [m]				
G	19.16	19.23	0.92	C	14.45	15.08	4.19	H	16.38	17.63	0.69	C	11.92	12.32	0.61
A	18.41	20.89	4.75	B	15.69	16.35	2.66	D	16.32	17.87	-0.15	A	9.66	14.47	3.54
B	18.89	21.77	-0.14	G	17.4	18.86	1.64	i	17.75	18.81	0.52	F	14.96	15.18	0.75
L	21.48	23.14	0.94	F	17.3	18.92	-1.18	F	15.57	19.9	0.95	I	15.46	15.96	1.38
E	17.44	23.57	5.37	A	14.0	18.96	1.45	Z	18.23	20.19	0.1	B	11.05	15.96	3.45
F	20.92	23.64	4.22	O	18.58	19.77	2.11	J	19.17	20.47	1.1	E	14.35	16.08	3.6
M	23.95	24.74	2.24	N	19.47	20.11	-1.16	C	15.15	21.48	0.07	G	15.47	16.98	1.28
C	16.92	24.75	0.22	Q	20.69	21.12	-1.38	B	14.39	21.82	9.84	N	17.34	17.94	1.72
D	16.92	24.78	3.12	M	20.7	21.31	1.04	A	13.2	22.26	4.63	O	17.92	18.73	2.49
H	20.85	24.90	3.87	L	19.22	21.43	3.35	L	19.49	22.55	1.7	P	18.19	18.84	2.13
N	23.04	25.00	0.89	D	16.74	22.04	1.94	E	15.66	22.57	2.01	Q	18.5	19.03	1.91
K	23.64	25.30	0.98	K	21.14	22.95	1.03	K	18.34	22.59	1.83	M	17.03	19.06	2.07
I	21.91	25.58	2.65	E	15.9	23.22	4.05					J	16.03	19.44	2.26
				i	17.97	23.38	3.59					L	16.34	19.66	1.57
				H	18.45	23.83	1.45					H	16.27	20.41	3.12
				R	21.92	24.08	-2.27					D	13.79	20.59	4.97
				T	22.73	24.68	-0.4								
				U	23.16	24.78	-0.56								
				P	20.89	25.08	2.91								
				V	23.09	25.09	0.91								
				S	21.9	25.5	-0.41								

Table 2: Classification of boughs as shade boughs (dark coloured cells) and sun boughs (light grey coloured cells) according to the extension of their leaf biomass in height and toward the south. Boughs in the table are sorted by maximum height extension of the appending leaf-biomass. Height ranks (x = line numbers of the table) and maximum height extensions (y, in meters) are visualised in the graphs below. The vertical lines in the graphs indicate the border between the two classes and were drawn arbitrarily, considering the steep light gradient in the upper crown and between south and north side of the crown, which is especially valid for the Buchenallee trees that are standing on a slope. The differentiation between the lowest sun bough and the highest shade bough was often facilitated by the higher maximum south extension of the lowest sun bough (see pairs of white cells in the table).

The relationship between basal area of leaf cloud supporting branches and the cumulated area of the affiliated leaf cloud branches that support the second 1m-segment of the leaf cloud was analysed based on data of the Großebene trees. Here branches with a high proportion of dead wood were excluded. The basal area reduction per meter was 84% in leaf clouds of oak Gr13 and 81% in leaf clouds of beech Gr12 (Fig. 8).

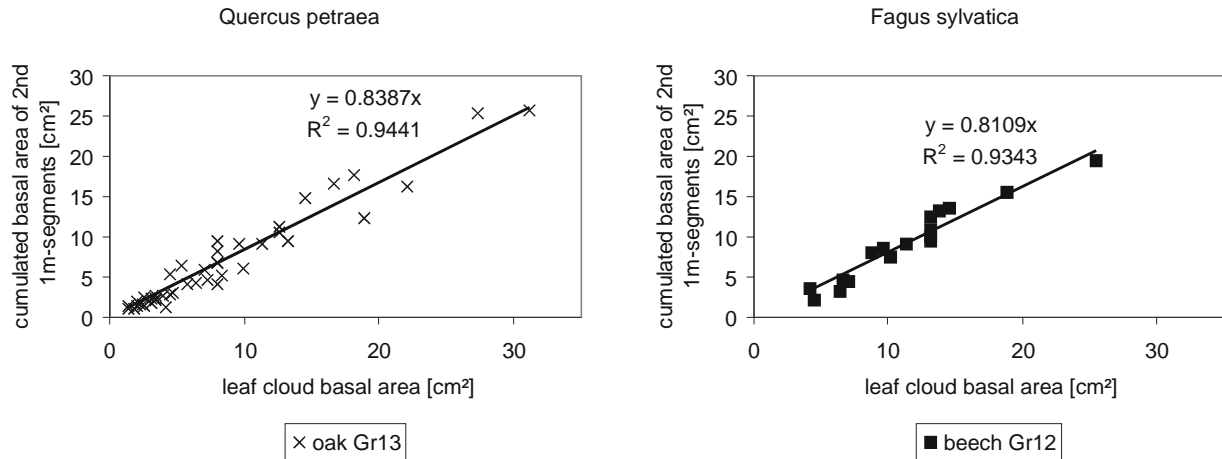


Fig. 8: Basal area relationship between leaf cloud supporting branches and the connected branches in the second 1m-segment of the leaf cloud

2.3.1.3 Allometric relationships between basal area and leaf area or leaf weight

The pipe-model theory (SHINOZAKI 1964) first advanced the principle that sapwood area in trees is related proportionally to foliage biomass (MÄKELÄ 1986). The theory reasons that each unit of foliage requires a unit pipeline of wood to conduct water from the roots and to provide physical support. As leaf area is a quantity that is interesting in terms of light interception and gas-exchange, the correlations presented here utilise leaf dry weight and one-sided leaf area as key variables. Though in the past, pipe-model relations have usually expressed biomass in relation to sapwood area, which yields strong linear correlations to leaf area and leaf weight of several species (GRIER & WARING 1974, KAUFMANN & TROENDLE 1981, ROGERS & HINCKLEY 1979, WARING ET AL. 1977) the current investigations are - like some newer publications (BARTELINK 1997, SUMIDA & KOMIYAMA 1997) - based on basal area of branches, boughs and stems, because sapwood area is difficult to measure non-destructively and, therefore, not suitable as an input-parameter for up-scaling and modelling purposes.

In leaf clouds of oak Gr13, basal area of the branch and appending *leaf biomass* was better correlated than basal area and *leaf area* (Fig. 9). The same was found for beech, when all beech observations were pooled: The leaf biomass / basal area ratio was 27.3 with an r^2 of 0.93, while the leaf area / basal area ratio over all beeches (0.364) had a lower r^2 of 0.89. The opposite was true if the beeches are analysed separately (see Fig. 9). The individual differences between the beech trees may partly be explained by lower leaf biomass and area of the subdominant and infected tree Bu45. In general, the concept of constant ratios between leaf area or biomass and basal area of the respective branch was better supported for beech leaf clouds than for those of oak Gr13.

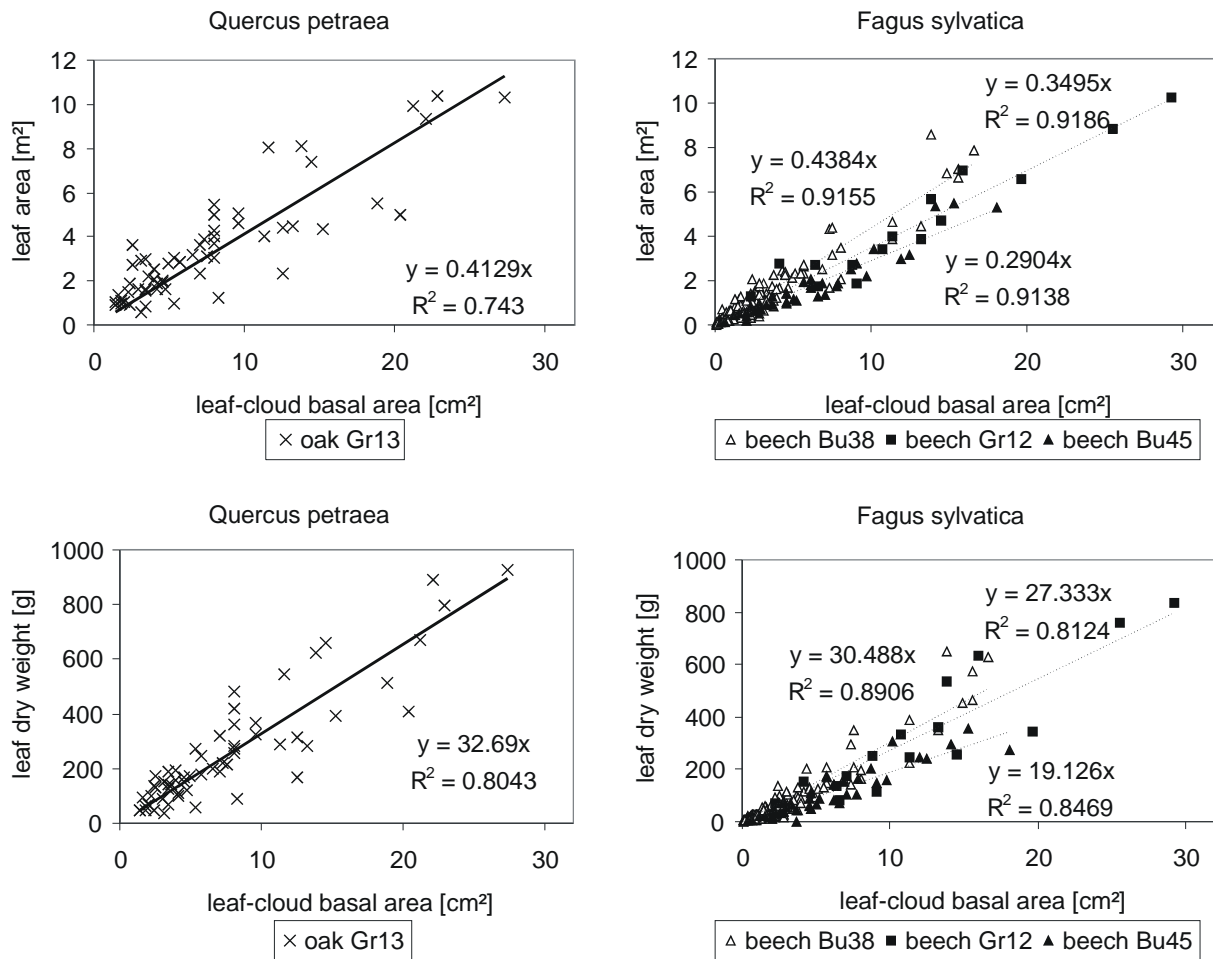


Fig. 9: Allometric relationships between leaf area or leaf biomass and basal area of the associated branch.

The same relationships on the level of trunk connected main boughs are illustrated in Fig. 10: Very high correlations were found for the ratio of leaf area or leaf biomass to basal area of sun-boughs of oak Gr13, while shade-boughs have lower leaf area and mass. A similar tendency was found in beeches, where the subdominant (shade-) tree Bu45 has less leaves per basal area than the dominant one (Bu38) of the two fully harvested beeches. Again, correlations for beech are higher when considered on a single tree basis. The ratios for the pooled data of beeches are 0.319 for leaf area and 0.0196 for leaf biomass and both have rather high coefficients of determination ($r^2 = 0.896$ and 0.904 , respectively). Coefficients of determination on the spatial level of boughs were, thus, higher than on the level of leaf clouds.

Ratios of leaf area to total basal area of boughs are compared to estimates of leaf area per trunk basal area in Fig. 11 to investigate, if this relationship may be extrapolated: Only the stem basal area of the subdominant beech tree Bu45 is compatible with a linear extrapolation from boughs to the stem. The stems of oak Gr13 and beech Bu38 support less leaf area, leaf biomass, and bough basal area per trunk basal area.

An overview of the different leaf area / basal area ratios for leaf cloud branches, boughs and stems indicates that the slope of all these linear regression lines decreases with increasing basal area of the woody element for all trees (see Table 3). Thus, an allometric relationship for all kind of wood from an individual tree becomes non-linear, although linear regression lines with high r^2 values may be determined on distinct levels of organisation.

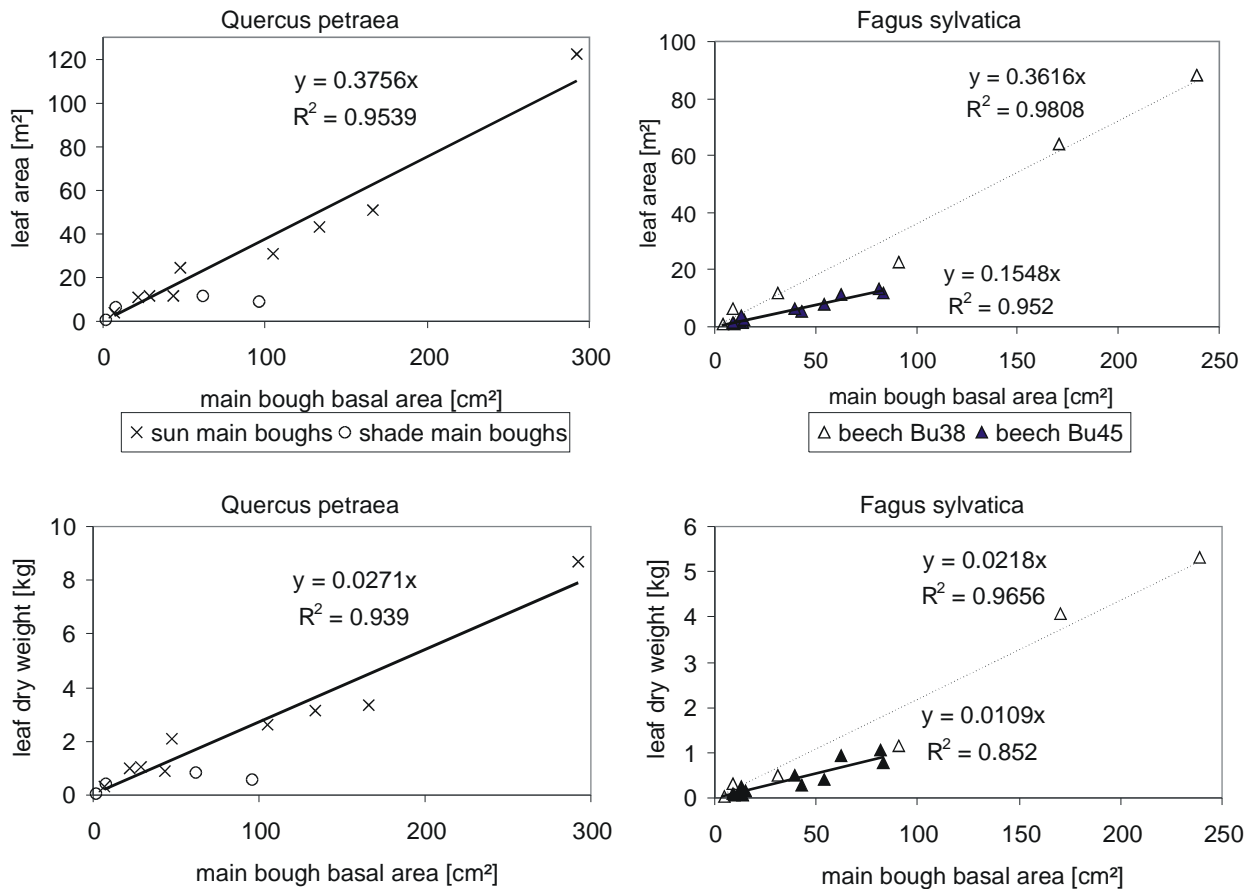


Fig. 10: Allometric relationship between leaf area or biomass and basal area of the associated bough

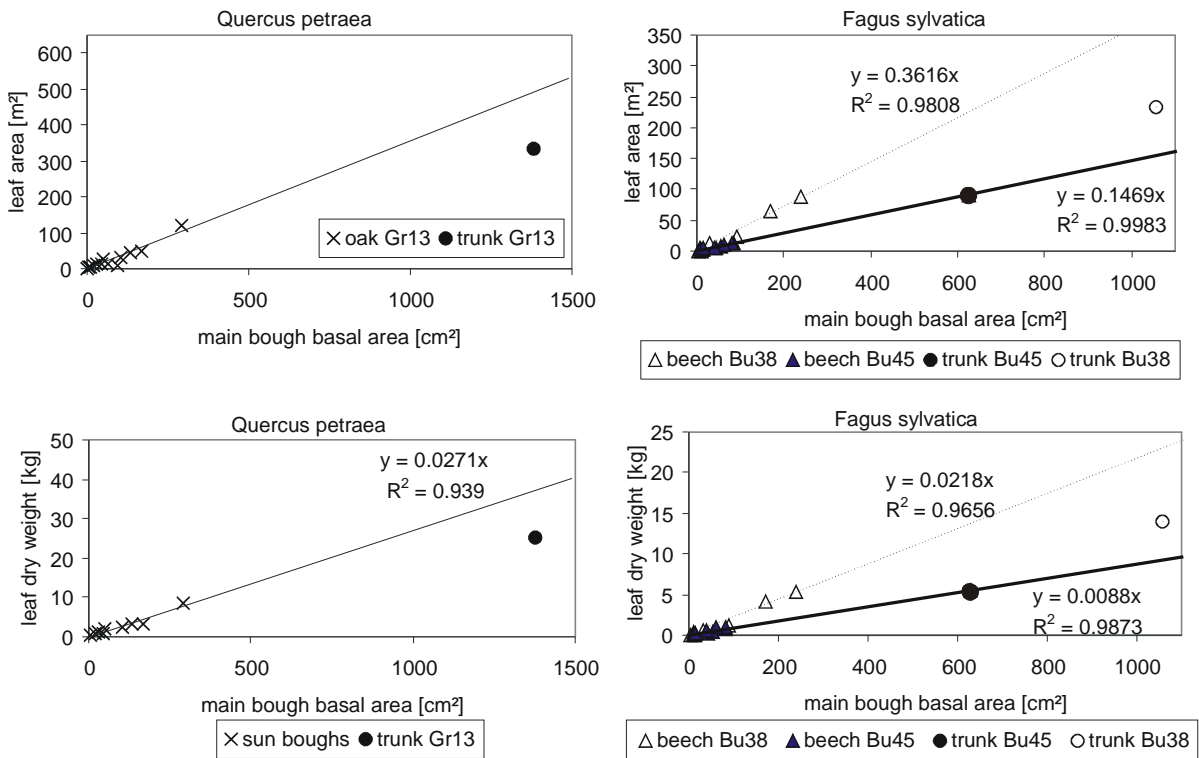


Fig. 11: Comparison of allometric relationships on the bough level with those of the trunk level. The correlation for beech Bu45 includes the trunk data

Table 3: Leaf vs. woody element ratios on different spatial levels

Allometric relationship	Oak Gr13		Beech Bu38		Beech Bu45	
	Leaf area (m ²) basal area (cm ²)	Leaf biomass (g) basal area (cm ²)	Leaf area (m ²) basal area (cm ²)	Leaf biomass (g) basal area (cm ²)	Leaf area (m ²) basal area (cm ²)	Leaf biomass (g) basal area (cm ²)
Leaf clouds	0,4129	32,69	0,4384	30,49	0,2904	19,13
Boughs	0,3756	27,1	0,3616	21,8	0,1548	10,9
Stem	0,2433	18,1	0,2216	13,3	0,1464	8,7

The transition from approximate linear to non-linear behaviour can be described with a power function, which increases the overall coefficients of determination. A linear regression line or model is only a special case of a power function (power function with exponent 1). Indeed r^2 -values increased to more than 0.99 when using a power function for the regression. All resulting fits have exponents lower than 1, which indicates the slight decline of the ratio between leaf area or mass and basal area of woody elements with increase in basal area as more stand structural complexity is included. (Fig. 12).

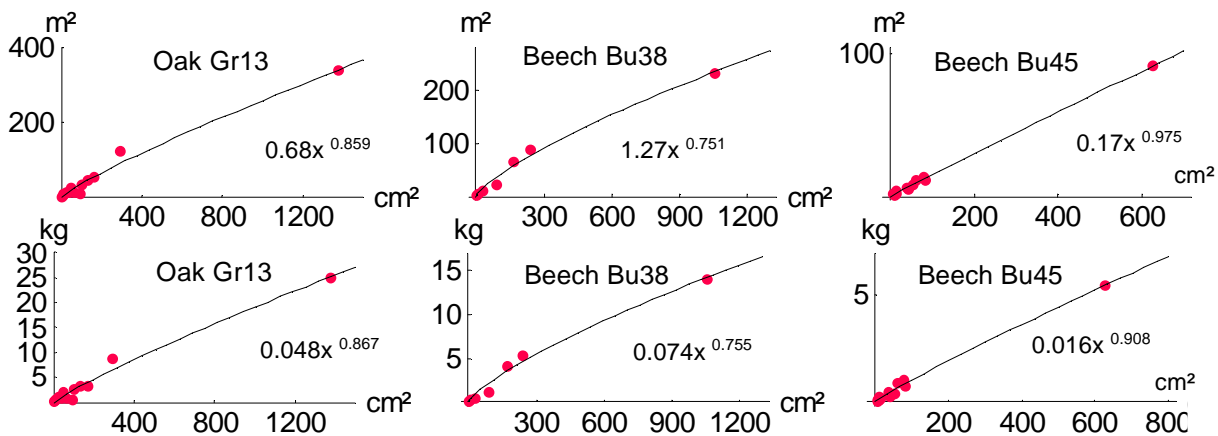


Fig. 12: Power function approximation of the area- and mass-based allometric relationship between basal area (cm²) and leaf area (m²) or leaf dry weight [kg] of boughs and stems of the three fully harvested trees.

When estimating parameters for the power function regressions it was found that trendlines produced by Microsoft Excel are based on the logarithmic transformed data of both variables (log-log-transformation), which is justified only for the special case that the log-log-transformed data show a better agreement with the normal distribution than the original data, because in this case the potential effect of lacking data would be considered. Because the agreement with the normal distribution was not tested separately in each case, only approximations to the original data were done using the programming and calculation software Mathematica (Wolfram Research, Champaign, Illinois). These approximations generally yield the best fit to the available data (compare Fig. 13).

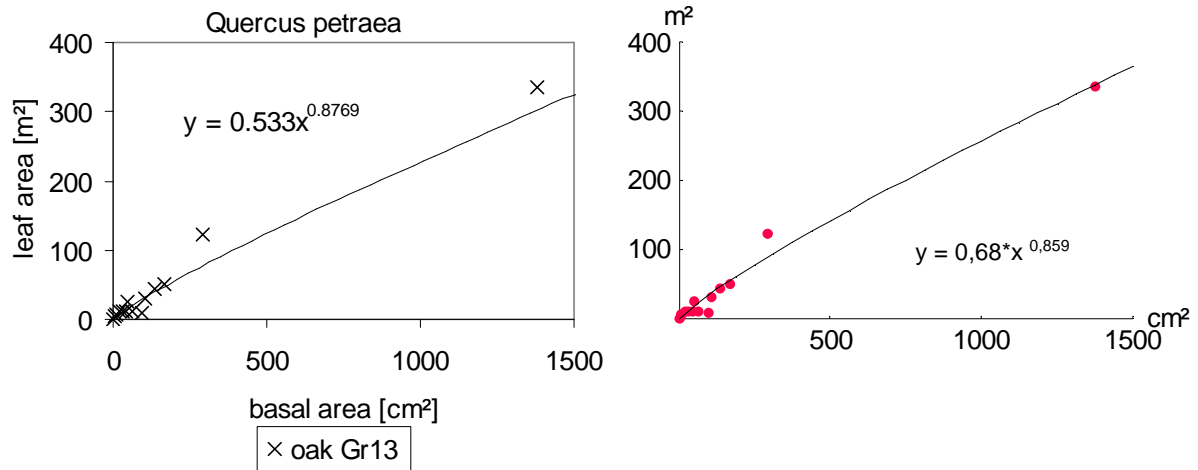


Fig. 13: Comparison of power function trendline (Excel) and power function approximation (Mathematica) on the same data set. The sum of squared errors (χ^2) was 3749,8 for the trendline and 2020.98 for the approximation.

A comparison was made between the allometric relationships of 2 beech species, 5 oak species and 5 additional broad-leaved tree species to examine, whether the decrease in ratios of leaf area to total basal area with increasing basal area of the stems may be systematically and generally described with a power function, and most data for this study were taken from literature. The investigated tree species are *Fagus crenata* (KAKUBARI & MARUYAMA, UNPUBLISHED), *Fagus sylvatica* (BARTELINK 1997, PELLINEN 1986, LEBAUPE ET AL. 2000 AND THE OWN MEASUREMENTS), *Quercus* spp. (including *Quercus petraea* and *Quercus robur*, BURGER 1947 AND THE OWN DATA), *Quercus alba* (MARTIN ET AL. 1998, ROGERS & HINCKLEY 1979), *Quercus coccinea*, *Quercus prinus*, and *Quercus rubra*, *Acer rubrum*, *Betula lenta*, *Carya* spp. (including *Carya glabra*, *Carya ovata* and *Carya tomentosa*), *Liriodendron tulipifera* and *Oxydendrum arboreum* (MARTIN ET AL. 1998).

The decrease in stem basal area to leaf area ratio at the level of main trunks was found in 11 of the 12 tree species, only the data set for *Betula lenta* showed a slight increase in this relationship, which seems to be an artefact due to one data point that represents the largest harvested *Betula lenta* tree (see Fig. 14). The power function approximation to all available tree data was $0,463 * x^{0,903}$.

2.3.2 Discussion of allometric relationships of the branch system

The inter-individually constant and inter-specifically similar relationship between basal area and sapwood area or area of outer rings of branches (Fig. 6) strengthens the hypothesis, that both relationships describe the same phenomenon. On the one hand, this constancy suggests that the distinguished central part of the cross-section of branches grows in constant relationship to the whole branch cross-section, which in turn indicates physiological changes in the central part of branches with increasing diameter, though heartwood formation has been shown not to take place in branches of several different species (SCHWEINGRUBER 1978).

On the other hand, it shows that the allometric relationship between basal area and leaf area at the level of leaf cloud supporting branches of both species is not influenced by alterations of sapwood area, because a constant ratio between basal area and sapwood area exists at this hierarchical level, but not on the level of boughs or trunks (Fig. 6, NAIR 1995).

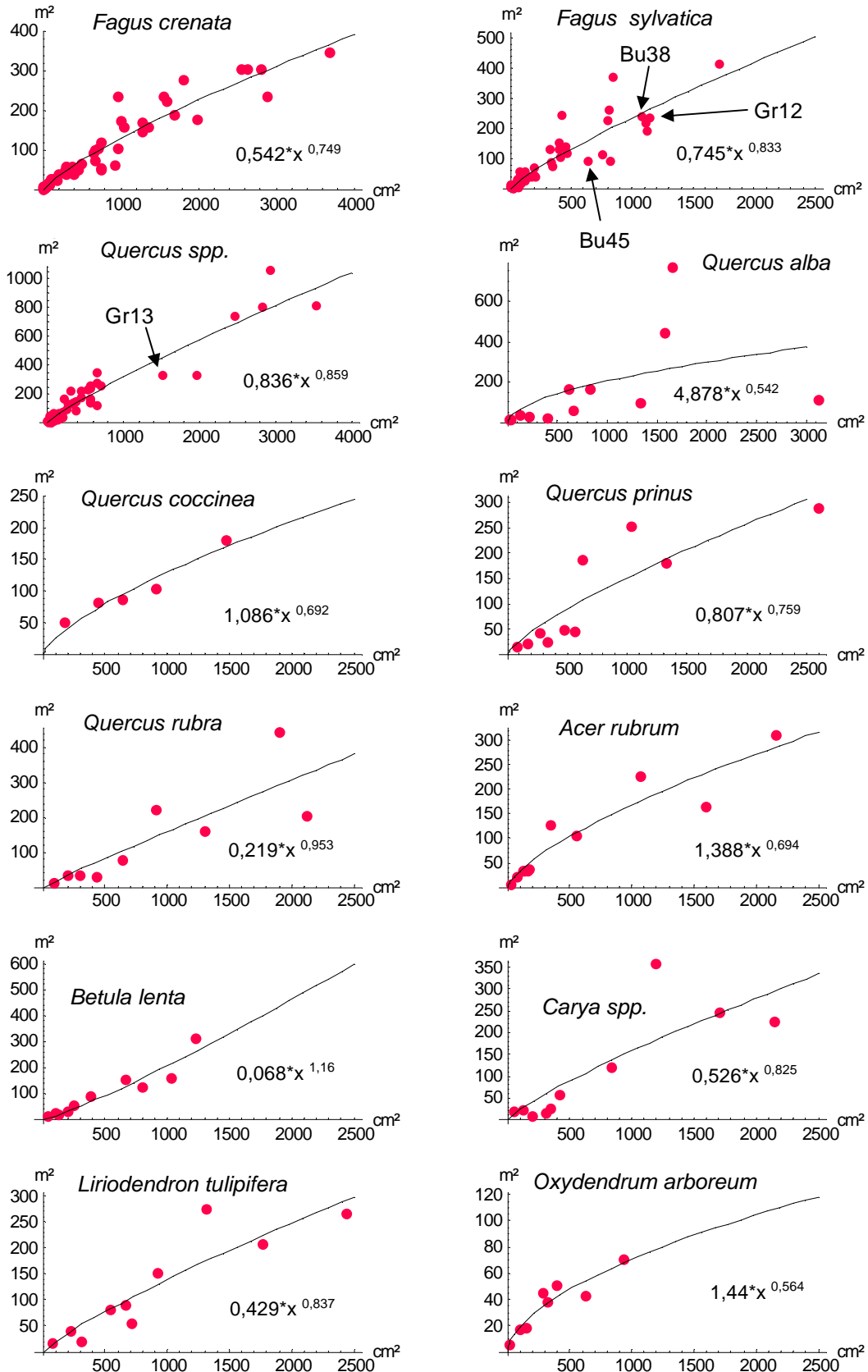


Fig. 14: Decrease of ratio between leaf area and basal area of 11 of 12 investigated tree species with increasing basal area. *Quercus petraea* and *Quercus robur* are not distinguished (“*Quercus spp.*”) and *Carya spp.* stands for *Carya glabra*, *Carya ovata* and *Carya tomentosa*.

The leaf area vs. basal area relationship is very robust (Fig. 9) and, thus, well suitable for up-scaling of leaf area along branch diameters of a crown. This could reduce the necessary work in biomass harvests to 10-20% of the leaf clouds, as is shown for beech Gr12. Nevertheless, the established relationship for oak shows considerable variation that can not solely be explained by measurement errors. The inter-individual differences between beeches and the scatter between leaf clouds may relate to variation in the regulation of processes affecting wood formation and differing demands placed on hydraulic conductivity according to the orientation, size and position of the leaf cloud on individual branches (MATTHECK 1995, PROTZ ET AL. 2000, MAHERALI ET AL. 1997). The leaf area / basal area ratio of boughs may also be useful for up-scaling, but here differences between sun- and shade-boughs of oak occur, and the inter-individual differences between beeches were larger than those observed at the branch level.

The azimuth direction of growth of main boughs from the stem was important for structure formation in the crown, at least in the case of oak. Also in beech trees Bu38 and Gr12, several main boughs reach the upper 1-2m of the crown, while one or two lower boughs exhibited an extreme extension to the south. This could be interpreted as light driven competition between boughs and gives a hint to the asymmetrical distribution of favourable conditions in the tree crown. The much lower number of living shade boughs in the oak crown and the phenomenon of several dead boughs below the living crown of oaks contrasts to the high number of living shade boughs in the three beech crowns. This indicates – together with the low leaf area / basal area ratio of shade boughs of oak - the higher shade tolerance of beech branches.

Species-specific differences in heartwood formation occur at the stem and bough level, but not at the level of leaf cloud supporting branches. Nevertheless, allometric relationships of ramification were remarkably similar at all three spatial levels for oak Gr13 and for beech trees (Fig. 7 and Fig. 8), which may be due to the common requirements in crowns of this size for structural stability.

The ratio between supported leaf area and basal area of stems declines in most species with increasing basal area. This trend is also found in the investigated oak and beech trees, considering the integration from branches to boughs and to main stems. Exponents lower than 1 for a power function relationship were also found in power function approximations for stem-connected boughs of *Quercus mongolica*, *Acer sieboldianum*, *Magnolia obovata*, *Betula platyphylla* and *Betula maximowicziana* (SUMIDA & KOMIYAMA 1997). Similar relationships at different spatial levels may indicate a common reason for the decline. While the leaf area / basal area ratio was linear and inter-individually constant at the level of branches (Fig. 9), differences between sun and shade boughs of oak and between the subdominant, infected tree and the dominant beech tree in the same stand occurred at the level of boughs (Fig. 10). These differences may be explained by cavitation due to dying of appertaining branches of the shade main boughs of oak. Cavitation may also be the reason for the generally lower leaf area / basal area ratio of the wholly infected beech Bu45.

The linearity of all investigated leaf area vs. basal area relationships on the bough and branch level apart from that for the shade boughs of oak strengthens this explanation. Cavitation is expected to have less impact on the leaf area / basal area ratio of young branches, because of the relatively short time of their exposition to stress situations. A linear relation in the leaf area / basal area ratio can also result, if cavitation affects all boughs or branches with the same probability due to their similar age, similar conditions in the same tree crown, or similar vitality (same exposure regarding infection as in Bu45). The age of trees, boughs, and branches may,

thus, explain the general decline of leaf area / basal area ratios across spatial scales. Different species-specific mechanisms to avoid cavitation under their different living conditions may be responsible for the high numerical differences in the investigated leaf area / basal area ratio between species, which may especially be seen between the biggest and therefore oldest trees (for example of *Fagus crenata* and *Quercus spp.* in Fig. 14 and Fig. 15).

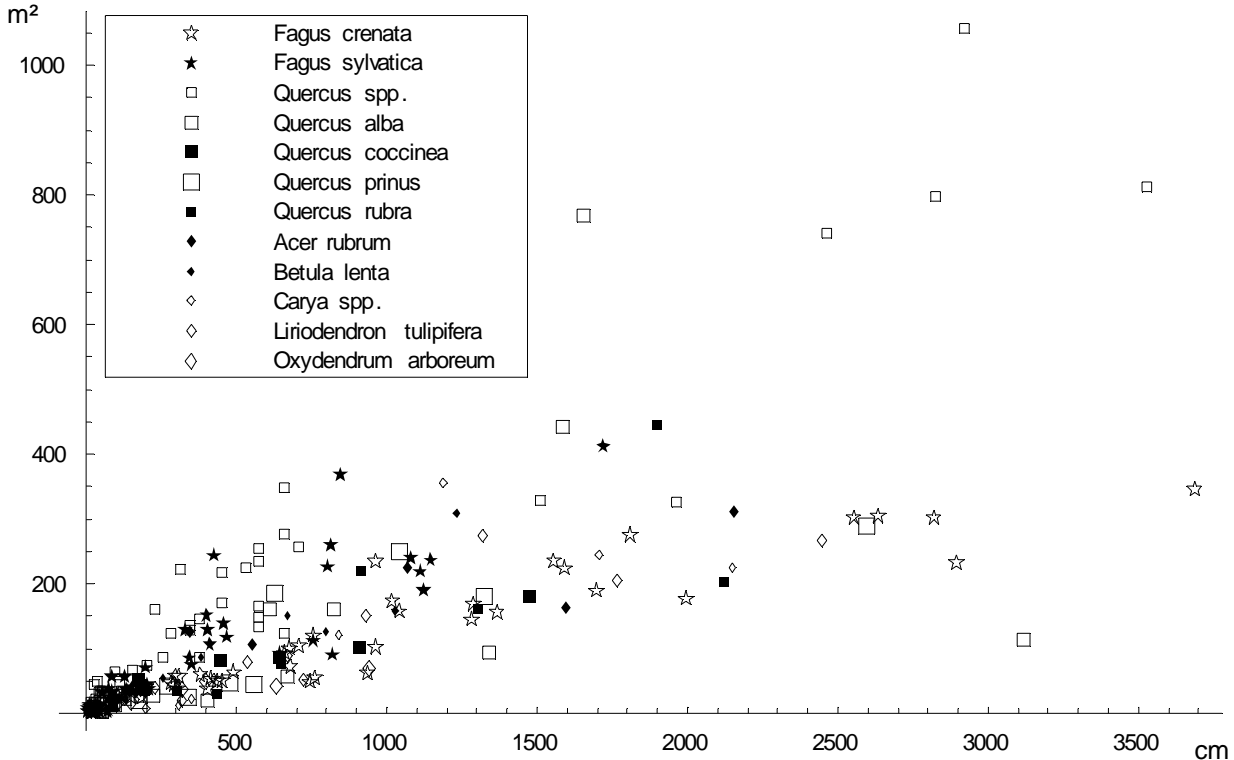


Fig. 15: Inter-specific variation of the ratio between basal area and leaf area of 261 trees of different species.

2.3.3 Leaf arrangement in whole tree crowns

2.3.3.1 3D-representation of leaf clumping

The arrangement of leaves in the canopy has a major influence on light climate in the tree crown and the light-dependent function of all assimilating tissues. In most tree species, leaf distribution is clumped along leaf cloud supporting branches, though there may also be some single leaves close to the stem or to a main bough that are far away from other leaves, and therefore, not part of a leaf cloud (as was found in the investigated *Quercus petraea* crown). A full description of the three-dimensional arrangement of leaf clouds in the crown was achieved for beech Bu38 (139 leaf clouds) and for oak Gr13 (88 leaf clouds) via direct measurement of the whole leaf biomass, while the leaf biomass of leaf clouds of beech Gr12 (66 leaf clouds) was calculated using the relationship found on a sub-sample of its branches (see Fig. 9). The results are shown below in 3-D-illustrations. The data listing the exact co-ordinates of all leaf cloud enveloping polyhedrons are long-term stored and available via the BITÖK sample collection.

3-D-graphs in the following are constructed with the software Mathematica (Wolfram research, Champaign, Illinois) using a light reflection model [Phong 1975] that simulates the reflectance of surfaces considering their orientation to light sources, thereby distinguishing between specular (low scatter-) and diffuse (high scatter-) light reflection. The resulting 3-D-effect can only be

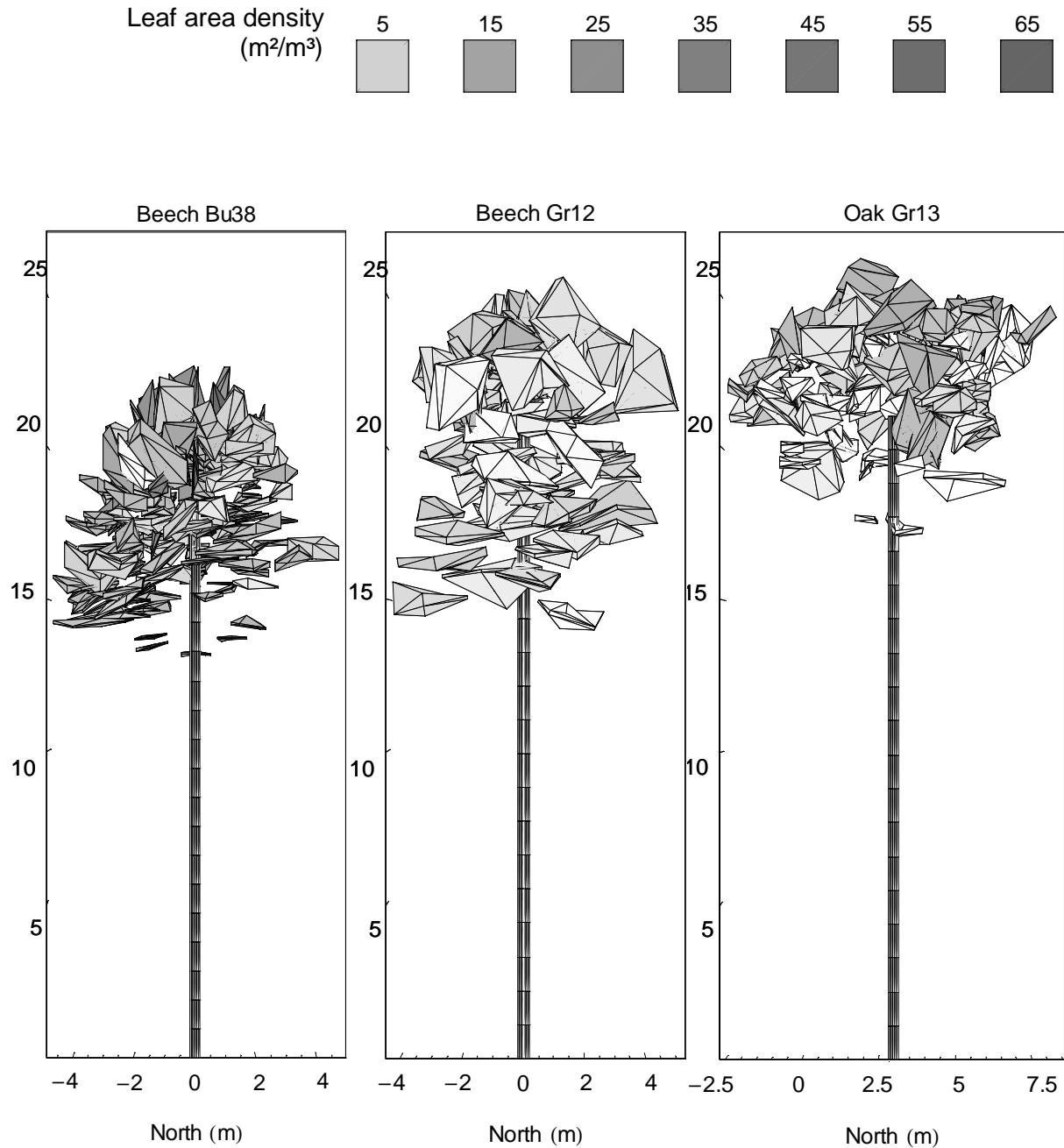


Fig. 16: 3-dimensional maps of tree crown structures and leaf area densities of leaf cloud enveloping polyhedrons in the canopies of beech Bu38, beech Gr12 and oak Gr13. Though beech Bu38 is smaller than the “Großebene”-trees, it is a dominant tree in its stand “Buchenallee” (see also Fig. 3). The y-axis of the graphs represents height above the floor (m). The origin of the co-ordinate system for oak Gr13 is the same as for beech Gr12, so that the stem base point of oak Gr13 is $(-4,79 \mid 2,96 \mid 0,14)$ [East/North/Height], while the other stem base points are situated in the origin. This and the legend are also valid for Figure 19 a and b, where horizontal sections of the polyhedrons of 1m thickness can be viewed from above. This and all following tree crown figures rely on the 3-D-representation model CRISTO (see chapter 4) that was built using the Mathematica programming language.

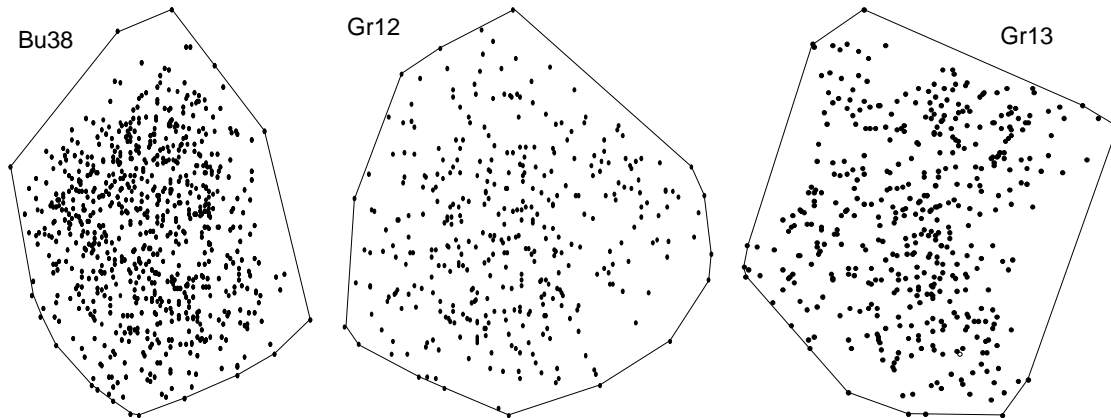


Fig. 17: Crown projected areas of individual trees using the convex hull of projected points. While the beech crown projections (Bu38, Gr12) were in fact largely convex, oak Gr13 actually had an asterisk-like projected crown shape with three large indentations (compare Fig. 18).

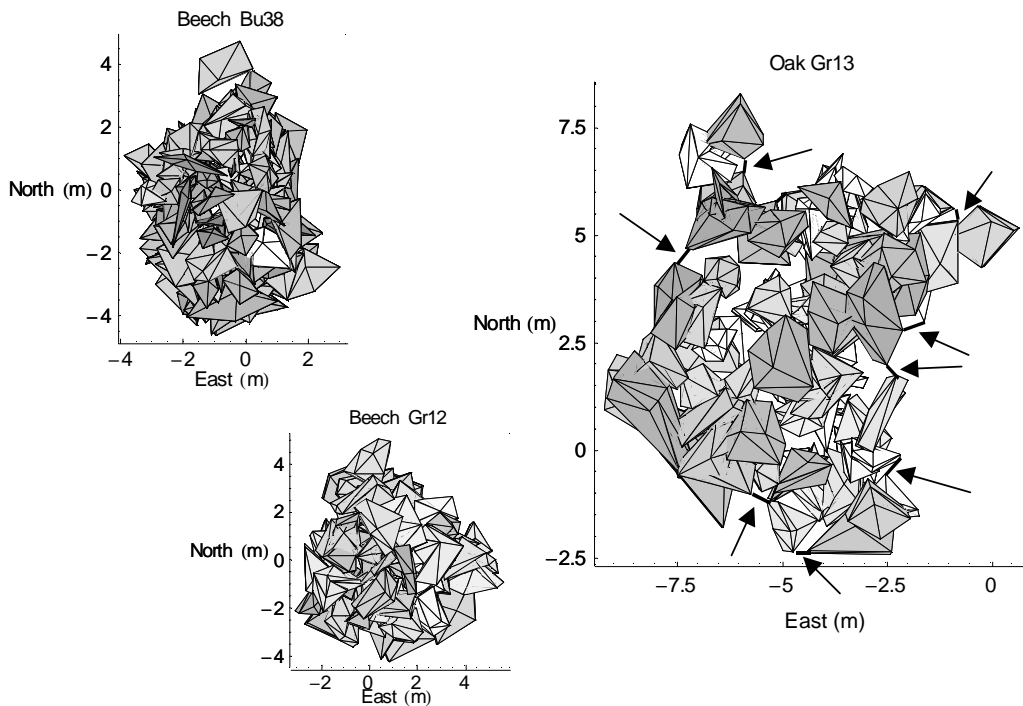


Fig. 18: Vertical view of the 3-D-representation of oak Gr13 and beeches Gr12 and Bu38. The shape was cut along the outermost line, which was completed in the case of oak Gr13 at the position of narrow but partly deep cavities by straight lines (see arrows).

achieved when reflectance dependent deviations from the original polyhedron surface colour are accepted. This side-effect has been kept to a minimum by simulating light conditions with more than one light source (usually 3) and diffuse reflection coefficients for the polyhedron surfaces, so that only very small, nearly invisible deviations from the original colour occur,

thereby enabling the 3-D-graphs to represent relative differences between leaf clouds in a tree by gradual changes in colour.

2.3.3.2 Tree Leaf Area Indices

Absolute leaf area of the three trees was 240.7m² (Bu38), 236.6m² (Gr12), and 328.3m² (Gr13). A tree specific leaf area index (TLAI) based on the measured data was defined as leaf area of the tree per projected area of its crown, thereby using the convex hull area of a horizontal projection of all measured co-ordinates within each tree as projected crown area (Fig. 17). The convex hull area of the projected points was 42,8m², 52,4m², and 69.4 m² respectively, resulting in a TLAI of 5.6, 4.5, and 4.7. The convex hull area is an easily determined measure for the projected crown area, which cannot lead to an underestimation of the projected crown area, because it represents the outermost line that can be drawn on a given group of points. In fact, this leads to an overestimation of the projected area, especially of concave crown shapes, as can be recognised by optical control of the convex hull data (Fig. 17). While the beech projections were largely convex, the projected crown of oak Gr13 had an asterisk-like shape with three large indentations, which cannot be accurately represented by the convex hull. As an alternative measure for crown projection area, the shape of a vertical view of the 3-D-representation of the tree crowns was cut from a print-out with a pair of scissors (Fig. 18) and its area was measured with the DIAS area meter (see methods). This area was related to the area of the printed co-ordinate system, which describes a rectangle of known area in the stand, and the corrected projected area of the three crowns was calculated as 36.0m², 47.5m², and 54.8m² respectively, resulting in corrected TLAI-values of 6.7, 5.0, and 6.0. Thus, the correction reduced the projected areas by 15.9%, 9.4% and 21%, respectively.

The subdominant beech Bu45 had a leaf area of 93.2 m² and an uncorrected projected crown area of 22.0m² (TLAI = 4.2).

2.3.3.3 Arrangement of leaf clouds

The arrangement of leaf clouds with different leaf area densities in different regions of the tree crowns is shown in Figures 19 a and b and 20. The optical 3-D-representation of the trees provides an opportunity to explore structural characteristics of these specific tree crowns, which may serve as an example of beech and oak canopy structure. Beech leaf clouds were very often adjacent to their horizontal neighbours equidistant to the stem, thus forming closed or open horizontal rings around a leafless central space, which is visible in Fig. 19a (beech Bu38, 2-6m below apex and beech Gr12, 3-6m below apex). The central leafless space is also visible in Fig. 20 (Bu 38 and Gr12, behind the stem). Adjacency in beech leaf clouds was more seldom in the vertical dimension than in the horizontal dimension (see Fig. 20). Fig. 20 also shows that the upper beech leaf clouds formed a more or less dense cupola or roof above the leafless space. Lower leaf clouds were partly grouped to layers, which were separated by coherent cavities from other leaf clouds (especially beech Bu38). The leaf layers of beech Bu38 were oriented parallel to the slope of the ground (Fig. 20, Bu38, in front of the stem). Considerable foliage of beech was found up to 10-11m (Bu38) below the apex of the crowns.

Oak leaf clouds were spread more irregularly, with gaps of similar size in horizontal and in vertical dimensions. The upper leaf clouds (Fig. 19a, 2-3m below apex) formed a roof which was less dense than that of the beeches. The layer below this roof had larger cavities in the central

part than in other layers, which can be seen in Fig. 19a and Fig. 20 (oak Gr13, behind the stem). Considerable amounts of oak leaves were in the range of 0 - 7m below apex.

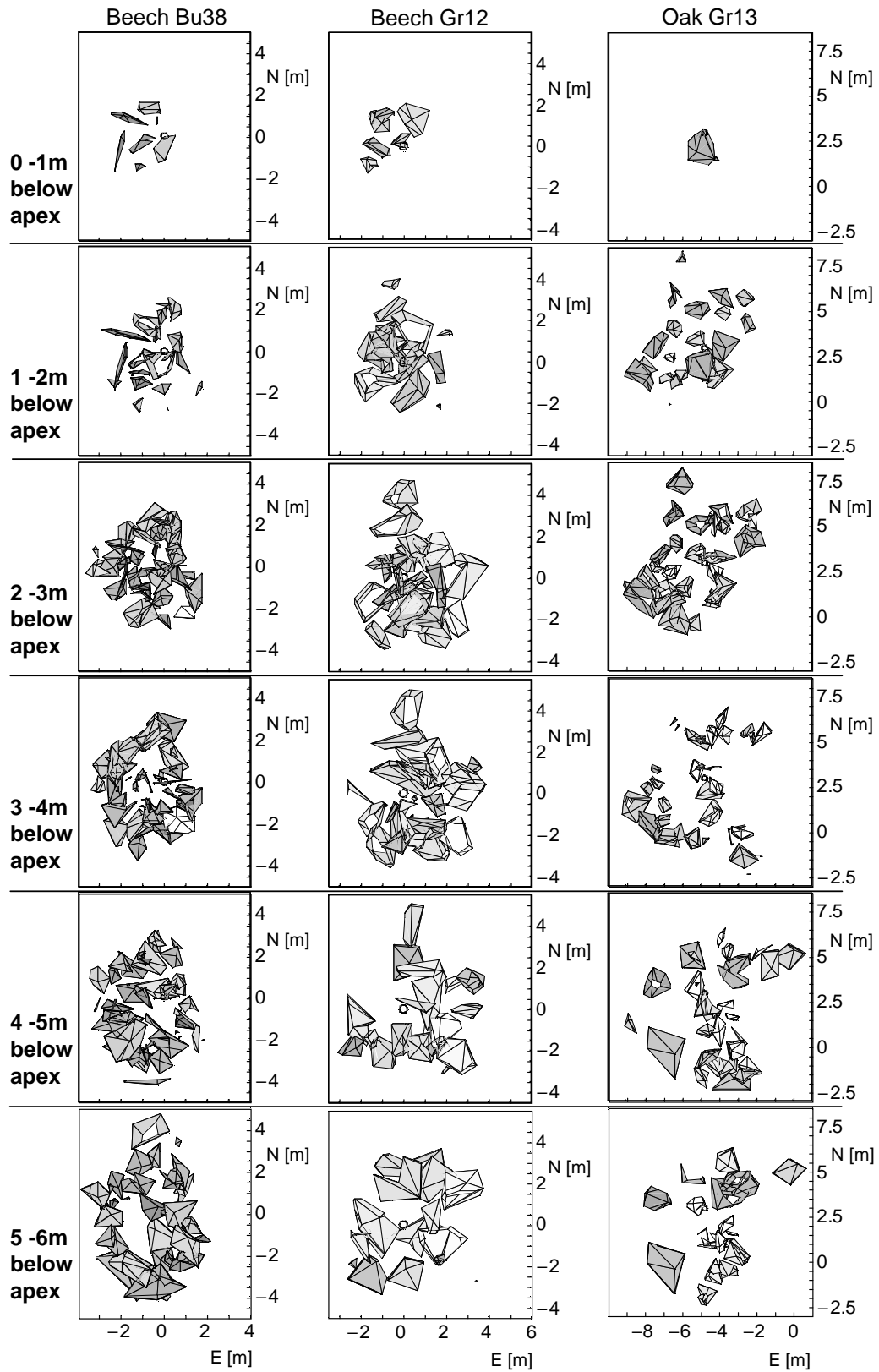


Fig. 19a: Leaf area densities in horizontal layers of canopies (E = east, N = north; see caption of Fig. 16)

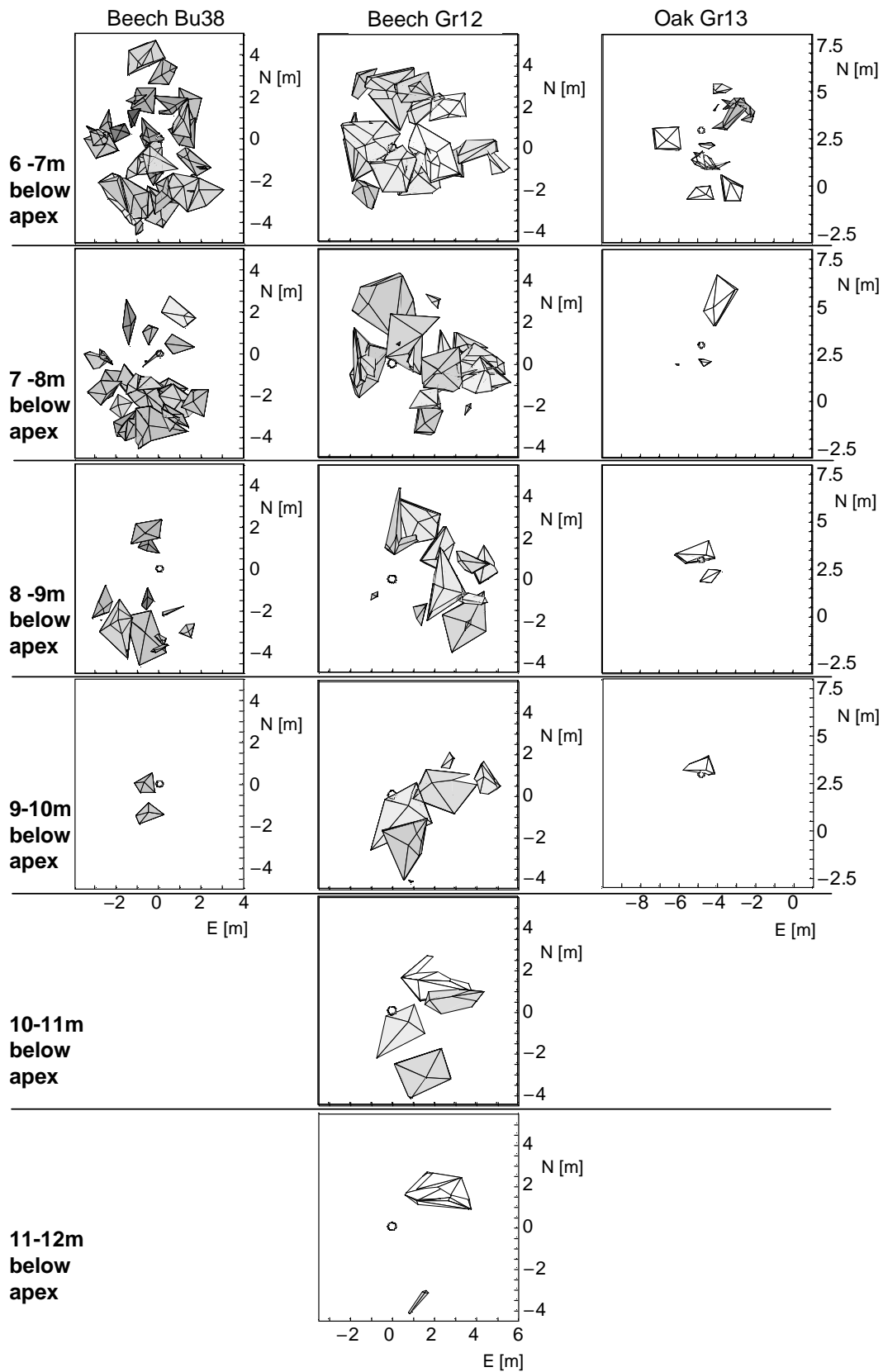


Fig. 19b: Leaf area densities in horizontal layers of canopies (E = east, N = north; see caption for Fig. 16)

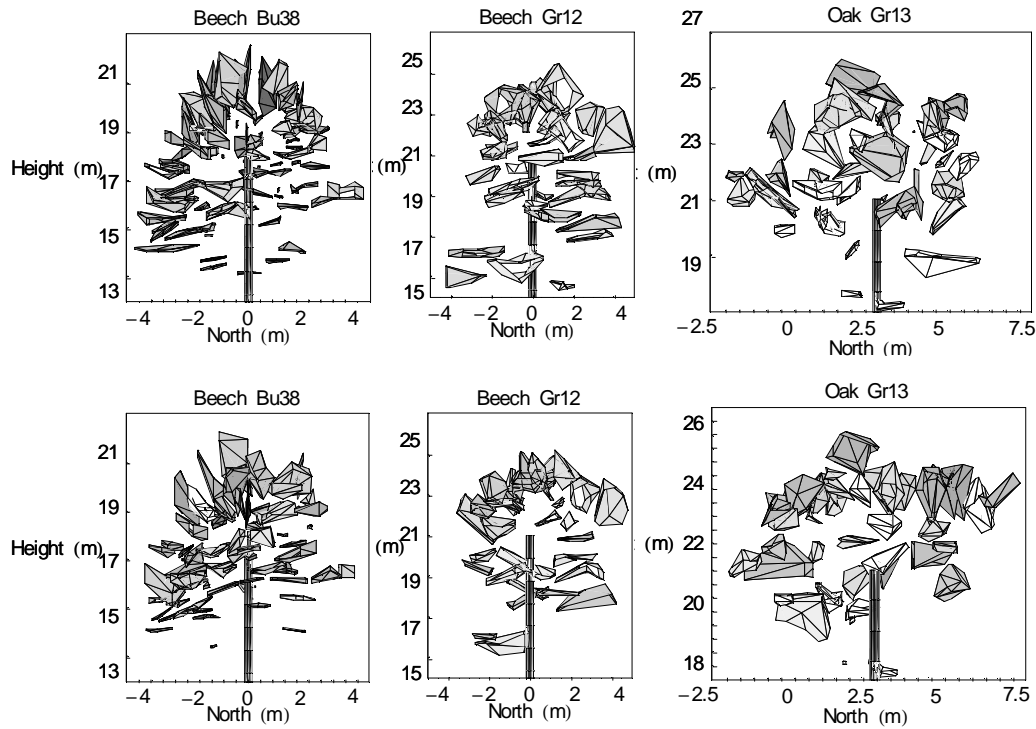


Fig. 20: View of leaf area densities and arrangement of leaf clouds from the east. The upper row shows the 1m thick vertical slice in front of the stem of each tree and the lower row the vertical slice up to 1m behind the stem. Height (m) is the y-co-ordinate of all 6 graphs.

2.3.4 Layer oriented description of leaf distribution in the crown

2.3.4.1 Leaf area of height layers

While leaf area densities of leaf clouds did not show a clear dependence on height (see 2.3.5.6), it is known from tree harvests that the amount of leaf area of oak and beech trees is generally higher in the upper parts of the crown and decreases from there towards the crown base (compare KAKUBARI 1987, LEUSCHNER 1994). The leaf cloud oriented description of the trees (see chapter 4) was used to check this relationship for the investigation trees with a high level of resolution. Assuming that leaf area of a leaf cloud is equally distributed over the height range of the cloud (height range homogeneity), leaf area of 1 dm layers ($LA_{L, dm}$) with constant horizontal extension was calculated as

$$LA_{L, dm} = \sum_{i=1}^n \frac{LA_{C_i}}{H_{C_{a_i}} - H_{C_{b_i}}} (H_{L_{a_i}} - H_{L_{b_i}}) \quad , \quad (1)$$

where LA_C denotes cloud leaf area, H_{C_a} and H_{C_b} are the height limits above and below the leaf cloud, H_{L_a} and H_{L_b} are the height limits above and below the height layer and n is the number of leaf clouds in that height layer. The underlying assumption of height range homogeneity of leaf clouds was chosen instead of volumetric homogeneity because of the different resolution of

leaf cloud geodetic measurements in Buchenallee and Großebene trees and the potential impact of species-specific differences in leaf cloud form on volume calculations.

Contrary to expectation the leaf area vs. height relationship had a non-monotone course in all cases, showing two or three (beech Gr12) main maxima in leaf area, which are separated by rather leaf-poor layers (Fig. 21).

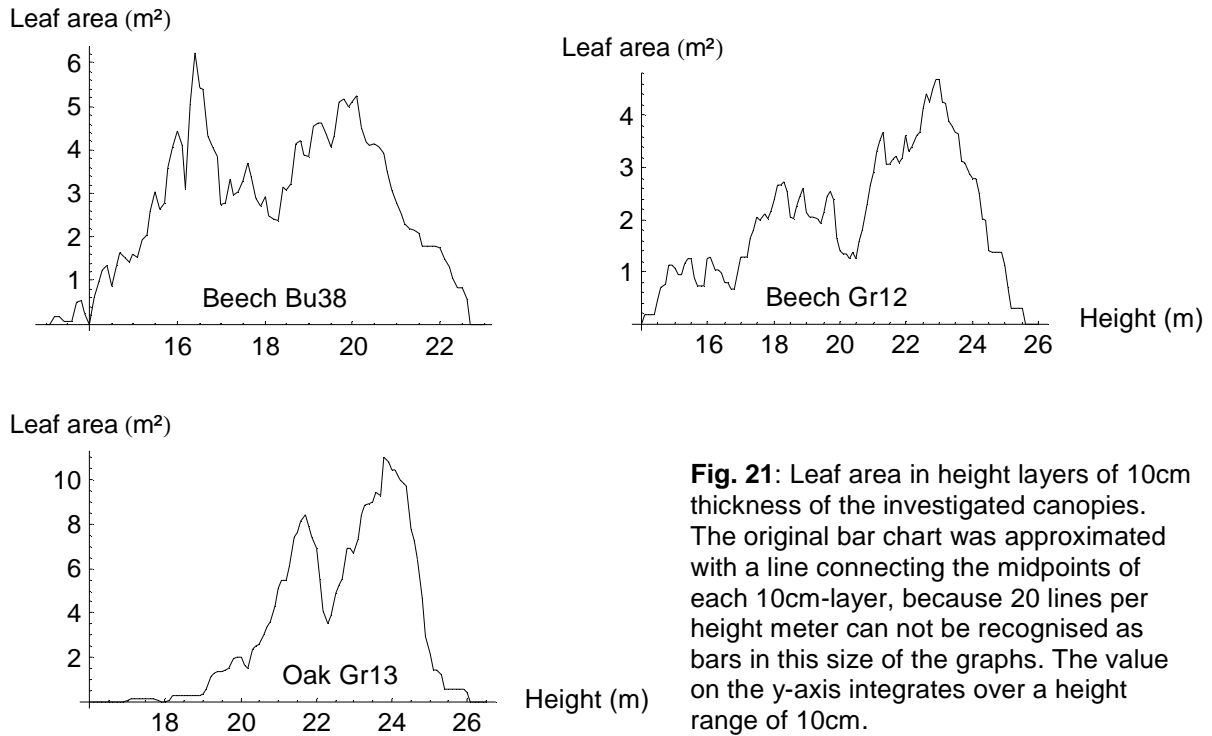


Fig. 21: Leaf area in height layers of 10cm thickness of the investigated canopies. The original bar chart was approximated with a line connecting the midpoints of each 10cm-layer, because 20 lines per height meter can not be recognised as bars in this size of the graphs. The value on the y-axis integrates over a height range of 10cm.

Leaf area maxima in lower heights were not in all cases less than in maxima found high in the canopy (beech Bu38). The separation into two separate crown sections was clearest for oak Gr13, where the courses between crown base, first peak maximum, separating minimum, second peak maximum, and crown apex were approximately monotonous ascending or descending. In contrast, several intermediate leaf area minima and maxima between main maxima occurred in the beech crowns. While the uppermost 10 layers of oak Gr13 enclosed very small amounts of leaf area (ca. 3% of the maximum value), beech Bu38 and Gr12 crown tops contained more leaf area (13% to 14% of the maximum value). This would lead the area below a good approximation function to this part of the bar-chart to be concave in oak Gr13 and convex in the beech trees. The greatest leaf area in the upper crown part was at 72%, 78%, and 75% (Bu38, Gr12, Gr13) of the height extensions of the tree crowns. Maxima of the neighbouring trees Gr12 and Gr13 were separated by only 0.8m in height distance.

The assumption of height range homogeneity in leaf clouds was compared with calculations on the basis of volumetric homogeneity, i.e., the assumption that leaf area of leaf clouds is equally distributed in their volume. Because this requires the segmentation of leaf cloud polyhedrons along horizontal planes and calculation of the segments' volumes these calculations were based on the lower resolution of 1m height layers. Segmentation and volume calculation were performed with the program CRISTO, which is best explained using an example, as is done in chapter 4 (see 4.1).

Leaf area calculations on the base of volumetric homogeneity confirm the non-monotone distribution over height layers that was shown for height range homogeneity (Fig. 22).

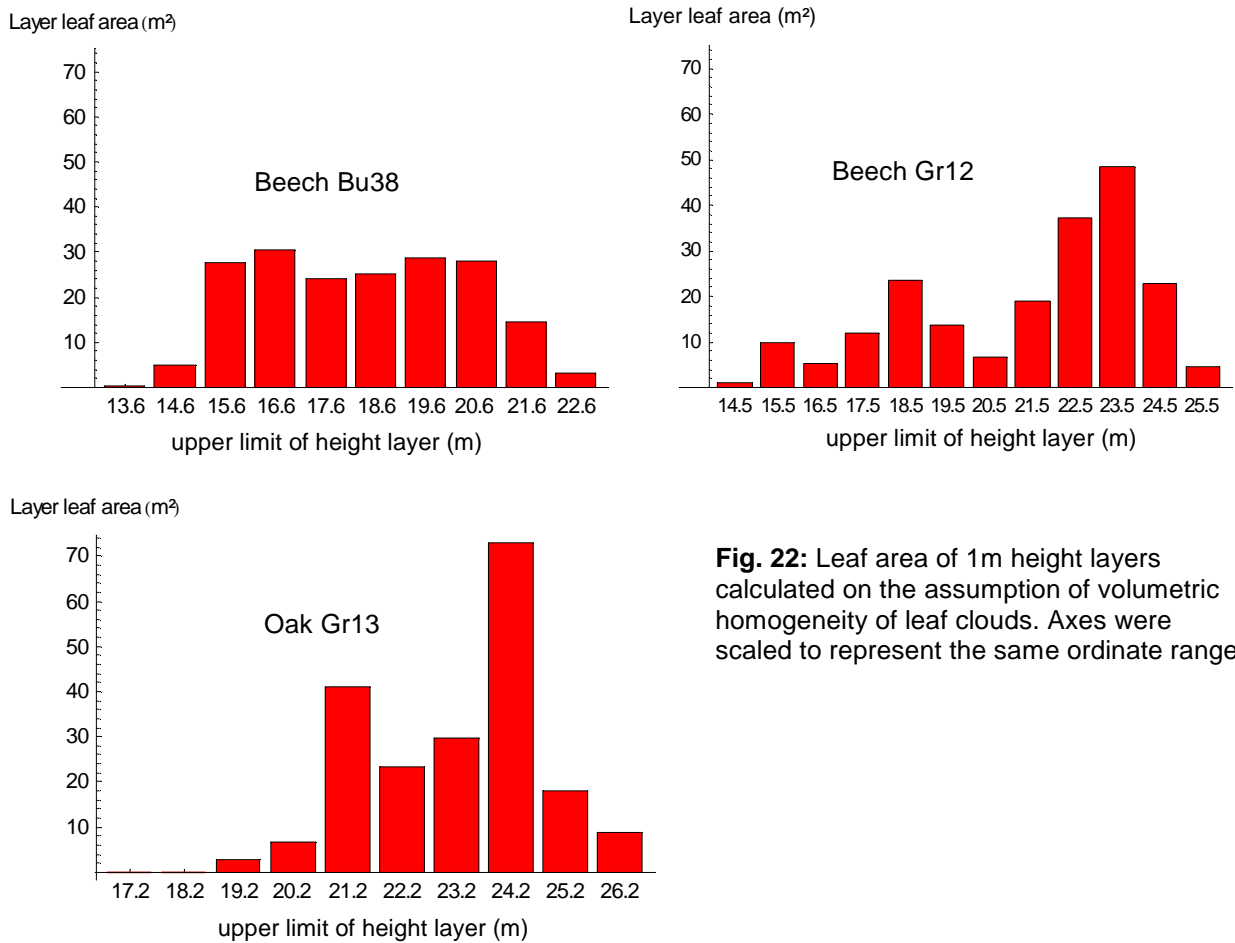


Fig. 22: Leaf area of 1m height layers calculated on the assumption of volumetric homogeneity of leaf clouds. Axes were scaled to represent the same ordinate range.

The same maxima and minima are apparent though the lower resolution smoothes the data so much that information from the finer resolution data is necessary to interpret the results. For example, the height layers 17.6m and 18.6m of beech 38 are here difficult to view as minimum layers. The volumetric homogeneity assumption tends to shift leaf area minima and maxima to lower levels. This is a consequence of the volume distribution over height range of the leaf clouds, which are usually wider in their lower, darker extent and smaller in the lighter and upper portion. Considering that leaf clouds usually grow towards lighter and higher regions (development of new leaves) and away from the lower and darker parts (die off of shaded parts), both methods seem to be justified approaches for examining structure.

2.3.4.2 Leaf area densities of height layers

Light harvest of tree crowns is not only influenced by the amount of leaf area at different heights, but also by the shadows cast on and by competing trees and on self-shading (LEUSCHNER 2000). The effective leaf area densities of height layers of single tree crowns depend on leaf area of the layer but also on the horizontal extension of the height layer, which is usually not constant. Height layer-related leaf area densities (LAD_L) were calculated on the base of $LA_{L, dm}$ -data, assuming that the volume of height layers may adequately be described by multiplying the layer height by the convex hull area of projected polygon corner points in that height layer. This assumption requires the height layers not be too small. For the sake of

simplicity, a height of 1m was chosen for all height layers and leaf area densities were calculated according to

$$\mathbf{LAD}_L = \frac{\sum_{i=1}^{10} \mathbf{LA}_{L, dm}}{\mathbf{V}_L} \quad , \quad (2)$$

where \mathbf{V}_L denotes the layer volume. The \mathbf{LAD}_L / height relationship was approximated by a polynomial function of \mathbf{LAD}_L versus relative height in the canopy (ranging from 0 to 1, see Fig. 23).

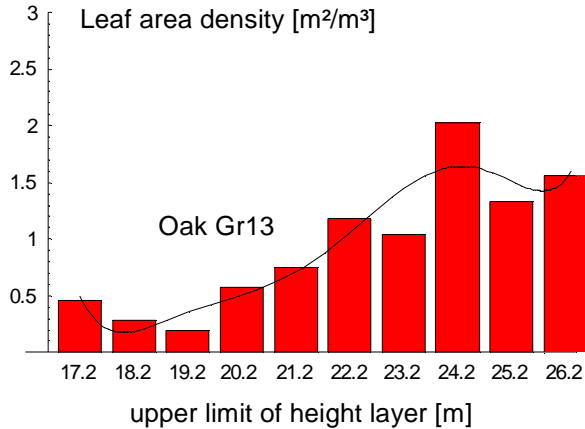
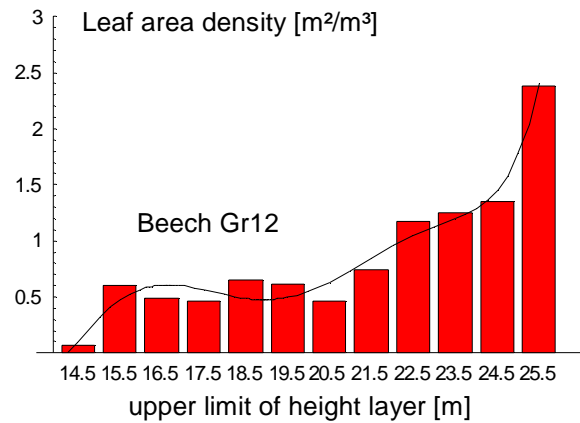
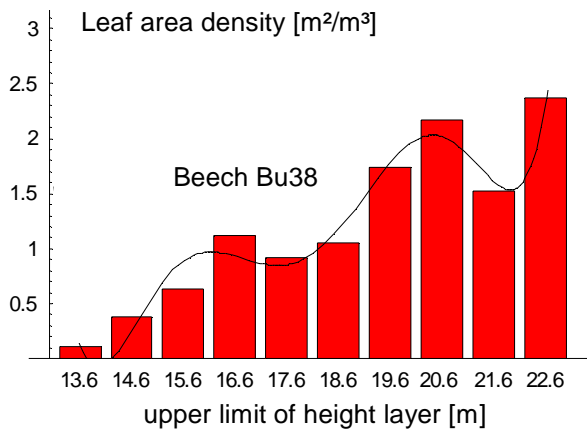


Fig. 23: Leaf area densities of 1m-height layers of the investigated canopies. The volume calculation is based on the convex hull of the projected polygon corner points of each layer times layer height (1m), and the LAD calculation assumes equal distribution of leaves over the height range of a leaf cloud. Polynomial approximations on the base of x = mean relative height in the canopy for beech Bu38, Gr12 and oak Gr13 were (respectively):

$$\mathbf{LAD}_L = 1111.3 x^6 - 3245.9 x^5 + 3605.8 x^4 - 1897.2 x^3 + 477.5 x^2 - 48.2 x + 1.6$$

$$\mathbf{LAD}_L = 211.9 x^6 - 544 x^5 + 495.9 x^4 - 176.9 x^3 + 11.4 x^2 + 5.2 x - 0.1$$

$$\mathbf{LAD}_L = 335.8 x^6 - 990.9 x^5 + 1119.2 x^4 - 615.2 x^3 + 174.7 x^2 - 22.8 x + 1.3$$

The results demonstrate a partly different situation in comparison to Figs. 21 and 22. A greater distribution of leaf area density toward the upper part of the crown occurs. Skewness of the \mathbf{LAD}_L -distribution was positive in all cases (see Table 5), indicating that the trees produce some single layers (those in the upper crown) with extremely high leaf area densities as compared to other layers. Especially the beech trees Gr12 and Bu38 had the highest leaf area densities in their uppermost crown layer, while oak Gr13 had its highest \mathbf{LAD}_L -values 2,5m below the apex.

While oak Gr13 had the greatest amount of leaf area in a higher region than the neighbouring beech Gr12 (Fig. 21), and even though this was more than twice as much leaf area than that of beech Gr12 in the peak layers, beech Gr12 (and also beech Bu38) had a higher maximum \mathbf{LAD}_L than oak Gr13. Furthermore, even though beech Gr12 was 0.7m shorter

than oak Gr13, beech Gr12 managed to produce its maximum LAD_L in a higher region than the maximum LAD_L of oak Gr13, which should be important in terms of shading.

The lower maximum LAD_L of oak Gr13 is not due to a generally higher volume of the whole tree crown, because the sum of all layer volumes of the two trees ($=LAD_{Crown}$) was nearly the same (see Table 5). Moreover, oak Gr13 had a higher absolute leaf area density related to the whole crown volume (LAD_{Crown} , Table 5), so that the higher maximum LAD_L of beech Gr12 only arises because of the much more positively skewed distribution of LAD_L -values in comparison to the distribution of oak Gr13 LAD_L -values, i.e., the high maximum LAD_L -value of beech Gr12 can under these circumstances only be achieved due to many height layers with low LAD_L -values. The crown of oak Gr13 on the other hand expands to enormously high layer volumes (40.1 - 58.8m³, compare Table 5) in the 2nd to 6th layer below apex, which leads despite their high amounts of leaf area to rather moderate LAD_L -values for these upper layers.

Table 5: canopy data

	Bu38	Gr12	Gr13
Leaf area (m ²)	240.7	236.6	328.3
Height range (m)	13.13 - 22.6	14.0 - 25.5	16.92 - 26.2
Crown volume (m ³)	229.3	312.0	310.1
Range of layer volumes (1m-layers, m ³)	4.8 – 39.5	3.6 - 37.6	0.6 - 58.8
Crown leaf area density LAD_{Crown} (m ² /m ³)	1.05	0.76	1.06
Range of layer leaf area densities LAD_L (m ² /m ³)	0.11 - 2.37	0.07 - 2.38	0.20 - 2.03
Skewness* of LAD_L –distribution	0.18	1.31	0.41
Standard deviation of LAD_L -values	0.74	0.61	0.60
Projected crown area (m ²)	42.8	52.4	69.4
Projected crown area (gap corrected, m ²)	36	47.5	54.8
Tree leaf area index $TLAI$ (m ² /m ²)	5.6	4.5	4.7
Tree leaf area index $TLAI_g$ (gap corrected, m ² /m ²)	6.7	5.0	6.0

*: Skewness calculation was based on maximum likelihood estimates of standard deviations

2.3.4.3 Effect of gap correction of leaf area densities

Separating the canopy into layers of constant depth does not relate in any way to a natural phenomenon and, therefore, the choice of other boundaries which could significantly influence the volume dependent determination of LAD_L –values could be considered. While horizontal boundaries spread the foliage by separating leaves of leaf clouds that are naturally clumped, vertical boundaries can additionally consider the form of the cross-section of a height layer in a finer or coarser manner. Reasonable definitions of layer projected areas are the same as those for projected crown areas and the convex hull area represents a definition that considers the overall shape of the cross-section but explicitly no cavities along the border of the cross-section. Another reasonable definition would be for example to consider all cavities of a given size or to consider only the biggest cavity, which can have a strong effect on the height dependence of LAD_L –values, when the roughness of the border of the cross-section of height-layers varies. The potential magnitude of this effect can be seen, when the calculated tree leaf area indices of the investigation trees with or without gap correction are understood as leaf area densities of a single large layer with constant height: Gap correction led to an increase of $TLAI$ in the range of 10 - 28% (Table 5).

A tree and cavity oriented layer definition assuming volumetric homogeneity of leaf clouds was tested for comparison on the data of beech Gr12: The height of horizontal boundaries between

layers was chosen by eye such that bigger cavities along the border of the cross-section were not hidden by leaf clouds above or below the cavities. The irregular form of horizontal cross-sections was approximated by 8 or 12 sectors of circles with different radii (see Figs. 112a, 112b). The assumption of volumetric homogeneity of leaf clouds again required the use of the program CRISTO (see chapter 4).

Using this approach led to a slightly different LAD_L vs. height relationship (Fig. 24).

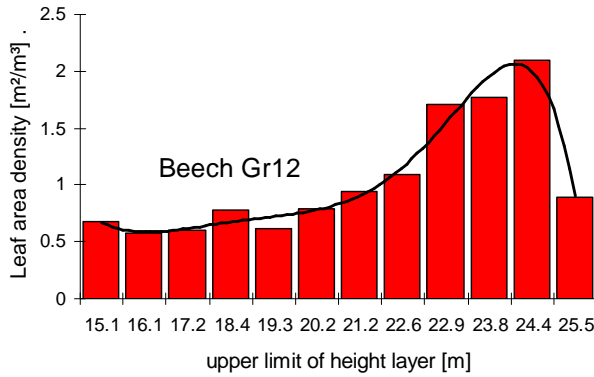


Fig. 24: Leaf area densities of irregular chosen height layers of beech Gr12. Layer volume is calculated as the sum of cylinder sector volumes with different radii and the LAD calculation is based on the assumption of volumetric homogeneity. The polynomial approximation on the base of $x =$ mean relative height in the canopy was:

$$LAD_L = -313.7 x^6 + 766.2 x^5 - 687.7 x^4 + 280 x^3 - 49.3 x^2 + 2.8 x + 0.6$$

The lowest and the uppermost layer were no longer extreme and their LAD_L -values were shifted towards values closer to the average. The highest LAD_L now occurs in the second layer from the top. This was again due to the assumption of volumetric homogeneity instead of height range homogeneity. The leaf area of leaf cloud top segments in the uppermost layer is overestimated and that of leaf cloud bottom segments in the lowest layer are underestimated, when their leaf area is assumed to be equally distributed over the height range. Though this is principally also true for the other layers, the effect appears to be weaker in the middle layers: The overall relationship between the middle layers agrees well with that obtained from 1m-height layers, which accounts for the fact that the middle layers contain bottom and top segments of leaf clouds, so that their contributions to relative over- and underestimation may cancel each other out. The general trend is still a monotonous and nearly exponential increase in LAD_L towards the uppermost layers. If no fundamental changes in the opposite direction would occur when oak Gr13 would be layered in this manner, the layer with highest LAD_L of beech Gr12 (mean height: 24.1m) would still be in a slightly higher region than that of oak Gr13 (mean height: 23.7m), though the beech is 0.7m shorter.

2.3.4.4 Volume gap fractions

The meaning of layer leaf area densities for light transmission and absorption in a canopy is strongly dependent on clumping of leaves and discontinuity of the tree canopy (CESCATTI 1998). Therefore the question arises, whether the leaf area density distribution from top to bottom of the canopy is due to changes in leaf area density of leaf clouds or in the leaf cloud density in different layers, i.e., the fraction of their volume with respect to the layer volumes (which can be inversely expressed as volume gap fraction). Volume of leaf cloud segments as calculated with the program CRISTO was summed for each layer and related to the layer-specific convex hull-based layer volume V_L for the calculation of layer gap fractions as

$$\text{Gap} = 1 - \frac{\sum_{i=1}^n V_{P_i}}{V_L} \quad (3)$$

where V_{P_i} denotes the volume of a polyhedron or polyhedron segment and n the number of polyhedrons and polyhedron segments in that layer. The 1m-height layer leaf area density was estimated from the leaf cloud leaf area data assuming volumetric homogeneity:

$$\text{LAD}_{L,m} = \frac{\sum_{i=1}^n \frac{V_{P_i}}{V_{C_i}} \times \text{LAC}_i}{V_L} \quad (4)$$

Here, V_{C_i} denotes the volume of the whole polyhedron, i. e., the leaf clouds volume and LAC_i is the leaf clouds leaf area. Finally, average leaf area density of polyhedrons and polyhedron segments in the layer (LAD_p) was calculated according to

$$\text{LAD}_p = \frac{\sum_{i=1}^n \frac{V_{P_i}}{V_{C_i}} \times \text{LAC}_i}{\sum_{i=1}^n V_{P_i}} \quad (5)$$

Volume gap fractions within the crown layers were rather high (90%, 82% and 89% on average for beech Bu38, beech Gr12 and oak Gr13), and ranged from 82% to 98%, 58% to 96%, and 72% to 98% for the three trees, respectively. While the lowest gap fraction of oak Gr13 was in

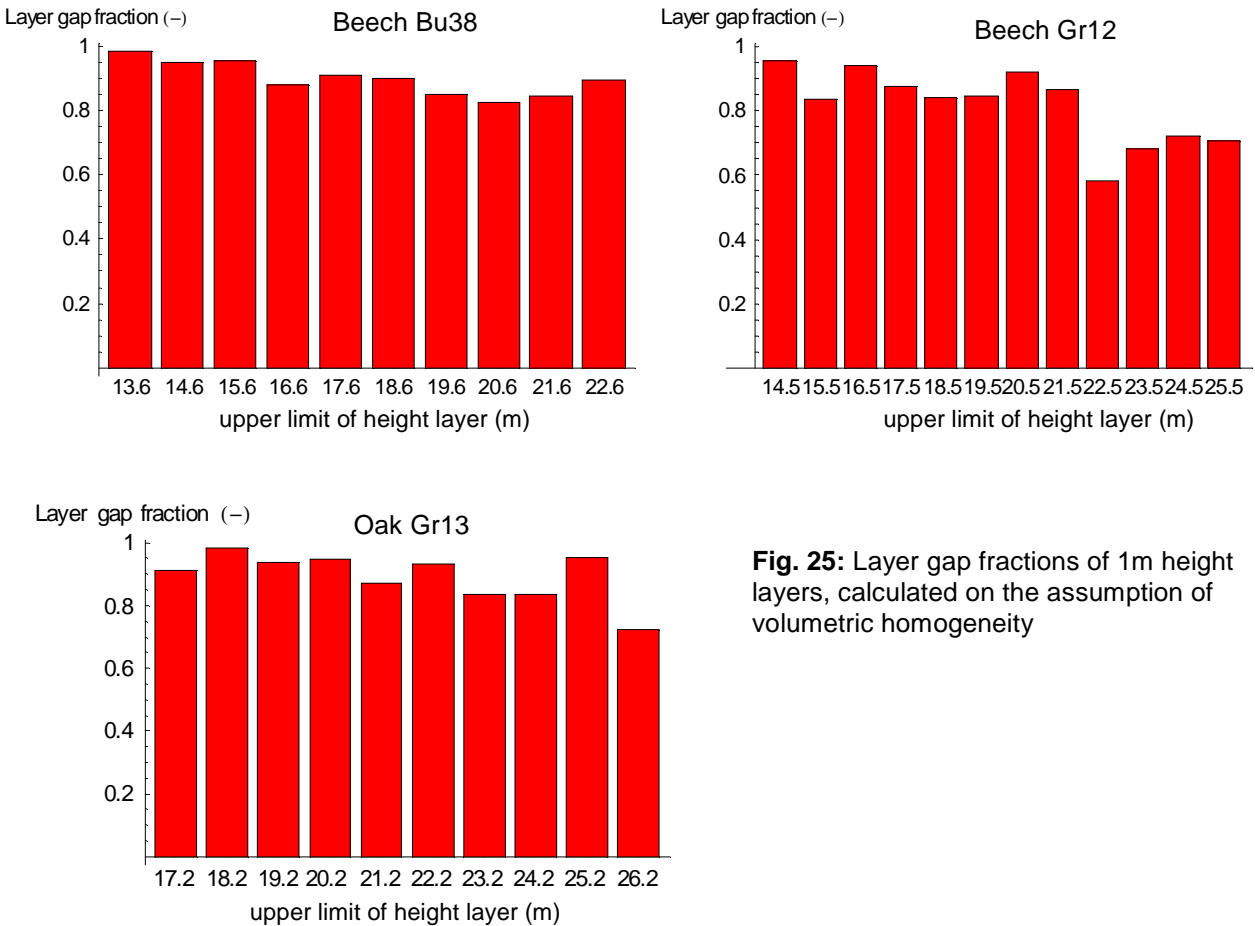


Fig. 25: Layer gap fractions of 1m height layers, calculated on the assumption of volumetric homogeneity

its uppermost layer, the lowest gap fraction of beech Bu38 and Gr12 was 2.5m and 3.5m below the apex (Fig.25).

In any case, the general trend was a more or less continuous decrease in gap fractions as one moved towards the top layer. Gap fractions explained 64%, 89%, and 89% of the variability of layer leaf area densities (Bu38, Gr12, and Gr13 respectively), which were significant relationships at the 1%-level. The regression on LAD_p was only significant for oak Gr13 ($r^2 = 0.51$), leading to the conclusion that the increase of layer leaf area densities of the beeches with height was basically due to decreasing gap volumes; which is also valid for oak Gr13, even though increasing leaf area densities of leaf clouds also occurred.

2.3.5 Leaf cloud oriented evaluation of leaf arrangement in the crown

Spatial and qualitative properties of leaf clouds were investigated because of their potential importance for up-scaling of photosynthesis and also because the arrangement of leaf clouds appeared to be quite regular (compare Fig. 16). The growth of tree crowns is generally understood as dependent on a complex interaction of species-specific rules and the research on this topic has been described in chapter 1. But though it has repeatedly been shown that the consequent application of growth rules in simulations over several growth periods leads to regular shaped, typical crown forms (KURTH & SLOBODA 1999, DE REFFYE ET AL. 1997, LIST & KÜPPERS 1997, SIEVÄNEN ET AL. 1997), a regular structure of real tree crown shapes in a mature forest has not yet been described in detail, while general concepts of typical crown forms exist already for a long time (HALLÉ ET AL. 1978). Therefore, it becomes questionable, if fractal simulations of tree growth are an adequate method for their description (LIST & KÜPPERS 1997). A common argument for these doubts is that the influence of tree growth patterns may become less visible in ageing trees due to the growing and accumulating influence of changing environmental conditions during its life-span and the influence of an inhomogeneous environment.

Regularities in canopy structure may have a significant impact on up-scaling methods since they suggest underlying patterns in flows of mass and energy. For example, as the directed separation of electrical charges across the thylakoid membrane of the chloroplast by the spatial organisation of the electron transport chain causes a powerful charge gradient (KARLSON 1999), the spatial organisation of tree crowns could influence the distribution of photosynthetically active radiation in the canopy via transmission and reflection. Transmittance and reflectance of PAR on typical leaf surfaces varies between 2 and 7%, and between 8 and 15%, respectively, with an average value of ca. 5% for transmittance and ca. 10% for reflectance (JONES 1992). Both processes are in virtually all canopy light models assumed to be randomly directed, knowing that reflection is dependent on the angle between incoming radiation and reflecting surface, and thereby considering the leaves and other crown elements to be randomly oriented. Even though 10% of the incoming radiation is a small proportion, the resulting irradiance after the first reflection lies often in the range of light saturation of photosynthetic light response curves of shade leaves (achieved at 100 – 200 $\mu\text{mol}/(\text{m}^2\cdot\text{s})$ for beech, LICHTENTHALER ET AL. 1981, SCHULTE 1992), while the incoming global radiation above the canopy is often higher than the saturation value for sun leaves (600 - 700 $\mu\text{mol}/(\text{m}^2\cdot\text{s})$ for beech).

It would be possible for tree crowns to optimise the use of radiation for photosynthesis, if the surplus of PAR in the upper part of the forest canopy could be passed to the lower layers by

directed reflection. Additionally, shade leaves could be spatially arranged such that the amount of reflected and transmitted radiation in the lower layers is optimally used.

The leaf cloud oriented three-dimensional description of the investigated trees can not be used to test the reflection of each leaf, but it can be used to check, whether regularities exist that support the use of reflected and transmitted light in the lower layers.

Leaf cloud properties may be described with a group of parameters that describe where the leaf cloud is situated in relation to the stem, to the canopy base, or to the forest floor; a second group of parameters that describe the influence of other crown elements on the environmental situation of the leaf cloud; a third group of quantities that describe the spatial properties (angles and extensions) of the leaf cloud, and, finally, a group of qualitative properties.

Location properties include the quantities:

H: relative height of the leaf cloud centre in the canopy (-),

H_{abs}: absolute height of the leaf cloud centre above the floor (m)

E: distance of the leaf cloud centre to the stem in east direction (m),

N: distance of the leaf cloud centre to the stem in north direction (m),

stemd: horizontal distance of the leaf cloud centre to the stem (m),

AZ_s: azimuth of the horizontal vector stem → leaf cloud centre, measured anti-clockwise from the north (°).

Crown environmental properties are:

CLA: sum of tree canopy leaf area above the leaf cloud (m²),

CVOL: tree canopy volume above the leaf cloud (m³),

CLAD: average tree canopy leaf area density above the leaf cloud (m²/m³).

Leaf cloud spatial properties are:

AZ_p: azimuth of the exposition of the leaf cloud plane, mathematically defined as azimuth of the upwards directed normal vector of the leaf cloud plane, measured anti-clockwise from the north (°),

α_n: leaf cloud angle; steepest angle of the leaf cloud plane towards a horizontal plane (°; positive and negative values),

α_{AZ}: inclination of the main growth direction of a leaf cloud towards the horizon. The main growth direction is here determined as that vector in the leaf cloud plane, that goes through the leaf cloud centre and comes from the stem. (°; positive and negative values),

α_s: angle of the main growth direction vector towards the idealised surface of the crown (°),

H_s: height of the intersection of main growth direction vector and idealised canopy surface (m),

D_s: derivative of the idealised canopy shape function at the point of intersection with the main growth direction vector (m/m),

area: vertically projected area of the leaf cloud (m²),

volume: volume of the leaf cloud (m³),

Hrange: vertical extension of the leaf cloud (m).

Qualitative properties include:

LAD: Leaf area density of leaf clouds (leaf area per leaf cloud volume, m²/m³),

WAD: Wood area density of leaf clouds (projected area of branches and twigs per leaf cloud volume, m^2/m^3)

CLA was calculated based on the cloud-related height and leaf area data, summing up leaf area of all leaf clouds whose centre lies above a certain relative height. **CVOL** relies on the volume calculations for height layers (compare Fig. 23), summing up all layer volumes above the relative height of the leaf cloud centre and the height-proportional upper part of that layer to which the leaf cloud centre belongs. **CLAD**, in contrast, is not related to crown form oriented layer volumes, but assumes a constant volume of each layer above the leaf cloud, thus considering the tree crown as a cylinder. This was done to enable an estimation of the self-shading effect of crown leaf area densities on leaf clouds on the basis of an application of Beer's law to height layers (see below). The volume of these height layers was, therefore assumed to equal the maximum of height layer volumes of each tree. Volume (**volume**) of leaf clouds has been estimated by calculation of their enveloping polyhedron's volume (see chapter 4.1.2.2).

The variables α_{AZ} , α_s , H_s , and D_s were introduced for the investigations on spatial regularities in the tree crown and require an approximate description of the canopy shape. The discontinuous real crown shape may not be used for their calculation, which reveals the idealising concept behind the word "canopy shape". The chosen concept to approximate the measured crown extensions shall enable the consideration of deterministic relationships between properties of crown elements and the canopy shape and therefore tries to describe a typical canopy shape for the given trees in a forest environment: It is assumed that homogeneously changing conditions of the environment do not fundamentally change the typical canopy shape, and that the observed variety of canopy shapes from the same species mainly results from their spatially inhomogeneous environments. Thus, the typical canopy shape may not be found in inhomogeneous environments like a forest, and it may be difficult to reconstruct it from the actual spatial situation, because this situation has changed during the life-span of a tree. The described typical crown shape therefore equalises the crown development in all horizontal directions by taking the maximum extension of height layers as the typical extension in every other direction. It is assumed that the canopy would have developed to this maximum extension in all horizontal directions, if no competition effects due to the inhomogeneity of the forest environment would exist.

The canopy surface was defined to be a surface of revolution around the stem on the basis of 5th order polynomial functions that were approximated to the maximum stem distances in each 1m-height layer. The lowest height layer of each tree was not considered in the approximation and the polynomial function was cut at the bottom of the tree crown (see Fig. 26). The approximations show a similar crown shape of both beeches which is different from the canopy surface shape for the oak. This can definitely be shown by a comparison of the derivatives of the three shape functions (Fig. 27). While the derivative of both beech crown shape functions has two maxima in the height range of the tree canopies, the oak's had only one, which is due to a great height range in the shape function curve, where the height layers have nearly constant and very high maximum stem distances, while the layers above and below this part are much smaller, so that the shape function monotonously decreases from the five maximum layers towards both ends of the crown.

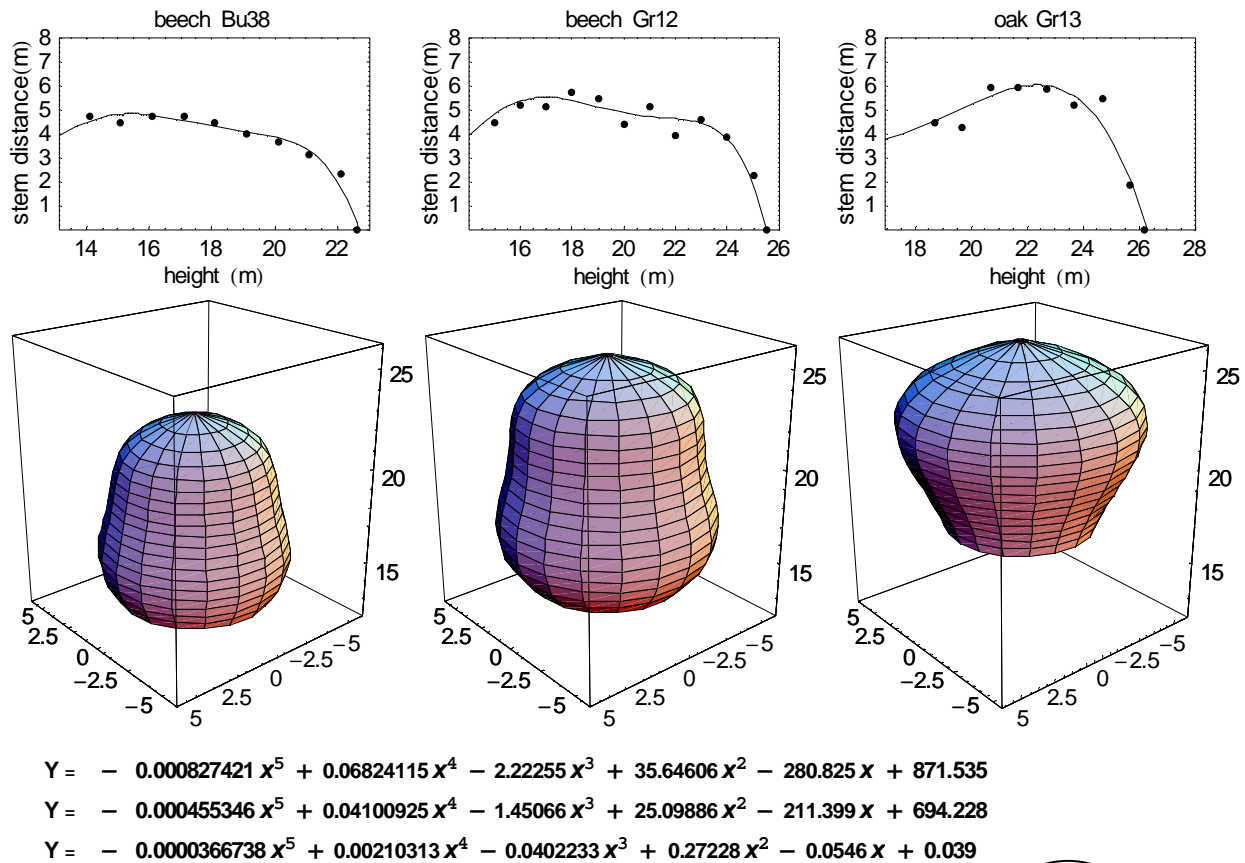
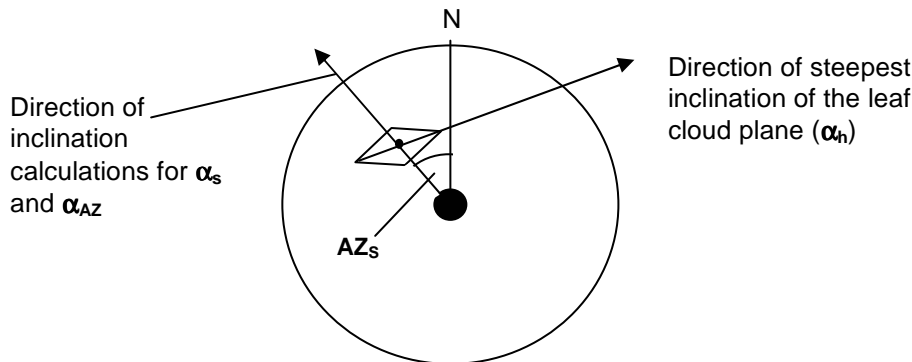


Fig. 26: Polynomial approximations to the maximum stem distance in each layer (first row). The canopy surface was assumed to be a surface of revolution of these functions around the x-axis (second row, all units in meters). The functions for the dependence of stem distance (Y) to height (X) are displayed below (Bu38, Gr12, and Gr13, respectively). The angle between leaf cloud plane and canopy surface (α_s) was determined at the point of intersection of a straight line through the leaf cloud and the calculated canopy surface (right side, side view). The straight line represents the main growth direction of the leaf cloud and goes through the central axis of the stem and the leaf cloud centre and lies in the leaf cloud plane.

While α_h is the steepest inclination of the leaf cloud plane, α_{AZ} is the inclination of the leaf cloud plane when measured in direction of its stem relative azimuth orientation AZ_s , which is illustrated in the graph below (view from above)



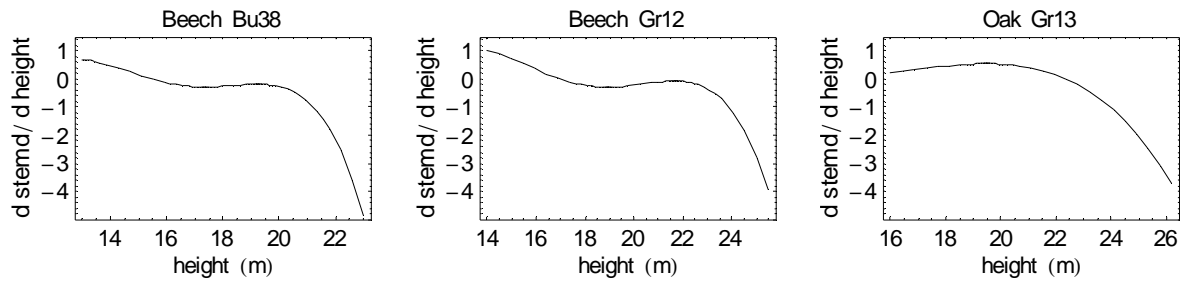


Fig. 27: Derivatives of the 5th order polynomial that approximates the maximum horizontal extensions of 1m-layers of the three trees. While the derivative of the beech functions has two maximums in their canopies' height range, only one maximum is to be found in the height range of oak Gr13, which is a consequence of the outstanding position of the 5 largest layers with nearly constant maximum stem distance relative to the other layers.

An important consequence of the described canopy shapes is that the maximum extension of the canopy of oak Gr13 lies in the upper half of the crown, while it is in the lower third of both beech canopies. Empirical evidence for the relatively higher position of the maximum extension of oak canopies was found in stand investigations on all trees from the Große Ebene and from the Steinkreuz stand: While the height of maximum extension in south, east, north, and west direction was on average 80% of the total tree height of 48 oak trees, it was on average 67% of the tree height of 58 beeches. Only trees higher than 15m were considered in this comparison and the range between first and third quartile was 76.7 - 84.9 % for oak trees and 57.2 - 75.6% for beech trees. The same value for all 80 beech trees higher than 15m from the Buchenallee stand was 45% with an interquartile range of 41% - 50.2%.

α_s was calculated by prolonging the main growth direction of the leaf cloud (a straight line in the leaf cloud plane that goes through the stem and the leaf cloud centre) to the canopy surface, thus considering the azimuth of the leaf cloud relative to the stem (\mathbf{AZ}_s) (Fig. 26). The angle was calculated between the main growth direction and the derivative \mathbf{D}_s of the polynomial function at the point of intersection of both lines in a two-dimensional co-ordinate system in the plane of the main growth direction and the stem ($x = \mathbf{H}_{abs}$, $y = \mathbf{stemd}$). The derivation of the parameters is described in the appendix.

2.3.5.1 Properties of the crown environment of each leaf cloud

Tree crown leaf area above each leaf cloud (CLA) reflects the pattern of leaf area in different height layers (Fig. 21) from the view point of a leaf cloud, thus, cumulating the leaf area above it. Though big changes in leaf area were found for 10cm height layers, these changes cause

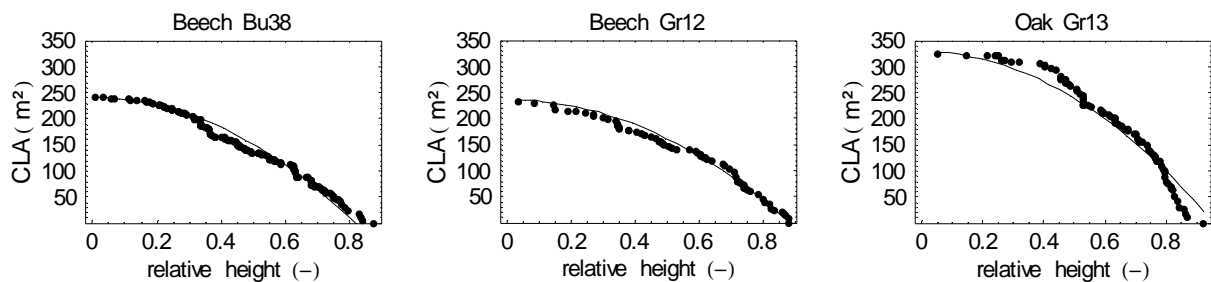


Fig. 28: Cumulative leaf area of leaf clouds in relation to relative height \mathbf{H} . The curvilinear relationship was approximated with one-parametric functions of the form: $\text{CLA} = \text{Tree leaf area} - k * \mathbf{H}^2$. The coefficient k was 358.3, 302.6, and 358.4, respectively with r^2 -values 0.97, 0.98, and 0.96 for the trees Bu38, Gr12, and Gr13.

only small deviations from a monotonously decreasing quadratic function that was fitted to the resulting height dependence of **CLA** (Fig. 28). The curvilinear relationship could be approximated with single-parametric functions of the form: $CLA = \text{Tree leaf area} - k * H^2$. The coefficient k was 358.3, 302.6, and 358.4, respectively with r^2 -values 0.97, 0.98, and 0.96 for the trees Bu38, Gr12, and Gr13.

Similar to **CLA**, **CVOL** reflects the changes of height layer volumes with height in a cumulative way. The volume calculations are based on the volume of height layers (see figure caption to Fig. 23). Like the **CLA** vs. **H** relationship, the height dependence of **CVOL** could be well approximated with a single-parametric equation (Fig. 29).

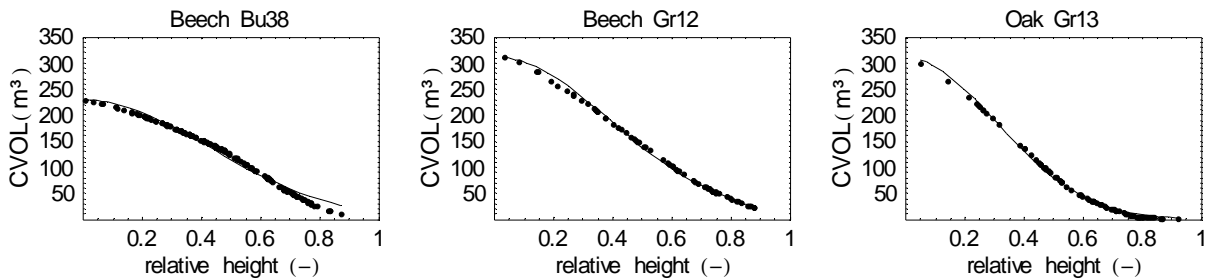


Fig. 29: Cumulative tree crown volume above leaf clouds in a certain relative height (**CVOL**). The volume calculations are based on the volume of height layers. The results were approximated using a one-parametric equation of the form: $CVOL = \text{Crown volume} / \text{Exp}[(H / k)^2]$, where the coefficient k was 0.599, 0.557, and 0.43, for the trees Bu38, Gr12, and Gr13, respectively. All r^2 -values were higher than 0.98.

The S-shape of the relationship was expressed by the equation: $CVOL = \text{Crown volume} / \text{Exp}[(H / k)^2]$, where the coefficient k was 0.599, 0.557, and 0.43, for the trees Bu38, Gr12, and Gr13, respectively. All coefficients of determination were greater than 0.98. Due to the very low volume of the uppermost height layer of oak Gr13 (compare Fig. 19a), the **CVOL**-values for oak Gr13 approach closer to the x-axis.

The dependence of **CLAD** on height was not as regular as that of **CLA** and **CVOL** (Fig. 30).

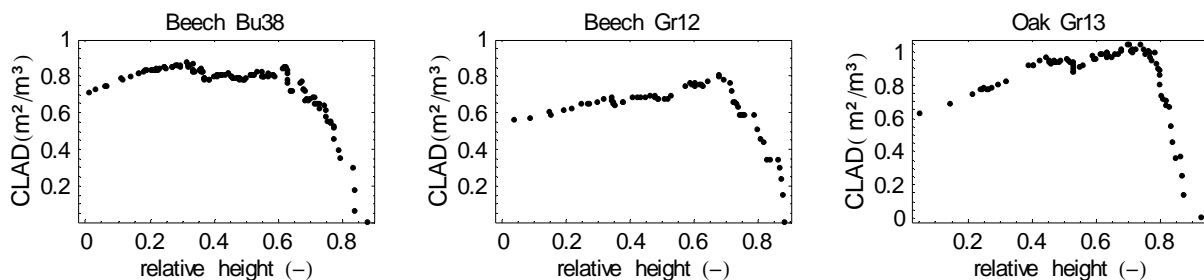


Fig. 30: Leaf area densities of tree crown parts above leaf clouds in a certain relative height (**CLAD**). Tree crowns were assumed to have the form of a cylinder to enable the application of Beer's law on height layers. The relationship reflects the ratio of cumulative leaf area to cumulative volume of a cylinder.

While most leaf clouds of beech Bu38 in the lower two thirds of the canopy were exposed to a constant crown leaf area density above them of around $0.8 \text{ m}^2/\text{m}^3$, built up by the cumulative increase in the upper 36% of the tree crown, **CLAD**-values of the Großebene trees had a maximum value at 33% (Gr12) and 26% (Gr13) below apex and decreased approximately linearly below this. Oak Gr13 had generally the highest **CLAD**-values with maximum leaf area densities of $1 \text{ m}^2/\text{m}^3$, while beech Gr12 reached $0.81 \text{ m}^2/\text{m}^3$ and beech Bu38 $0.89 \text{ m}^2/\text{m}^3$. The oak

leaf clouds in the relative height range of 0.38 - 0.8 were therefore exposed to higher **CLAD**-values than all leaf clouds of the neighbouring beech Gr12.

The consequences of **CLAD** for the relative amount of radiation flux density that reaches the leaf clouds may be approximately estimated from Beer's law:

$$I = I_0 * \text{Exp}[-k d] \tag{6}$$

Here **I** denotes radiation flux density in or below the medium, **I₀** is the flux density above the medium, **d** is the distance travelled in the medium and **k** is an extinction coefficient which accounts for concentration and optical properties of small particles like for example leaves in a canopy. This equation can be used to approximate the light profile in plant canopies (JONES 1992). Assuming that the optical properties of the investigated oak and beech leaves are not different and that light comes from above through horizontal height layers, the ratio **I/I₀** for leaf clouds that is achieved due to self-shading can therefore be calculated as

$$\frac{I}{I_0} = \text{Exp}[-\text{CLAD} * (H_{\text{apex}} - H_{\text{abs}}) * c] \tag{7}$$

, where **H_{apex}** is absolute height of the canopy apex above the floor and **c** is a constant representing the effect of optical properties due to transmittance, reflectance, angle distribution of leaves, etc. The calculated quantity **Exp[-CLAD * (H_{apex} - H_{abs})]** can therefore be used to express the relative changes of **I/I₀** for leaf clouds due to self-shading.

Fig. 31 reveals that nearly all leaf clouds of oak Gr13 are more strongly subjected to self-shading than those of the neighbouring beech Gr12 and those of beech Bu38, when leaf clouds in the same relative height of the canopy are compared.

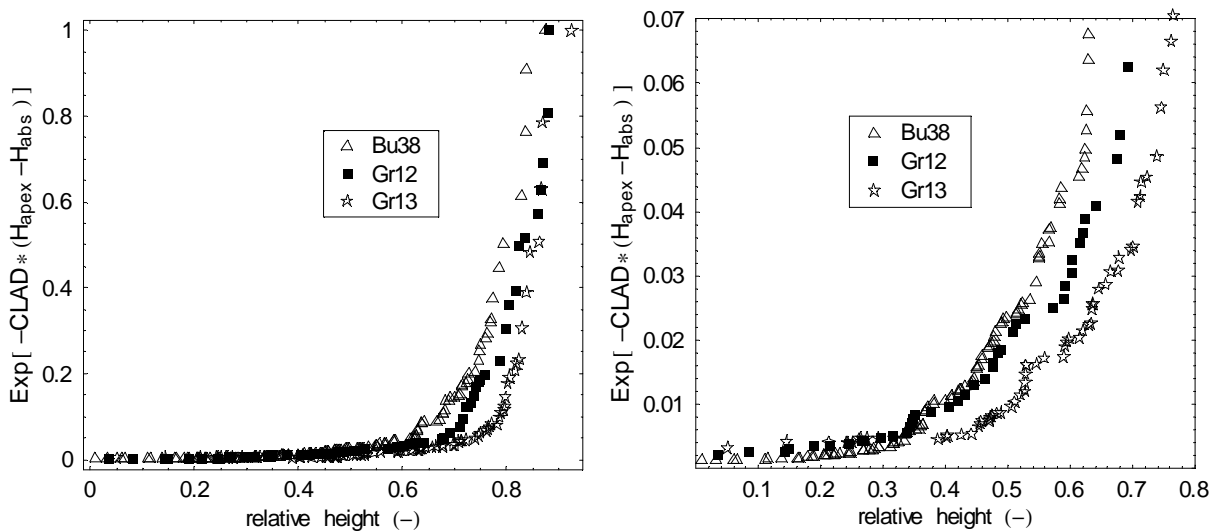


Fig. 31: Effect of leaf area density of the crown above a certain height (**CLAD**) on self-shading as estimated according to Beer's law. The quantity **Exp[-CLAD * (H_{apex} - H_{abs})]** may approximately express the relative differences in self-shading, when light extinction properties of oak and beech leaves due to leaf angle distribution, reflectance, transmittance, etc. are assumed to be the same. The left graph shows the whole data set and the right graph magnifies the region below 0.07.

This is mainly a consequence of the strong and immediate increase in **CLAD** in the uppermost 20% of the crown of oak Gr13. Only those leaf clouds below the height range of 0.32 have partly higher I/I_0 -ratios due to self-shading than the comparable beech leaf clouds. The lowest relative light intensities were found for leaf clouds of beech Bu38 and they were half of that of the lowest leaf cloud of beech Gr12 and one third of that of oak Gr13. A comparison between the neighbouring trees in the Große Ebene is shown in Fig. 32 based on the absolute height above the floor in the stand (H_{abs}). Again, leaf clouds of oak Gr13 are subjected to stronger self-shading than those of beech Gr12.

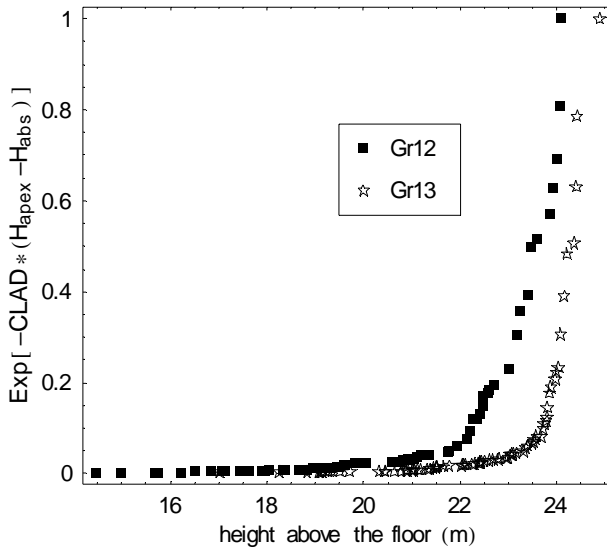


Fig. 32: Comparison of the light situation of leaf clouds of the neighbouring trees in the Große Ebene stand as influenced by self shading. All leaf clouds of oak Gr13 have lower I/I_0 ratios due to self-shading when compared to the leaf clouds of beech Gr12 in the same height.

2.3.5.2 Angles of the leaf cloud plane

Leaf cloud angles towards a horizontal plane (α_h) can be positive and negative values, when the leaf cloud plane is considered to have a direction from the origin to the leaf cloud's tip. This differentiation is not important for light absorption by the leaf cloud leaves, when the surrounding structure is assumed to be randomly distributed, but it reflects a tree specific organisation scheme that may as a whole have an influence on light capture. For beeches Bu38 and Gr12 leaf cloud angle α_h showed a significant ($p < 0.001$) increase with relative height in the canopy (H), though the correlation was not very strong ($r^2 = 0.47$ and 0.46 , see Fig. 33).

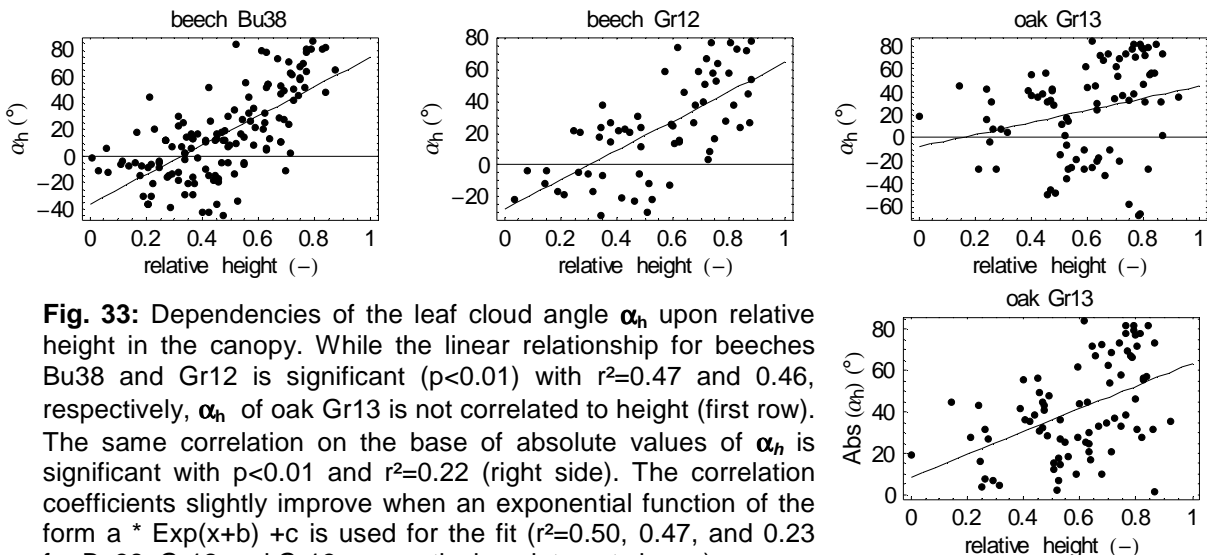


Fig. 33: Dependencies of the leaf cloud angle α_h upon relative height in the canopy. While the linear relationship for beeches Bu38 and Gr12 is significant ($p < 0.01$) with $r^2 = 0.47$ and 0.46 , respectively, α_h of oak Gr13 is not correlated to height (first row). The same correlation on the base of absolute values of α_h is significant with $p < 0.01$ and $r^2 = 0.22$ (right side). The correlation coefficients slightly improve when an exponential function of the form $a * \text{Exp}(x+b) + c$ is used for the fit ($r^2 = 0.50, 0.47$, and 0.23 for Bu38, Gr12 and Gr13, respectively – data not shown).

While no trend was observed in the α_h / H relationship of oak Gr13, the situation changed when the absolute values of α_h were taken ($r^2=0.22$, Fig. 33). Mean values \pm standard deviation of α_h were $15.5 \pm 32.6^\circ$, $22.7 \pm 30.4^\circ$, and $23.6 \pm 40.9^\circ$, respectively for beech Bu38, beech Gr12 and oak Gr13.

No useful correlations were found between α_h and other basic quantities (**N**, **E**, **stemd**, **AZ_s**), though the relationship to **stemd** was significant with $p < 0.001$. The relationship between leaf cloud angle α_h and the height dependent quantities **CVOL** and **CLA** was slightly better than the relationship to height in the case of beeches Bu38 ($r^2=0.52$ and 0.50) and Gr12 ($r^2=0.47$ and 0.46) and slightly worse in the case of oak Gr13 ($r^2=0.22$ and 0.20 , absolute value of α_h) ($p < 0.001$, data not shown). Absolute values of leaf cloud angles increased with height range of the leaf clouds (Fig. 34) and this seems to be a consequence of the unidirectional growth of leaf clouds especially of beech, which allows height extension primarily by length growth. The r^2 -values for this significant ($p < 0.001$) relationship were 0.58 , 0.41 and 0.33 (Bu38, Gr12, and Gr13, respectively).

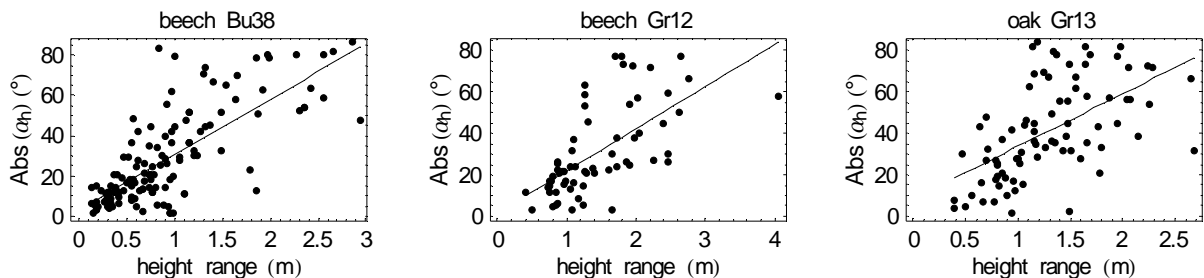


Fig. 34 : Increase of leaf cloud angle with height range of leaf clouds ($p < 0.001$). r^2 was 0.58 , 0.41 and 0.33 for beech Bu38, beech Gr12 and oak Gr13, respectively.

2.3.5.3 Main growth directions of leaf clouds

Main growth directions of leaf clouds in a tree crown are the result of the application of species-specific growth mechanisms in a unique environmental situation. It is questionable if the environmental impact may fully hide the species-specific growth patterns during the long life of trees. If this is not the case, the species-specific arrangement of branches may result in a species-specific distribution of leaf biomass, which is likely to have an influence on the use of irradiation. Main growth directions of leaf clouds may, thus, indicate structural regularities on the level of whole crowns.

Fig. 35 shows the main growth directions of leaf clouds from the three trees, projected by rotation around the stem into a two-dimensional co-ordinate system. The majority of leaf clouds in the lower third of the crowns was growing horizontally or slightly downwards away from the stem. The angle to the horizon increased for most leaf clouds with height in the canopy, as can be seen in the increase of absolute values of α_{AZ} with height in the canopy (Fig. 36). Though the increase of α_{AZ} appears to be continuous at least in the beech trees, coefficients of determination for this relationship were rather low, which is due to a number of leaf clouds that grow horizontally even two or three metres below apex, where most leaf clouds have steep inclinations (Fig. 35). The steep inclinations in the upper metres of the crowns were not only due to branches that grow towards light and thereby promote height extension of the crown, but also

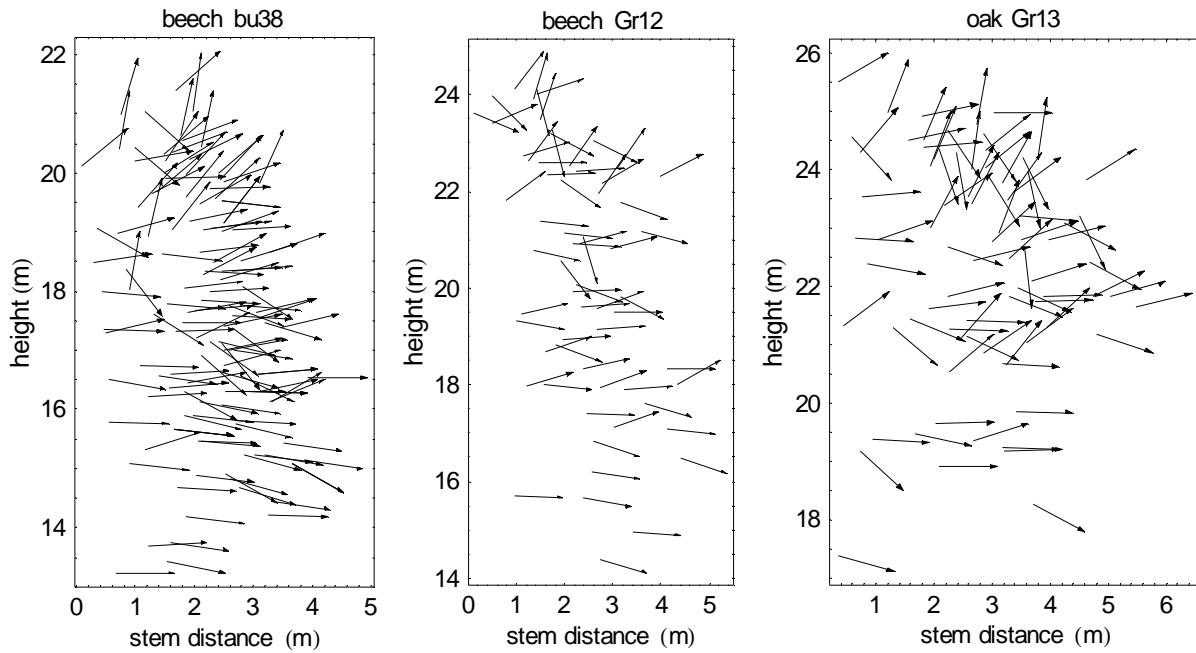


Fig. 35: Main growth directions of leaf clouds from the three investigated trees. Each vector is rotated around the stem into a common plane for all vectors of a tree and starts at the (rotated) centre point of its leaf cloud.

to steeply downwards directed branches, that are often close to rectangular inclined towards the main growth direction of their neighbours in height.

The similar shape of the beech canopies may be anticipated from Fig. 35: Both canopies had a dent in their hull (between 17.5m and 19m (Bu38) and between 19m and 21m (Gr12)) that was partly due to downwards inclined leaf clouds below the dent and upwards inclined leaf clouds above it. An alternation of crown parts with upward directed leaf clouds and downwards inclined leaf clouds may be described for beech Bu38: All leaf clouds below 16m were growing remarkably similar and on average -9.2° downwards, seemingly following inflected lines from the stem towards the canopy surface. Leaf clouds in the canopy part directly above 16m were also following a line, but this was slightly upwards directed ($\alpha_{AZ} = +0.3^\circ$). The majority of leaf clouds between 17m and 18m was directed towards the floor ($\alpha_{AZ} = -6.9^\circ$ on average), while the next layer between 18m and 19m consists prevalingly of upwards directed leaf clouds ($\alpha_{AZ} = +30.1^\circ$ on average). In the next height metre from 19m to 20m, leaf clouds are on average $+31.5^\circ$ inclined towards above, the lower half of leaf clouds of this layer had an average α_{AZ} of

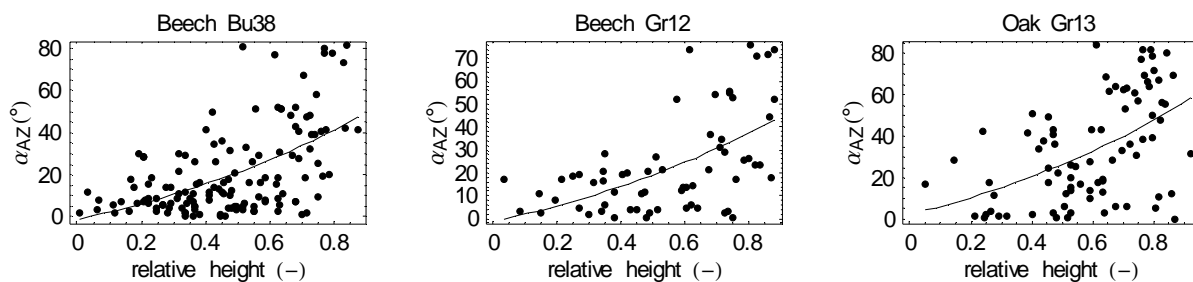


Fig. 36: Absolute values of the leaf clouds' inclinations in their main growth direction (α_{AZ}) versus relative height in the canopy (H). The general trend is an increase of α_{AZ} –inclinations with height. The exponential approximations of the form $\text{Abs}[\alpha_{AZ}] = a \cdot \text{Exp}[H+b]+c$ had an r^2 of 0.32, 0.33, and 0.35, respectively.

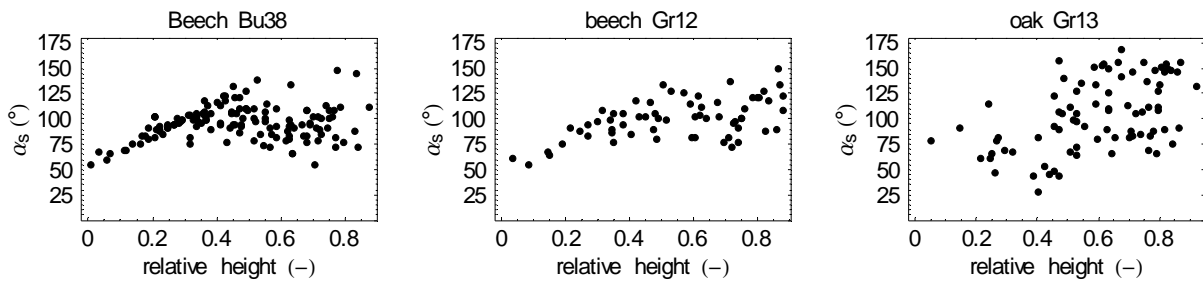


Fig. 37: Angle between leaf cloud plane and canopy surface (α_s) versus relative height in the canopy (H). The relationship for both beech trees was similar and different from that of oak Gr13.

22.4°. α_{AZ} between 20 and 21m was 60.2° and that above 21m was 65.4° on average. While a similar alternation may be seen in the crown of beech Gr12, it was not found for oak Gr13, but both tree structures have been determined with lower resolution than that of beech Bu38.

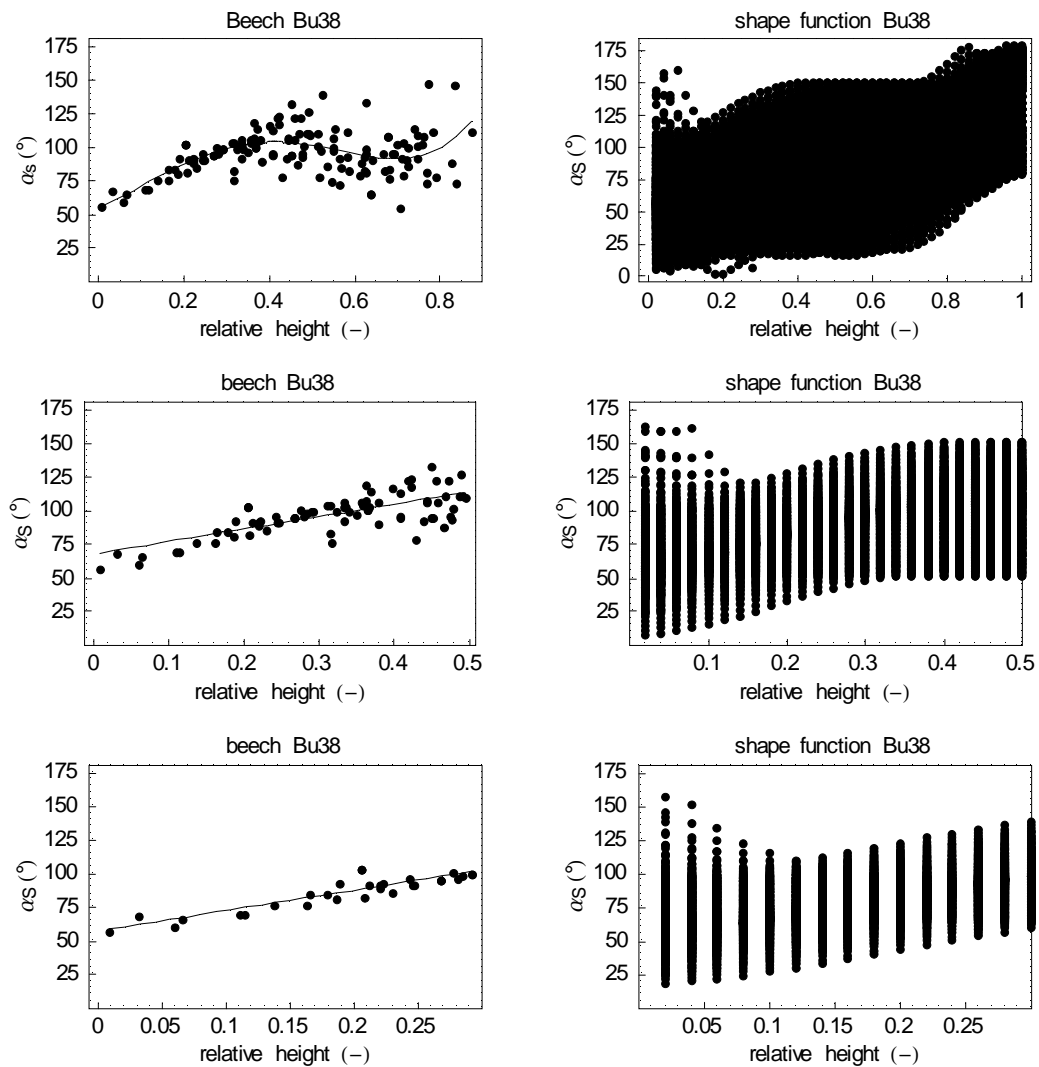


Fig. 38: The range of achievable values for α_s is limited by the applied shape function in a given height range: The observed α_{AZ} angles in a given height range (left side: whole crown, lower half of the crown, lowest 30% of the crown) may principally cause α_s -angles in the range of values that was calculated for a 10cm-grid of positions in the crown as depicted on the right side.

The angle between main growth direction of leaf clouds and the idealised canopy surface (α_s) had a similar height dependence for both beech trees, while it was different from that of oak Gr13 (Fig. 37).

The range of achievable values in this relationship is partly limited by the tree-specific canopy shape function that was derived from measured data for all trees using the same polynomial function. Fig. 38 shows that the similarity in the α_s vs. height relationship of beech crowns was not completely due to the similar canopy shape of both trees: The consideration of all α_{AZ} - angles of beech Bu38 allows a much bigger range of α_s -values than was measured and this is even true, when only the lower variation in α_{AZ} -angles from the bottom part of the crown is considered in the simulation of α_s -angles for their height range.

The similarity of main growth directions of leaf clouds from the two beech trees may also be observed without relating them to the idealised canopy shape: Fig. 39 shows the vector fields of the main growth directions of leaf clouds from both trees, i. e., the graphs from Fig. 35 two-dimensionally scaled to a common height range and superimposed.

Leaf clouds of both trees occupied nearly the same space relative to apex and crown base, which would not be the case when the vector field from oak Gr13 would be superimposed. Thus, the similar crown shape with a dent between 0.45 and 0.6 relative height is still visible. Neighbouring vectors from both trees follow often the same direction and the main patterns that have been described for beech Bu38 vectors are still valid. The alternation of height ranges with

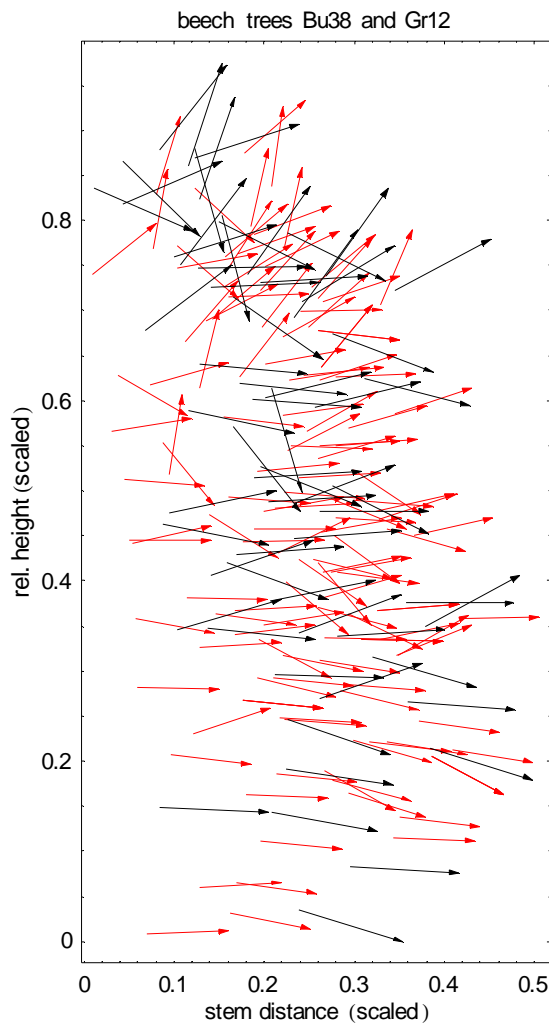


Fig. 39: Main growth direction of leaf clouds of beech Gr12 (entire, dark, and longer arrows) and of beech Bu38 (dotted, light (red), and shorter arrows). The graphs from Fig. 35 were two-dimensionally scaled to a common height range for both crowns.

more upwards and more downwards inclined leaf clouds in the lower part of the crown may still be shown, when the absolute height ranges from beech Bu38 are recalculated to relative heights (Fig. 40).

Assuming that these similarities reflect a species-specific trend in mature beech crowns, the α_s vs. height relationship of both trees was approximated with a single curve for both data sets (Fig. 41). The geometrical meaning of this curve is that leaf clouds in the crown were on average fanned-up towards the canopy surface.

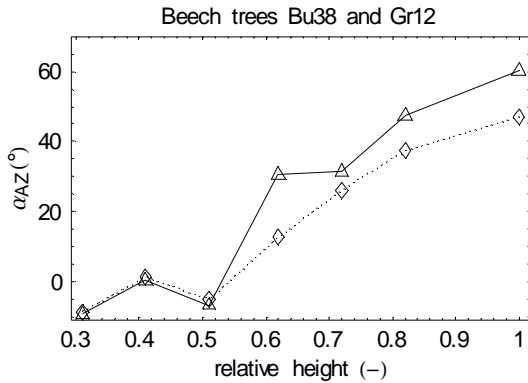


Fig. 40: Average inclination of the main growth direction of leaf clouds towards the horizon (α_{AZ}) in layers of beech trees. Open triangles represent beech Bu38, while the rhombi stand for the superimposed vector field of both beech trees (Fig. 39).

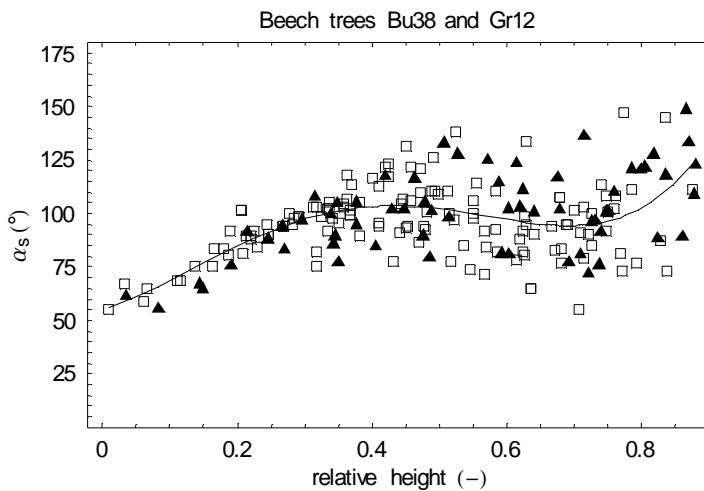


Fig. 41: A unique relationship has been drawn for the similar relationships between α_s and relative height for both beech trees (Bu38: filled triangles, Gr12: open squares). The approximated fourth order polynomial function was $y = 1259.85 x^4 - 1778.46 x^3 + 569.83 x^2 + 96.89 x + 54.83$.

2.3.5.4 Azimuth angles

Though significant correlations were not found between the azimuth orientation of the leaf cloud plane (AZ_p) and any other tree inherent quantity, the comparison between the neighbouring trees Gr12 and Gr13 reveals a significant similarity in both distributions ($r^2=0.41$, $p<0.01$, Fig. 42). Thus, the AZ_p -distribution appears not to be regularly distributed, but is possibly dependent on environmental factors that affect both trees.

A regularity of AZ_s angles could only be found in relation to the azimuth of the slope where the trees were standing. While the largest portion of leaf clouds of beech Bu38 was oriented towards the Buchenallee slope azimuth, this was not true for the Großebene trees. No significant correlations were found to the AZ_s frequency distributions, which indicates if the tree crown was developed symmetrical in all directions. The 30° angle classes of the AZ_s frequency distributions correspond to radial sectors of the tree crown. While the beech trees had the relatively most leaf clouds in the azimuth direction of the slope of their stand, oak Gr13 had the highest frequency of leaf clouds in that angle class, that was 30° closer to south (Fig. 43).

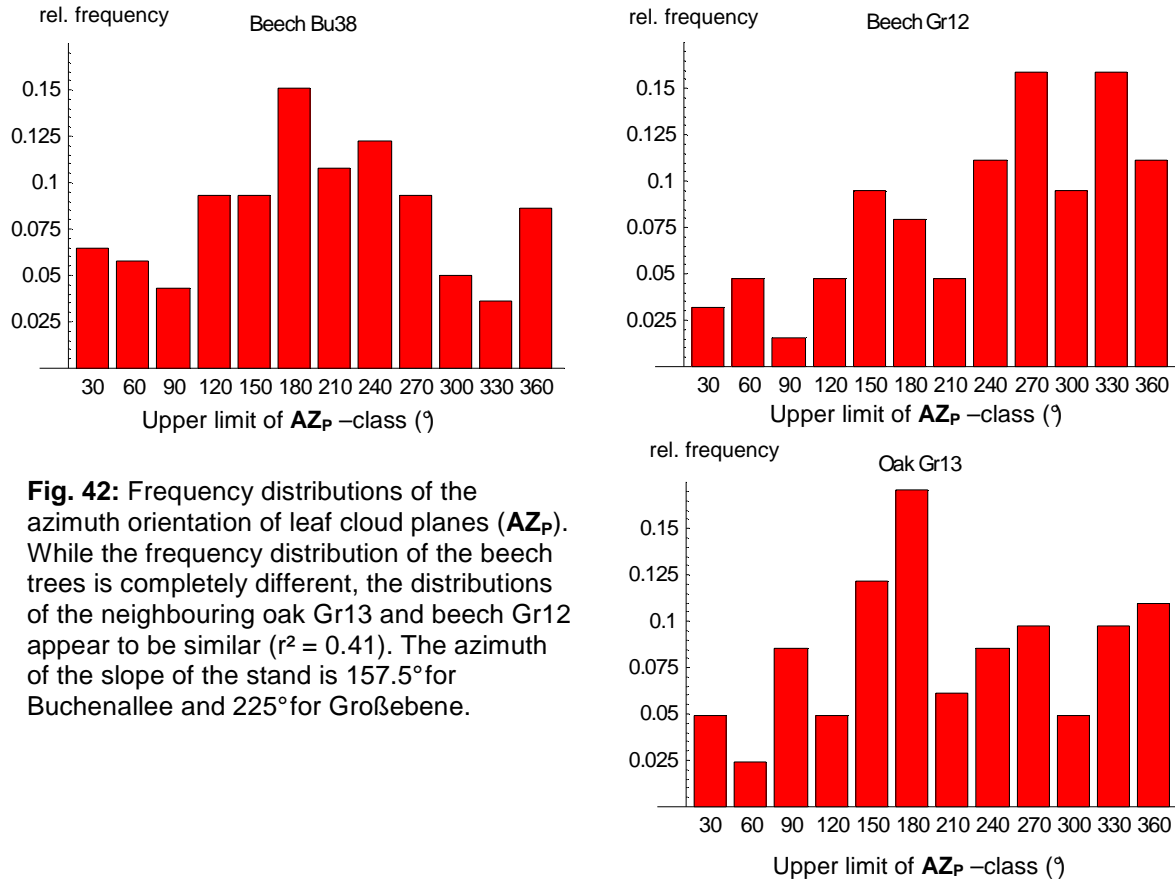


Fig. 42: Frequency distributions of the azimuth orientation of leaf cloud planes (AZ_P). While the frequency distribution of the beech trees is completely different, the distributions of the neighbouring oak Gr13 and beech Gr12 appear to be similar ($r^2 = 0.41$). The azimuth of the slope of the stand is 157.5° for Buchenallee and 225° for Große Ebene.

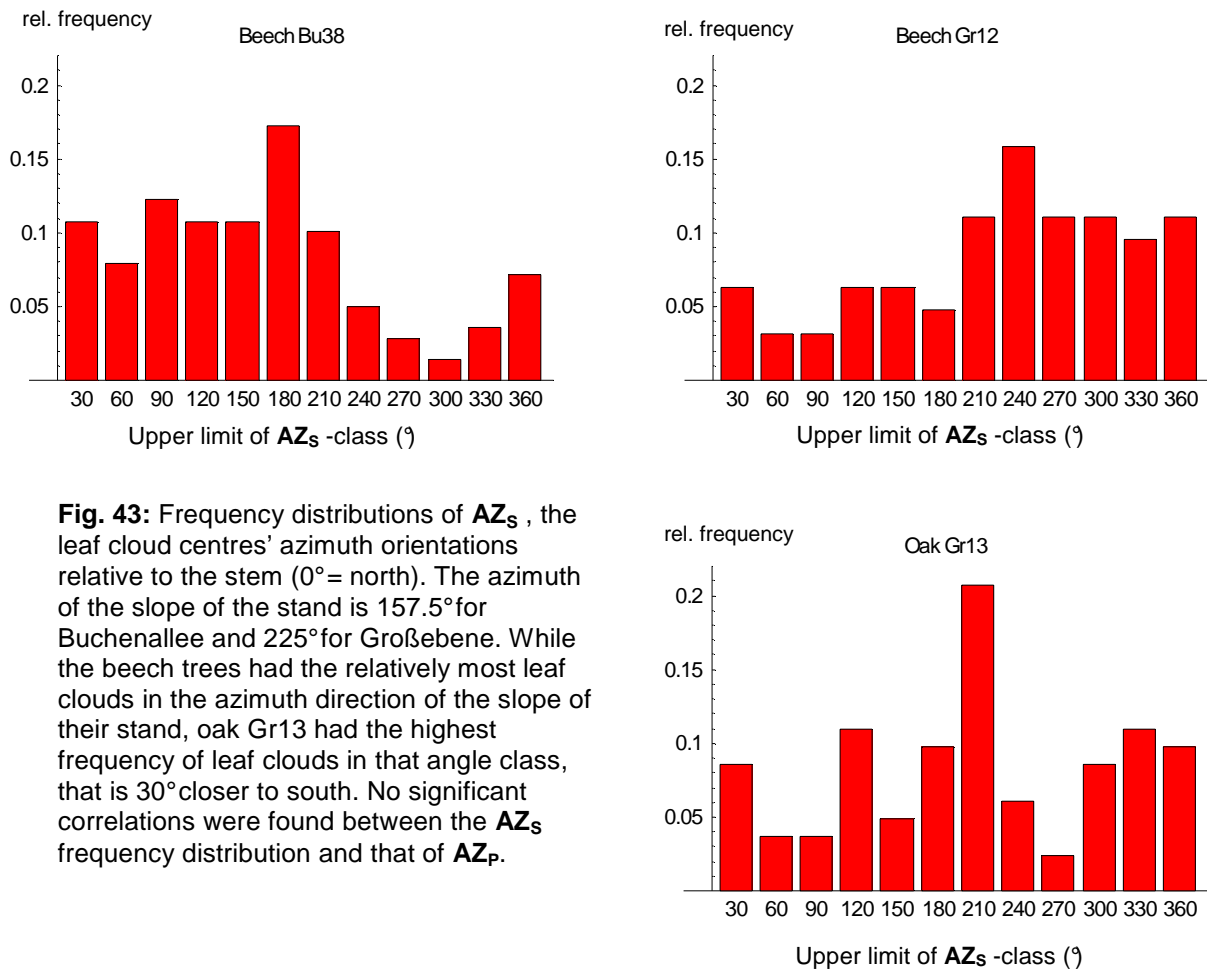


Fig. 43: Frequency distributions of AZ_S , the leaf cloud centres' azimuth orientations relative to the stem ($0^\circ = \text{north}$). The azimuth of the slope of the stand is 157.5° for Buchenallee and 225° for Große Ebene. While the beech trees had the relatively most leaf clouds in the azimuth direction of the slope of their stand, oak Gr13 had the highest frequency of leaf clouds in that angle class, that is 30° closer to south. No significant correlations were found between the AZ_S frequency distribution and that of AZ_P .

A comparison of the average leaf cloud azimuth angles (AZ_P) in 30° AZ_S -sectors is shown in Fig. 44. While the mean leaf cloud azimuth (AZ_P) in most sectors of beech Bu38 was between

south-east and south-west (135° - 225°), the leaf clouds in direction of the slopes azimuth (157.5°) are oriented towards north. The prevailing average leaf cloud azimuth of beech Gr12 sectors was between east-south-east and north-north-east (247.5° - 337.5°). No unique range of AZ_P -angles was preferred in the sector averages of oak Gr13. These results are only examples of the azimuth orientations of growth in these trees, that were evaluated in order to assure a complete representation of the data set. Further studies on other trees would be necessary to investigate if the found tendencies have a general meaning.

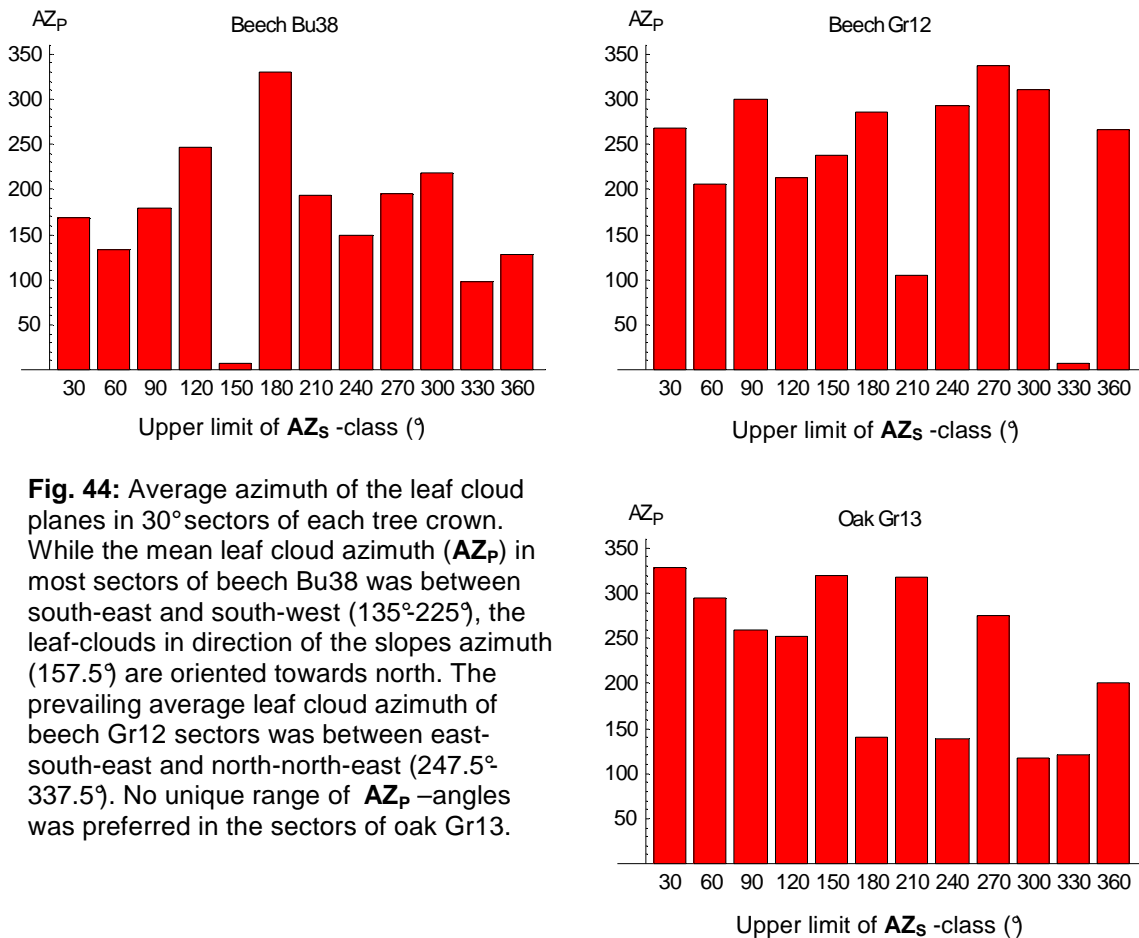


Fig. 44: Average azimuth of the leaf cloud planes in 30° sectors of each tree crown. While the mean leaf cloud azimuth (AZ_P) in most sectors of beech Bu38 was between south-east and south-west (135° - 225°), the leaf-clouds in direction of the slopes azimuth (157.5°) are oriented towards north. The prevailing average leaf cloud azimuth of beech Gr12 sectors was between east-south-east and north-north-east (247.5° - 337.5°). No unique range of AZ_P -angles was preferred in the sectors of oak Gr13.

2.3.5.5 Spatial extension of leaf clouds

The quantities which describe the spatial extension of leaf clouds are partially dependent on each other, because projected area and height range may be used to calculate a volume around the leaf cloud plane with two horizontal borders above and below and vertical borders along the leaf cloud shape towards the side. The relationship between projected area times height range (**area * Hrange**) and calculated volume (**volume**) of the leaf cloud enveloping polyhedron is shown in Fig. 45. It was better correlated for oak Gr13 ($r^2=0.9$) than for beech Bu38 ($r^2=0.67$) and beech Gr12 ($r^2=0.74$). The slope of the linear equations was very similar for all trees (0.30, 0.30, and 0.33 for the trees Bu38, Gr12, and Gr13, respectively).

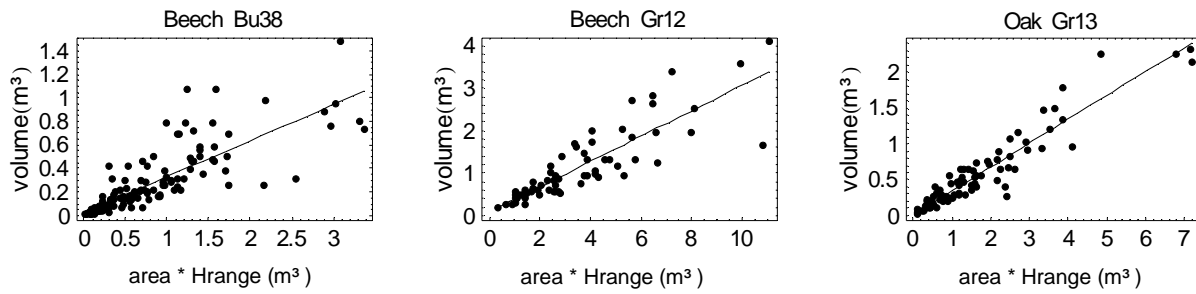


Fig. 45: The relationship between projected area times height range (**area * Hrange**) and calculated volume (**volume**) of the leaf cloud enveloping polyhedron was better correlated for oak Gr13 ($r^2=0.9$) than for beech Bu38 ($r^2=0.67$) and beech Gr12 ($r^2=0.74$). The slope of the linear equations was 0.30, 0.30, and 0.33 for the trees Bu38, Gr12, and Gr13, respectively.

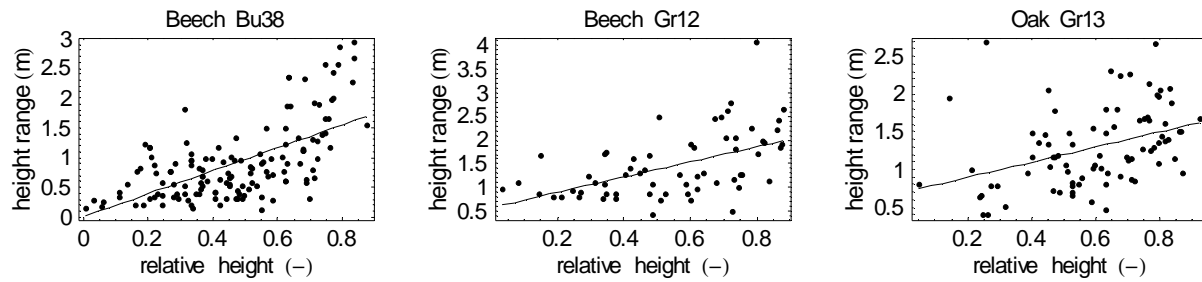


Fig. 46: The height extension of the leaf clouds (**Hrange**) showed a significant ($p<0.001$) tendency to increase with relative height in the canopy. R^2 -values were higher for the beech trees (0.38 and 0.28, respectively) than for oak Gr13 (0.14).

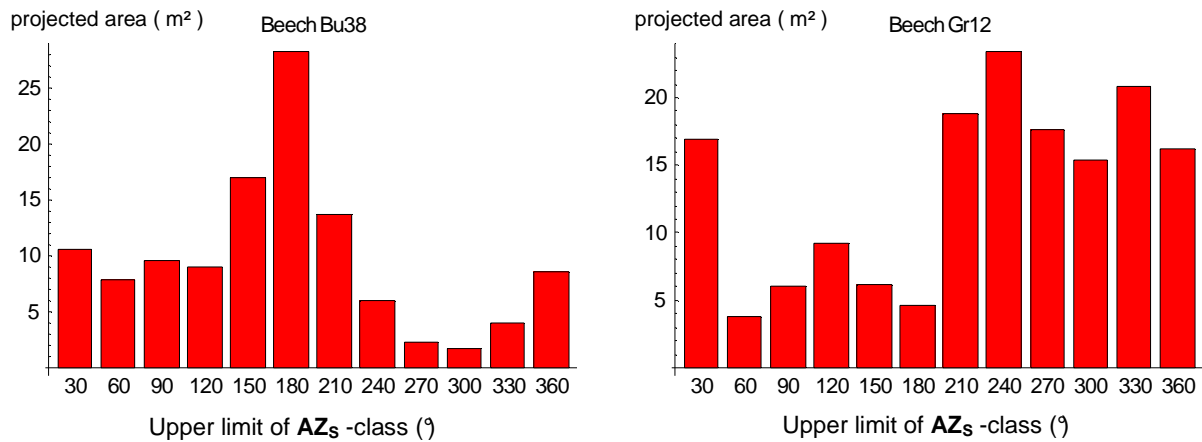
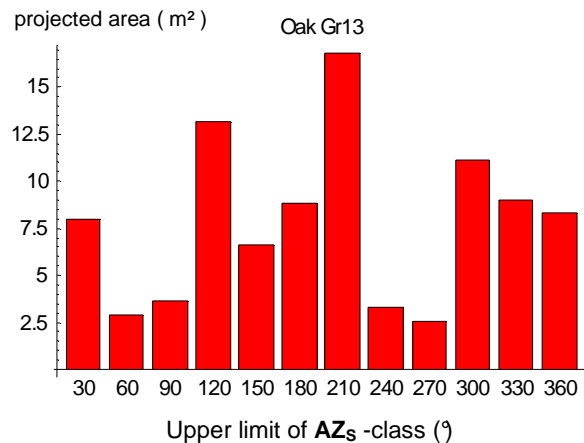


Fig. 47: Projected area of leaf clouds (**area**) summed for twelve different **AZ_s**-angle classes (radial sectors of the tree crown). The distribution pattern is similar to Fig. 43 and shows that the beeches had the highest amount of leaf cloud projected area in direction of the slope of their stand (157.5° and 225°) and that they preferred a unique range of angles for strengthened development, while **area** of oak Gr13 leaf clouds was highest in that angle class that is 30° closer to south than the slope of the Großebeene stand (225°).



area, **volume**, and **Hrange** were only weakly correlated to height or position of the leaf cloud. The strongest relationship was found between **Hrange** and **H** (Fig. 46) with coefficients of determination below 0.4. R^2 -values were only in some cases higher than those of Fig. 46, when the relations are based on the crown environmental properties **CLA**, **CVOL**, or **CLAD**. For

example the relationship between **Hrange** and **CVOL** had an r^2 of 0.45 for beech Bu38 and the relationship between **Hrange** and **CLAD** slightly improved the r^2 -value of oak Gr13 to 0.16.

Only minor changes to the patterns of frequency distributions of **AZ_s** in Fig.43 were detected, when volume (data not shown) or projected area (**area**) of the leaf clouds in each 30° angle class of **AZ_s** are considered. The position of the leaf cloud centre relative to the stem was decisive for the classification of leaf clouds. Figure 47 shows that the beeches had the largest amount of leaf cloud projected area in the direction of the slope of their stand (157.5° and 225°) and that they preferred a unique range of angles for strengthened development, while **area** of oak Gr13 leaf clouds was highest in that angle class that is 30° closer to south than the slope of the Große Ebene stand (225°). In addition to this, oak Gr13 shows strengthened development in three different **AZ_s** -angle ranges (90-120°, 180-210°, and 300-390°) when compared to the sectors between these ranges.

2.3.5.6 Leaf area densities of leaf clouds

Leaf area densities of leaf clouds could be key parameters to a leaf cloud oriented 3D-light-model of single trees and it was therefore necessary to investigate in some detail if they are randomly distributed in the canopy space or if they depend on any other quantity, which would facilitate the parameterisation of a leaf cloud oriented light model.

Measured leaf area densities were partly influenced by the measurement method. Leaves of very small leaf clouds were often arranged along one branch axis or in one plane, so that gaps between two branches or between different leaf-layers did not occur. This increased their calculated leaf area density. Additionally, very small leaf clouds often had a more regular form that fits more accurately into a plane bordered polyhedron than those of larger leaf clouds. Both

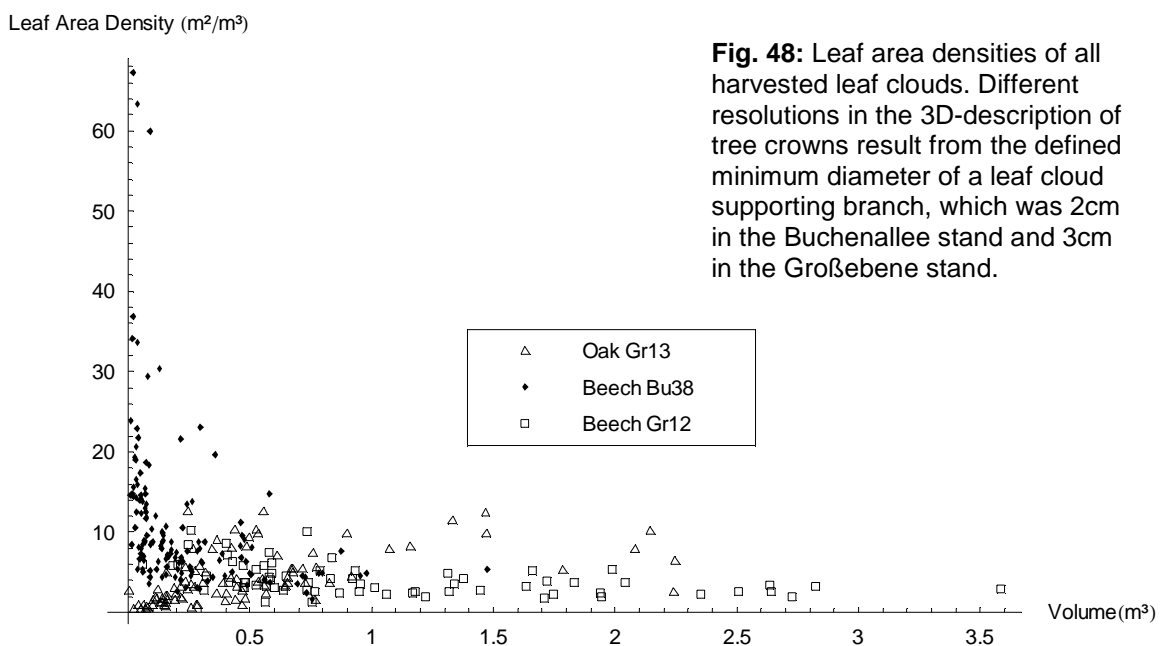


Fig. 48: Leaf area densities of all harvested leaf clouds. Different resolutions in the 3D-description of tree crowns result from the defined minimum diameter of a leaf cloud supporting branch, which was 2cm in the Buchenallee stand and 3cm in the Große Ebene stand.

effects led to some extremely high leaf area densities in very small leaf clouds of beech Bu38, as can be seen in Fig. 48. Therefore, geodetic measurements on the Großebene trees were performed without considering very small leaf clouds as separate units (see methods). Then no similar effects were observed (compare Fig. 48). Leaf area densities were in the range of 1.63-67.7 m²/m³ in beech Bu38 (139 leaf clouds), 1.31-10.2 m²/m³ in beech Gr12 (66 leaf clouds) and 0.26-13.5m²/m³ in oak Gr13 (88 leaf clouds).

No clear relationship of leaf area density could be demonstrated by regression analysis on each of the investigated leaf cloud properties (see above) for each tree. However, when leaf area densities of leaf clouds were averaged per height layer, all trees showed a more or less clear tendency to increase leaf area densities of leaf clouds with height. (Fig. 49).

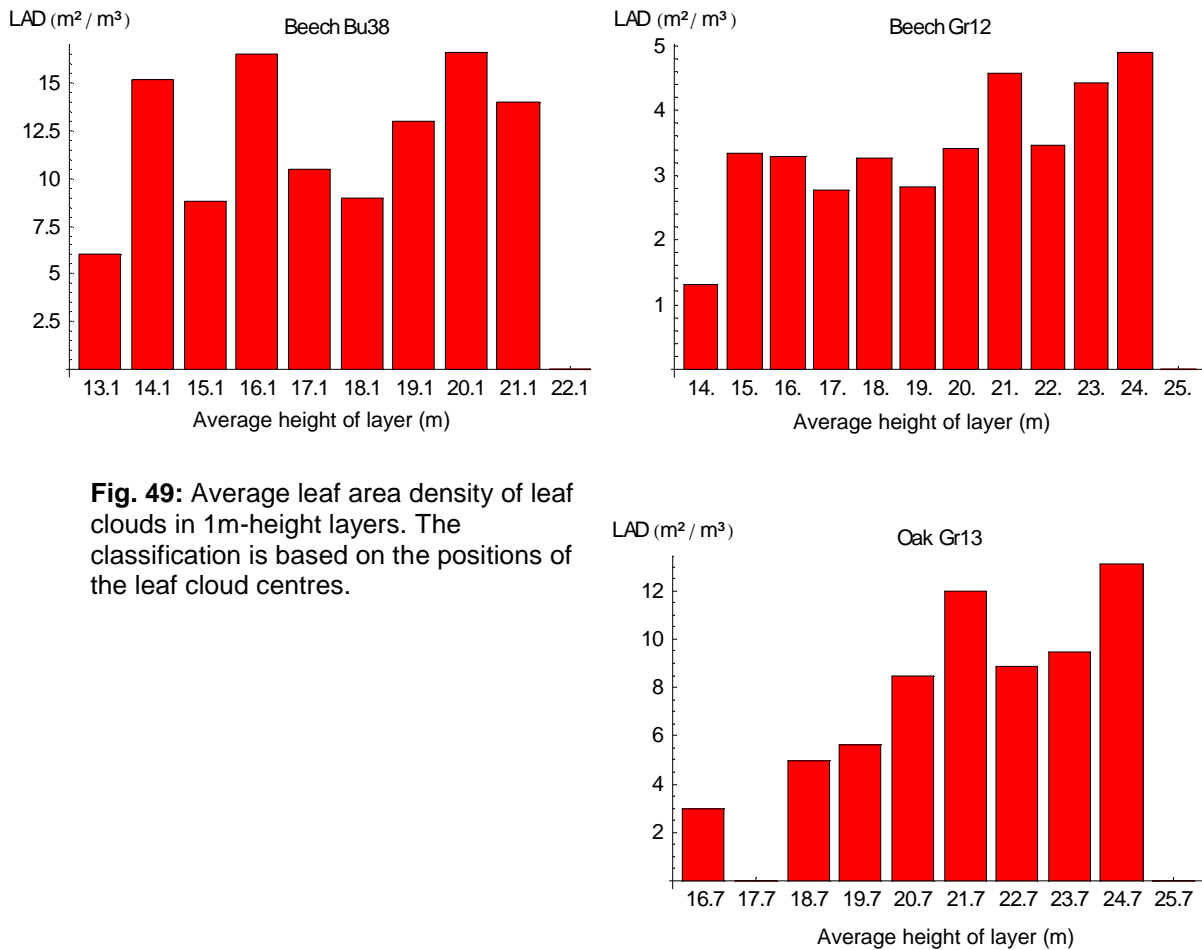


Fig. 49: Average leaf area density of leaf clouds in 1m-height layers. The classification is based on the positions of the leaf cloud centres.

The average leaf area densities of leaf clouds in distinct radial sectors of the trees are shown in Fig. 50. A weak similarity in the angular distributions of **LAD** has been found between the beeches in the different stands ($r^2 = 0.22$) and it turned out that this was due to a remarkable similarity of the angular distribution in the north half of the crowns ($r^2 = 0.80$, $p < 0.05$), which was also found, when the angle classes were larger (45° : $r^2 = 0.93$, $p < 0.05$) or smaller (15° : $r^2 = 0.56$, $p < 0.01$). Though no similarity was found to the oaks angular distribution of **LAD**, this might be chance and can not be interpreted as species-specific. Apart from this similarity, **LAD** was irregularly distributed over **AZ_s**-angle classes. A comparison of the angular **LAD**-distribution of the neighbouring trees oakGr13 and beech Gr12 (Fig. 51) shows that neighbourhood effects could have an influence on **LAD** of oak leaf clouds: The sectors with high average **LAD** of leaf

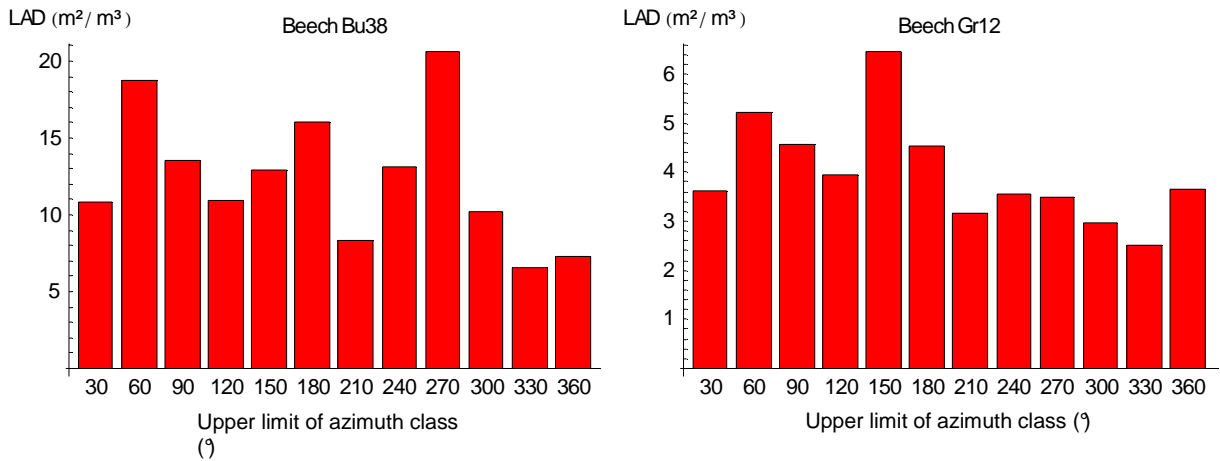


Fig. 50: Average leaf area densities (LAD) of leaf clouds in radial sectors of the tree crown given by the azimuth of the leaf cloud centre relative to the stem (AZ_S).

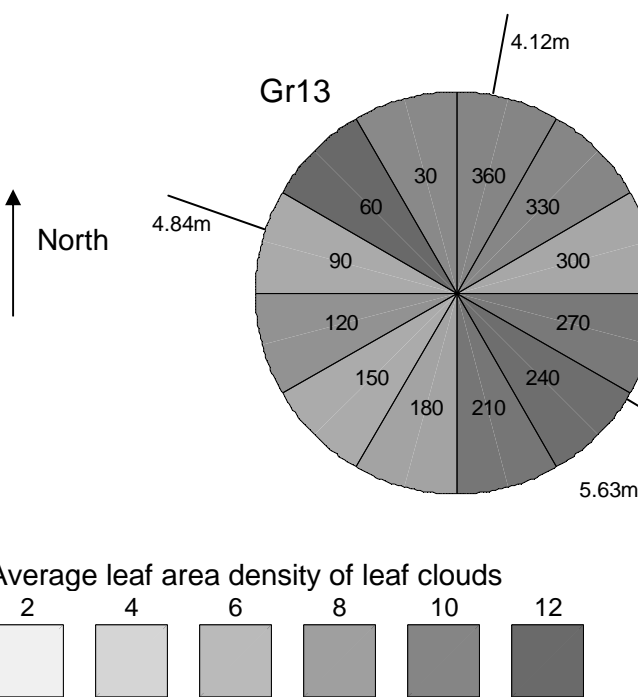
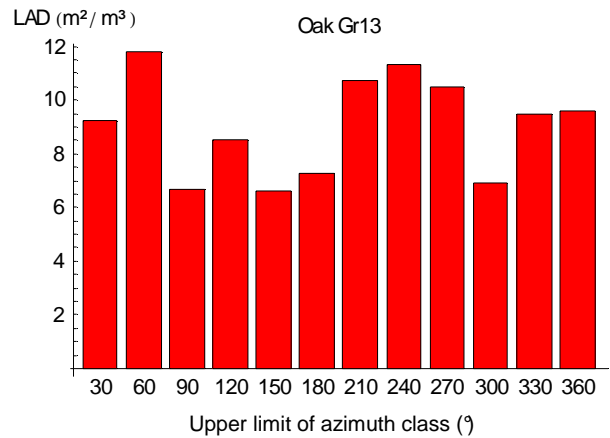
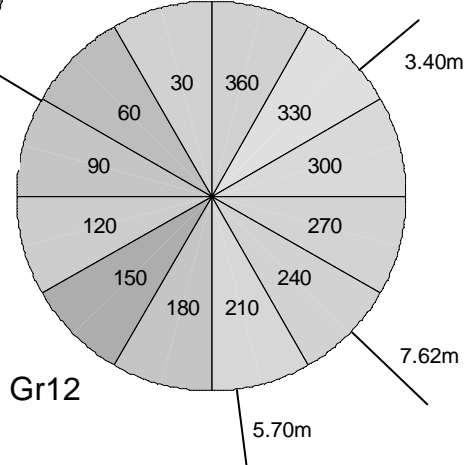


Fig. 51: Average leaf area densities of leaf clouds in radial sectors of the canopies of beech Gr12 and oak Gr13. The crowns are situated in their stems' relative angular position to each other. Angles and distances towards the nearest neighbouring trees are indicated.



clouds were more or less clearly directed towards the three closest tree stem positions of neighbouring trees. Beech Gr12 did not show this coincidence.

Data of the three trees were separately used for a multiple regression analysis of **LAD** on 8 quantities (**H**, **N**, **E**, α_h , absolute value of α_h , **AZ_p**, **AZ_s**, **Area**). The quantities were chosen because of their expected potential to explain leaf area density distribution inside tree crowns:

- Leaf area densities are likely to increase with height (**H**), because leaves cannot survive without light and the lower parts of the crown get less light than the upper parts. Nevertheless it is questionable if this effect may be found in leaf area densities of leaf clouds, because the absolute amount of leaves in a height layer depends on leaf area density of leaf clouds and as well on leaf cloud density in the height layer. Though number and leaf area density of leaf clouds were low in the lowest layers of crowns of oak and beeches (Fig. 19b), no obvious trend in leaf area densities of leaf clouds was found in relation to height (data not shown).
- A dependence of leaf area density on distances to the stem in east and north direction, leaf cloud inclination at the point of attachment, or azimuth orientation relative to the stem (**E**, **N**, α_b , **AZ_p**, **AZ_s**) could reflect a species-specific internal organisation scheme of the tree crown. For example, if the leafless space in the central part of the crown develops via partial thinning of leaves of leaf clouds over time, this should have a remarkable effect on the relationship between distances (**E,N**) and leaf area density, or if leaf clouds on the south side of the canopy would have generally higher leaf area densities when they were oriented to the east, this would affect the relationship between **LAD** and the azimuth angles.
- Angle and projected area of the leaf cloud plane (α_p , **Area**) may be correlated with leaf area density because they have a major influence on light harvesting of the leaf cloud and, thus, may be influential if leaf area densities partly depend on the light situation.

Because regression analysis assumes normal distribution of the dependent variable (ENGEL 1997), the probability density functions of leaf area density data was analysed. A first logarithmic transformation showed much better agreement with the normal distribution than the original distribution (for example beech Bu38, see Fig. 52).

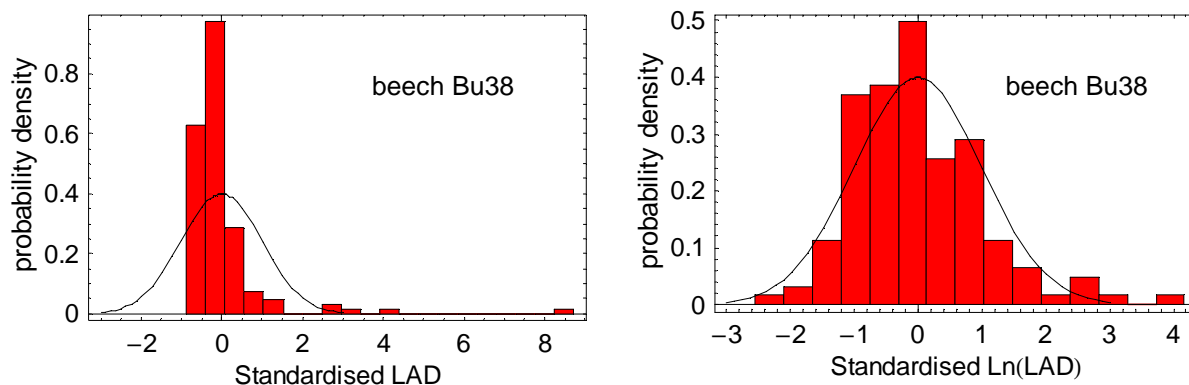


Fig. 52: Comparison of the distribution of leaf area densities of leaf clouds of beech Bu38 (left side) with the normal distribution. The same data after logarithmic transformation are in better agreement with the normal distribution. The original data were standardised by shifting their mean value to zero and scaling their variance to unity.

This was confirmed by an r^2 -value of 0.97 for the relationship between probability densities of $\text{Log}(\text{LAD})$ and the corresponding values of the normal distribution. The original data were

standardised for comparison with the normal distribution by shifting their mean value to zero and scaling their variance to unity. A scatter plot of both quantities (normal probability plot, see Fig. 53) reveals a curvilinear relationship behind this r^2 -value, indicating that the log-normal distribution is left skewed in the case of beech Bu38 (compare Fig. 52).

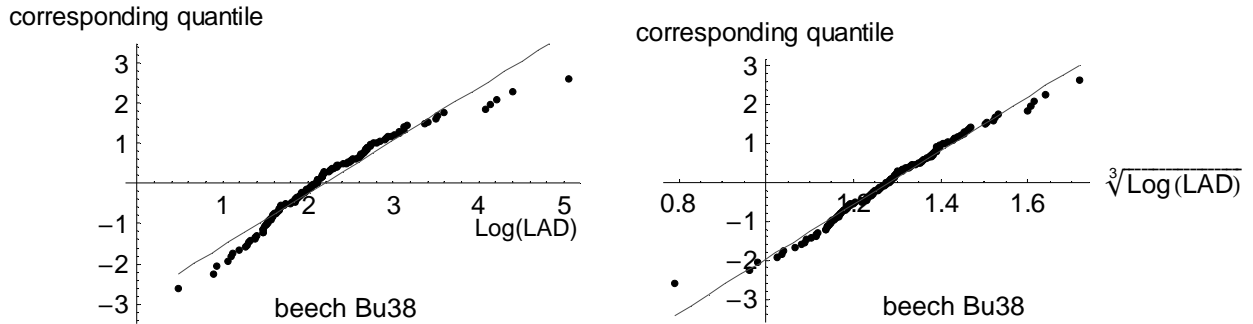


Fig. 53: Normal probability plots of logarithmic transformed LAD data of beech Bu38 against corresponding quantiles of the normal distribution and the cubic root logarithmic transformation of LAD against corresponding quantiles of the normal distribution. The cubic root transformation made the relationship more linear and improved the regression from $r^2=0.97$ to $r^2=0.993$.

Thus, a second transformation taking the cubic root of $\text{Log}(\text{LAD})$ was employed to make the relationship more linear, resulting in an r^2 -value of 0.993 to the normal distribution. The cubic root transformation was found by the maximum-likelihood method according to (Box & Cox 1964), where the conditional maximised log likelihood of a given power transformation with respect to the normal distribution is calculated and iteratively evaluated for a range of exponent values. The same procedure for the Großebene trees led to the transformation $\text{Log}^{3/2}(\text{LAD})$ for both trees ($r^2=0.986$ for beech Gr12 and $r^2=0.996$ for oak Gr13). Because the natural logarithm of the lowest LAD-value of beech Gr12 was negative (-0.48), a constant of 0.5 had to be added to enable the Box-Cox transformation, which requires positive values.

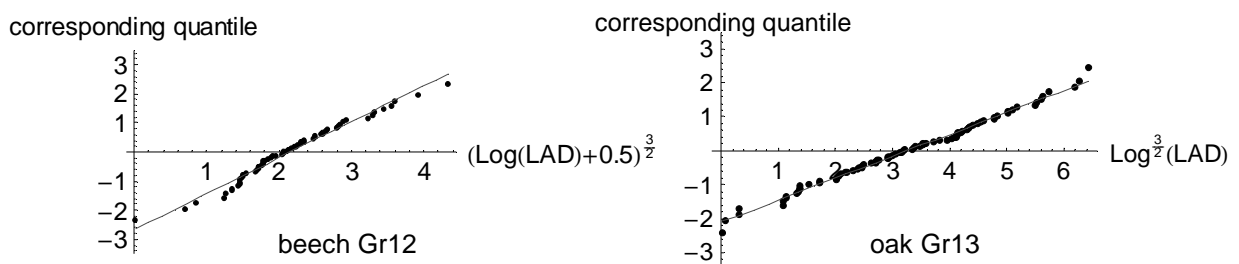


Fig. 54: Normal probability plots of transformed LAD data of beech Gr12 (left) and oak Gr13 (right) against corresponding quantiles of the normal distribution.

Multiple regressions were based on a linear combination of all quantities of the form

$$y_i = \beta_1 f_{1i} + \beta_2 f_{2i} + \dots + \beta_p f_{pi} + e_i \quad (8)$$

where y_i is the i^{th} response, f_{pi} is the p^{th} quantity evaluated at the i^{th} case, and e_i is the error of the i^{th} case. Estimates of the coefficients β_i are calculated to minimise the residual sum of squares.

The multiple regression for the transformed **LAD**-values showed no strong influence of any single variable nor of a combination of these variables. This was also valid when products of all pairs of the questionable variables and power-transformations of the variables were linearly included in the multiple regression. The most significant combination of independent variables for beech Gr12 were **Area * H**, **H**, and **E**, but a fitted model of these three variables explained only 41% of the observed variance, though it was significant with $p < 0.01$. The same variable combination was found to be most significant for beech Bu38 ($r^2 = 0.36$, $p < 0.01$), while in oak Gr13 the most significant combination was $\text{Log}(\text{Area})$, **H**, and **AZ_s** ($r^2 = 0.36$, $p < 0.01$). An application of the model

$$y_i = \beta_1 \text{Area} H + \beta_2 H + \beta_3 E \tag{9}$$

to **LAD** data of oak Gr13 yielded a slightly worse correlation ($r^2 = 0.29$, $p < 0.01$, see Fig. 55).

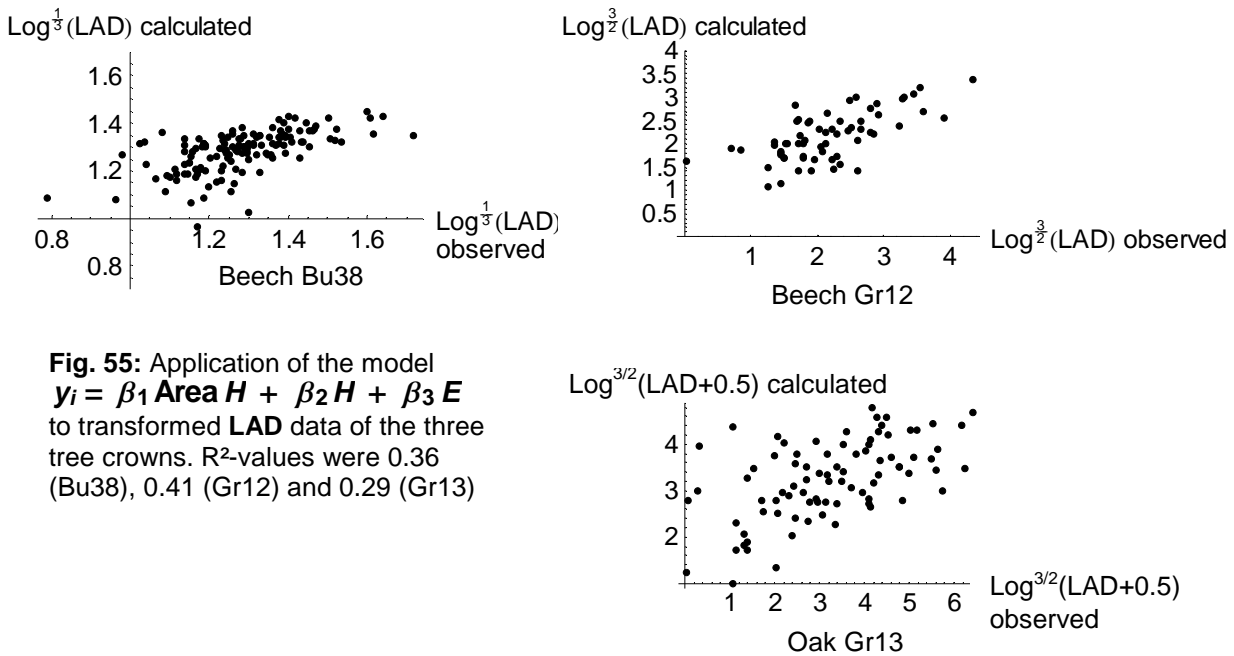


Fig. 55: Application of the model $y_i = \beta_1 \text{Area} H + \beta_2 H + \beta_3 E$ to transformed **LAD** data of the three tree crowns. R^2 -values were 0.36 (Bu38), 0.41 (Gr12) and 0.29 (Gr13)

A comparison of the coefficients for this model (see table 4) shows that **H** had a much bigger influence on the calculation for oak than for the beeches and that **E** was – in association with the other variables - negatively correlated to transformed **LAD** data for the beeches while it was positively correlated for oak Gr13. **LAD** was negatively correlated to **Area*H**, which is proportional to the canopy volume directly below the leaf cloud and sums to a constant value with **Area *(1-H)**, which is proportional to the canopy volume directly above the leaf cloud. The influence of **Area*H** is partly explained by its correlation to leaf cloud volume ($r^2 = 0.6$, 0.38, and

Table 4: model coefficients

	β_1	β_2	β_3
Beech Bu38	-0.35	0.20	-0.002
Beech Gr12	-0.69	1.41	-0.19
Oak Gr13	-1.74	4.59	0.08

0.51 for beeches Bu38 and Gr12 and oak Gr13, respectively), which is part of the calculation of **LAD**.

The low coefficients of determination found for the relationships between LAD of leaf clouds and 8 potentially relevant quantities show that LAD of leaf clouds may - in a first approximation - be considered in a 3D-light model as randomly distributed.

2.3.5.7 Wood area densities of leaf clouds

Projected area of leaf cloud wood was estimated on a sub-sample of 20 leaf clouds of beech Bu38. Projected area of the dry samples was measured 3 years after their harvest and an average weight loss of only 0.37% during this time confirms that the samples were already dry enough after 6 days in the oven. The average relationship between projected area and dry weight of wood was $3.54 \pm 0.78 \text{ m}^2/\text{g}$. This factor was used to estimate projected area of woody organs of each leaf cloud. Weight of woody organs was correlated to leaf biomass of leaf clouds ($r^2 = 0.77$, Fig. 56) and also the relationship between projected area of wood and leaf area was well correlated ($r^2=0.83$, Fig. 56). Thus, wood area density was strongly correlated to leaf area density and therefore constant relationships can be employed to calculate it from leaf area density or vice versa.

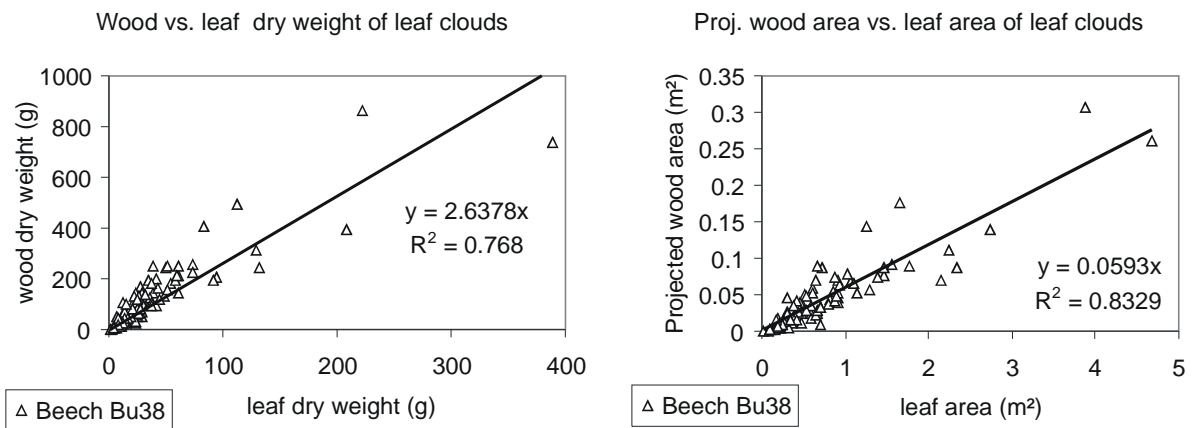


Fig. 56: Weight and area relationship between leaves and woody organs of leaf clouds of beech Bu38.

2.4 Interpretation of investigations on leaf clumping and arrangement

The investigations of leaf clumping and leaf cloud arrangement in the crowns show that the general assumption of homogeneous distribution of leaf area in the canopy is not valid on a single tree basis, thus supporting hypothesis **H1**. Instead the three investigated crowns consisted of more than 80% leafless spaces between leaf clouds (Fig. 25) and these were in part arranged to form coherent cavities, leafless central spaces, and leaf layers. This led to a natural partitioning of the tree crowns into 2-3 distinguishable crown sections with large amounts of leaf area that were separated by leaf-poor layers (Fig. 21). The proportion of gaps between leaf clouds was the main cause for the different leaf area densities of height layers of all three canopies.

The shape of oak crowns in the investigated stands was generally different from those of the beech trees, which supports hypothesis H3. This may be concluded from the height of maximum crown breadth of 106 trees from the Steigerwald stands, which was in oak on average higher (80% of total height) than that of beech trees (67% of total height). The different

height of maximum crown breadth was confirmed with a polynomial approximation to maximum extensions of crown layers from beech Bu38, beech Gr12, and oak Gr13 (Fig. 26), where the height of maximum breadth was 68%, 66%, and 84% of total height, respectively. The large horizontal extension of layers in the upper mid-part of the crown altered the crown shape of oak from that of beech trees.

While the beech trees grew asymmetrically preferring a unique range of azimuth angles in the direction of their stands exposition for enhanced growth, oak Gr13 developed strongly in several separate directions (Fig. 47). This produced an asterisk like, concave shape to the crown projection of oak Gr13, while the crown projections of both beech trees were largely convex (Fig. 17 and Fig. 18). Leaf area densities of leaf clouds of oak were particularly high in those crown sectors adjacent to even high neighbouring trees, whereas the azimuth sector of the crown of beech Gr12 with high leaf area density of leaf clouds was in direction of a gap in the stand (Fig. 51). The angle of leaf clouds was dependent on height in beech trees, but not in oak Gr13 (Fig.33) and leaf cloud height ranges were more strictly dependent on leaf cloud angles in the beech crowns (Fig. 34).

Different space capture strategies were observed on the trees Gr12 and Gr13. Higher leaf area densities and lower gap fractions were generally found in the uppermost layers of all trees, which was clearest for beech Gr12 (Fig. 23, Fig. 25). The tendency to build some single leaf layers with extremely high leaf area densities was also found in all trees, but it was stronger in the trees of the mixed stand Großebeene (Table 5) and strongest in beech Gr12. Through the combination of both strong tendencies, beech Gr12 managed to produce a higher leaf area density in a higher region than the neighbouring oak Gr13, though oak Gr13 was 0,7m taller and had more leaves (also more leaves in the upper part of the crown). The volume of the uppermost height layers was higher in oak Gr13 than in beech Gr12. Thus, the arrangement of leaves in layers of beech Gr12 was optimally used to cast a deep shadow on leaves in the surrounding stand. The leaf area of oak Gr13 casted less deep shadow on probably more leaves by occupying large volumes in the upper region, thereby exhibiting lower leaf area densities. The consequences for self-shading of these strategies were estimated to be more severe for oak Gr13 than for beech Gr12 (Figs. 30-32).

The canopy structure of even mature beech trees is still stamped by a species-specific growth scheme. While the leaf clouds of oak Gr13 appeared to be more irregularly arranged, a regular, fan-shaped formation of leaf clouds opening towards the canopy surface was observed in both beech tree crowns and supports hypothesis **H2** in that the arrangement of leaf clouds in beech is regular. The similarity in branch orientations from two beech trees in different stands suggests a deterministic growth scheme that is detectable even after decades of development. The fan-shaped formation of branches probably enables radiation coming from the side to penetrate deeper into the crown. Considering that the source of reflected and transmitted radiation in a tree canopy is not a point-source but may be assumed to be equally distributed over the canopy surface, shade leaves of beech might better profit from reflected and transmitted radiation or from direct radiation in the early morning or in the evening, when the sun stands close to the horizon. Even if the light gain due to this structural orientation would in some periods and for some leaves be as low as only $10 \mu\text{mol}/(\text{m}^2\cdot\text{s})$, these leaves would likely be able to improve their assimilation rate in the order of $0.5 \mu\text{mol}/(\text{m}^2\cdot\text{s})$ due to the strong inhibitory effect of even low light intensities on respiration rates (ATKIN ET AL. 2000). Thus, hypothesis **H2** is plausible though not provable, due to the low number of investigated trees.

Useful dependencies for the 3-dimensional description of tree crowns were found for the measurement of leaf cloud volumes on the base of projected area and height range of the leaf clouds (Fig. 45). Canopy leaf area and canopy volume above a certain leaf cloud may be described with single-parametric equations. Leaf area densities of leaf clouds were largely irregular and the description with an empirical model remains insufficient, though a weak height dependence existed for LAD of leaf clouds of oak Gr13 (2.3.5.6).

Resolutions for the description of tree crown structure may be too low but also too high. While 1m height layers could not adequately express the partitioning of tree crowns into 2-3 crown sections (Figs. 21, 22), a high resolution during the geodetic measurements caused artificially high leaf area densities for small leaf clouds (Fig. 48). The LAI of single trees may strongly be underestimated, when concavity of crown projections is not considered (Figs. 16, 17).

3 Spatial distribution of leaf properties in tree crowns

3.1 Materials and methods

Additional to the harvested leaves of each leaf cloud of the trees Bu38, Bu45, Gr12, and Gr13 that were used for leaf area and dry weight determinations (see 2.1.4), single leaves were chosen for the determination of leaf angle, leaf form parameters, leaf area, leaf dry weight, nitrogen content, carbon content, relative irradiance, and leaf photosynthetic capacities. These leaf measurements took place in July and August 1997 and 1998 on the standing trees with a highlift (see 2.1.1), i. e., after the structural measurements and before the biomass harvests of them. The sampled leaves of the Buchenallee trees were taken in different heights along four vertical lines per tree at the upper border of leaf clouds. Selected leaves of the GroÙebene trees were taken in different light situations on those 12 leaf clouds that were used by M. SCHMIDT (DEPARTMENT OF PLANT ECOLOGY, UNPUBLISHED) for sapflow measurements.

3.1.1 Structural leaf parameters

At least ten leaf angles (defined as the angle between leaf blade and horizon) per investigation point were measured with a plummet equipped protractor in direction of the steepest inclination of the optically estimated mean planes of the leaves. The angle of 10-15 branches and twigs in the above surrounding of each sampled leaf of the Buchenallee trees to the horizon was also measured. Considering that most leaves were not entirely flat but occupy a space of 0.5 to 3cm in height, width and height of this space were measured as leaf-form parameters on beech and oak leaves. Leaf area and width of the flat leaf were measured after detaching with the portable leaf area meter CI-202 (CID, Idaho, USA), averaging 5 repetitions. Each leaf was oven-dried (80°C for at least 48h), dry weight was determined and leaf mass per area (LMA) was calculated. Nitrogen and carbon content of each leaf was measured with an elemental analyser (CHN-O-Rapid, Foss Heraeus GmbH, Hanau, Germany).

The measured leaf angle distribution of at least 30 leaf angles was fitted using a one-parametric ellipsoidal function, which is based on the assumption that the angular distribution of leaf area in the canopy is identical to the distribution of area on the surface of an oblate spheroid (CAMPBELL 1986, CAMPBELL & NORMAN 1989). The single parameter k is the ratio between horizontal and vertical semi-axis of the ellipsoid, so that the distribution becomes the spherical distribution at $k = 1$. When $k > 1$ (oblate spheroid), the function is given as:

$$f(\theta) = \frac{2k^2 \sin \theta}{M(\cos^2 \theta + k^2 \sin^2 \theta)^2} \quad , \quad (10)$$

with

$$M = 1 + \frac{\ln\left(\frac{1 + \sqrt{1 - k^2}}{1 - \sqrt{1 - k^2}}\right)}{2k^2 \sqrt{1 - k^2}} \quad . \quad (11)$$

3.1.2 Relative irradiance

Hemispherical photographs (Minolta MF camera equipped with Soligor 0.15x fisheye adapter, Soligor GmbH, Leinfelden-E., Germany) were taken above each sampled leaf in the Buchenallee stand and as a spot check above 8 leaves in the Großebene stand. From the hemispheric images, the fractions of penetrating diffuse solar radiation of open sky (I_D , diffuse site factor) and of potential penetrating direct solar radiation of open sky (I_B , direct site factor) were calculated according to EVANS & COOMBE (1959) and ANDERSON (1964). The diffuse site factor, I_D , was computed from the measurements of relative area of canopy gaps (9 sky bands, 40 angle districts in each sky band) for uniformly overcast sky conditions. The direct site factor, I_B , was found as the hourly evaluated canopy gap fraction along solar tracks between 22nd of April and 22nd of August, which were calculated based on standard equations from LINACRE (1992) and GATES (1980). Both I_D and I_B calculations took account of the angular distribution of diffuse and direct radiation over the sky, and the angular fractions were cosine corrected to assess radiation incident on a horizontal plane (s. EVANS & COOMBE 1959, ANDERSON 1964). Relative irradiance (Q_{rel}), i. e., the quantum flux density over the period from 22nd of April to 22nd of August 1997 for a specific leaf in relation to the quantum flux density for this period above the canopy was calculated as:

$$Q_{rel} = I_D F_D + I_B F_B \quad , \quad (12)$$

where F_D is the relative proportion of integrated above-canopy diffuse quantum flux density, which sums to 1 with F_B , the relative proportion of integrated above-canopy direct quantum flux density (Niinemets et al. 1998). F_D and F_B were 0.46 and 0.54, as derived from measurements of diffuse and direct radiation at the BITÖK investigation site Waldstein in the Fichtelgebirge (Fig. 1) during April 22 – August 22, 1998. Total solar radiation at the Waldstein was measured with the pyranometer CM-11 (Kipp & Zonen) and diffuse radiation with another pyranometer (Model 8101, Philipp Schenk GmbH Wien & Co KG, Austria) equipped with a shadow band.

3.1.3 Gas-exchange Measurements

Gas-exchange measurements were performed with the portable open photosynthesis measurement system LI-6400 (LiCor Inc., Lincoln, Nebraska, USA) directly on each of the leaves at their location inside the canopies of beech Gr12 and oak Gr13 before the hemispherical photo was taken. On each leaf, 3 A/C_f -curves were measured at high, low, and ambient temperature (span: ca. 15°C), under the saturating PPFD of 2000 $\mu\text{mol}/(\text{m}^2 \cdot \text{s})$, which was achieved with the appertaining LED red light source with a peak centred at 670nm in the spectral output. External CO_2 -concentration was varied between 50, 150, 350, 600, 1000 and 1500 $\mu\text{mol}/\text{mol}$, while vapour pressure deficit between air and leaf (around 2 mmol/mol) was

held constant during each curve. A total coefficient of variation of 2% over the last 30 seconds was allowed to assure stability of the measurement conditions in the chamber. This total coefficient of variation is the sum of the coefficients of variation for CO₂-concentration, water vapour concentration, and flow rate. The two IRGAS for sample and reference gas analysis were matched automatically before each date was recorded.

Transpiration (E), stomatal conductance (g_{sw}), net photosynthesis (A), and intercellular CO₂-concentration (C_i) were calculated with the OPEN software, which is part of the LI-6400 and is based on the equations derived by VON CAEMMERER & FARQUHAR (1981). The underlying equations are:

$$E = \frac{u_i (w_o - w_i)}{ar (1 - w_o)} \quad , \quad (13)$$

where u_i is the measured incoming flow rate of the chamber (mol/s), w_i and w_o are measured incoming and outgoing water mole fractions (mol H₂O / mol air), and ar is leaf area (m²).

Stomatal conductance to water vapour, g_{sw} (mol H₂O / (m²*s)), is obtained from the total conductance by removing the contribution from the boundary layer:

$$g_{sw} = \frac{1}{\frac{1}{g_{tw}} - \frac{k_f}{g_{aw}}} \quad . \quad (14)$$

Here g_{tw} is the total leaf conductance to water vapour and g_{aw} is the boundary layer conductance (mol H₂O / (m²*s)), which is corrected by the correction factor k_f . k_f is given by

$$k_f = \frac{K^2 + 1}{(K + 1)^2} \quad , \quad (15)$$

where K is the fraction of stomatal conductances of one side of the leaf to the other, which is close to 0, when nearly all stomata are on one side of the leaf as in beech or oak leaves (STRASBURGER 1991).

Total leaf conductance to water vapour, g_{tw} (mol H₂O / (m²*s)), is given by

$$g_{tw} = \frac{E \left(1000 - \frac{W_i + W_s}{2} \right)}{W_i - W_s} \quad , \quad (16)$$

with the sample water mole fraction W_s (mmol H₂O / mol air) and W_i , the molar concentration of water vapour within the leaf (mmol H₂O / mol air), which is computed from leaf temperature and atmospheric pressure.

Net photosynthesis A (μmol / (m²*s)) is calculated as

$$A = \frac{u_i (C_i - C_o)}{ar} - EC_o \quad , \quad (17)$$

where c_i and c_o are incoming and outgoing mole fractions of carbon dioxide (mol CO₂ / mol air).

The intercellular CO₂ concentration (C_i) is given by

$$C_i = \frac{\left(g_{tc} - \frac{E}{2} \right) C_s - A}{g_{tc} + \frac{E}{2}} \quad . \quad (18)$$

Here C_s is the mole fraction of CO₂ in the sample air stream (μmol CO₂ / mol air) and g_{tc} is the total conductance to CO₂ (mol CO₂ / (m²*s)), given by

$$g_{tc} = \frac{1}{\frac{1.6}{g_{sw}} + \frac{1.37 k_f}{g_{aw}}} \quad . \quad (19)$$

The results allowed the calculation of temperature normalised values for carboxylation capacity ($V_{c_{max}}$), electron transport capacity (J_{max}) and day respiration (R_d) with the program RACCIA (see below).

Additional estimations of J_{max} , the electron transport capacity were achieved by chlorophyll fluorescence measurements. They were performed using the portable pulse-modulation fluorometer PAM-2000 (Heinz Walz GmbH, Effeltrich, Germany), equipped with leaf clip holder 2030-B, on some of the oak leaves before the gas-exchange measurement on the same leaves. These leaves were darkened for at least 30 minutes with aluminium foil to enable one measurement of minimum and maximum fluorescence, F_o and F_m , with a saturating light pulse on dark adapted leaves (SCHREIBER ET AL. 1994). Fluorescence of the illuminated leaves (F_m') was afterwards determined with saturating light pulses of increasing light intensities up to 2500 $\mu\text{mol}/(\text{m}^2\cdot\text{s})$ or even more, when the resulting light response curve of the electron transport rate did not yet appear to saturate. At least three repetitions per light level were done. Quantum yield of the illuminated leaves (Y) was calculated as

$$Y = (F_m - F_m') / F_m' \quad (20)$$

(SCHREIBER ET AL. 1994). The electron transport rate J was calculated according to GENTY ET AL. (1989):

$$J = 0.5 * 0.84 * Y * I \quad (21)$$

where I is incident quantum flux density and the factor 0.84 accounts for absorptance of leaves. Electron transport capacity J_{max} was found as electron transport rate J at a quantum flux density of 2000 $\mu\text{mol}/(\text{m}^2\cdot\text{s})$, which was determined by extrapolation of the measured electron transport rates at other quantum flux densities on the base of equation (29), which was fitted to the maximum measured values per light level.

3.1.4 Evaluation of A/C_i -curves with RACCIA

The measurement of A/C_i -curves has been described as a cumbersome procedure in the past (LAISK & LORETO 1996), which is probably due to the necessity of long stabilisation times for the conditions in the chamber after changing the C_a -value and to the use of large CO_2 -storage and mixing systems, that made it necessary to work in the laboratory. This situation has changed to some extent due to the development of small portable photosynthesis measurement systems with small CO_2 -mixing units, small cuvettes, short distances for gas-supply and IRGA-measurements, and automatic immediate calculations on the measured data, which facilitate the assessment of stability of cuvette conditions. Therefore much more data can be measured in the same time and have to be evaluated. The program RACCIA (Routine for A/C_i curve evaluation) was developed to automate the time-consuming derivation of species-specific key parameters of leaf photosynthesis from these measurements, as they are used in different variations of the Farquhar model of leaf photosynthesis (FARQUHAR & VON CAEMMERER 1982). Because this is typically done by non-linear fits on a low number of data points along the A/C_i curve (HARLEY & TENHUNEN 1991), a plausibility check is enabled by automatic graphical representation of the data and each fit on the screen during the automatic evaluation process. RACCIA is based on the equations of the HARLEY/TENHUNEN photosynthesis model (HARLEY & TENHUNEN 1991), which links a modification of the biochemical Farquhar model (FARQUHAR &

VON CAEMMERER 1982) with the Ball/Berry model of stomatal conductance (BALL ET AL. 1987), and on the calculation of day respiration and CO₂-compensation point according to BROOKS and FARQUHAR (1985).

3.1.4.1 The HARLEY/TENHUNEN model of leaf photosynthesis

The HARLEY/TENHUNEN model basically expresses net assimilation rate (**A**) as the sum of carboxylation rate (**V_c**), oxygenation rate (**V_o**), and day respiration (**R_d**), i. e., the rate of CO₂-evolution from processes other than photorespiration that continues in the light:

$$\mathbf{A} = \mathbf{V}_c - 0.5 \mathbf{V}_o - \mathbf{R}_d \quad (22)$$

(all quantities in μmol/(m²*s)). Photorespiration losses are expressed dependent on **C_i** and the photocompensation point **Γ*** (μmol/mol), that **C_i**-value, at which **A** would be 0, if no other source of respiration than oxygenation of ribulose-1,5-bisphosphate catalysed by rubisco would occur. It is assumed that **V_c** is limited by the velocity of three processes, so that equation (22) is transformed to the common form of balance equation of most photosynthesis models:

$$\mathbf{A} = \left(1 - \frac{\Gamma^*}{\mathbf{C}_i}\right) \min\{\mathbf{W}_c, \mathbf{W}_j, \mathbf{W}_p\} - \mathbf{R}_d \quad (23)$$

W_c denotes the carboxylation rate limited by rubisco activity and **W_j** is the carboxylation rate limited by regeneration of RuBP in the Calvin-cycle, which is light dependent. The phosphate limited carboxylation rate **W_p** is not included in most photosynthesis models and was not considered in the parameter derivation with RACCIA nor in leaf gas exchange calculations with the HARLEY/TENHUNEN model.

The remaining two expressions for **W_c**-limited assimilation rate (**A_v**) and **W_j**-limited assimilation rate (**A_j**) are basically the same as in (FARQUHAR & VON CAEMMERER 1982):

$$\mathbf{A}_V = \mathbf{V}_{c_{\max}} \frac{\mathbf{C}_i - \Gamma^*}{\mathbf{K}_{M,C}(1 + \mathbf{O}/\mathbf{K}_{M,O}) + \mathbf{C}_i} - \mathbf{R}_d \quad (24)$$

Here **V_{c,max}** stands for the enzyme-specific maximum rate of carboxylation, **K_{M,C}** (μmol/mol) and **K_{M,O}** (mmol/mol) stand for the Michaelis-Menten constants of rubisco (ribulose-1,5-bisphosphate carboxylase-oxygenase) for carboxylation and oxygenation of ribulose-1,5-bisphosphate, and **O** (209 mmol/mol air at 101.3 kPa atmospheric pressure) is the leaf internal O₂-concentration.

W_j is given as

$$\mathbf{W}_j = \frac{\mathbf{P}_m}{1 + 2\Gamma^*/\mathbf{C}_i} \quad , \quad (25)$$

with **P_m** (μmol/(m²*s)), the CO₂ saturated rate of photosynthesis at any given irradiance and temperature. On the assumption that 4 electrons are required for the regeneration of a single RuBP in the Calvin cycle, **A_j** is expressed as

$$\mathbf{A}_J = \mathbf{J} \frac{\mathbf{C}_i - \Gamma^*}{4\mathbf{C}_i + 8\Gamma^*} - \mathbf{R}_d \quad , \quad (26)$$

where J ($\mu\text{mol e}^-/(\text{m}^2\text{s})$) is the electron transport rate over the thylakoid membrane and equals $4P_m$. Γ^* in the above equations is defined as

$$\Gamma^* = \frac{0.5 O}{\tau}, \quad (27)$$

with the dimensionless rubisco specificity factor τ . Temperature dependence of this parameter and also of $K_{M,C}$, $K_{M,O}$, and R_d is expressed in exponential equations, which were converted in the used version of the leaf model to be based on the parameter values at a temperature of 298.16K:

$$\text{parameter} = \text{parameter}_{298} * \text{Exp}\left[\frac{H_a * (T - 298.16)}{298.16 R T}\right] \quad (28)$$

parameter_{298} stands for the temperature dependent parameter at a temperature (T) of 298.16K, R is the gas constant, and H_a (J/mol) is the activation energy for the parameter.

P_m and thereby J is the only light dependent quantity:

$$P_m = \frac{\alpha I}{\sqrt{1 + \frac{\alpha^2 I^2}{P_{ml}^2}}} \quad (29)$$

(Smith-equation). Here I ($\mu\text{mol}/(\text{m}^2\text{s})$) is incident quantum flux density, P_{ml} is P_m at light saturation, and α (mol/mol) stands for the initial slope of the curve relating CO_2 -saturated photosynthesis to irradiance. P_m and P_{ml} in this equation may be replaced by J and J_{max} (maximum electron transport rate), when α is multiplied by four.

The temperature dependence of P_{ml} and Vc_{max} is described in a 4-parametric thermodynamic equation (JOHNSON ET AL. 1942, SHARPE & DEMICHELE 1977), which may be expressed based on the parameter value at a temperature of 298.16K:

$$Vc_{max} = Vc_{max, 298} \text{Exp}\left[\frac{H_a(T - 298.16)}{298.16 R T}\right] \frac{1 + \text{Exp}\left[\frac{298.16 S - H_d}{298.16 R}\right]}{1 + \text{Exp}\left[\frac{S T - H_d}{R T}\right]} \quad (30)$$

Here, $Vc_{max, 298}$ stands for the parameter value at $T = 298.16$ K, H_a and H_d (J/mol) are the energies of activation and deactivation for Vc_{max} , and S (J/(K*mol)) stands for a Vc_{max} -specific entropy term. The same equation with P_{ml} or J_{max} -specific energies and entropy term is applied for P_{ml} or J_{max} .

A in the above equation system is dependent on C_i , which is in turn dependent on A and stomatal conductance g_{sw} :

$$C_i = C_a - 1.6 A / g_{sw} \quad (31)$$

C_a ($\mu\text{mol}/\text{mol}$) stands for the external CO_2 -concentration and 1.6 accounts for the different diffusivities of water vapour and CO_2 in air. Additionally, g_{sw} is linearly dependent on A and C_a as was first described by BALL ET AL. (1987):

$$g_{sw} = g_{min} + \frac{g_{fac} A h_s}{C_s} \quad (32)$$

Here g_{min} (mol/(m²*s)) is the constant cuticular conductance for water vapour, h_s (-) and C_s (μmol/(m²*s)) are relative humidity and CO₂-concentration on the leaf surface and g_{fac} is an empirically found factor that is derived from (BALL ET AL. 1987). To calculate h_s and C_s from rh (external relative humidity) and C_a , the boundary layer conductance for water vapour (g_{aw} , mol/(m²*s)) is taken into account (FALGE 1997):

$$h_s = rh - \frac{rh - 1}{1 + \frac{g_{aw}}{g_{sw}}} \quad (33)$$

$$C_s = C_a - \frac{1.37(C_a - C_i)}{1.37 + 1.6 \frac{g_{aw}}{g_{sw}}} \quad (34)$$

The used version of the model solves iteratively for C_i , thereby finding that C_i -value that is compatible with net assimilation rate A (equation (23)) and stomatal conductance g_{sw} (equations (32), (33), and (34) combined), and where A and g_{sw} are related according to equation (31).

3.1.4.2 RACCIA routine for species-specific parameterisation

The species-specific parameterisation of the HARLEY/TENHUNEN model and other Farquhar models with RACCIA is focused on the determination of three key parameters that are not rubisco-specific. Due to the - among higher plants - similar structure of the rubisco molecule and its highly conserved active sites (KELLOGG & JULIANO 1997), species-specific variations in rubisco kinetic parameters ($K_{M,C}$, $K_{M,O}$, τ , Γ^*) are expected to be relatively small (BERNACCHI ET AL. 2001). *In vitro* measured values for τ and Γ^* of many different species generally vary about ±20% around a mean value of 2560 (dimensionless) and 42 μmol/mol at 25°C for all species (EPRON ET AL. 1995), and rather big (±10%) intra-specific variations were found under the same measurement conditions (PARRY ET AL. 1987). However, also single outlying measurements (-50% for τ and +100% for Γ^*) exist for *Fagus sylvatica* and *Castanea sativa* (EPRON ET AL. 1995). The *in vivo* derivation of τ and Γ^* from *Nicotiana tabacum* and *Spinacia oleracea* (VON CAEMMERER ET AL. 1994) yielded τ -values of 2710 and 2975, which equals Γ^* -values of 38.8 and 35.3 μmol/mol at 25°C, when oxygen concentration O is assumed to equal 210000 μmol/mol (equation 29). These measurements are the only ones, where carboxylation dependent limitation of the assimilation rate is assured by the use of transgenic plants with low rubisco content.

The term $K_{M,C}(1+210 / K_{M,O})$ from the calculation of A_V (equation (24)) varies for the low number of measured species between 410 and 750, (MAKINO ET AL. 1988, HARLEY & TENHUNEN 1991, VON CAEMMERER ET AL. 1994, BERNACCHI ET AL. 2001), though $K_{M,C}$ and $K_{M,O}$ are not expected to vary among higher plants (VON CAEMMERER ET AL. 1994). It has been argued that this variation might be due to the *in vitro* measurement method. The two newer measurements use transgenic *Nicotiana tabacum* plants that shall assure the rubisco limitation of assimilation for *in vivo* measurements and end up with 710 and 746 for the term mentioned above (VON CAEMMERER ET AL. 1994, BERNACCHI ET AL. 2001).

Rubisco-specific parameters and their temperature dependencies may, thus, be considered as constant among higher plants, meaning that species-specific variations in assimilation rates that are not due to stomatal limitations prevalingly result from the quantities P_{ml} , $V_{C_{max}}$, R_d , and α .

RACCIA and the appertaining photosynthesis measurements were designated to estimate the quantities P_m , $V_{c_{max}}$, and R_d that are crucial for the calculation of leaf gas-exchange, because α is the most conservative parameter out of the four and may approximately be estimated to equal 0.06 mol CO₂/mol photons among C₃ species under most conditions (HARLEY & TENHUNEN 1991, EHLERINGER & BJÖRKMAN 1977).

While equations (24) and (26) are a common part of most so-called Farquhar models, different types of equations are employed to describe light dependence of electron transport rate J , temperature dependencies, and effects of stomatal regulation, if considered. The original Farquhar model (FARQUHAR & VON CAEMMERER 1982) for example employs a hyperbolic relationship instead of equation (29) to express the saturating relationship of electron transport rate J on irradiance I :

$$J = \frac{J_{max} I}{I + 2.1 J_{max}} \quad (35)$$

The factor 2.1 in this equation has to be changed under certain conditions. J_{max} stands here for the electron transport capacity, the maximum electron transport rate under saturating light conditions, and it is by definition of J and P_m equal to $4P_m$. RACCIA can be used to derive both quantities, when A/C_r -measurements are made at light saturation, because it then only uses the common equations (24) and (26).

Published values for J_{max} and $V_{c_{max}}$ range from 17 to 372 $\mu\text{mol}/(\text{m}^2\cdot\text{s})$ and from 6 to 194 $\mu\text{mol}/(\text{m}^2\cdot\text{s})$ (WULLSCHLEGER 1993), which has due to the multiplication in equations (24) and (26) an immense impact on calculated species-specific photosynthesis rates. The effect of day respiration (R_d) is often smaller due to its additive consideration and rather low absolute values: Published estimates of R_d at about 25°C according to the method of LAISK (1977) and BROOKS & FARQUHAR (1985) lie prevalingly in the range from 0 to 0.8 $\mu\text{mol}/(\text{m}^2\cdot\text{s})$ (HÄUSLER ET AL. 1996, HÄUSLER ET AL. 1999, JACOB & LAWLOR 1993, HERPPICH ET AL. 1998, BROOKS & FARQUHAR 1985, SUMBERG & LAISK 1995, LAISK & LORETO 1996, ATKIN ET AL. 1997), but also higher values were measured (3.4 $\mu\text{mol}/(\text{m}^2\cdot\text{s})$ for *Encelia farinosa*, ZHANG ET AL. 1995), partly with another method (1.1 $\mu\text{mol}/(\text{m}^2\cdot\text{s})$ for *Pinus sylvestris*, WANG ET AL. 1996).

RACCIA first calculates R_d as the negative assimilation rate that would be measured at $C_i = \Gamma^*$, prolonging the linear initial slope of each A/C_r -curve towards lower values (see Fig. 57, BROOKS & FARQUHAR 1985). The needed Γ^* -value is calculated from the temperature dependence of Γ^* and τ , which are connected by equation (27). The used temperature dependence has been found by JORDAN & OGREN (1984) on spinach and was confirmed by later measurements on spinach and wheat (BROOKS & FARQUHAR 1985), French bean (GHASHGHAIE & CORNIC 1994), potato (HÄUSLER ET AL. 1999), and *Eucalyptus pauciflora* (ATKIN ET AL. 2000), where it is expressed as a formula:

$$\Gamma^* = \Gamma^*_{25} + 1.88 (T - 298.16) + 0.036 (T - 298.16)^2 \quad (36)$$

However, a different temperature dependence was found for *Epilobium hirsutum* at temperatures below 18°C (GHASHGHAIE & CORNIC 1994). A Γ^* -value of 38.8 $\mu\text{mol}/\text{mol}$ at 25°C and 210,000 $\mu\text{mol}/\text{mol}$ oxygen concentration in the air was derived from the measurements of

VON CAEMMERER ET AL. (1994) and was applied considering equation (27) and correcting O for air pressure of the measurement.

The temperature dependent Michaelis-Menten constants for rubisco catalysed oxygenation and carboxylation, $K_{M,O}$ and $K_{M,C}$, are calculated according to equation (28) based on the measurements of VON CAEMMERER ET AL. (1994) and the specific H_A -values of HARLEY & TENHUNEN (1991), which are similar to those from BERNACCHI ET AL. (2001).

The data points below $350 \mu\text{mol/mol}$ CO_2 -concentration inside the leaf intercellular spaces (C_i) are then used for a non-linear regression (based on the Levenberg-Marquardt method) of equation (24) on each curve, thereby assuming that $V_{C_{max}}$ is limiting photosynthesis in that part of the curve, so that $A = A_V$ (Fig. 57).

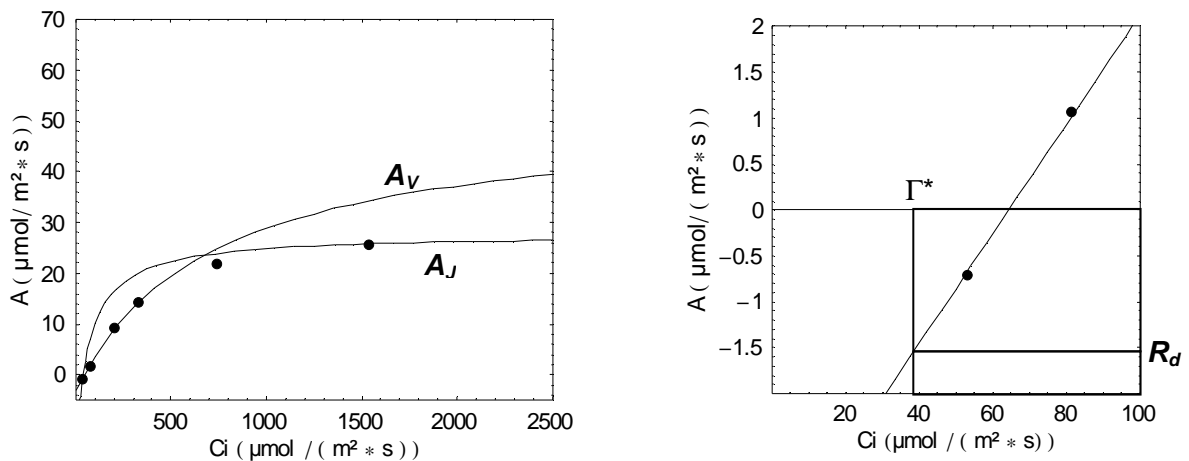


Fig. 57: Determination of $V_{C_{max}}$ and J_{max} with non-linear approximations of equations (24) and (26) (left graph), and determination of R_d from the initial slope of the A/C_i -curve.

Similarly, equation (26) is fitted to the points above $350 \mu\text{mol}/(\text{m}^2 \cdot \text{s})$, where $V_{C_{max}}$ is not limiting and J_{max} is equal to J due to saturating irradiance ($2000 \mu\text{mol}/(\text{m}^2 \cdot \text{s})$) during the measurement. RACCIA then evaluates groups of A/C_i -curves that belong to the same leaf (or to the same group of leaves, if desired) and were measured at different temperatures. A non-linear regression of equation (30) is performed on the calculated $V_{C_{max}}$ values of these A/C_i -curves versus temperature. An additional data point in the $V_{C_{max}}$ versus temperature diagram results from complete enzyme inactivation of rubisco, which was shown to occur at 60°C (GEZELIUS 1975). At least three additional $V_{C_{max}}$ values at different temperatures are necessary, because equation (30) is used to estimate four parameters.

The same equation for J_{max} is fitted to the J_{max} values of at least three A/C_i -curves at different temperatures again completed by a Zero-value, which was estimated from ARMOND ET AL. (1978) and NOLAN & SMILLIE (1976) to occur at 50°C . 4 data points were sometimes not enough for these approximations, especially when the measured values were close to each other, so that a completely different shape of the curve better fulfilled the requirements of the χ^2 merit function given by the sum of squared residuals. In this case, data points were weighted and an additional Zero-value at -30°C was added with 10% of the weight of the measurement-derived data to assure that the functional relationship starts with low values at 0°C instead of very high ones.

3.2 Results

3.2.1 Light and height dependence of leaf properties

3.2.1.1 Relative Irradiance

Beer's law is the reason to expect an exponential decrease of relative irradiance with depth in the canopy (MONSI & SAEKI 1953). The decrease of relative irradiance at the position of sampled leaves with vertical distance from the tree apex was close to exponential in the dominant beech Bu38 ($r^2=0.91$) and no significant differences were found in the decrease of relative irradiance between its 4 vertical lines of investigation points. Relative irradiances from the subdominant tree Bu45 were much more scattered ($r^2 = 0.44$, Fig. 58).

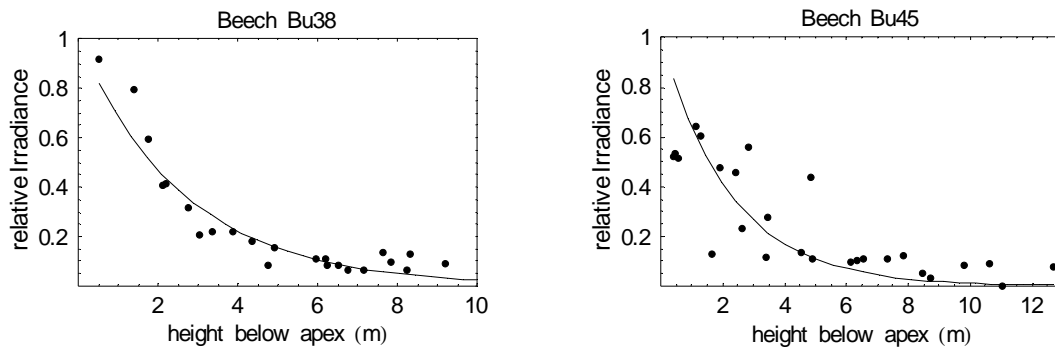


Fig. 58: Exponential decrease of relative irradiance in the tree crowns with vertical distance to their apex. The approximated lines were $y = \text{Exp}[-0.3764x]$ ($r^2 = 0.91$) for beech Bu38 and $y = \text{Exp}[-0.4428x]$ ($r^2 = 0.44$) for beech Bu45.

An explanation for the higher scatter in the data of the subdominant tree Bu45 is that its light climate is much more dependent on neighbouring trees than that of beech Bu38. Therefore, depth in the canopy is often higher than the vertical distance to the tree apex. This has been considered by separate approximations on the four vertical lines of investigation points based on a modification of the exponential fit for beech Bu38, which allows for the correction of vertical distance (Fig. 59). The resulting idealised height correction (parameter b) was in the range from -0.68 m to 1.72 m. The height correction improved the coefficient of determination for data of beech Bu45 to 0.8 .

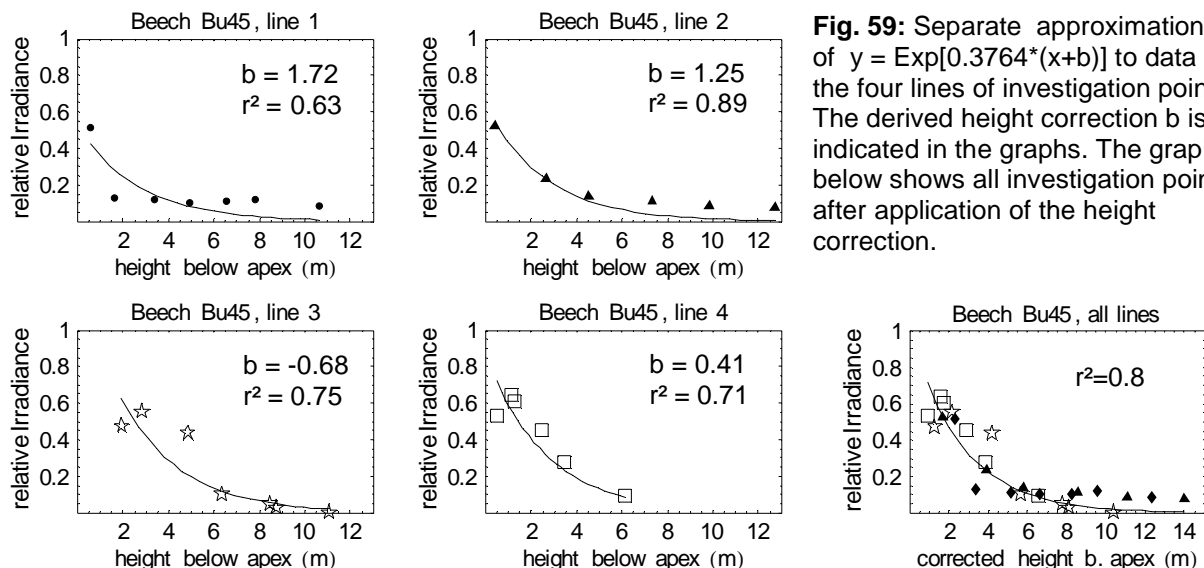


Fig. 59: Separate approximations of $y = \text{Exp}[0.3764*(x+b)]$ to data of the four lines of investigation points. The derived height correction b is indicated in the graphs. The graph below shows all investigation points after application of the height correction.

Spatial distribution of leaf properties in tree crowns

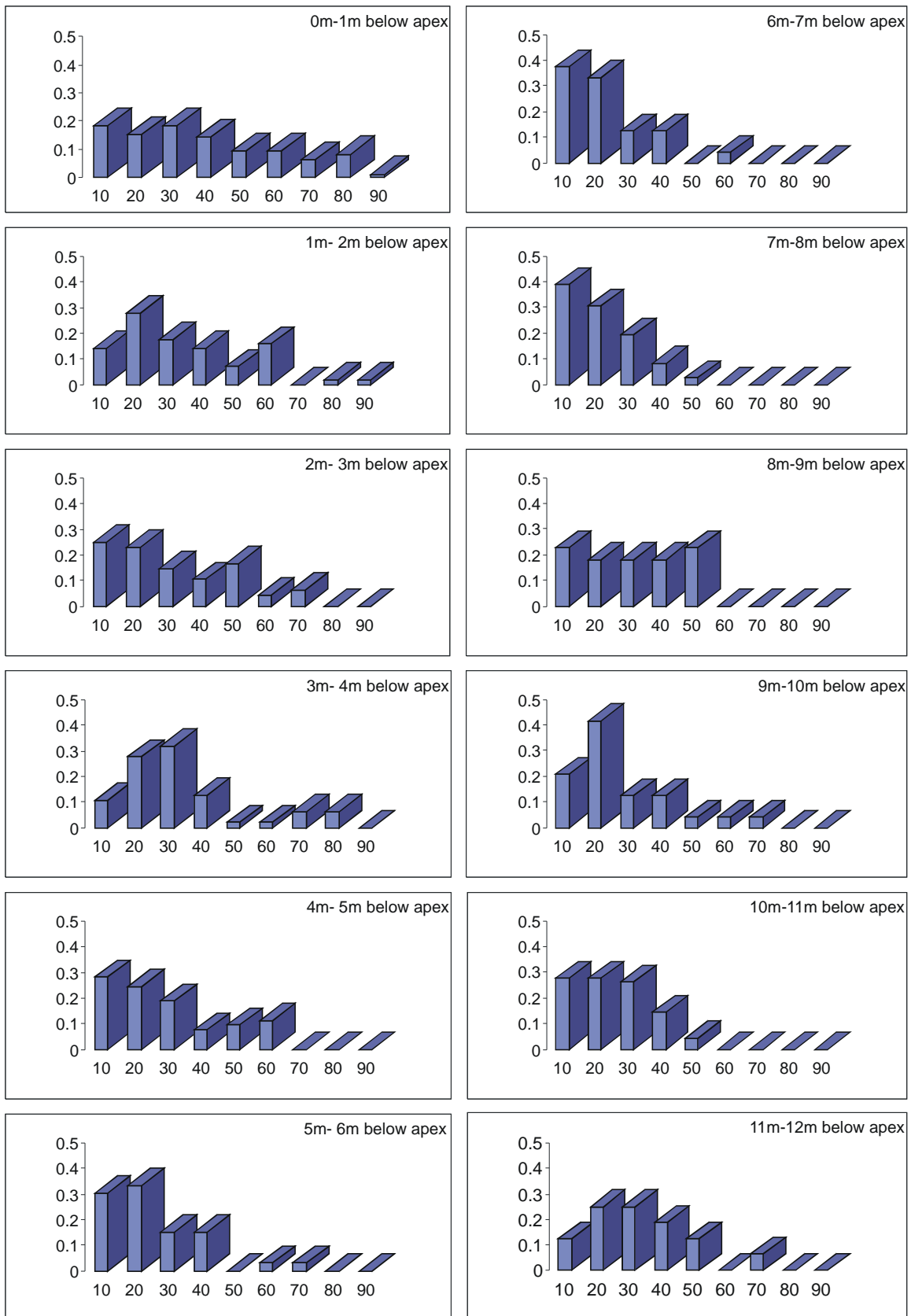


Fig. 60: Leaf angle distributions for 1m-height layers of the tree crown of beech Bu45 in angle classes of 10°.

3.2.1.2 Leaf angles

Leaf angles to the horizon from both Buchenallee beech trees were in the range from 0° to 86°, low inclinations being much more abundant than steep inclinations. Data of investigation points were grouped in 1m-height layers to assure that at least 30 leaf angles are evaluated per data point. In a first approximation, leaf angle distributions of height layers did not appear to be regular, despite the fact that very steep inclinations above 70° did not occur in the lower half of both crowns, but were relatively abundant in the upper two metres (compare Fig. 60). A general trend towards higher average leaf angles in regions of higher irradiance was observed (Fig. 61), but large variations occurred in this relationship.

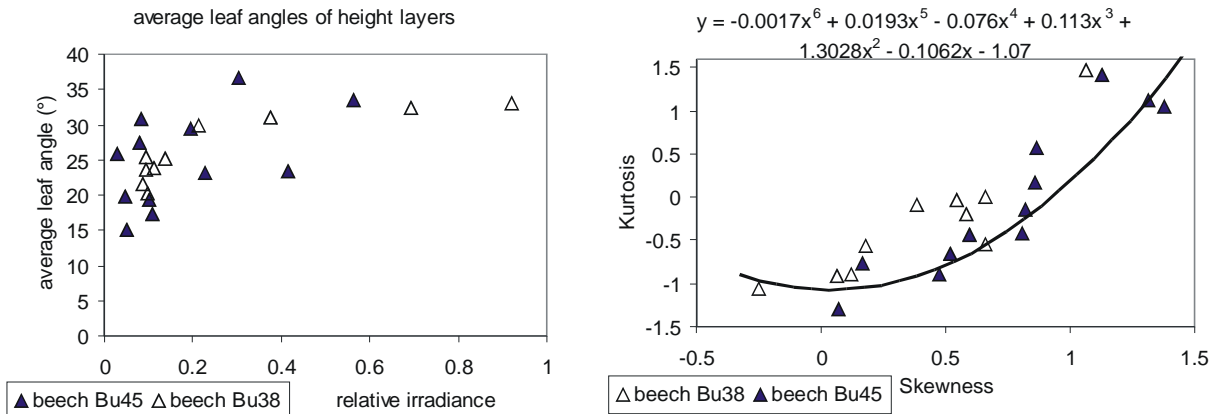


Fig. 61: General increase of average leaf angles of height layers with relative irradiance (left) and relationship between kurtosis and skewness of all leaf angle distributions (right). The curve in the right graph indicates the relationship between kurtosis and skewness of ellipsoidal distributions with varying parameter k , which may also be expressed as a 6th order polynomial function ($r^2 = 1$). R^2 for the regression between this line and the data points was 0.83.

Anyway it turned out that these leaf angle distributions are regular and belong to the same family of distributions: A more detailed analysis of skewness and kurtosis of the angle distributions of both trees revealed that a close to linear relationship can be drawn between both properties. This has among other things the meaning that leaf angles in each crown region were never normal distributed, because skewness and kurtosis of the normal distribution are 0 and the point (0,0) lies apart from the close to linear relationship. The non-normal distribution of leaf angles is also apparent from Fig. 60. Instead, the relationship between skewness and kurtosis of the measured leaf angle distributions lies close to that relationship that is obtained for the ellipsoidal distribution derived from an oblate spheroid, which was proposed for the description of leaf angle distributions (CAMPBELL 1989), thereby providing empirical evidence for the adequacy of this type of distribution for the description of leaf angle distributions in beech crowns (Fig. 60).

k -values of each ellipsoidal distribution, derived by non-linear approximations of the ellipsoidal distribution function (integrated over 10° angle classes, average $r^2 = 0.73$), showed a strong dependence on absolute vertical distance from the apex, which was similar for both beech trees (Fig. 62). However, only a weak dependence on relative irradiance was found: While the height dependence shows a clear linear increase of k -values up to 6 or 7 m below apex and a linear decrease from this point towards the bottom of both tree crowns, no linear decrease can be observed in the region of lower irradiances. This is mainly due to the steep light gradient which

condenses the points that belong to leaf angle distributions of lower layers to a cloud of points in the graph.

The relationship between average leaf angle of height layers and the k-value of the associated ellipsoidal leaf-angle distribution was slightly different for both trees as can be seen in Fig. 63.

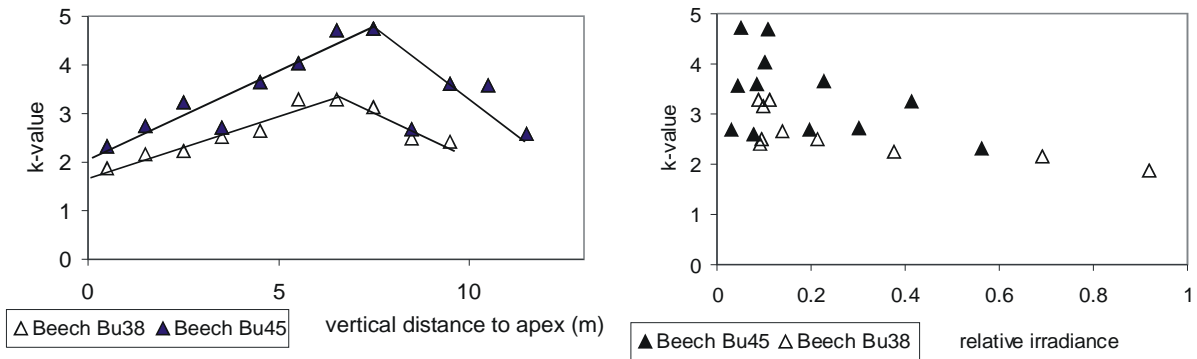


Fig. 62: Dependence of the k-value of the approximated ellipsoidal distribution of leaf angles on vertical distance to the tree's apex (left) and relative irradiance (right). The trendlines in the left graph were drawn by hand and equal $y = 0.24x + 1.67$ and $y = -0.38x + 5.85$ in the case of beech Bu38.

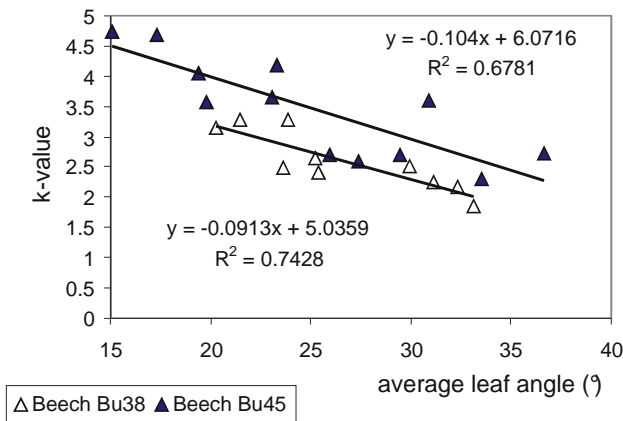


Fig. 63: Relationship between k-value and average leaf angle of leaf angle distributions of both beech trees.

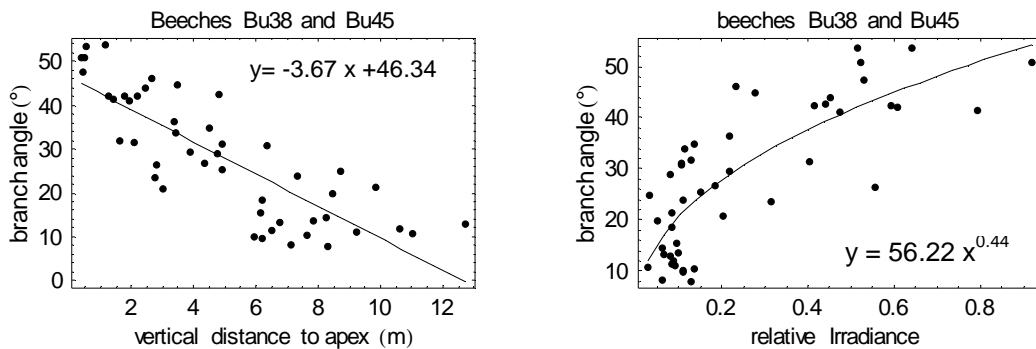


Fig. 64: Average branch angles of branches and twigs closely above the leaf at each investigation point as dependent on height (m below apex) and relative irradiance. R^2 -values were 0.68 and 0.64.

3.2.1.3 Angles of neighbouring branches

Mean angles of branches and twigs closely above each investigation point in the Buchenallee beech trees were linearly dependent on height, while a non-linear relationship was employed to describe the dependence on relative irradiance (Fig. 64). The decrease of branch angles with distance from the apex means that lower branches and twigs grow more horizontally, which may reflect a tendency of branches to grow in direction of the shortest distance to the canopy surface.

The correlation between leaf angle and mean angle of branches was significant but weak ($p < 0.0001$, $r^2 = 0.32$).

3.2.1.4 Leaf Form

Because beech and oak leaves are not entirely flat, they occupy a three-dimensional space with a height of around 1cm and a width that is somewhat smaller than width of the leaf blade, while lengths of leaf space and leaf blade are mostly the same. The width reduction due to bending of the leaves has a meaning for light interception, because it reduces the light exposed projected area of the leaf.

The width of leaf spaces of beech was on average 80.7 % that of the leaf blades ($n = 340$). Average width of leaf blades and average leaf area of beech leaves at each investigation point were closely related ($r^2 = 0.97$, Fig. 65), which is a consequence of the regular form of beech leaves of the same tree (compare ROLOFF 1986). Deviations from the approximated functional relationship in Fig. 65 may be explained with damaged leaves due to herbivorous insects or other mechanical impacts.

Due to the variability in leaf bending, width of leaf space was not as strictly related to leaf area ($r^2 = 0.53$ for 23 oak leaves and 0.6 for 340 beech leaves, Fig. 65). Fig. 66 shows, that this variability is light-driven for beech: While the average width of leaf blades was not dependent on relative irradiance at the investigation point, the effective widths of leaf spaces decrease with increasing irradiance. The largest widths of leaf spaces were reached 6-7m below apex, and smaller widths were found in the lowest parts of the crowns, though relative irradiance was not higher in this part of the crown.

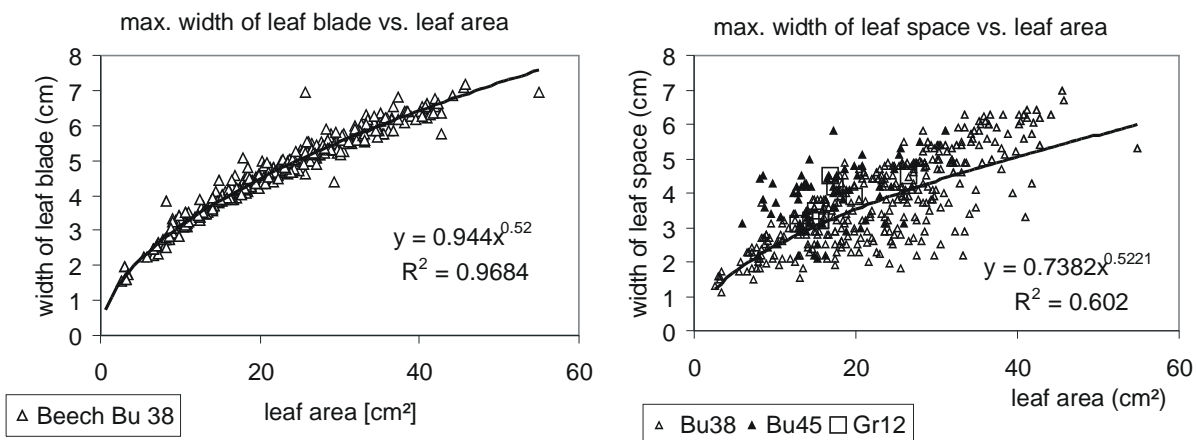


Fig. 65: The regular form of beech leaf blades causes a functional relationship between area and maximum width of leaf blades of beech ($n = 340$, left), while the relationship to the maximum width of leaf space is more scattered (right), which is a consequence of variable bending of the leaf blade. The depicted trendlines were fitted to the data of beech Bu38.

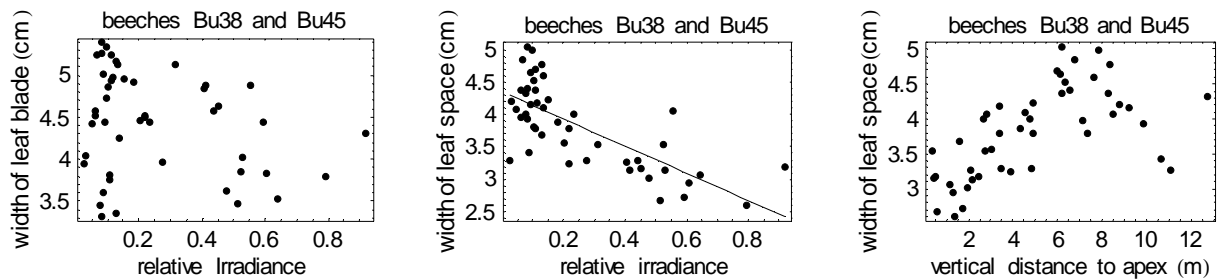


Fig. 66: While the average width of leaf blades ($n \geq 10$) was not dependent on relative irradiance (left), average width of leaf space ($n \geq 10$) decreased with increasing irradiance ($r^2 = 0.53$, $p < 0.0001$; in the middle). The average width of leaf spaces was highest at 6 – 7 m below apex and decreased from there towards both ends of the tree crown (right).

Height of leaf space was expected to be a consequence of the width reduction through leaf bending, but both quantities were not well correlated ($r^2 = 0.20$ for beech trees and 0.01 for oak Gr13). The dependence of height of leaf space on relative irradiance (Fig. 67) was significant with $p < 0.0001$ but relatively weak ($r^2 = 0.42$). The calculated leaf space ratio between height and width of leaf space was better correlated to relative irradiance than both single quantities ($r^2 = 0.65$, $p < 0.0001$). Linear approximations of the leaf space ratio's (y) dependence on height (x , m below apex) were $y = -0.026 x + 0.375$ for all beeches ($r^2 = 0.53$) and $y = -0.049 x + 0.548$ for oak Gr13 ($r^2 = 0.52$, data not shown).

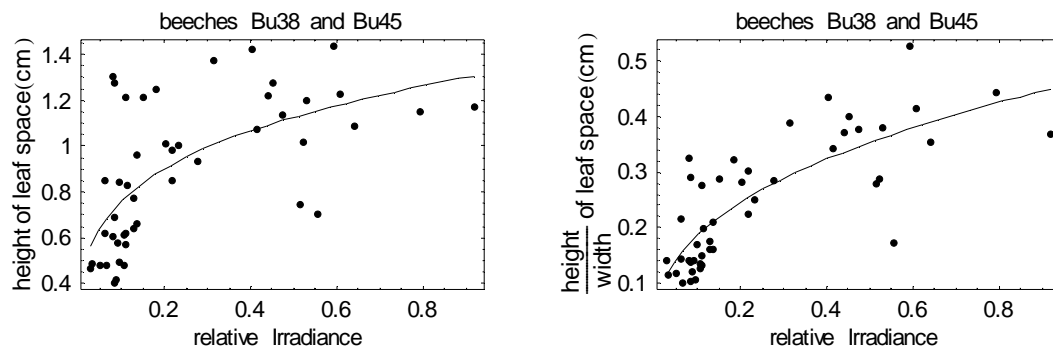


Fig. 67: Height of leaf space (left) and leaf space ratio (height divided by width, right) versus relative irradiance. The approximations are $y = 1.33x^{0.24}$ and $y = 0.47x^{0.4}$, respectively.

3.2.1.5 Leaf mass per area (LMA)

Leaf mass per area could be evaluated from the single leaf measurements as well as from the samples for the biomass harvest (chapter 2) and ranged from 24 to 110 g/m² in beech Bu38, 26 to 99 g/m² in beech Bu45, 23 to 128 g/m² in beech Gr12, and 10 to 135 g/m² in oak Gr13, with mean values of 56.6 g/m² ($n = 772$), 49.9 g/m², ($n = 105$), 80.1 g/m² ($n = 231$), and 70.3 g/m² ($n = 552$), respectively. These ranges for beech are similar to those recently found by other investigators (BARTELINK 1997, HAGEMEIER 1997, GRATANI ET AL. 1987), while older investigations often report lower values (SCHULZE 1970), even for free standing trees that were not shaded by their neighbours (LICHTENTHALER 1981, ELLER ET AL. 1981, TANNER & ELLER 1986, compare Table 5). Average LMA-values of 21 mature beeches (age of 75 to 128 years) from 7 different stands were in the year 1945 as low as 13 to 37 g/m² (BURGER 1945), and 1947,

average LMA-values of 18 oak trees (63 - 155 years) from 6 stands were in the range from 25 to 44 g/m² (BURGER 1947).

Table 5: Comparison of LMA-ranges from different investigation years

Author	Year of publication	LMA-range (g/m ²)	Species
Ramann	1911	25 - 51	averages of two codominant beeches
Burger	1945	13 - 36	averages for different beech trees
Burger	1947	25 - 44	averages for different oak trees
Schulze	1970	20 - 60	mature beech in a stand
Lichtenthaler	1981	25 - 83	free standing beech
Eller et al.	1981	31 - 97	free standing beech
Ducrey	1981	30 - 99	mature beech in a stand
Tanner & Eller	1986	30 - 94	free standing beech
Pellinen	1986	30 - 73	beech trees
Gratani et al.	1987	27-114	beech trees
Jayasekera & Schleser	1988	46 - 103	beech
Schulte	1992	50 - 110	mature beech in a stand
Hagemeier	1997	25 - 105	beech trees from different stands
Bartelink	1997	29 - 125	beech trees
Own measurements	2001	23 - 128	beech trees

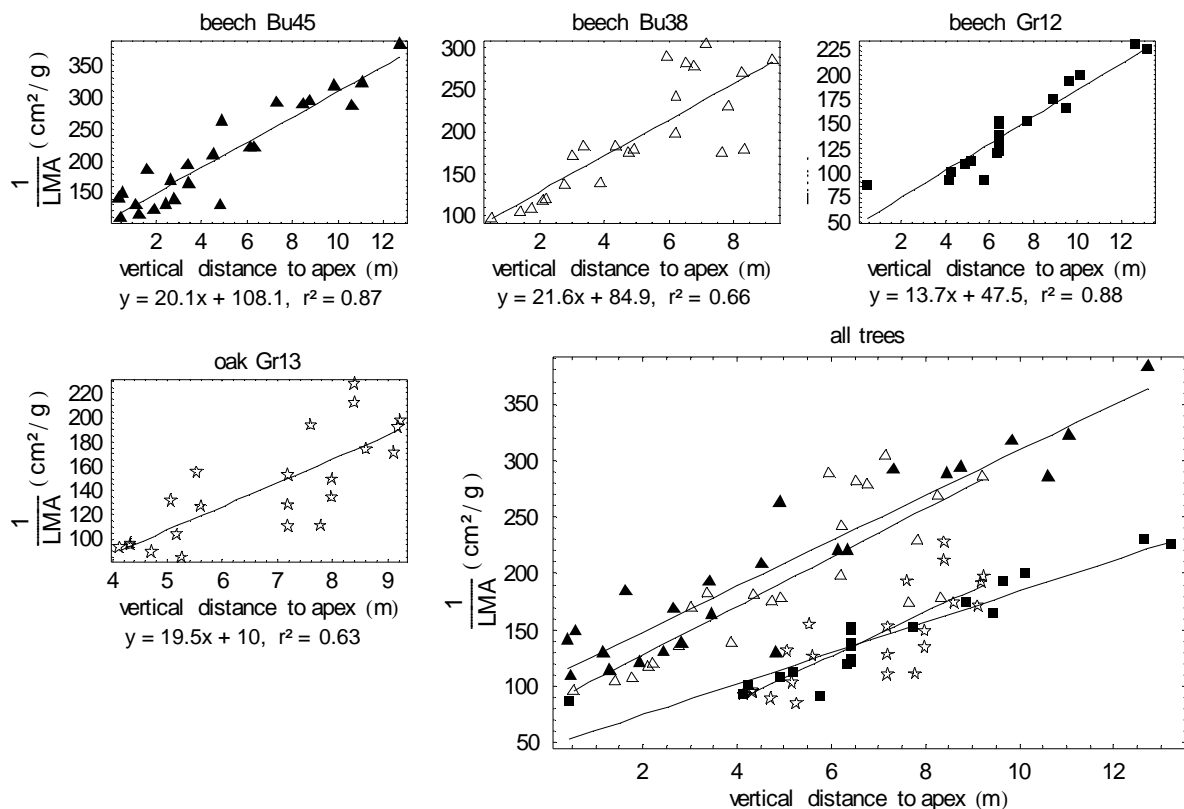


Fig. 68: Leaf area per mass (1/LMA) was linearly correlated to canopy depth of each tree (vertical distance to apex). Data points for the Große Ebene trees are measurements of single leaves, while each point of the Buchenallee trees represents an average of at least 10 leaves.

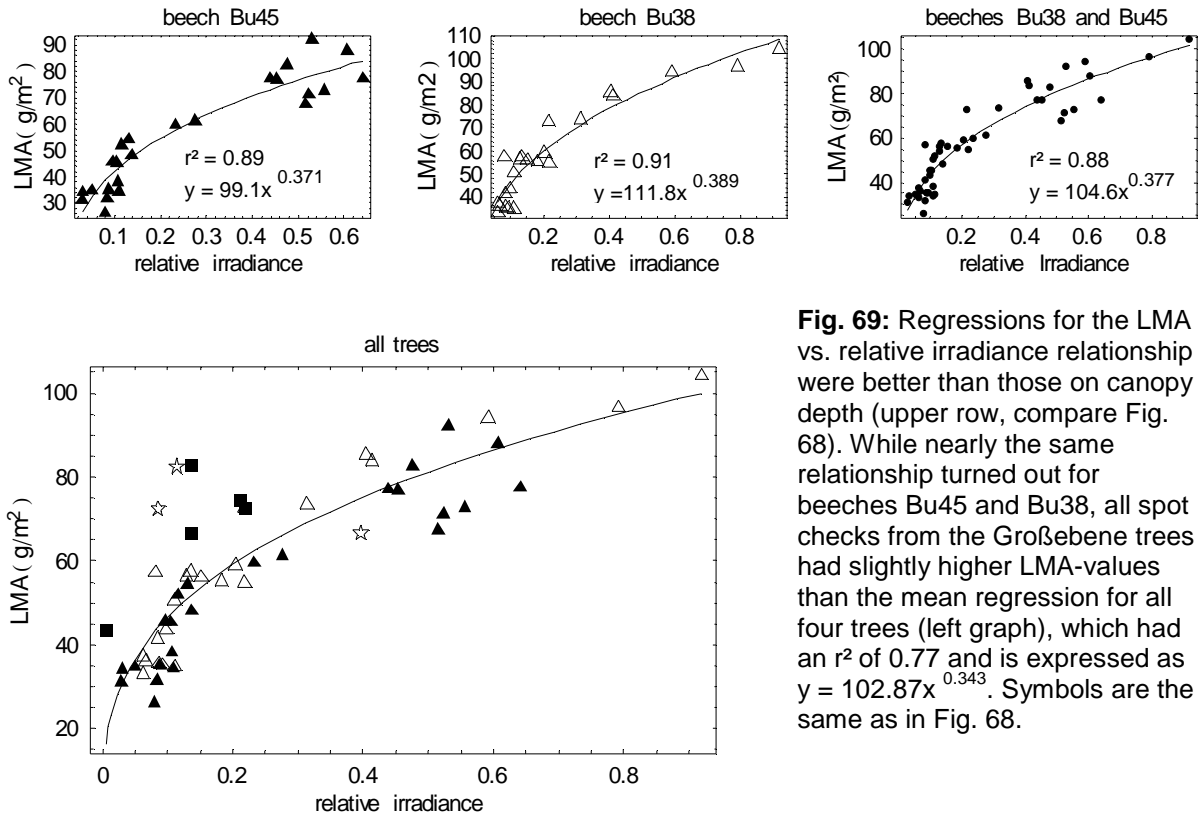


Fig. 69: Regressions for the LMA vs. relative irradiance relationship were better than those on canopy depth (upper row, compare Fig. 68). While nearly the same relationship turned out for beeches Bu45 and Bu38, all spot checks from the Großebene trees had slightly higher LMA-values than the mean regression for all four trees (left graph), which had an r^2 of 0.77 and is expressed as $y = 102.87x^{0.343}$. Symbols are the same as in Fig. 68.

The lower average LMA-values of the Buchenallee trees and the about 50% higher values of beech Gr12 and oak Gr13 may indicate a stand-specific difference, that may also be observed in the LMA-dependence on canopy depth: Leaf mass per area was inversely correlated to canopy depth (vertical distance to apex) of each tree with coefficients of determination between 0.63 and 0.88 (Fig. 68). The regression lines for trees of each stand were similar and at the same time different from those of the other stand.

The partly high scatter (Beech Bu38) in these data disappeared, when the relationship to relative irradiance was drawn (Fig. 69). Coefficients of determination for beech Bu45 and beech Bu38 improved from 0.87 to 0.89 and from 0.66 to 0.91. Possible stand-specific but no species-specific differences may be derived from the spot checks on five beech leaves and three oak leaves from the Großebene trees.

Leaf mass per area of leaves in leaf clouds was not constant, but generally increased from the

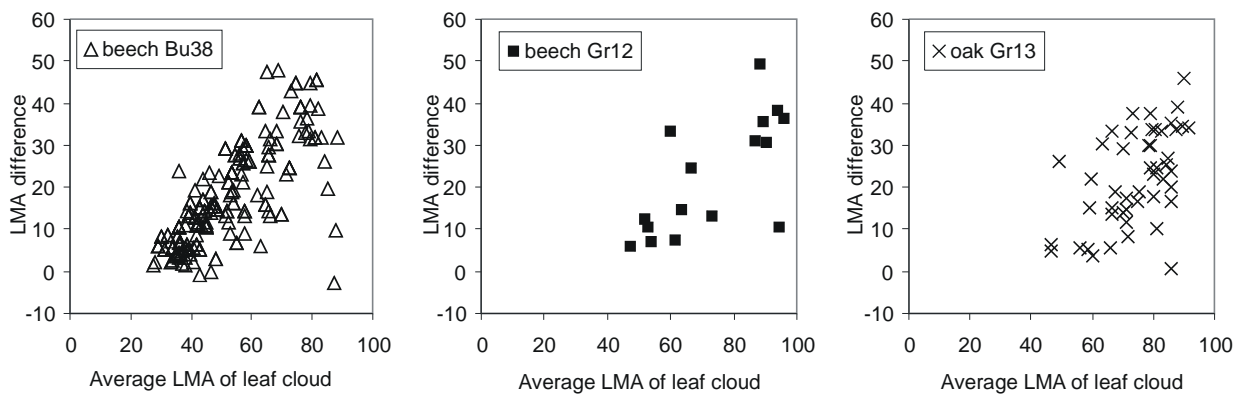


Fig. 70: The LMA difference between distal and proximal leaves of leaf clouds increases with average LMA of the leaf cloud.

proximal, inner side of the leaf cloud towards the outermost distal end of it (Fig. 70), thus reflecting the light dependence of LMA.

The LMA difference between distal and proximal leaves was positive in nearly all leaf clouds and increased with increasing average LMA of the leaf cloud, i. e., with increasing relative irradiance. The leaf clouds with highest average LMA were the uppermost leaf clouds of each tree and were fully sun-exposed due to the dominant or codominant position of the trees in their stand. The light-gradient on these leaf clouds may be small, when self-shading is less severe and so was the LMA gradient between their distal and proximal leaves.

3.2.1.6 Leaf nitrogen and carbon contents

Carbon and nitrogen belong to the 4 most abundant elements in leaf biomass. Carbon prevailingly occurs as part of cellulose, lignin, proteins, carbohydrates or in secondary metabolites as tannins, whereas nitrogen is most abundant as part of proteins. Around 30% of leaf nitrogen are bound in rubisco (EVANS 1989) – nitrogen may therefore generally be seen as functionally important and carbon as important for mechanical stability.

Leaf nitrogen contents per dry weight ranged from 2.1 to 3.5 % dry weight in oak Gr13, from 2.2 to 3.2 % dry weight in beech Gr12, from 2 to 2.6% in beech Bu45, and from 2.2 to 2.7% in beech Bu38.

While mass-related carbon contents of beech leaves were to some extent dependent on relative irradiance (Fig. 71), mass-related leaf nitrogen concentrations of the beech trees Bu 38 and Bu45 were scattered when viewed against any of the reported leaf properties. Carbon content

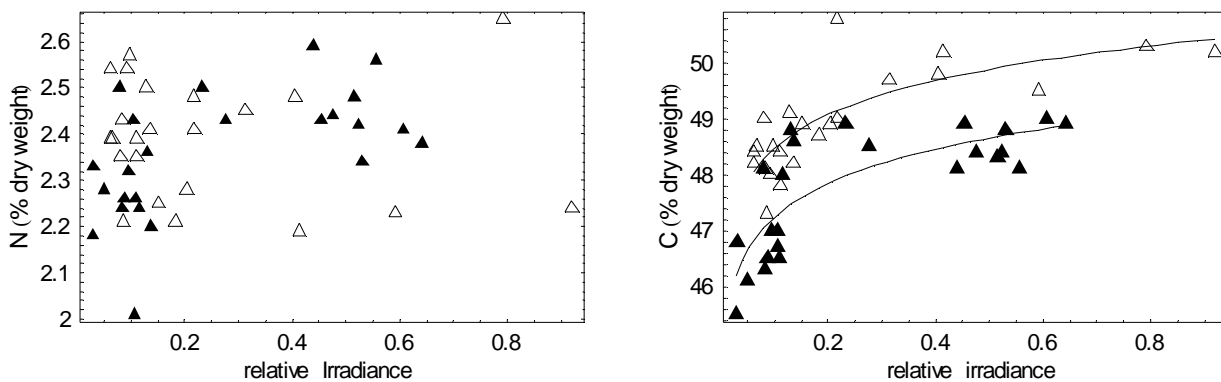


Fig. 71: Average mass related nitrogen and carbon contents of $n \geq 10$ leaves per investigation point in relation to relative irradiance. Regression lines could only be drawn for leaf carbon. The approximation for beech Bu45 (filled symbols) was $y = 49.28x^{0.018}$ ($r^2 = 0.64$) and that for beech Bu38 (open symbols) was $y = 50.51x^{0.018}$ ($r^2 = 0.63$).

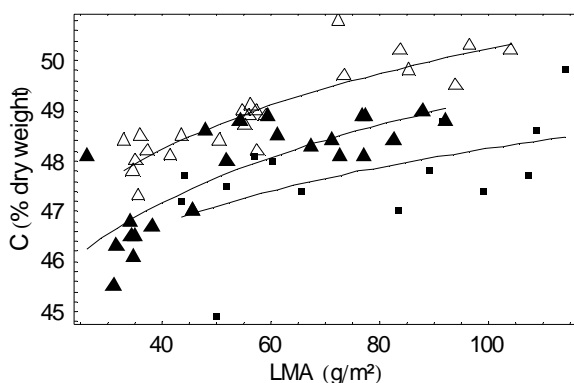


Fig. 72: The mass related carbon content of leaves of all beech trees increased with increasing leaf mass per area. The approximation lines for each tree were

Bu45 (filled triangles): $y = 39.7x^{0.0466}$, $r^2 = 0.63$;
 Bu38 (open triangles): $y = 40.96x^{0.044}$, $r^2 = 0.77$;
 Gr12 (filled squares): $y = 41.1x^{0.035}$, $r^2 = 0.29$.

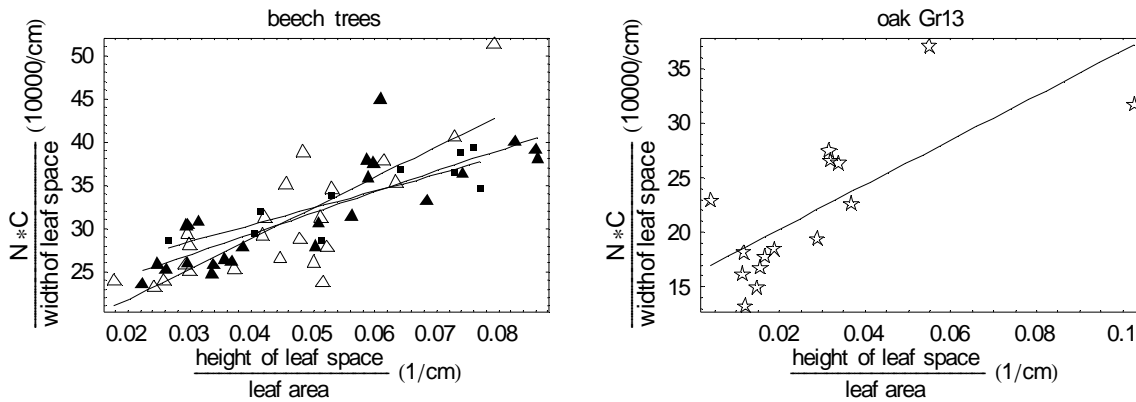


Fig. 73: Correlation between the product of nitrogen and carbon contents (% dry weight) per width of leaf space and leaf bending, which is expressed as height of leaf space per leaf area. r^2 -values were: 0.65 for beech Bu38 (open triangles), 0.7 for beech Bu45 (filled triangles), 0.73 for beech Gr12 (filled squares), 0.66 for all beech leaves, and 0.56 for oak Gr13 (open stars).

of all beech leaves increased with growing LMA ($r^2 = 0.6$, Fig. 72) and a tendency to increase was also found with increasing leaf angle, space ratio (height / width of leaf space) and height of leaf space (all $r^2 < 0.5$, data not shown), which may be seen in the context of the role of carbon for mechanical stability of the leaves.

A co-factorial relationship was found between both leaf mass-related concentrations and leaf bending, which may be expressed as the height of leaf space that is realised by bending of a given leaf area (Fig. 73). Carbon and nitrogen concentrations had to be divided by width of leaf space to build a significant relationship ($p < 10^{-13}$) for all beech leaves, which could also be observed on the low number of investigated oak leaves ($p < 0.001$). Coefficients of determination were 0.66 for all beech leaves and 0.56 for the oak leaves.

A similar co-factorial relationship based on relative intercepted irradiance was observed on the two beech trees of the Buchenallee stand: relative intercepted irradiance was calculated as relative irradiance divided by light exposed area, which was estimated to be equal to projected leaf area (leaf area times cosine of leaf angle). A functional relationship to relative intercepted irradiance times height of leaf space was found, which had r^2 -values of 0.73 (beech Bu38) and 0.74 (beech Bu45), when the product of nitrogen and carbon content (% dry weight) was divided by width of leaf space (Fig. 74). Thus, the scattered relationship between nitrogen concentration and relative irradiance (Fig. 71) turned into a more regular relationship, when the relation between carbon concentration and leaf form parameters is multiplied.

Nitrogen content per leaf area was closely correlated to leaf mass per area as was reported earlier for other species (KLEIN ET AL. 1991, NIINEMETS 1997, ELLSWORTH & REICH 1993, KULL & NIINEMETS 1993, DEJONG & DOYLE 1985). Similarly to leaf mass per area, also nitrogen per area

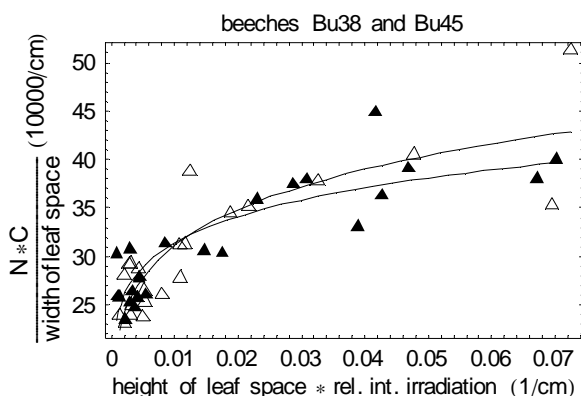


Fig. 74: The same combination of quantities on the y-axis as in Fig. 72 versus the product of height of leaf space and relative intercepted irradiation. R^2 -values were 0.74 for beech Bu45 (filled triangles) and 0.73 for beech Bu38 (open triangles).

of leaves of the Buchenallee trees was therefore dependent on relative irradiance ($r^2 = 0.87$, Fig. 75). The same was principally true for carbon concentrations.

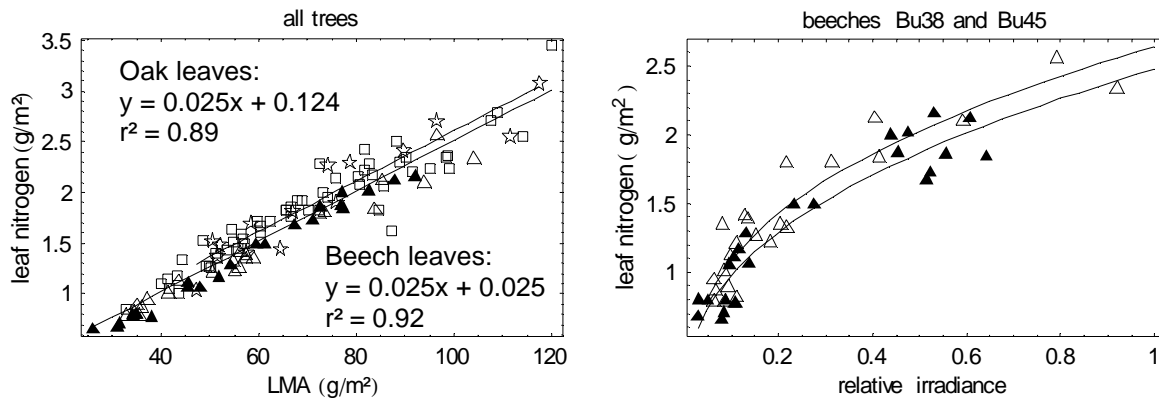


Fig. 75: Area related nitrogen content of leaves versus leaf mass per area (left) and relative irradiance (right). Open squares in the left graph stand for leaves from 2 beeches in the Steinkreuz stand, beech Gr12, and 3 additional beeches in the Großebene stand, all other symbols are the same as in Fig. 73. Data points of beeches Bu38 and Bu45 are averages of at least 3 neighbouring leaves, r^2 for these data only against LMA was 0.97 and 0.99, respectively. The relationships to relative irradiance were $y = 2.64x^{0.383}$ ($r^2 = 0.88$) for beech Bu38, $y = 2.48x^{0.405}$ ($r^2 = 0.9$) for beech Bu45, and $y = 2.54x^{0.389}$ ($r^2 = 0.87$) for both beech trees.

3.2.2 Photosynthesis measurements

3.2.2.1 Comparison of PAM-2000 and RACCIA estimates of J_{max}

J_{max} estimations from fluorescence and gas exchange measurements on the same leaf should lead to comparable results, when they are performed under the same conditions, thus principally providing an opportunity to check accuracy of the measurements. But field conditions were variable and they could only partly be manipulated: While the LICOR-6400 portable gas exchange measurement system can alter temperature in the measurement chamber in the range of ambient temperature $\pm 7^\circ\text{C}$ and maximum light intensity of the appertaining LED light source (LED 6400-02B) is $2000\mu\text{mol}/(\text{m}^2\cdot\text{s})$, fluorescence measurements with the PAM-2000 under field conditions do not allow any adjustment of temperature, but light intensity can be varied in a wide range. Additionally, time of day of the measurement may play a role for the result and differences could also occur between subsequent days at the same hour.

A comparison between results of both methods was enabled by measuring a light response curve of J with the fluorometer PAM-2000 at a more or less constant ($\pm 2^\circ\text{C}$) temperature and a temperature dependence curve of J with the LICOR-6400 at the constant maximum PPFD of $2000\mu\text{mol}/(\text{m}^2\cdot\text{s})$ on the same leaf. The temperature variation in the light response curve is a result of the variation in ambient conditions and warming of the leaf due to the light source. Assuming that the maximum electron transport rate J_{max} is achieved at $2000\mu\text{mol}/(\text{m}^2\cdot\text{s})$, the evaluation of A/C_T -curves with RACCIA can provide a segment of the temperature dependence curve of J_{max} , representing the maximum temperature range that can be obtained with the LICOR-6400 under the actual ambient conditions. The extrapolation of this curve to the temperature of the PAM-2000 measurement can be compared with the electron transport rate at $2000\mu\text{mol}/(\text{m}^2\cdot\text{s})$ that is derived from the light response curve using a non-linear fit of equation (29) for interpolation.

Five leaves of oak Gr13 were selected in different light expositions and fluorescence measurements were performed directly after gas-exchange measurements, except in one case (leaf eb2_1, 20°C), where no gas-exchange measurements could be performed due to a sudden rain event (30.7.99). This leaf was measured twice on two subsequent days during the same hours of the day (11.00 h - 13.00 h), but at different temperatures. The results of fluorescence and gas-exchange measurements are shown in Figs. 76 and 77.

The light response curve of leaf 3eb2_1 was different at both measurement temperatures in its initial slope, which was 0.25 in the 20°C and only 0.1 in the 28°C measurement, while maximum values did not differ so much. The light response curve at the highest temperature (leaf 3eb2-2, 32°C) had also a rather low initial slope (0.12), while all other estimations for the initial slope were in the range from 0.22 to 0.3. It can therefore not be excluded that the two leaves under the highest temperatures suffered stress to some extent, though they were able to achieve high

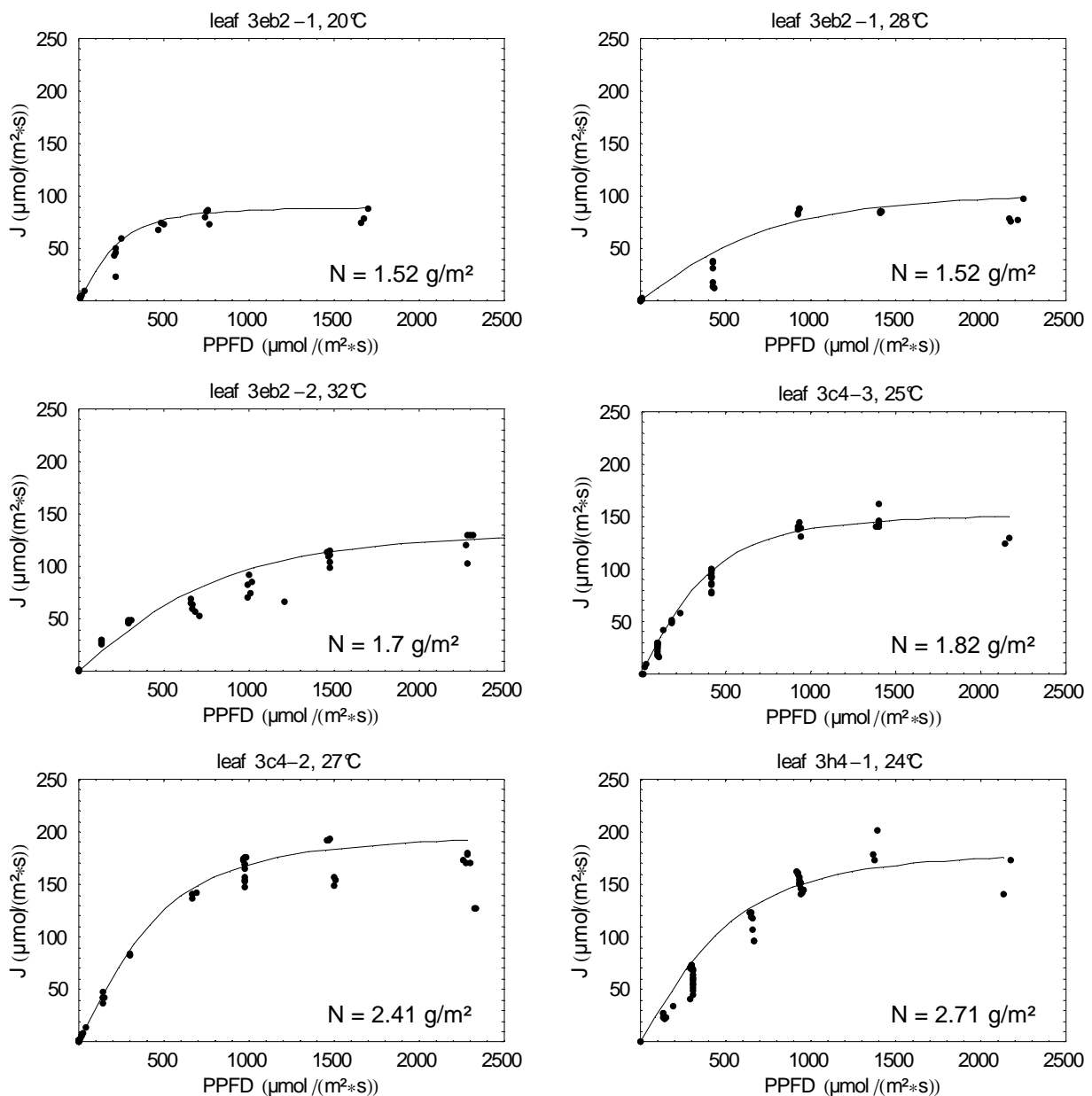


Fig. 76: Light response curves of electron transport rate J of 5 leaves of oak Gr13, derived from fluorescence measurements with the PAM-2000 fluorometer at 6 different temperatures (sorted by nitrogen content). The highest measured value per light level was used for a non-linear approximation of the light dependence function for J from the HARLEY/TENHUNEN model (equation 29).

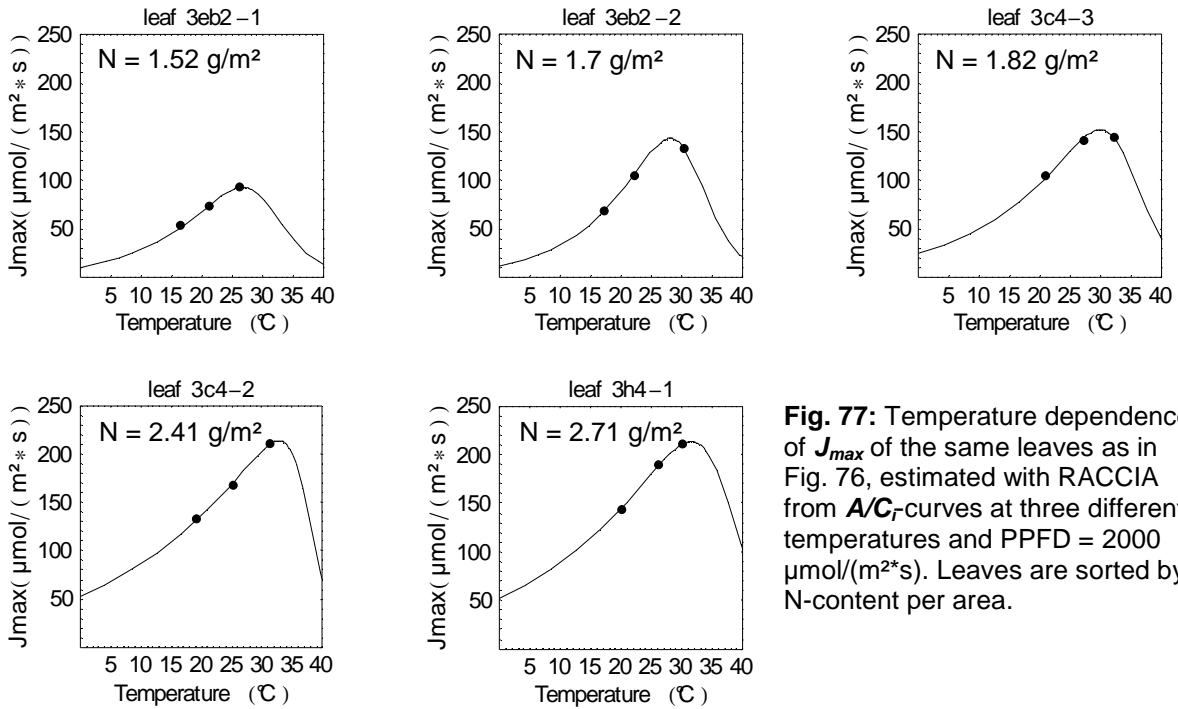


Fig. 77: Temperature dependence of J_{max} of the same leaves as in Fig. 76, estimated with RACCIA from A/C_r -curves at three different temperatures and PPFD = 2000 $\mu\text{mol}/(\text{m}^2\cdot\text{s})$. Leaves are sorted by N-content per area.

maximum electron transport rates. Some fluorescence measurements seem to indicate that the light dependence of J was not monotonously increasing, but achieved a maximum value below 2000 $\mu\text{mol}/(\text{m}^2\cdot\text{s})$. But this may also be attributed to effects of the long measurement period before measuring the high PPFD values and the effect of the 1-2°C higher temperature at these PPFD values due to leaf warming by the lamp.

Shade leaves with lower nitrogen content per area had generally lower J_{max} values than sun leaves according to both methods.

A high correlation ($r^2=0.93$) was found between the J_{max} estimations of both methods (Fig. 78). The PAM-2000 estimations were generally slightly higher than those derived with RACCIA from gas-exchange measurements, and this situation improved a bit, when average values instead of

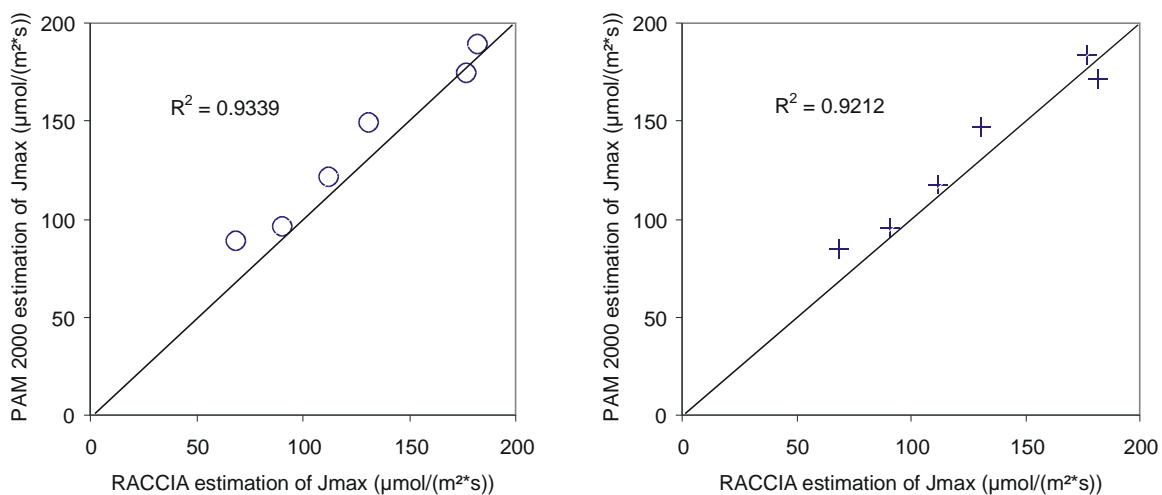


Fig. 78: Comparison of J_{max} estimations from two different methods (RACCIA and PAM-2000). The circles in the left graph represent J_{max} estimations with the PAM-2000 based on approximations to the maximum measured values per light-level, while the crosses in the right graph rely on approximations to average values.

maximum values were used for the approximation of equation (29) to the measured data of the light response curve, though correlation was somewhat lower than ($r^2=0.92$).

3.2.2.2 Day respiration (R_d)

All determined day respiration rates were in the range from 0 to $2.7 \mu\text{mol}/(\text{m}^2 \cdot \text{s})$ for leaves of beech Gr12 and from 0 to $2.7 \mu\text{mol}/(\text{m}^2 \cdot \text{s})$ for leaves of oak Gr13. R_d of the same leaf was generally higher under higher temperatures and the gradual increase with temperature was greater for sun leaves with high nitrogen content per area than for shade leaves of both species. Therefore, temperature dependence of day respiration was investigated for groups of leaves with similar nitrogen content separately using equation (28). All following approximations of equations (28) and (30) are done to interpolate between measurements at different temperatures. For this, A/C_T -data of leaves were sorted by nitrogen content (see appendix) and

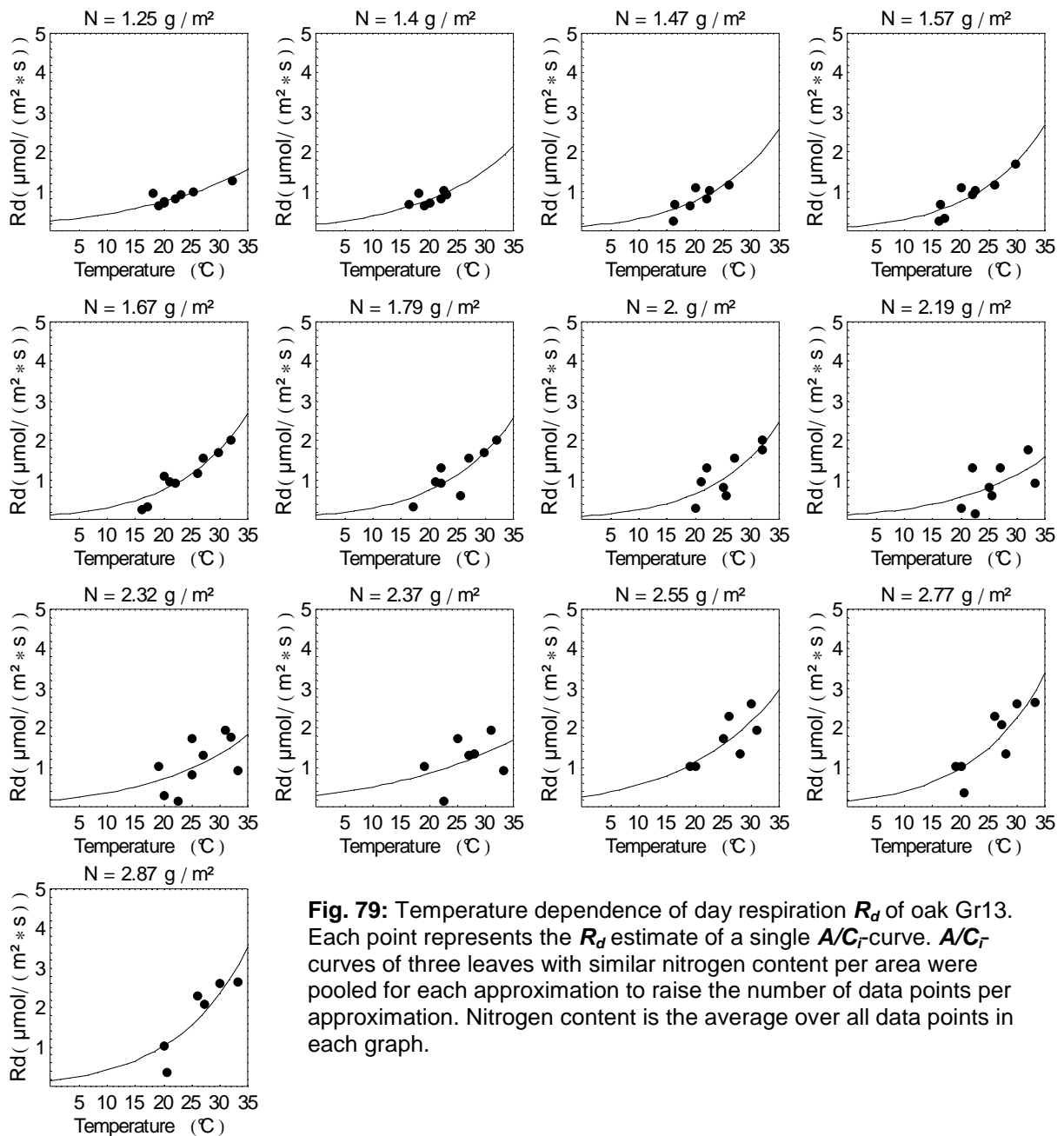


Fig. 79: Temperature dependence of day respiration R_d of oak Gr13. Each point represents the R_d estimate of a single A/C_T -curve. A/C_T -curves of three leaves with similar nitrogen content per area were pooled for each approximation to raise the number of data points per approximation. Nitrogen content is the average over all data points in each graph.

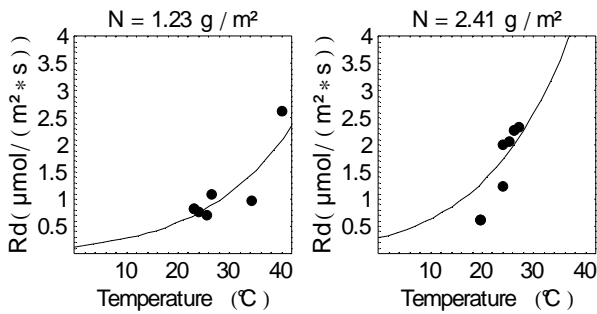


Fig. 80: Temperature dependence of day respiration R_d of beech Gr12. All R_d -values were splitted into two non-overlapping groups with low and high nitrogen contents. The approximation with equation (28) was performed with the condition that H_a does not exceed a threshold value of 50kJ/mol.

groups of consecutive leaves in this row were combined in the evaluation. Groups were partly overlapping. Fig. 79 shows that the gradual increase of R_d of oak leaves with temperature was very low for some shade leaves, while it was greater for most of the sun leaves. For comparison: The occasionally determined gas-exchange rate of an oak leaf with 2.33 g N/m² at 25°C, measured after 6 minutes of darkness, was $-1.85 \mu\text{mol}/(\text{m}^2\cdot\text{s})$.

The low number of data points and their concentration on a narrower range of temperatures was a problem for the approximations with the exponential equation (28) for beech, because extremely high curvatures (H_a in equation (28)) gave the best approximation even when the beech data were splitted in only two groups. Because this would have resulted in unrealistic or at least never measured R_d -values of more than $10 \mu\text{mol}/(\text{m}^2\cdot\text{s})$ at temperatures above 30°C, H_a in the regressions for beech (Fig. 80) and beech seedlings (Fig. 81) was not allowed to reach values above 50 kJ/mol. This was also done considering recent observations that respiration continuing in the light not necessarily follows an exponentially increasing function, but may also decrease above a maximum value at 25 or 30°C (A TKIN ET AL. 2000).

Additional A/C_r -measurements have been searched to enlarge the data basis for beech. M. FORSTREUTER AND J. STRASSEMAYER (Technische Universität Berlin) meritoriously made available their partly published A/C_r -measurements (MEDLYN ET AL. 1999) on beech seedlings at different temperatures for the evaluation with RACCIA. The nitrogen content per area of these investigated leaves varied in a narrower range than that of the leaves of mature trees in Steigerwald or Fichtelgebirge (0.71 - 0.98 g/m² for these investigated leaves, 0.5 - 1.5 g/m² for all measured seedling leaves, 0.6 - 2.6 g/m² for beech leaves from the Fichtelgebirge, and 1.0 - 3.4 g/m² for beech leaves from the Steigerwald), which was due to less variation in leaf mass per area. Nitrogen content per area was on average lower than that of shade leaves from mature trees in both stands. A/C_r -curves of seedlings were separated into three groups (low, middle, and high nitrogen) and were analysed separately (Fig. 81). H_a in these approximations was between 33.9 and 42 kJ/mol, while it reached the maximum allowed value of 50kJ/mol in the approximations for beech Gr12.

Respiration rates at 25°C (R_{d298}) did not show a clear dependence on nitrogen content, though leaves with similar nitrogen content tended to have similar values of R_{d298} (Fig. 82). The results

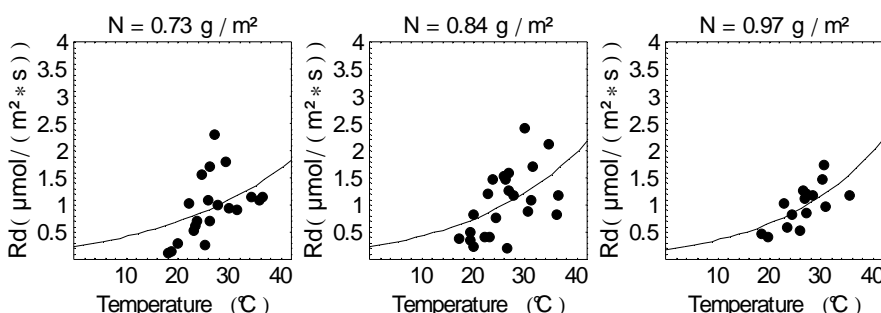


Fig. 81: Approximation of equation (28) to R_d -estimations from A/C_r -curves measured on seedlings (A/C_r -measurements of Forstreuter and Strassemer (MEDLYN ET AL. 1999))

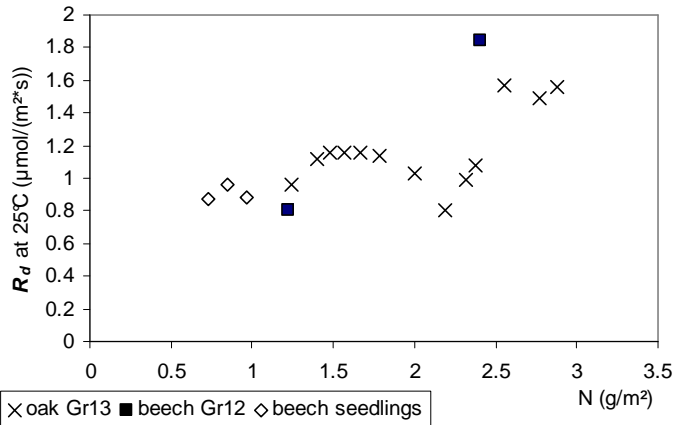


Fig. 82: Variation of day respiration at 25°C with nitrogen per leaf area. Temperature interpolation was done based on the results of Figs. 79-81.

for oak Gr13 show a slight increase in respiration from the shade leaves with low nitrogen content towards a nitrogen content of 1.7 g/m², slightly lower respiration rates between 1.7 and 2.5 g/m² and a sudden increase towards the leaves with nitrogen contents above 2.5 g/m². The general trend over all leaves is an increase of respiration rates with nitrogen per area.

3.2.2.3 Carboxylation capacity $V_{C_{max}}$ and electron transport capacity J_{max}

Non-linear approximations of equation (30) were used for the description of temperature dependence of $V_{C_{max}}$ and J_{max} of both species (Figs. 83 - 87). Because both quantities had obviously lower values for shade leaves than for sun leaves, A/C_r -data were grouped in the same manner as for the evaluation of R_d versus temperature (see 3.2.2.2) in order to separate nitrogen classes.

$V_{C_{max}}$ of oak leaves was generally higher than $V_{C_{max}}$ of leaves of beech Gr12, reaching a maximum value of 158 μmol/(m²*s) at 33°C in the investigated leaf with the highest nitrogen content (3.1 g/m²), while the maximum determined value of beech leaves was 63 μmol/(m²*s) at 24°C (N = 2.8 g/m²). This corresponds to the maximum values for J_{max} , which were 231 μmol/(m²*s) (32°C, N = 2.3 g/m²) for oak Gr13 and only 132 μmol/(m²*s) for beech Gr12 (25°C, N = 2.2 g/m²). $V_{C_{max}}$ and J_{max} generally increased with nitrogen content per leaf area, which was also true for seedlings (see below).

Additional A/C_r -curves from beech seedlings (MEDLYN ET AL. 1999) were investigated and showed to have much lower $V_{C_{max}}$ - and J_{max} -values (Fig. 87), which may be a consequence of their low nitrogen contents per area. Maximum values were 47 μmol/(m²*s) and 56 μmol/(m²*s) at a temperature of 31°C and 30°C, respectively, measured on a leaf with a nitrogen content of 0.96 g/m². Thus, $V_{C_{max}}$ and J_{max} of beech seedlings appear to lie closer to each other than those of beech Gr12.

Nearly all $V_{C_{max}}$ -values of oak Gr13, beech Gr12, and beech seedlings were found to be on the ascending part of the approximation curve, while J_{max} -values from the same A/C_r -curves were more often on the descending part, indicating a lower temperature optimum for J_{max} than for $V_{C_{max}}$.

The relationship between both capacities was found to be relatively constant for a high number of species (WULLSCHLEGER 1993, LEUNING 1997), with an average $J_{max} / V_{C_{max}}$ ratio between 2.16 and 2.68 at 20°C (depending on the used temperature function). The above temperature dependencies were therefore used to interpolate for a temperature corrected value of $V_{C_{max}}$ and J_{max} at 20°C for each nitrogen class in order to investigate the general relationship between

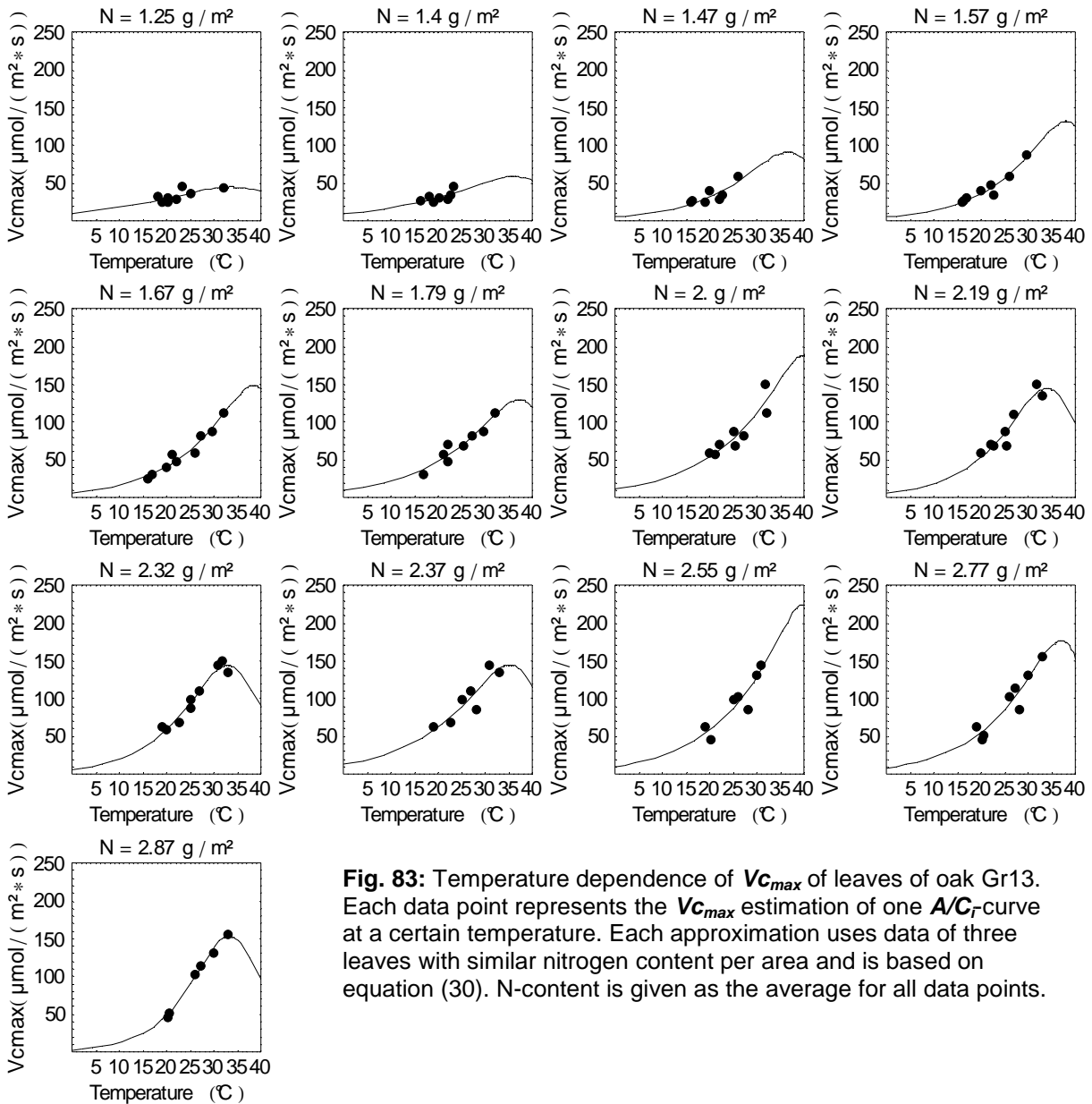


Fig. 83: Temperature dependence of $V_{C_{max}}$ of leaves of oak Gr13. Each data point represents the $V_{C_{max}}$ estimation of one A/C_p -curve at a certain temperature. Each approximation uses data of three leaves with similar nitrogen content per area and is based on equation (30). N-content is given as the average for all data points.

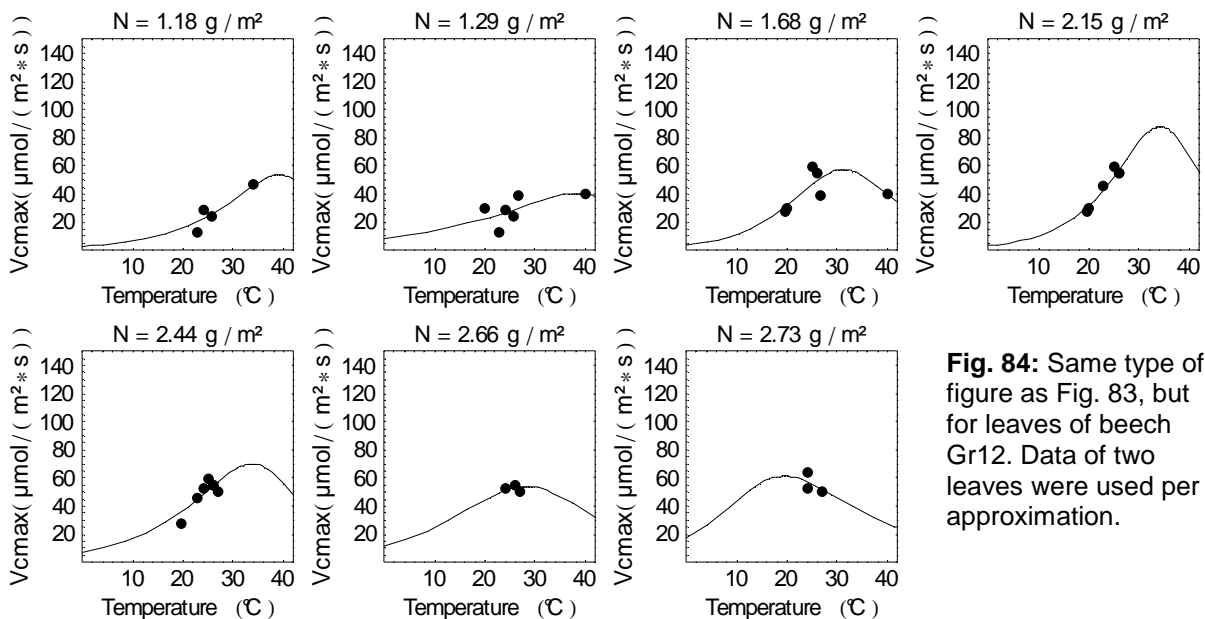


Fig. 84: Same type of figure as Fig. 83, but for leaves of beech Gr12. Data of two leaves were used per approximation.

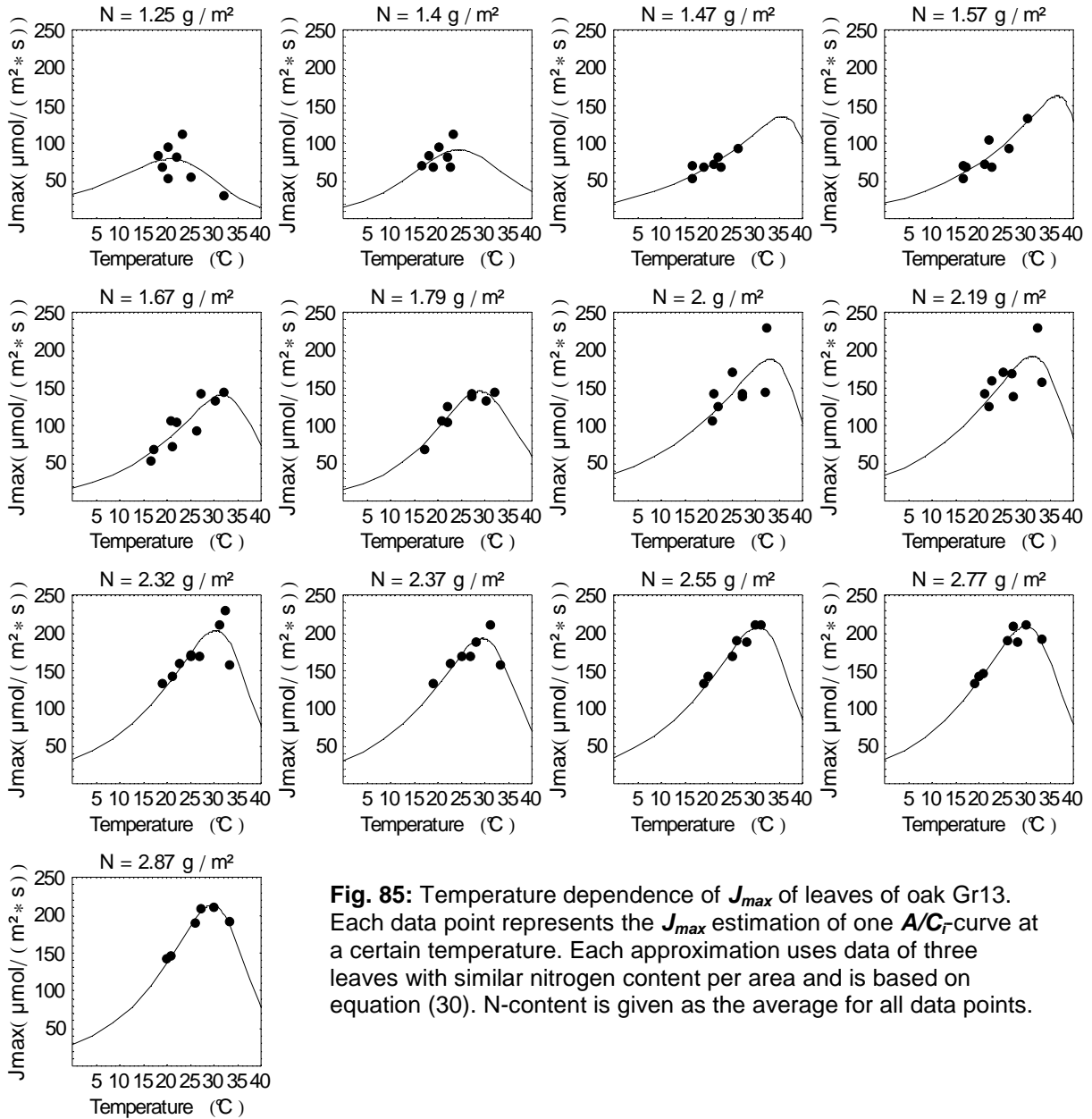


Fig. 85: Temperature dependence of J_{max} of leaves of oak Gr13. Each data point represents the J_{max} estimation of one A/C_T -curve at a certain temperature. Each approximation uses data of three leaves with similar nitrogen content per area and is based on equation (30). N-content is given as the average for all data points.

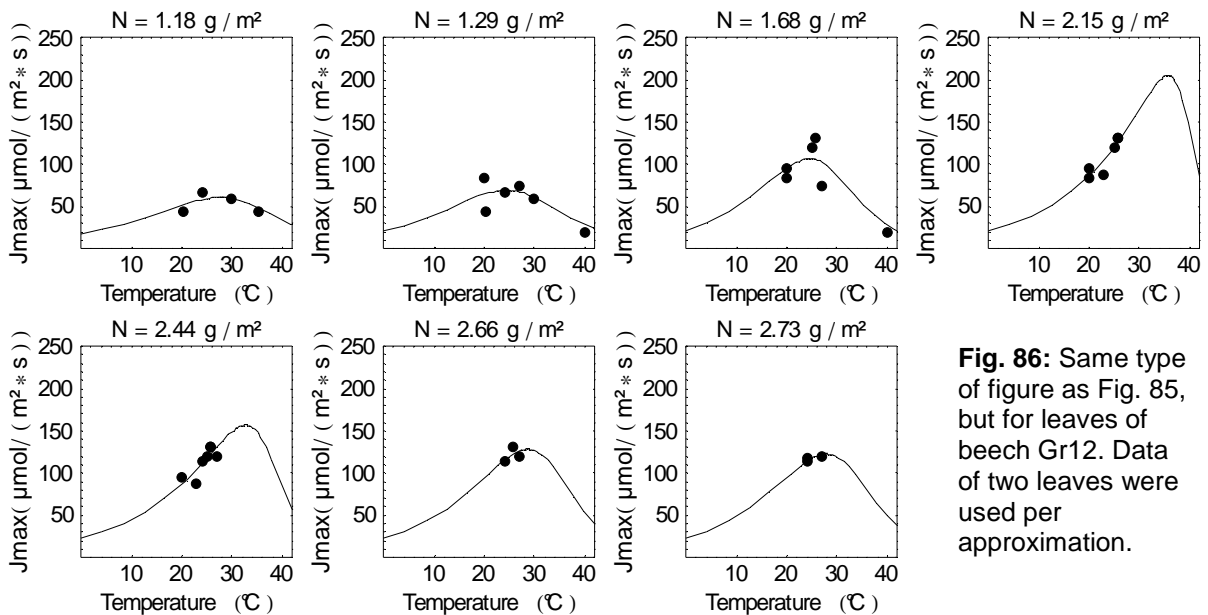


Fig. 86: Same type of figure as Fig. 85, but for leaves of beech Gr12. Data of two leaves were used per approximation.

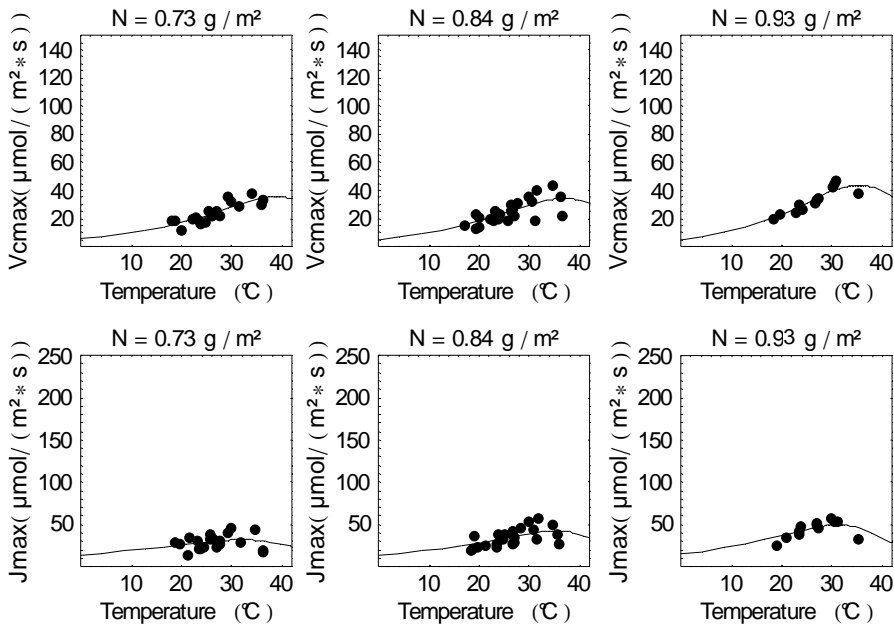


Fig. 87: Temperature dependence of $V_{c_{max}}$ (upper row) and J_{max} (below) of beech seedlings as determined with RACCIA.

both quantities. Those temperature dependence functions without $V_{c_{max}}$ or J_{max} values below 21°C were excluded from this analysis. Fig. 88 shows that all data lie relatively close to the regression line, which represents a general ratio of 2.28 ($r^2 = 0.86$) and lies in the range of previously found ratios (LEUNING 1997). Nevertheless, $J_{max}/V_{c_{max}}$ ratios varied: While the ratio for investigated leaves of oak Gr13 was nearly the same as the mean response (2.24, range: 1.97 - 2.79), leaves of beech seedlings had a lower average $J_{max}/V_{c_{max}}$ ratio (1.58, range: 1.51 - 1.64) and leaves of beech Gr12 a higher one (2.72, range: 2.38 - 3.23). Thus, the high coefficient of determination for the overall relationship does not necessarily mean that $V_{c_{max}}$ may be derived from J_{max} estimations, because species- or age-specific differences are evident.

3.2.2.4 Nitrogen dependence of J_{max} and $V_{c_{max}}$

The increase of J_{max} and $V_{c_{max}}$ with nitrogen content of the leaves is obvious from Figs. 83 - 86 and was investigated on the base of the temperature corrected value at 25°C for each nitrogen class of leaves, which is one parameter of equation (30) ($J_{max, 298}$ and $V_{c_{max, 298}}$) and was

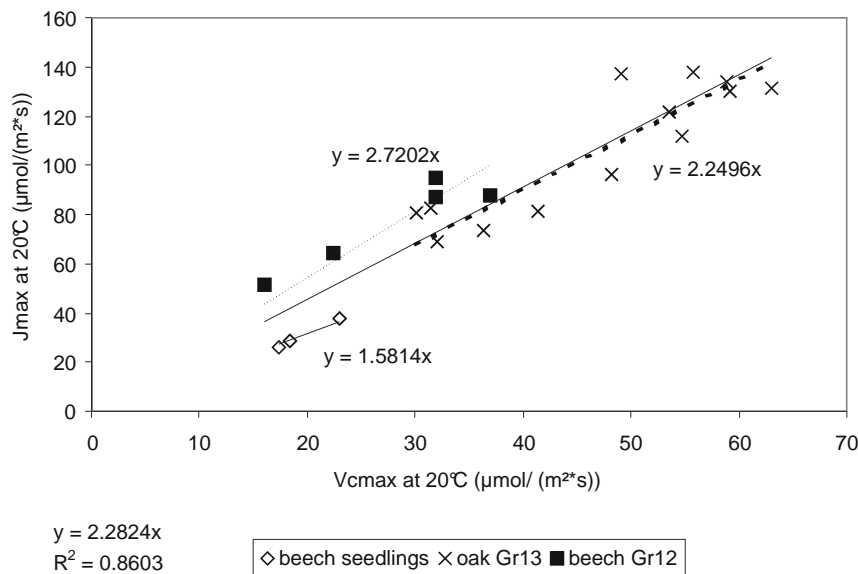


Fig. 88: Ratio between J_{max} and $V_{c_{max}}$ at 20°C for investigated nitrogen classes of leaves of beech Gr12, oak Gr13, and beech seedlings (MEDLYN ET AL. 1999). The interpolation to 20°C was based on the temperature response curves of Figs. 83-87, except those without values below 21°C. The mean ratio for all data was 2.28 ($r^2 = 0.86$, long solid line)

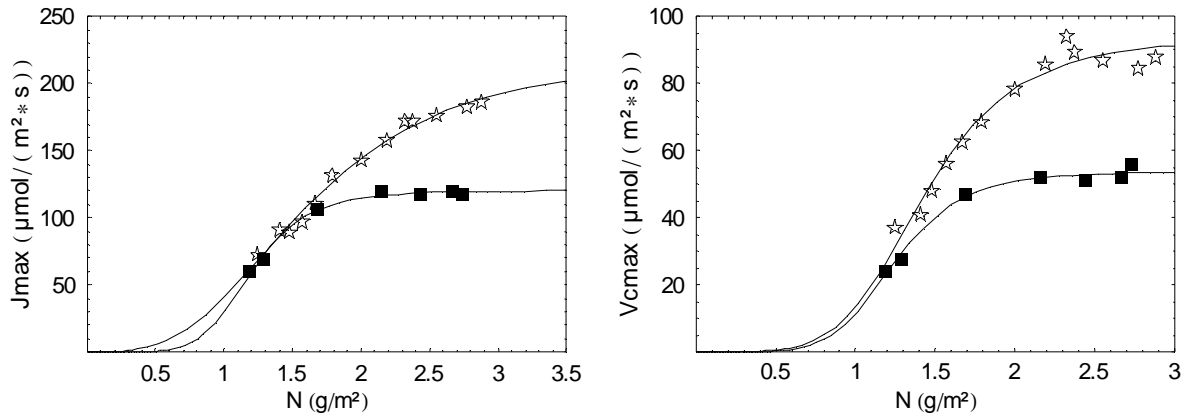


Fig. 89: Variation of J_{max} and $V_{c_{max}}$ at 25°C of leaves of oak Gr13 (open stars) and beech Gr12 (filled squares) with nitrogen content per area. Each data point represents the temperature interpolated value from nitrogen classes of leaves as in Figs. 83 - 86. The observed saturation at higher nitrogen contents was described with an approximation function of the type $y = a x^b / (x^b + c)$. Coefficients a, b, and c were 120.3, 5.94, and 3.02 (J_{max} , $r^2 = 0.99$) and 53.9, 5.85, and 3.68 ($V_{c_{max}}$, $r^2 = 0.99$) for beech Gr12. Coefficients for oak Gr13 were 221.1, 3.07, and 4.44 (J_{max} , $r^2 = 0.99$) and 93.7, 4.93, and 5.9 ($V_{c_{max}}$, $r^2 = 0.96$), respectively.

measured or could be interpolated for all described nitrogen classes. Fig. 89 confirms the strict tendency of increasing capacities with increasing nitrogen content, but it also shows that the relative increase with increasing nitrogen content per area became smaller and finally disappeared at higher nitrogen contents of leaves in the upper sun crown. Above a nitrogen threshold of around 2.2 g/m², additional nitrogen per area did not raise photosynthesis capacities of leaves of beech Gr12. While $V_{c_{max}}$ of oak Gr13 was nitrogen saturated at a nitrogen content of 2.3 g/m², J_{max} of oak Gr13 still increased with increasing nitrogen per area up to 2.9 g/m², but the slope of the J_{max} vs. nitrogen relationship was already decreasing at this nitrogen content. The non-linear approximation of arbitrarily chosen functions of the type $y = a x^b / (x^b + c)$ represents the data very well ($r^2 \geq 0.96$) and may be extrapolated to a saturating nitrogen content above 4.5 g/m² in this case.

6 additional A/Ci-curves from leaves of mature *Fagus crenata* (Blume) trees (SAITO & KAKUBARI 1999), measured at 21°C, were evaluated with RACCIA and the nitrogen dependence of their

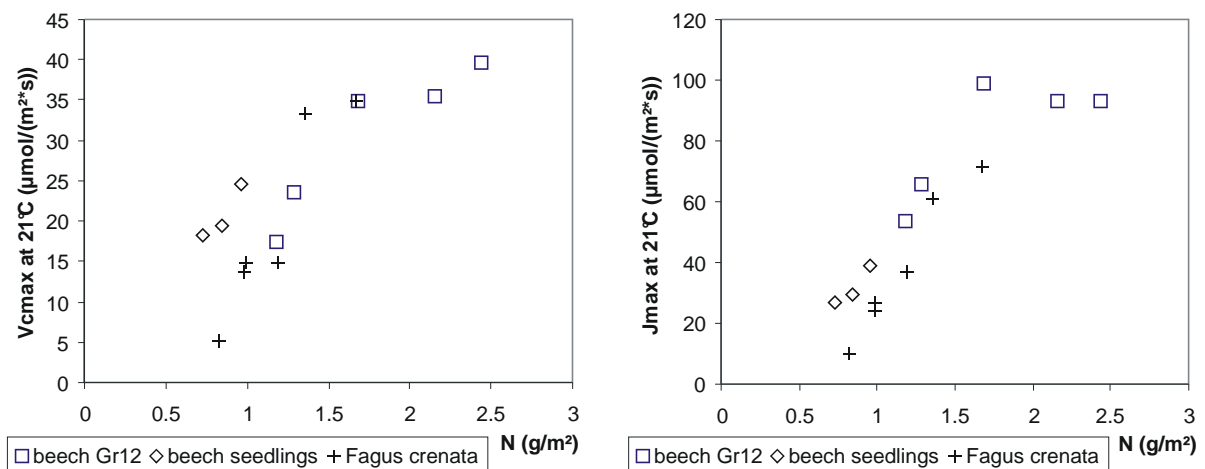


Fig. 90: Comparison of $V_{c_{max}}$ (left) and J_{max} (right) at 21°C of beech Gr12 with data from beech seedlings and from mature *Fagus crenata* trees.

capacities at 21°C was compared with that of beech Gr12 and beech seedlings (MEDLYN ET AL. 1999). Those temperature dependence functions without $V_{c_{max}}$ or J_{max} values below 22°C were excluded from this analysis to ensure a reasonable temperature interpolation. The results are depicted in Fig. 90 and show that only small differences exist between the three groups of leaves, those from *Fagus crenata* exhibiting generally similar capacities to those from beech Gr12 leaves with similar nitrogen content per area. Possibly due to lower nitrogen contents, the relationship of capacities vs. nitrogen per area of *Fagus crenata* did not show a saturation. While J_{max} -values of *Fagus sylvatica* seedlings seem to follow the same line as those from beech Gr12, $V_{c_{max}}$ -values were relatively higher than those of the mature trees.

3.2.2.5 The shape of temperature dependence functions for J_{max} and $V_{c_{max}}$

The three thermodynamic parameters of the temperature dependence function (equation (30)) from the evaluation of nitrogen classes with RACCIA did not show a clear dependence on nitrogen content per area. Range and average values for J_{max} - and $V_{c_{max}}$ -specific activation energies H_a , deactivation energies H_d and entropy terms S for leaves of both investigated trees are listed in table 6.

Table 6: range and average values of temperature dependence parameters

Quantity	Unit	Beech Gr12	Ø	Oak Gr13	Ø	
J_{max} -specific quantities	H_a	kJ/mol	37.3 - 53.5	46.4	37.2 - 66.3	47.4
	H_d	kJ/mol	140.6 - 269.3	213.7	149.4 - 417.7	251.4
	S	J/(K* mol)	464.5 - 1257	694.6	500.1 - 1330	814.3
$V_{c_{max}}$ -specific quantities	H_a	kJ/mol	33.3 - 79	61.4	37.3 - 92.8	61
	H_d	kJ/mol	121.7 - 226.8	170.4	140.1 - 410.2	268.7
	S	J/(K* mol)	403.5 - 717.7	551.9	448 - 1296	857.2

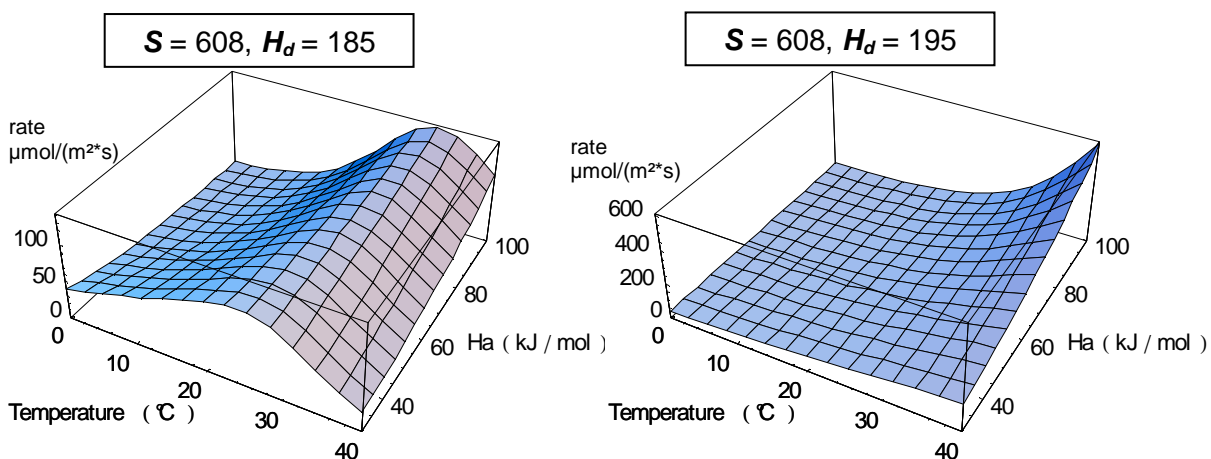


Fig. 91: Influence of relatively small changes of parameter H_d on the shape of the temperature dependence function for $V_{c_{max}}$ and J_{max} , when S is held constant at the average $V_{c_{max}}$ -specific value of beech Gr12 (608 J/(K * mol)). H_d is 185 kJ/mol in the left graph and 195 kJ/mol in the right graph, while the approximation to the measured data yielded an average value of 189 kJ/mol. The influence of parameter H_a can be seen from the third axis in the figure. The fourth parameter (rate at 25°C) was held constant equalling 100 $\mu\text{mol}/(\text{m}^2\cdot\text{s})$.

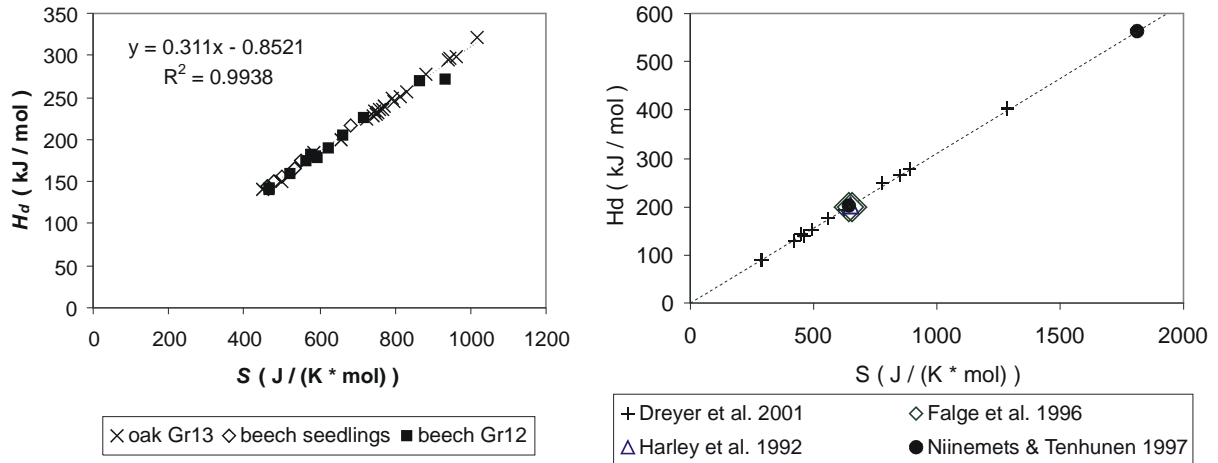


Fig. 92: Strong linear correlation between entropy terms and deactivation energies of equation (30) from the derived values for beech Gr12, oak Gr13, and beech seedlings (left graph). The same regression line gives a good approximation to previously published values (right graph).

In equation (30), the optimum temperature at which maximum rates are achieved is mainly determined by the parameters S and H_d , which interact in its third term. The ratio between both quantities is decisive for the result of this term and even small variations in one of both quantities without change of the other one were found to have an immense effect on the optimum temperature (Fig. 91). The high sensitivity of the shape of equation (30) on the ratio between both parameters is probably the reason for a strong correlation, that has been found between all the derived values for J_{max} - and V_{cmax} -specific parameters S and H_d (Fig. 92). The found linear relationship gave also a good approximation to previously published values, indicating the narrow range of reasonable values for these parameters, given that the optimum temperature lies somewhere between 20°C and 40°C. Considering the strong impact of small variations, the regression line in Fig. 92 was not forced through the origin.

S and H_d do not impose fundamental changes on the ecophysiologicaly interesting part of the temperature response curve, when their values move along the found linear relationship. Higher S and H_d values lead in this case to a more pronounced, peak-like temperature optimum with

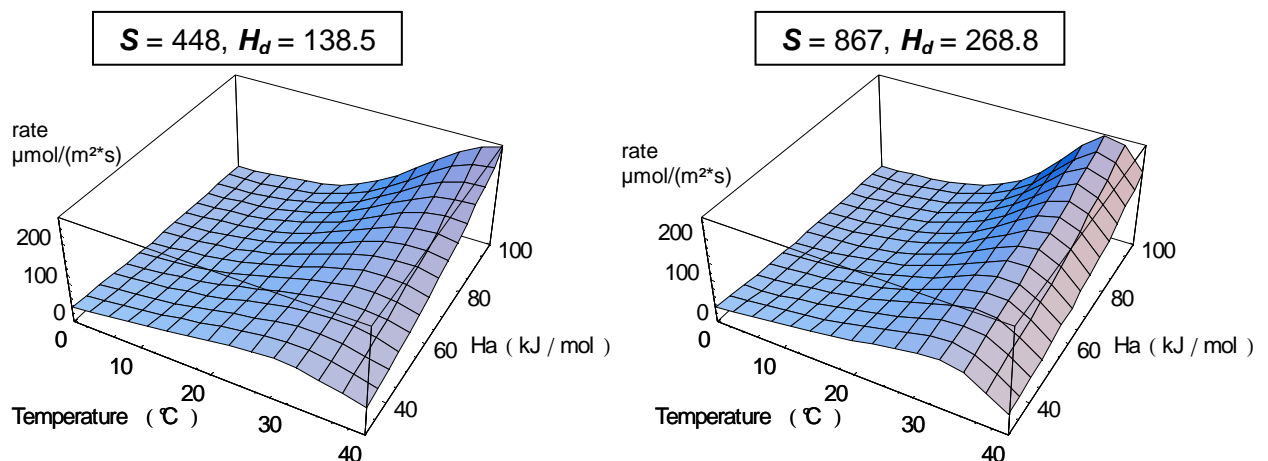


Fig. 93: Effect of simultaneously changing parameters S and H_d on the shape of the temperature dependence function for J_{max} and V_{cmax} (equation (30)). S and H_d were changed according to the linear relationship $H_d = 0.311S - 0.8521$, using the derived minimum value of S from oak Gr13 (left graph) and the maximum value from beech Gr12 (right graph). The rate at 25°C equals 100 $\mu\text{mol}/(\text{m}^2\cdot\text{s})$.

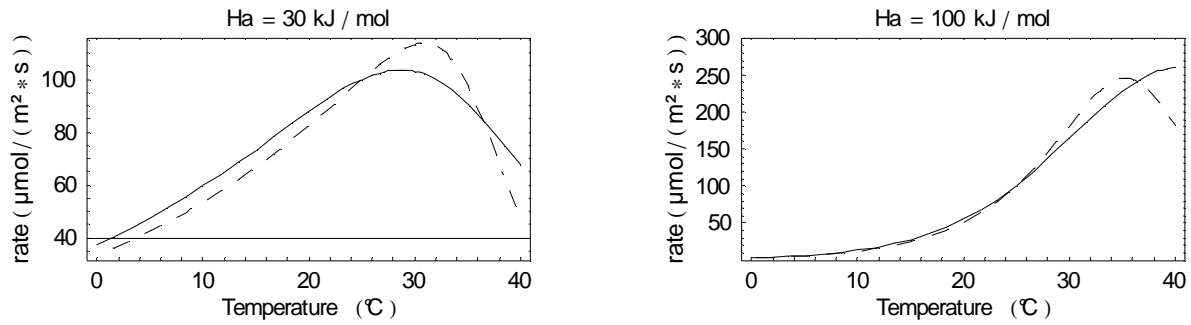


Fig. 94: Comparison of temperature dependence functions with minimum parameters of beech Gr12 ($S = 448 \text{ J}/(\text{K}^*\text{mol})$, $H_d = 138.5 \text{ kJ}/\text{mol}$, solid lines) and with maximum parameters of beech Gr12 ($S = 867 \text{ J}/(\text{K}^*\text{mol})$, $H_d = 268.8 \text{ kJ}/\text{mol}$, dashed lines). While the rate at 25°C was held constant at $100 \mu\text{mol}/(\text{m}^2*\text{s})$, activation energy H_a equals $30 \text{ kJ}/\text{mol}$ in the left graph and $100 \text{ kJ}/\text{mol}$ in the right graph.

more steeply ascending and descending slopes (Fig. 93), but the found differences in S -values and in H_d -values of different leaves or nitrogen classes induce only relatively small numerical changes in the resulting rates over the temperature range from 0°C to 40°C (Fig. 94). The effects of these differences on the optimum temperature were dependent on H_a , but also small. H_a mainly determines the curvature of the ascending slope of the temperature dependence curve, as can be seen in Figs. 93 and 94. While the rates below 25°C become lower, the rates above 25°C may easily become much higher when H_a -values are increased. Thus, rate calculations with equation (30) are more sensitive to the rate at 25°C and H_a than to parameters S and H_d , when the average linear relationship between S and H_d is assumed.

While J_{max} and Vc_{max} at 25°C have been shown to be strictly nitrogen dependent (Fig. 89), a weaker tendency was found for activation energies, H_a increasing with nitrogen per area ($r^2 = 0.35$ (Vc_{max}) and 0.25 (J_{max}) for all beech data and $r^2 = 0.27$ (Vc_{max}) and 0.01 (J_{max}) for oak Gr13, data not shown). Stronger relationships were observed between J_{max} at 25°C and H_a and between Vc_{max} at 25°C and H_a (Fig. 95). The unique H_a vs. J_{max} relationship for beech seedlings and beech Gr12 had a very high coefficient of determination (0.91), while the Vc_{max} -specific relationship was weaker (0.45), similar to that of oak Gr13 ($r^2=0.47$). No clear relationship was found between J_{max} and H_a of oak Gr13 leaves ($r^2 = 0.03$), which may be due to the low number

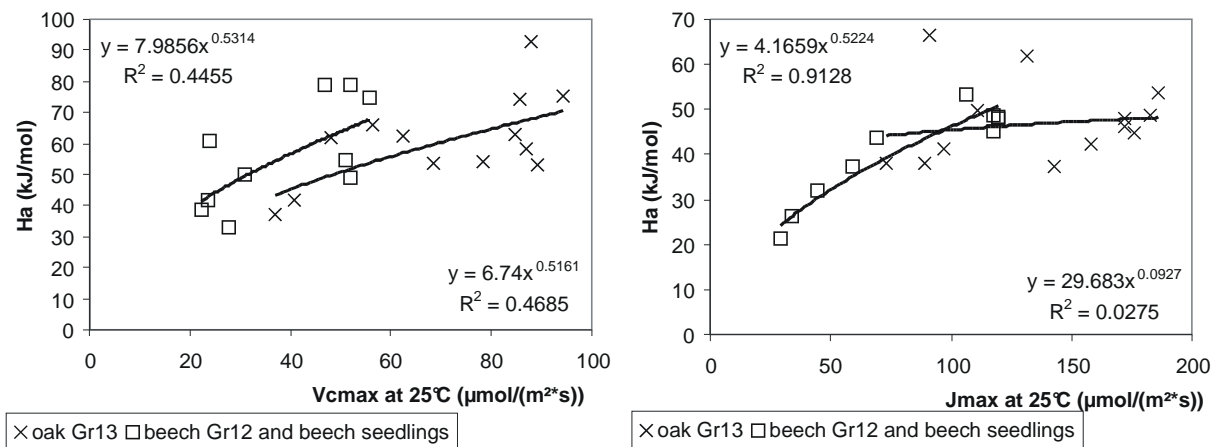


Fig. 95: Relative increase of activation energies H_a for Vc_{max} (left graph) and J_{max} (right) with their appertaining rates at 25°C . Equations and coefficients of determination in the upper left corner are for beech and those in the bottom right corner of each graph are for oak.

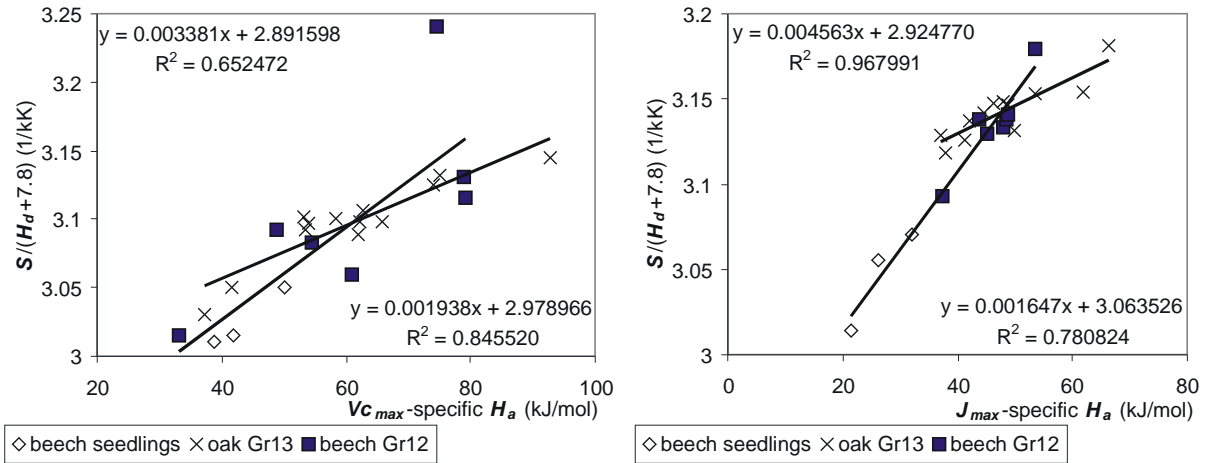


Fig. 96: Empirically found relationships between H_a and $S/(H_d+7.8)$ for the temperature dependence function of Vc_{max} (left) and J_{max} (right). The similar relationship for beech Gr12 and beech seedlings was considered with a unique regression line. The regression line for oak Gr13 had a smaller slope coefficient. Equations and coefficients of determination in the upper left corner are for beech and those in the bottom right corner are for oak.

of data points for the whole investigation, since the exclusion of only three points would result in an r^2 of 0.73.

As stated above, the ratio between S - and H_d -values was not really constant due to the addition of a small, but possibly powerful constant value. Thus, the term $S / (H_d + 0.8521)$ may be seen as constant in a first approximation. The examination of the small deviations from this approximation showed no clear tendency in relation to nitrogen or other leaf-related quantities, but the weak correlations that were found in relation to H_a ($r^2 \leq 0.3$) fundamentally improved, when the constant value was arbitrarily increased to a number close to 7.8 (Fig. 96). This was valid for J_{max} and Vc_{max} data from oak Gr13, beech Gr12, and beech seedlings. The empirical relationship between H_a and $S/(H_d+7.8)$ was nearly the same for beech seedlings and beech Gr12, while it was different for oak Gr13.

Thus, J_{max} and Vc_{max} are fully determined by nitrogen content and temperature:

- J_{max} and Vc_{max} at 25°C are dependent on nitrogen (Fig. 89).
- H_a may be expressed as function of J_{max} or Vc_{max} at 25°C (Fig.95), though the coefficients of determination for oak were low.
- Two equations (Figs. 92 and 96) describe the relationship between S and H_d , when H_a is known, and may be solved simultaneously for the determination of S and H_d .

If all found relationships between parameters of equation (30) and the relationship from Fig. 89 may be accepted as empirical relationships (which can only be proven in further investigations that increase the number of data points), J_{max} and Vc_{max} of *Fagus sylvatica* and *Quercus petraea* would be determined by temperature and nitrogen per area as is shown in Fig. 97.

3.2.2.6 Ball-Woodrow-Berry-coefficient of stomatal sensitivity (g_{fac})

The coefficient of stomatal sensitivity (g_{fac}) may be estimated from photosynthesis measurements on the base of equation (32). The relationship between stomatal conductance to H_2O and the product of A (net assimilation), rh (relative humidity at the leaf surface), and $1/C_s$ (CO_2 -concentration at the leaf surface) is expected to be linear (BALL ET AL. 1987) and the slope

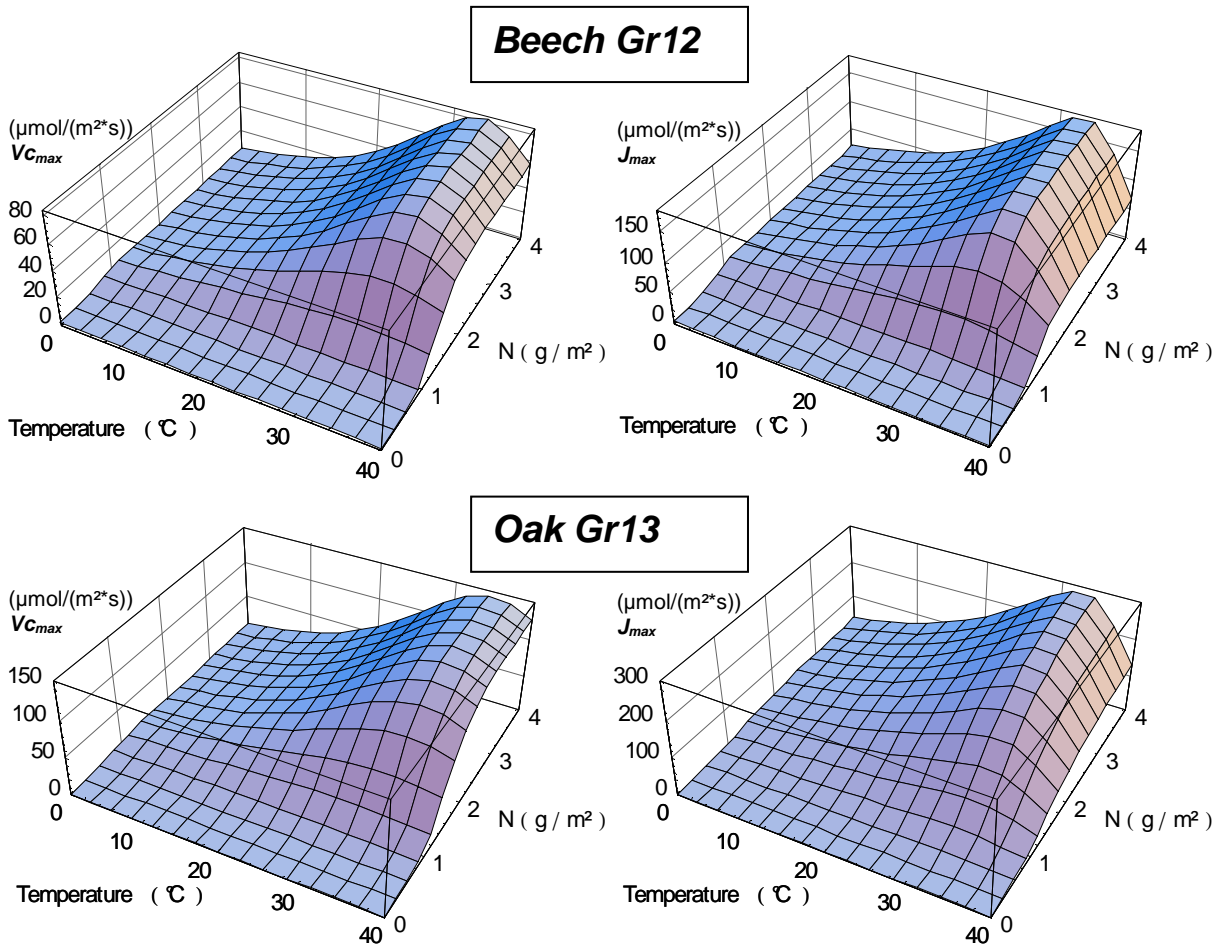


Fig. 97: Shape of the average dependence of V_{cmax} and J_{max} from beech Gr12 (upper row) and oak Gr13 (below) on temperature and nitrogen per leaf area.

of this relationship is an important parameter in the HARLEY/TENHUNEN model, linking photosynthesis and transpiration. It is not clear, if the stomatal sensitivity is purely dependent on the time course of climatic conditions during the day of measurement or if it partly also belongs to the structural leaf properties, that may change with changing leaf structure in mature tree crowns. Two simplifications were made to investigate the latter point: First, relative humidity (rh) and CO_2 -concentration at the leaf surface (C_s) were set equal to external CO_2 -concentration and humidity. This simplification did not remarkably change the numerical value of g_{fac} , because

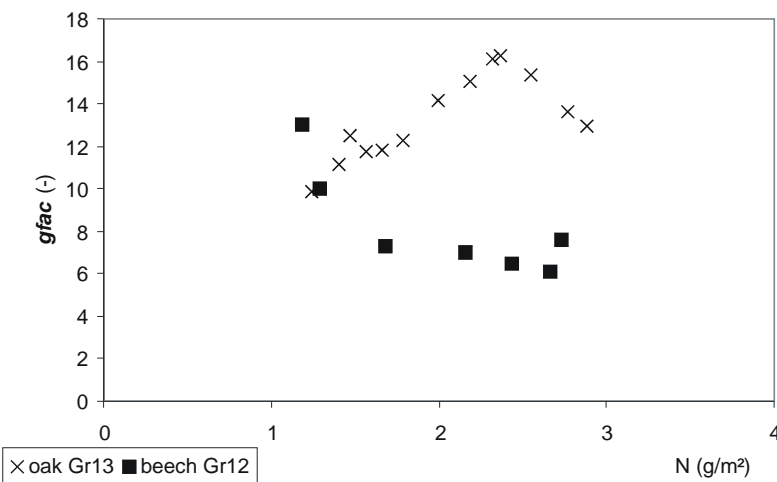


Fig. 98: Relationship between the Ball/Woodrow/Berry-coefficient of stomatal sensitivity (g_{fac}) and nitrogen per leaf area for nitrogen classes of leaves of both mature trees.

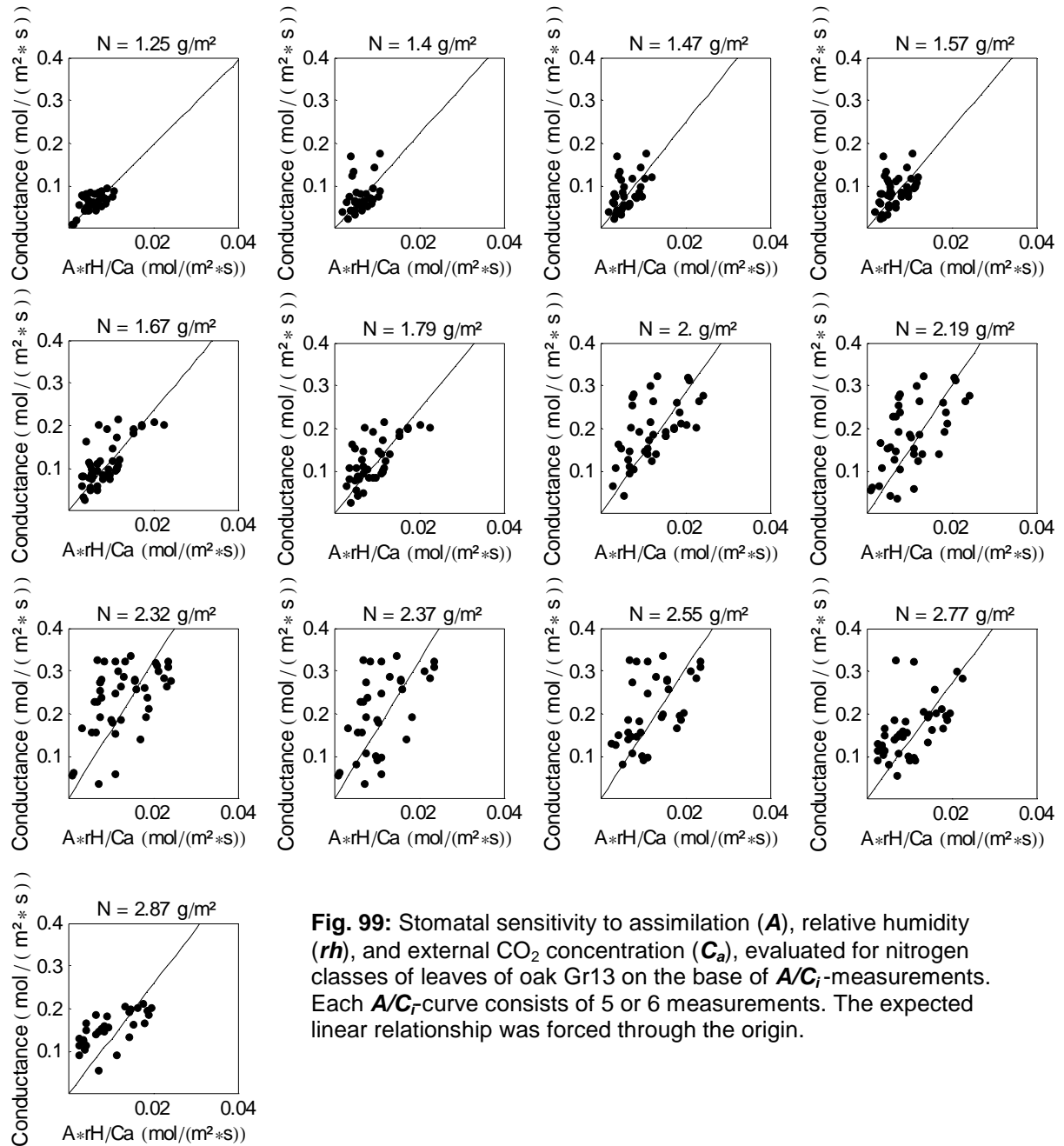


Fig. 99: Stomatal sensitivity to assimilation (A), relative humidity (rh), and external CO_2 concentration (C_a), evaluated for nitrogen classes of leaves of oak Gr13 on the base of A/C_i -measurements. Each A/C_i -curve consists of 5 or 6 measurements. The expected linear relationship was forced through the origin.

boundary layer conductances in the A/C_i -measurements were high and constant due to constant flow rates in the chamber ($g_{aw} = 1.42 \text{ mol}/(\text{m}^2\text{s})$). Second, g_{min} in equation (32) was set to 0 to make the different estimations for g_{fac} directly comparable, without any dependence on a second parameter.

A variation of the stomatal sensitivity of oak Gr13 leaves and beech Gr12 leaves with nitrogen per area was observed (Figs. 99 and 100). g_{fac} of beech leaves was generally lower and varied between 6.1 and 13, while it was generally higher in oak leaves (9.9 - 16.3). The comparison of the nitrogen relationship of g_{fac} of both trees showed a fundamental difference between the trends for oak Gr13 and beech Gr12 (Fig. 98). Shade leaves of beech were relatively sensitive to changes in the $A * rh / C_a$ -ratio, but the sensitivity coefficient g_{fac} steeply decreased with increasing nitrogen content to a constant value around 7, which was maintained for leaves between 1.7 and 2.7 g nitrogen / m^2 . Nearly the opposite trend was found in oak leaves: g_{fac} of

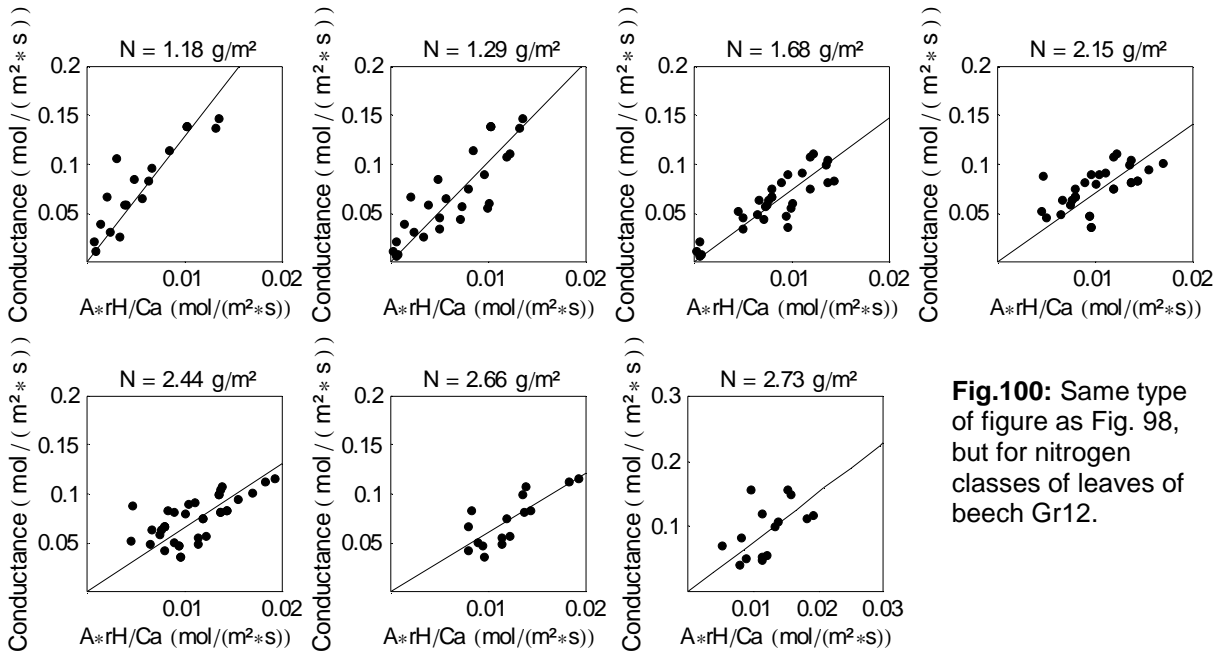


Fig.100: Same type of figure as Fig. 98, but for nitrogen classes of leaves of beech Gr12.

extreme shade leaves was lowest (9.8) and increased linearly with increasing nitrogen content up to a maximum value of 16.3 at 2.4g/m². Above this value, g_{fac} of oak Gr13 leaves tended to decrease.

3.2.3 Nitrogen dependent model of leaf photosynthesis for beech

3.2.3.1 Model description

Nitrogen per leaf area correlated with those leaf properties of oak Gr13 and beech Gr12 that are most important for the determination of photosynthesis rates and it has been shown to be dependent on relative irradiance in tree crowns of beech. It is therefore well suitable for up-scaling along light gradients in tree crowns. The nitrogen dependent model of leaf photosynthesis extends the model of HARLEY and TENHUNEN (1991) as described above in order to consider the found nitrogen dependent variation in photosynthesis capacities of leaves in tree

crowns of beech. Thus, it combines the above findings on nitrogen dependence of J_{max} , $V_{C_{max}}$, and R_d in the calculation of photosynthesis rates for single leaves.

The N-dependent parameterisation of equation (30) for J_{max} and $V_{C_{max}}$ is done according to the equations displayed in Figs. 89, 92, 95, and 96. Thus, rates at 25°C are dependent on nitrogen, H_a is dependent on the rate at 25°C and S and H_d depend on H_a according to the following equations:

J_{max} -specific:

$$J_{max,298} = \frac{120.3 N^{5.94}}{N^{5.94} + 3.02} \quad (37)$$

$$H_a = 4.1659 J_{max,298}^{0.5224} \quad (38)$$

$$\frac{S}{H_d + 7.8} = 0.004563 H_a + 2.925 \quad (39)$$

$V_{C_{max}}$ -specific:

$$V_{C_{max},298} = \frac{53.9 N^{5.85}}{N^{5.85} + 3.68} \quad (40)$$

$$H_a = 7.9856 V_{C_{max},298}^{0.5314} \quad (41)$$

$$\frac{S}{H_d + 7.8} = 0.003381 H_a + 2.89 \quad (42)$$

H_d in equations (39) and (42) is assumed to follow the relationship

$$H_d = 0.311 S - 0.8521 \quad (43)$$

R_d was also described as nitrogen dependent. While H_a from equation (28) for R_d was held constant at 70 kJ/mol, a linear increase of $R_{d,298}$ with nitrogen per leaf area (N) was assumed, that was derived from the two data points for beech Gr12 in Fig. 82:

$$R_{d,298} = 0.874 N - 0.269 \quad (44)$$

(compare Fig. 80).

While g_{min} was held constant equalling 0, g_{fac} was varied according to a quadratic fit to the beech data in Fig. 100 ($R^2 = 0.9$):

$$g_{fac} = 5.0071 N^2 - 22.704 N + 31.884 \quad (45)$$

3.2.3.2 Parameterisation

Nearly all parameters that are not rubisco-specific constants were replaced by a nitrogen dependent function, so that the number of parameters for the calculation of photosynthesis and transpiration of single leaves was reduced from 18 to 8, as can be seen in table 7.

rubisco-specific constants ($K_{M,C}$, $K_{M,O}$, τ) and the $K_{M,C}$ - and $K_{M,O}$ - specific H_a -values for equation (28) were taken from the *in vivo* measurements of VON CAEMMERER ET AL. (1994). The τ -specific H_a -value was taken from HARLEY & TENHUNEN (1991), which produced Γ^* -values very close to those from equation (36), when equations (27) and (28) were applied in the model (Fig. 101). This formulation was preferred, because it includes the dependence of Γ^* on oxygen concentration of the atmosphere.

α was set constant to 0.06 mol CO₂/mol photons.

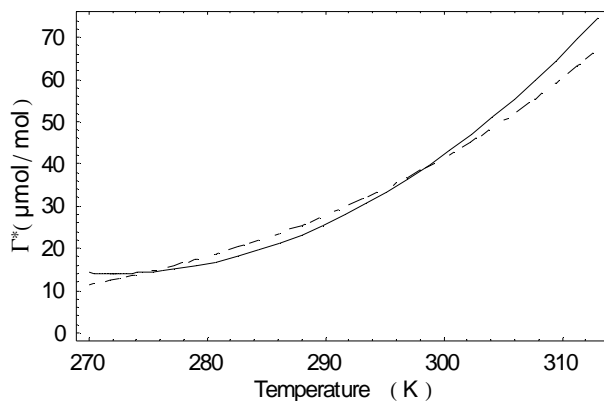


Fig. 101: Similar result of alternative formulations for the temperature dependence of Γ^* . While the entire line represents equation (36) (ATKIN ET AL. 2000), the dotted line is the result of equations (27) and (28) for an atmospheric oxygen concentration of 209 mmol/mol, using parameters τ from VON CAEMMERER ET AL. (1997) and H_a from Harley & Tenhunen (1991).

Table 7: Parameters of the leaf models

	HARLEY/TENHUNEN model	Nitrogen dependent model	Numerical value in the nitrogen dependent model
Rubisco-specific constants	$K_{M,O}$	$K_{M,O}$	248 mmol/mol
	$K_{M,O}$ -specific H_a	$K_{M,O}$ -specific H_a	35000 J/mol
	$K_{M,C}$	$K_{M,C}$	404 μ mol/mol
	$K_{M,C}$ -specific H_a	$K_{M,C}$ -specific H_a	63500 J/mol
	τ	τ	2710
	τ -specific H_a	τ -specific H_a	-28990 J/mol
Light-use parameters	α	α	0.06 mol CO ₂ /mol photons
	$P_{mI,298}$		
	H_a		
	S		
	H_d		
Carboxylation parameters	$V_{Cmax,298}$		
	H_a		
	S		
	H_d		
Respiration parameters	$R_{d,298}$		
	H_a		
Conductance parameters	g_{fac}		
	g_{min}		
Nitrogen		N	variable

3.2.3.3 Validation Measurements

While A/Ci-measurements took place between 27th of July and 6th of August 1998, validation measurements at ambient CO₂-concentrations were performed on 7th and 8th of August 1998, which were two of the driest and warmest days of that year in the Steigerwald (Fig. 102). Photosynthesis was measured two to four times during the day for around 20 minutes on each leaf, alternating between different leaves of both trees, whereby single points of the daily course

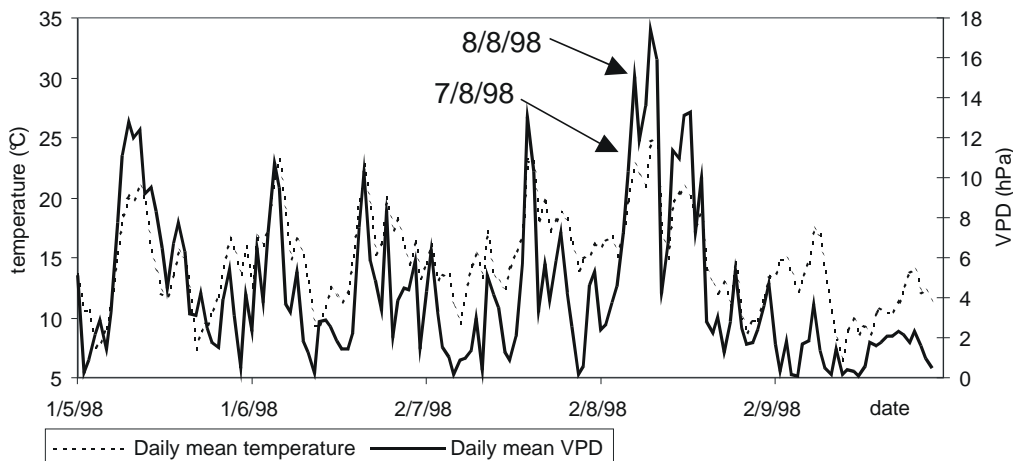


Fig. 102: Time course of VPD and temperature of summer 1998. 7th and 8th of August were two of the driest days of this year.

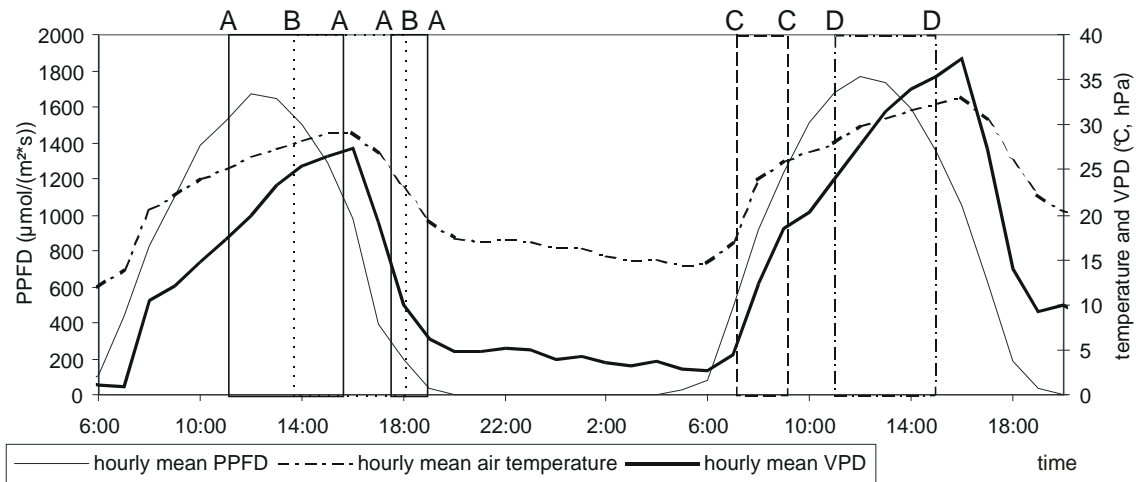


Fig. 103: Course of climate variables during the measurement period, measured five metres above the floor on a nearby clear-cut. Vertical lines indicate the average point of time of each measurement. The letters above each line indicate the name of the leaf.

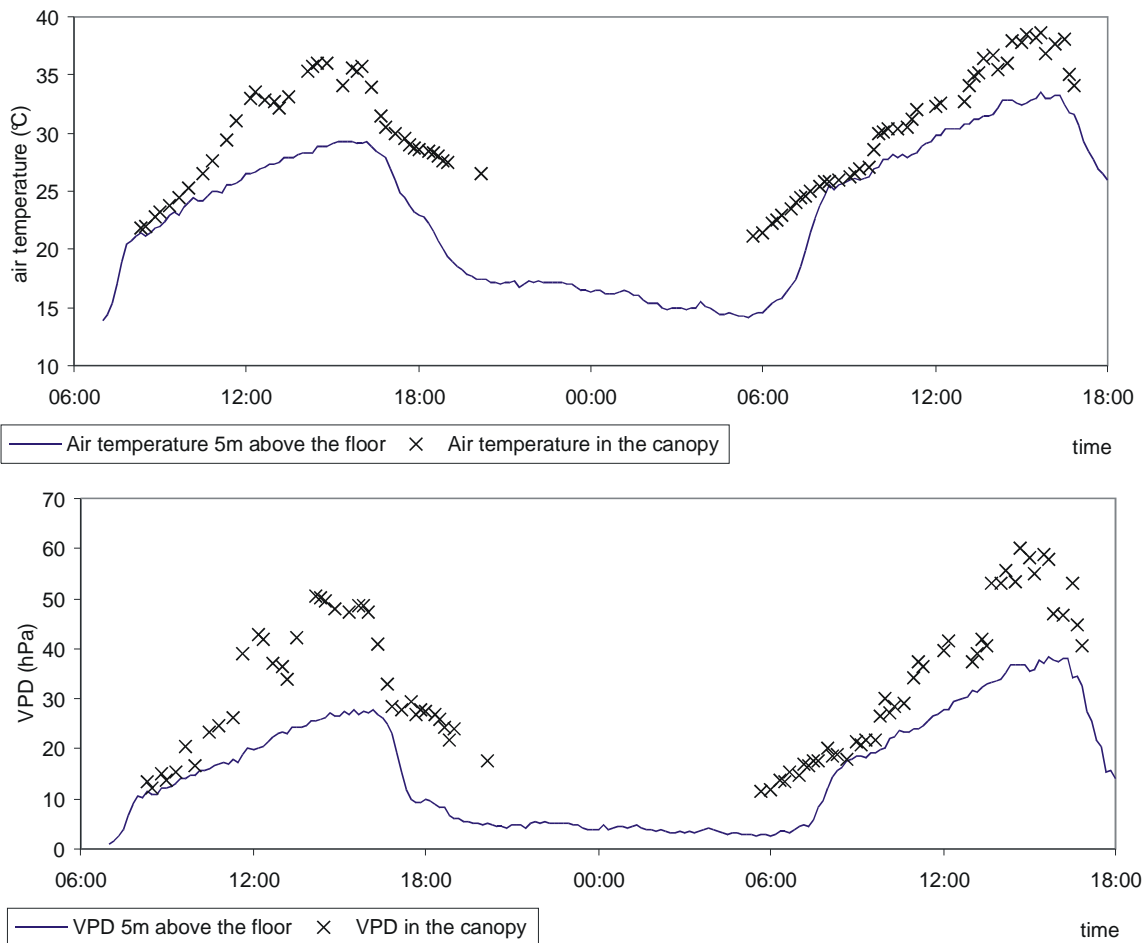


Fig. 104: Course of air temperature and VPD during 7th and 8th of August 1998. The measured values in the canopy were recorded in a height of 19 m above the floor on the south side of beech Gr12 and oak Gr13, while the values 5m above the floor were measured above a clear-cut.

of photosynthesis could be determined for each leaf. The objective to measure leaves with different nitrogen content and light exposition in the crowns of both species was only partly reached, because leaves of oak Gr13 were even in the morning hours not responding to light and stomata of most measured oak leaves remained at low conductances during the whole day. Less of the measured leaves of beech Gr12 seemed to be affected by drought, and their nitrogen content turned out to range from 1.8 to 2.3 g/m². All beech leaves were measured in the same height above the floor (19m), two leaves with 1.83 and 1.85 g N/m² represent a position shaded by other leaves and closer to the stem (leaves B and C), while leaves A and D were fully sun-exposed and had nitrogen contents of 1.96 g/m² and 2.28 g/m².

Day time of these measurements and climate conditions are depicted in Fig. 103. PPF_D, air temperature, and VPD were measured five metres above the floor on a nearby clear-cut. Though they differ from the conditions at the positions of the leaves, they may give insight into the relative changes of climate conditions over the two days. The deviation from these conditions at the position of a leaf in the canopy may be derived from the validation measurements in the canopy (Fig. 104). Air temperature was on average 4.2°C higher than 5m above the floor and a maximum temperature difference of 9°C was reached in the afternoon. VPD was on average 12.3 hPa higher with a maximum difference of 25 hPa. This may partly be attributed to the fact that the clear-cut is surrounded by forest, which casts a shadow in the early morning and in the late evening on the measurement station and may be the source of cooler and more humid air that is exchanged even at low wind velocities. On the other hand it may reflect the increased temperature of sun-exposed leaves and branches that are sun-exposed and poorly cooled by wind and transpiration, thus warming up the surrounding air. Between 12:00 and 16:00 MET, the average measured difference between temperature of leaves and air temperature was 1.1°C with a maximum value of 3.1°C, measured at 13:51 MET on 8th of August at a sun-exposed oak leaf.

Increasing irradiances were under these circumstances generally accompanied by dramatic changes in VPD, which is probably the reason for an unusual light response that was observed when the photosynthesis rates of all leaves are viewed against PPF_D (Fig. 105). The photosynthesis rates of beech leaves at above 1000 μmol/(m²*s) PPF_D were all lower than the rate of leaf A at 660 μmol/(m²*s).

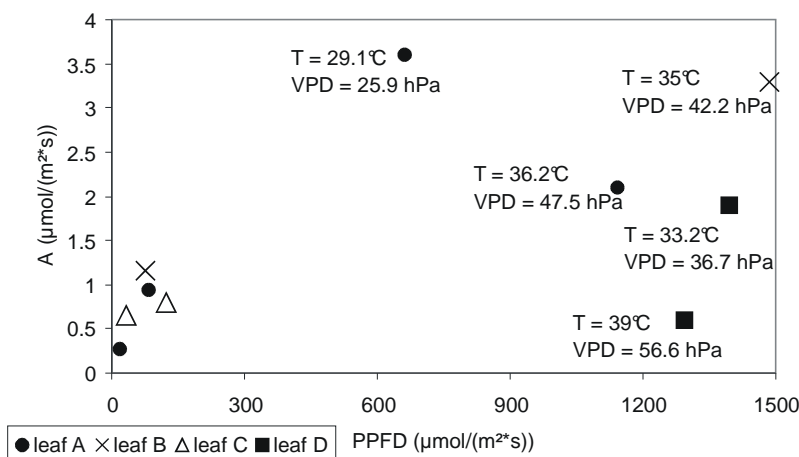


Fig. 105: Light dependence of assimilation rates of four different leaves in the crown of beech Gr12. Average leaf temperature and VPD at the leaf's position during the measurement are given for the measurements under high PPF_D. Nitrogen contents of the leaves were A: 1.96 g/m², B: 1.83 g/m², C: 1.85 g/m², and D: 2.28 g/m²

3.2.3.4 Model validation

The comparison between modelled and measured values of assimilation (A) and stomatal conductance (g_{sw}) revealed a general overestimation by the model: The difference between modelled and measured values was on average $0.52 \mu\text{mol}/(\text{m}^2\cdot\text{s})$ and $1.89 \text{mmol}/(\text{m}^2\cdot\text{s})$, respectively, which corresponds to 34% and 9% of the mean of measured values (mean absolute error, MAYER & BUTLER 1993). The high percentage for A is a consequence of the relatively low photosynthesis rates that were measured during the validation measurements, but it also reflects the partly big deviations from the 1:1 line in Fig. 106. The agreement between measured and modelled values may adequately be described by the root mean square error ($\sqrt{\frac{1}{n} \sum \epsilon^2}$, JANSSEN & HEUBERGER 1995), which was $1.1 \mu\text{mol}/(\text{m}^2\cdot\text{s})$ for A and $6.8 \text{mmol}/(\text{m}^2\cdot\text{s})$ for g_{sw} .

This overestimation was already expected from their unusual light response (Fig. 105), which must be seen with respect to the unusually dry conditions for the leaves on the measurement days. The strongest observed impact of the low relative humidity on leaf photosynthesis was that oak leaves had permanently low conductances, thus reducing assimilation to values below $1 \mu\text{mol}/(\text{m}^2\cdot\text{s})$. Though only some beech leaves with extremely low conductances were observed (data not shown), the question arises, if their stomatal reaction to drought has been assessed as accurately as necessary.

It has been shown that stomatal aperture of several species including beech is generally not uniform but patchy distributed over the leaves (KÜPPERS ET AL. 1999, ECKSTEIN 1997). The phenomenon of stomatal patchiness may lead to an overestimation of photosynthesis rates, when - like in the used model - only the average response of the stomata is considered (CHEESEMAN 1991). This overestimation is expected to be most severe in heterobaric leaves, where lateral gas diffusion is restricted, which causes different C_f -values in different parts of the leaf (VON WILLERT ET AL. 1995). In leaves of mediterranean plants, but also of *Quercus petraea*, *Picea abies*, and *Abies alba*, selective stomatal closure is known to be a response to low air humidity and may cause more or less big parts of the leaf to be excluded from photosynthetic activity, while other parts remain physiologically active (EPRON & DREYER 1993, BEYSCHLAG ET AL. 1992, BEYSCHLAG ET AL. 1994). Stomatal patchiness has also been shown to be light induced (KÜPPERS ET AL. 1999) and has been discussed as a mechanism to avoid photoinhibition (BEYSCHLAG & ECKSTEIN 1997).

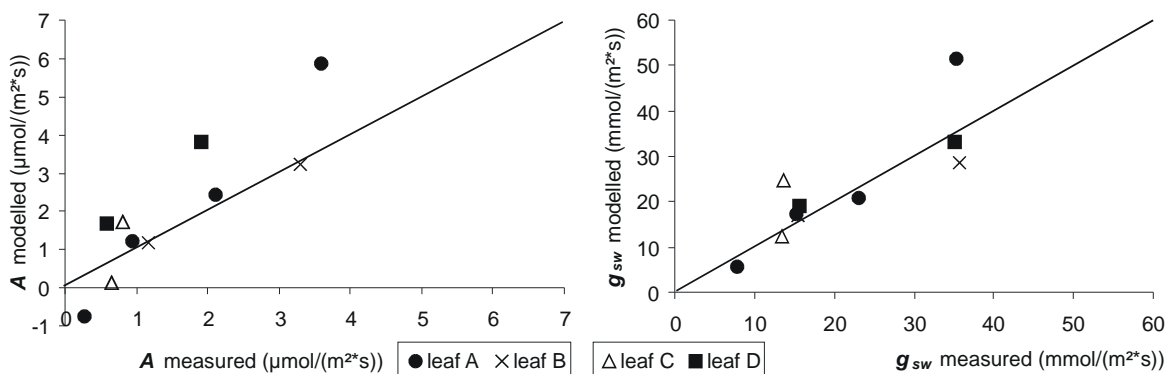


Fig. 106: Modelled versus measured values of assimilation rate A (left) and stomatal conductance to water vapour g_{sw} (right). The line represents the ratio 1 between modelled and measured data.

Since *Fagus sylvatica* leaves have a septate leaf anatomy due to sklerenchymatic tissues (“Sklerenchymscheide”) around the leaf veins, which causes the leaf to be heterobaric (VON WILLERT ET AL. 1995), it seems to be plausible, that the measured assimilation rates and conductances may be influenced by stomatal patchiness.

A simple test was performed to evaluate the effect of inactivated leaf parts on the model calculations: It was assumed that the shaded leaves inside the crown (B and C) still behave as the model expects, while the sun-exposed leaves (leaves A and D) are partly inactivated. 30% of their leaf area is assumed to be completely inactivated, while the rest of the leaf is physiologically active and behaves as the model expects. Under these circumstances, $V_{c_{max}}$, J_{max} , and R_d have to be reduced to 70% (BEYSCHLAG & ECKSTEIN 1997), while the average sensitivity of the stomata to humidity, assimilation, and CO₂ (g_{fac}) remains unchanged.

The effect of these changes on the comparison between model results and measurements is shown in Fig. 107. The previously reported overestimation of assimilation (**A**) and conductance (g_{sw}) disappeared: The average difference between modelled and measured values was 0.17 $\mu\text{mol}/(\text{m}^2\cdot\text{s})$ for **A** and -1.1 $\text{mmol}/(\text{m}^2\cdot\text{s})$ for g_{sw} , which is an overestimation of 11% of the mean of measured assimilation rates and an underestimation of 5% of the mean of measured stomatal conductances. The root mean square of errors improved to 0.48 $\mu\text{mol}/(\text{m}^2\cdot\text{s})$ and 4.9 $\text{mmol}/(\text{m}^2\cdot\text{s})$, when the inactivation of parts of the sun-exposed leaves was considered this way. This improvement in modelled assimilation rates was a consequence of lowered assimilation rates (due to decreased $V_{c_{max}}$ and J_{max}) as well as of one increased assimilation rate of leaf A, which is attributed to the decrease in R_d .

3.3 Summary and discussion

The investigations to relative irradiance above leaves along vertical lines confirm the general validity of Beer’s law in the investigated beech crowns, though deviations from a strictly exponential decrease were also found. These deviations were mainly found on the smaller tree, whose light climate is strongly influenced by the different height of neighbouring trees and they may partly be attributed to the effects of gaps between leaf clouds. Additional deviations occur in the lowest third of both crowns, where relative irradiances are not as low as an exponential approximation would suggest.

The scatter in the relationship between relative irradiance and distance to apex allows one to

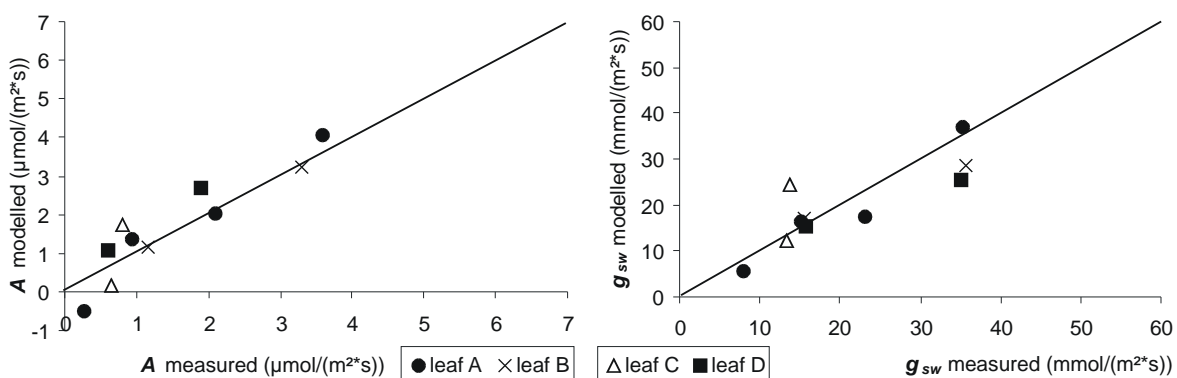


Fig. 107: Modelled versus measured values of **A** (left) and g_{sw} (right) under the condition that the photosynthetically active leaf area of the two sun-exposed leaves is reduced to 70%. The line represents the ratio 1 between modelled and measured data.

distinguish between deterministic and adaptive leaf properties: While height below apex may not be experienced by a leaf, irradiance is the most important driver for its physiological activity. Hence, strongly light dependent quantities appear to be a consequence of the environmental conditions, while height dependent quantities may simply be determined by regularities of growth.

In this sense, leaf angle distributions in the canopies of beech trees were found to be deterministic: The leaf angle distribution of each height level was an ellipsoidal distribution and the single parameter k of these distributions was linearly dependent on height, while it did not show a clear relationship to relative irradiance. That the linear dependence changes its direction in the lower third of the tree crowns may not be the result of changing irradiance, because only very small differences in relative irradiance occur in this part of the crown.

The theory of PPFD extinction in homogeneous canopies with ellipsoidal leaf angle distribution (CAMPBELL & NORMAN 1989) would expect a functional relationship that allows the calculation of a constant extinction coefficient for Beer's law from an assumed constant parameter of the ellipsoidal distribution and the zenith angle, but the assumption is not confirmed by this investigation. The vertical gradient in parameter k of the ellipsoidal leaf angle distributions must be considered in such calculations with the consequence of deviations from a strictly exponential decrease of irradiance with height. Thus, the deviations from Beer's law in beech Bu45 and beech Bu38 are partly a consequence of the deterministic change in leaf angle distributions.

Comparable results have been found for a mature tree crown of *Quercus robur* (KULL ET AL. 1999) and were interpreted as light dependent. The low number of six data points in this data set allows to draw an exponential relationship on canopy light transmittance with $r^2 = 0.89$, but the re-evaluation of these data shows, that also a linear relationship to height exists ($r^2 = 0.85$, data not shown).

A deterministic and adaptive change of leaf properties was found in the branch angles of their above neighbourhood. This may be understood on the assumption of autonomous growth of branches towards a better light situation, which would result in more horizontal growth towards the surface of the canopy in the lower part and increasing branch angles with increasing height, as was found in the measurements. Since this adaptive growth form was probably more successful in evolution than others it may have become part of a deterministic growth scheme and may therefore not be classified as adaptive or deterministic.

Width of leaf space is a more important quantity for light transmission through the canopy than width of leaf blade. Similarly to the parameter k of leaf angle distributions it followed a quasi-linear trend and increased up to 7m below apex but then the direction of the quasi-linear relationship changed towards decreasing widths. This effect contributes to the "better than by Beer's law expected" relative irradiances in the lower third of the canopies since it increases the transmission through the lowest leaf layers. The much more scattered relationship between width of leaf blade and height indicates the relative irrelevance of this quantity for light absorption and transmission.

Height of leaf space was surprisingly not simply a consequence of leaf bending by width reduction, but had together with width of leaf space a meaning for the relationship between light interception and chemical composition of the leaf, as may be derived from Fig. 74. Though it is not easy to find reasons for this highly significant relationship, it shows that leaf bending is more important for the interception of radiation than could be expected. The similar relationship in Fig.

73 describes a relationship between leaf space dimensions and nitrogen and carbon concentration of the leaf biomass and may be interpreted in terms of structural requirements to achieve a given leaf form.

Leaf mass per area was primarily light dependent and not as strictly height dependent, which suggests an adaptation to environmental conditions. Stand-specific differences are obvious from Figs. 68 and 69, whereas species-specific differences between oak Gr13 and beech Gr12 were not detected. Because nutrient and deposition situation of both stands were similar, other growth conditions like length of vegetation period, average humidity, or average temperature come into question as reasons for stand-specific differences.

Though stand-specific differences exist, it is probably not chance that the maximum leaf mass per area measured on beech Gr12 was the highest value when compared with published values from the last 110 years. The estimated average leaf mass per area of all three investigated beech trees was more than double that of mature trees from 1945! The same was also found for oak Gr13 when compared with data from 1947. Fig. 108 shows that the data from the studies mentioned in table 5 describe a more or less continuous increase of maximum LMA-values during the last decades. Thus, the extremely high maximum LMA-value from beech Gr12 is not interpreted as a special quality of the stand but as part of a general trend towards increasing leaf mass per area in beech leaves in Europe during the last 110 years. A potential reason for this trend is the parallel change in the environmental situation due to CO₂-increase and nitrogen depositions. However, (PETERSON ET AL. 1999) describe only weak effects of high CO₂ on LMA of leaves of beech seedlings, while other seedlings were more susceptible to CO₂-induced increases of LMA.

The strong relationship between relative irradiance and leaf mass per area ($r^2 = 0.88$, Fig. 68) was even valid for the variation of LMA in leaf clouds. It corresponds to the similar relationship between relative irradiance and nitrogen per leaf area (Fig. 75) and both together provide a solid basis for up-scaling purposes, since the variation in most photosynthesis parameters has been found to be nitrogen dependent.

The measured leaf nitrogen contents were partly very high. While the 'normal range' of nitrogen concentrations per dry weight of leaves in adult forest stands is 1.8 to 2.91% of dry weight (*Quercus petraea*, VAN DEN BURG 1990) and 1.8 to 2.78% of dry weight (*Fagus sylvatica*, VAN DEN BURG 1990), a range from 2.2 to 3.1% has been found in beech leaves from the upper third of the crowns along a European transect (BAUER ET AL. 1997). Thus, oak Gr13 had leaves with extremely high nitrogen concentrations, while beech Gr12 had normal to high concentrations

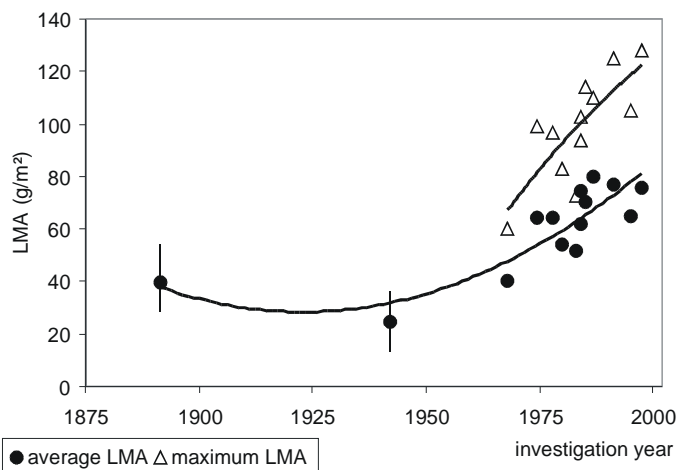


Fig. 108: Increase of maximum and estimated average values of leaf mass per area of mature beech trees during the last 30-110 years as derived from published values.

Average values for the newer studies since 1970 were estimated as the mean of minimum and maximum values, which was a 10% overestimation in the case of beech trees from the own harvest. The range of means from older whole tree harvests is indicated as error bars.

and the Buchenallee beeches had leaves with absolutely normal nitrogen concentrations per dry weight. These concentrations combined with the found high LMA-values result in the presented high leaf nitrogen contents per area for the Großebene trees. A direct effect of nitrogen depositions on these values could not be found due to the similar amount of nitrogen depositions in Buchenallee and Großebene, although the C/N ratio of the humus layer was slightly higher in the Buchenallee stand.

The dependence of carbon concentrations on relative irradiance may be interpreted as a consequence of increasing leaf mass per area with relative irradiance, which leads in addition to the construction of additional tissue to increased requirements for mechanical stability of the leaf, thus requiring more structural carbon. The production of more excess carbohydrates for storage under higher irradiance may not be the cause due to the low carbon content of carbohydrates (NIINEMETS & KULL 1998).

Extremely high LMA-values and nitrogen concentrations correspond to relatively high $V_{C_{max}}$ and J_{max} values that were derived for oak and beech, when compared with previously published data: While mean values of an overview of temperate hardwoods were $47 \mu\text{mol}/(\text{m}^2 \cdot \text{s}) \pm 33(\text{SD})$ for $V_{C_{max}}$ and $104 \mu\text{mol}/(\text{m}^2 \cdot \text{s}) \pm 64(\text{SD})$ for J_{max} (WULLSCHLEGER 1993), oak Gr13 reached at 25°C maximum values that were 100% and 81% higher. $V_{C_{max,298}}$ and $J_{max,298}$ of beech Gr12 were 21% and 15% higher than the mean values for temperate hardwoods. The reported values for *Fagus sylvatica* seedlings at 20°C from TAYLOR & DOBSON (1989) were much lower ($11 \mu\text{mol}/(\text{m}^2 \cdot \text{s})$ and $35 \mu\text{mol}/(\text{m}^2 \cdot \text{s})$). Values for different *Quercus* species (*Q. alba*, *Q. rubra*, *Q. stellata*) from this overview were also lower and varied between 18 and $51 \mu\text{mol}/(\text{m}^2 \cdot \text{s})$ ($V_{C_{max}}$) and 29 and $127 \mu\text{mol}/(\text{m}^2 \cdot \text{s})$ (J_{max}). Only DREYER ET AL. (2001) report similar values to those found in this study from an experiment with N-fertilised seedlings, that were 8% and 18% lower for *Quercus petraea* and 16% and 7% higher for *Fagus sylvatica* than the values measured on the Großebene trees and, thus, confirm this study.

The good agreement between the nitrogen dependence of $V_{C_{max}}$ and J_{max} of both species with a saturating curve (Fig. 89) may be interpreted as nitrogen saturation of photosynthesis. Though a nitrogen dependence of $V_{C_{max}}$ and J_{max} or of the maximum photosynthesis rate A_{max} has also been observed by other investigators (HARLEY ET AL. 1992, NIINEMETS & TENHUNEN 1997, PORTÉ & LOUSTEAU 1998, LE ROUX ET AL. 1999, MEDLYN ET AL. 1999, KAZDA ET AL. 2000, and KAKUBARI 2000 (personal communication)), a saturation has not yet been observed. This may have several reasons:

First, nitrogen per leaf area in the mentioned studies was often in a lower range than that of the Großebene trees ($0.3 - 2.4 \text{ g}/\text{m}^2$, $0.4 - 1.1 \text{ g}/\text{m}^2$, $1.3 - 2.4 \text{ g}/\text{m}^2$, $0.9 - 3.0 \text{ g}/\text{m}^2$, $0.5 - 1.7 \text{ g}/\text{m}^2$, $1.3 - 2.8 \text{ g}/\text{m}^2$, and $0.5 - 2.5 \text{ g}/\text{m}^2$ in the order of studies mentioned), while oak Gr13 reached $1.3 - 2.8 \text{ g}/\text{m}^2$ and beech Gr12 reached $1.3 - 2.7 \text{ g}/\text{m}^2$. Thus, an effect that appeared above $2.3 \text{ g}/\text{m}^2$ may hardly be recognised in some of these studies.

Secondly, differences between mature trees and seedlings or annual plants, that were used in some studies (HARLEY ET AL. 1992, MEDLYN ET AL. 1999) might exist.

And thirdly, all studies with maximum nitrogen contents above $2.4 \text{ g}/\text{m}^2$ were interpreted as linear relationship, though more or less clear tendencies towards saturation may be observed, when the data are re-evaluated. This is especially valid for the study with the highest nitrogen contents on *Juglans regia* (LE ROUX ET AL. 1999), where maximum $V_{C_{max}}$ and J_{max} are achieved at $2.4 \text{ g}/\text{m}^2$, while 3 more data points up to $3 \text{ g}/\text{m}^2$ show lower or even high rates. The A_{max} - data of KAZDA ET AL. (2000) for *Quercus robur* ($1.4 - 2.8 \text{ g}/\text{m}^2$) are partly scattered, but nearly

the maximum photosynthesis rate is achieved at 2.1 g/m², and only one data point at 2.8 g/m² has a less than 10% higher rate. A similar saturation effect may principally be observed in the data for *Fraxinus angustifolia* from the same study. Maximum A_{max} values for lowland *Fagus crenata* trees in the data of PROF. KAKUBARI were achieved at 1.7 g/m², while 3 additional data points with higher nitrogen content had lower rates. Upland *Fagus crenata* trees reached their highest rates at 2.37 g/m², but only one data point with higher nitrogen content (and lower rate) was measured.

Thus, the studies with high nitrogen content at least do not reject the observation of a nitrogen saturation of photosynthesis and partly confirm it. One possible physiological reason for this saturation may be seen in sink-limitation: Leaf photosynthesis of trees with high nitrogen uptake could become sink-limited when too much nitrogen is invested in photosynthetically relevant compounds like rubisco, chlorophyll or components of the electron transport chain. Therefore these trees may invest more nitrogen in other compounds or simply store it as nitrate, as is known from N-fertilised agricultural plants. ALI ET AL. (1999) have shown that rubisco concentrations increased due to nitrogen fertilisation in *Prunus persica* seedlings up to a certain level of fertilisation, but even doubling the fertiliser amount did not lead to increased rubisco concentrations above this threshold value.

A general relationship between S and H_d of the temperature dependence of J_{max} and $V_{C_{max}}$ has been found that describes the small range of reasonable values for these parameters also for previous studies. The average relationship of these parameters would allow a variation of the optimum temperature between 26°C and 40°C (Fig. 94), but the consideration of additional empirical relationships between the parameters resulted in a more or less constant optimum temperature (over different nitrogen concentrations) for $V_{C_{max}}$ of sun and shade leaves of both species, which was approximately 34.5°C and a slightly lower constant optimum temperature for J_{max} (around 33°C, Fig. 97). This corresponds to the found small variability of optimum temperatures for J_{max} of *Tilia cordata* and *Populus tremula* (NIINEMETS ET AL. 1999), which varied between 40.1 and 41.4°C and 32.7 and 34.1°C, respectively. Higher optimum temperatures and larger ranges have been found for the seedlings investigated by DREYER ET AL. (2001): 36.5 - 39.7°C (*Fagus*) and 37.4 - 52.2°C (*Quercus*) for $V_{C_{max}}$, and 34.0 - 35.6°C (*Fagus*) and 36.8 - 37.4°C (*Quercus*) for J_{max} . Differences to this study may arise because of differences between seedling leaves and those of mature trees, the latter being stronger differentiated into sun- or shade leaves. Optimum temperatures of the investigated seedling leaves of *Fagus sylvatica* from FORSTREUTER and STRASSEMAYER were also higher than those of beech Gr12 (Fig. 87).

4 Application of a 3D-light model to the 3D-representation of beech Gr12 and its stand

4.1 Methods

4.1.1 STANDFLUX-SECTORS

STANDFLUX-SECTORS (FALTIN 2001) is a 3D-light model for single trees in forest stands that modifies the light model of the 3D gas-exchange model STANDFLUX (FALGE 1997), which is

based on the light model of RYEL (1993) and calculates direct and diffuse irradiation along a rectangular grid of matrix points in the stand. It considers the light extinction of direct beams from the simulated course of the sun to the matrix point and of diffuse beams from 9 elevation angles in 6 azimuth classes as they pass through compartments of different leaf and wood area density in the stand. The contributions to light extinction of all compartments on the way from the sky to the matrix point are summed up, assuming homogeneous conditions in these compartments.

The share of sun exposed leaf area at each matrix point k (P_k) is given as (FALGE 1997)

$$P_k = \text{Exp} \left(- \sum_{j=1}^j I_{jk} * (L_j F_{l_{j\theta}} + S_j F_{s_{j\theta}}) \right), \quad (46)$$

where L_j and S_j are the leaf and wood area densities of compartment j , $F_{l_{j\theta}}$ and $F_{s_{j\theta}}$ are the Warren-Wilson-Reeve ratios (whole area / projected area, DUNCAN 1967) of leaves and woody elements of the compartment at a sun elevation θ , and I_{jk} is the length of the beam through this compartment. The Warren-Wilson-Reeve ratios are dependent on average leaf and branch angles.

Analogously, the diffuse irradiation from a given azimuth and elevation angle reaching matrix point k (M_k) is given as

$$M_k = D_{\text{sky}} \text{Exp} \left(- \sum_{j=1}^j I_{jk} * (L_j F_{l_{j\theta}} + S_j F_{s_{j\theta}}) \right), \quad (47)$$

where D_{sky} stands for the diffuse irradiation on a horizontal plane above the stand.

Upwards and downwards directed reflected and transmitted irradiation are calculated for layers of matrix points on the base of the reflectance and transmissivity of leaves according to NORMAN (1979) and RYEL ET AL. (1993).

The more or less homogenous compartments result from the division of modelled three-dimensional tree crowns in the stand in height layers, sectors and sections and the assumption of homogeneity is best fulfilled when the resolution in this structure description is high.

Each simulated tree crown is divided into height layers of variable height. The height layers consist of sectors of cylinders concentric to the stem, which may vary in radius and angle. Each sector may be subdivided into sections that result from the intersection with additional concentric cylinders. These sections need not extend over the whole height range of their layer, nor need they include any leaves or woody elements, so that even gaps in the crown may be represented, when the appertaining data are available (Figs. 112 -113). A high resolution in the structure description allows the derivation of light dependent quantities like those in Fig. 75 with the model.

4.1.2 Representation of 3D-data with CRISTO

The 3D-model CRISTO (optically controlled crown internal structure representation) has been constructed to handle the vast amount of 3D-data from geodetic location measurements on leaf clouds and tree crowns in order to enable the use of these data in a spatially explicit physiological description of the investigated trees. It sorts the measured points in space under optical control of the user to coherent oriented polygons that form leaf cloud enveloping or tree crown approximating polyhedrons. Volume and leaf area density may be calculated and may like any other measured data from the leaf clouds or tree crowns be analysed in relation to

spatial characteristics like volumes, angles, or positions and may be represented in three-dimensional maps of the tree or the stand. Considering the rarity of highly detailed structure descriptions the model allows the recalculation of these data into various structure descriptions, thereby enabling their use in different forms of 3D-models.

4.1.2.1 Representation of stand structure with crown approximating polyhedrons

While tree stems were represented as cylinders with the radius of the stem in 1,35m height and reaching the middle height of the tree crown, tree crown approximating polyhedrons were constructed similarly to leaf cloud enveloping polyhedrons (compare Figs. 4 and 5) from located points on their surface. The co-ordinates of crown surface points had to be estimated from projections, because it was not possible to bring a reflector to the point of interest. East and north co-ordinates of the outermost crown surface points in eight azimuth directions from the stem have been determined by optical projections using a vertical tube. The instrument consists of a 20cm long, hand-held tube mounted on a universal joint to make it hang vertically during operation. Crossed hairs are mounted in the upper end of the tube and a mirror is fixed in the lower end. More detailed descriptions are given by JOHANSSON (1985). The height co-ordinate of the outermost surface points in these directions was measured using the hand-held forest survey laser Criterion 400 (Laser Technology Inc., Englewood, Colorado), which measures compass directions, vertical angles and distances. The Criterion 400 was positioned in a distance of 50 to 100m in west direction from the stem to take the bearings of the outermost surface points in north and south direction of the crowns. The height co-ordinates were calculated from the vertical angles to these points and the measured distance to the stem. The same procedure was done on the south side of the stem to estimate the heights of the outermost surface points in east and west direction. The heights of the outermost surface points in south-east, north-east, south-west, and north-west direction were in most cases derived from these measurements assuming a medium height between the two neighbouring outermost surface points for these points, which was tested successfully in a few cases (data not shown). Height of crown base and apex were also measured with the Criterion 400.

These geodetic measurements were performed on 145 trees in the Großebene stand, 126 trees from the Buchenallee stand (data not shown), and 182 trees in the Steinkreuz stand (crown projections not from all trees, data not shown).

The determined ten points on the canopy surface were used for the construction of a canopy approximating polyhedron by joining the eight outermost surface points with straight lines along the canopy surface. Each corner of the resulting ring is then connected with lines to the crown base point and apex (compare Fig. 109). Tree crown approximating polyhedrons are in most cases not crown enveloping polyhedrons because many canopies have convex borders instead of linear ones. Thus, they may only give an estimation of the space where most of the leaf mass of a tree is placed.

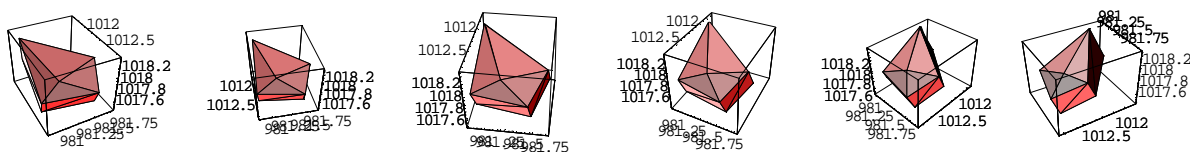


Fig. 109: Quarter of a rotation of a leaf cloud enveloping polyhedron around a vertical axis as shown by the CRISTO routine for optical control of measured spatial data.

4.1.2.2 Volume and leaf area density calculation of polyhedrons

The volume of polyhedrons was calculated as the sum of volumes of tetrahedrons that are constructed from each of its side-triangles and the origin, using the volume equation for a 4 point system (BRONSTEIN ET AL. 1995):

$$V_{\text{Tetrahedron}} = \frac{1}{6} \begin{vmatrix} x & y & z & 1 \\ x_1 & y_1 & z_1 & 1 \\ x_2 & y_2 & z_2 & 1 \\ x_3 & y_3 & z_3 & 1 \end{vmatrix} \quad (48)$$

Here, $P(x,y,z)$, $P_1(x_1,y_1,z_1)$, $P_2(x_2,y_2,z_2)$, and $P_3(x_3,y_3,z_3)$ are the four corner points of a tetrahedron with $x=y=z=0$. The determinant in equation (48) gives a positive result only when the orientation of the vectors from the origin to P_1 , P_2 and P_3 is equal to that of the co-ordinate system, otherwise the result is negative (BRONSTEIN ET AL. 1995). The absolute value of the sum of all positive and negative volumes of all tetrahedrons from the triangles of a complete polyhedron equals the polyhedron's volume, when all its triangles ($P_1P_2P_3$) are oriented in the same direction (either counter-clockwise or clockwise), which may be termed "coherent orientation" (J. LINHART, University of Salzburg, pers. communication).

Therefore, all side-polygons of leaf cloud enveloping or tree crown approximating polyhedrons were formulated as triangles. While the order of measurements on tree crown approximating polyhedrons was always the same and pre-determined by the given azimuth directions, the order of geodetic measurements on leaf cloud enveloping polyhedrons can for practical reasons not be pre-determined. The occurrence of concave and convex forms and the difficulty to take one's bearings in a canopy environment may be a source of fundamental errors, when the measured points are connected with lines to form a polyhedron. Therefore, CRISTO involves a routine for optical control of the measured data, which allows the user to sort the measured border points in the order of the leaf cloud's shape. The routine for optical control first shows the measured border points in direction of the normal vector of the leaf cloud plane, so that the user can put them in the right order referring to the measurement protocol. This order and the end points of the central axis are the base for the definition of a polyhedron with coherent oriented triangles, which is pre-formulated for leaf clouds with 3-9 border points. The routine finally shows an animation of the resulting polyhedron rotating along a chosen axis to the user for plausibility control (Fig. 109).

Leaf area of polyhedrons is taken from the harvested leaf area of the leaf cloud or from allometric relationships relating to the cross-sectional area of the leaf cloud supporting branch (Fig. 9) or to the basal area of tree stems (Fig. 14), which allows the calculation of volume-related leaf area densities. Other information like species, LMA-data, wood area density, or LMA-dependent variables (nitrogen content per area, photosynthesis capacities) may be stored associated to the appertaining polyhedron and shown in three-dimensional maps for further analysis (compare Figs. 16, 19a,19b,110,111 and figures in the appendix).

4.1.2.3 Segmentation of polyhedrons

One advantage of the leaf cloud oriented description of canopies is that it may provide a data base for different spatial schemes from various 3D-modelling approaches, because the usually necessary segmentation into compartments is not pre-defined by the method of harvest. The

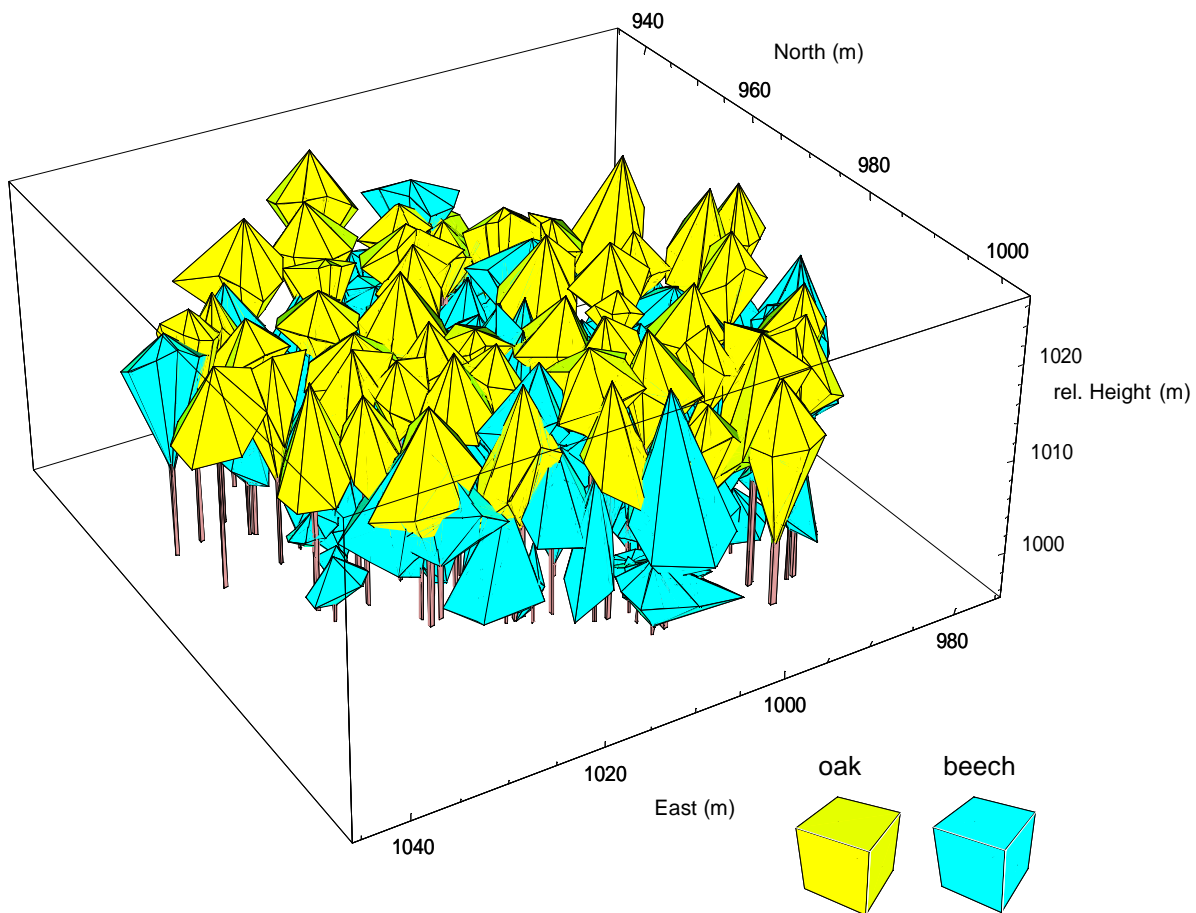


Fig. 110: Map of the species composition in the stand Großebene

segmentation routine in CRISTO may generally be applied to convex polyhedrons, which have to be provided using the routine for optical control to split concave polyhedrons into convex parts. The user defines an equation for the surface of intersection with the polyhedrons, for example

$$Ax + By + Cz + D = 0 \quad (49)$$

as definition of a plane with the normal vector (A,B,C). All polygon edges whose two endpoints (x_1, y_1, z_1) and (x_2, y_2, z_2) lead to one positive and one negative result when their co-ordinates are set into the left part of equation (51) are then chosen for the calculation of intersection points with the plane, using Newton's method to find out the point on each edge, where equation (51) is fulfilled. Each intersected polygon is split into two parts along the new edge between the intersection points. Resulting polygons with more than three corners are divided into triangles using the Delaunay triangulation method.

The Delaunay triangulation method is also used to form a boundary surface between the two polyhedron fragments on both sides of the plane, which serves as a lid closing the cut end of the fragments in order to complete the two new polyhedrons. In case of a cylinder as surface of intersection, given as

$$x^2 + y^2 - r^2 = 0, \quad (50)$$

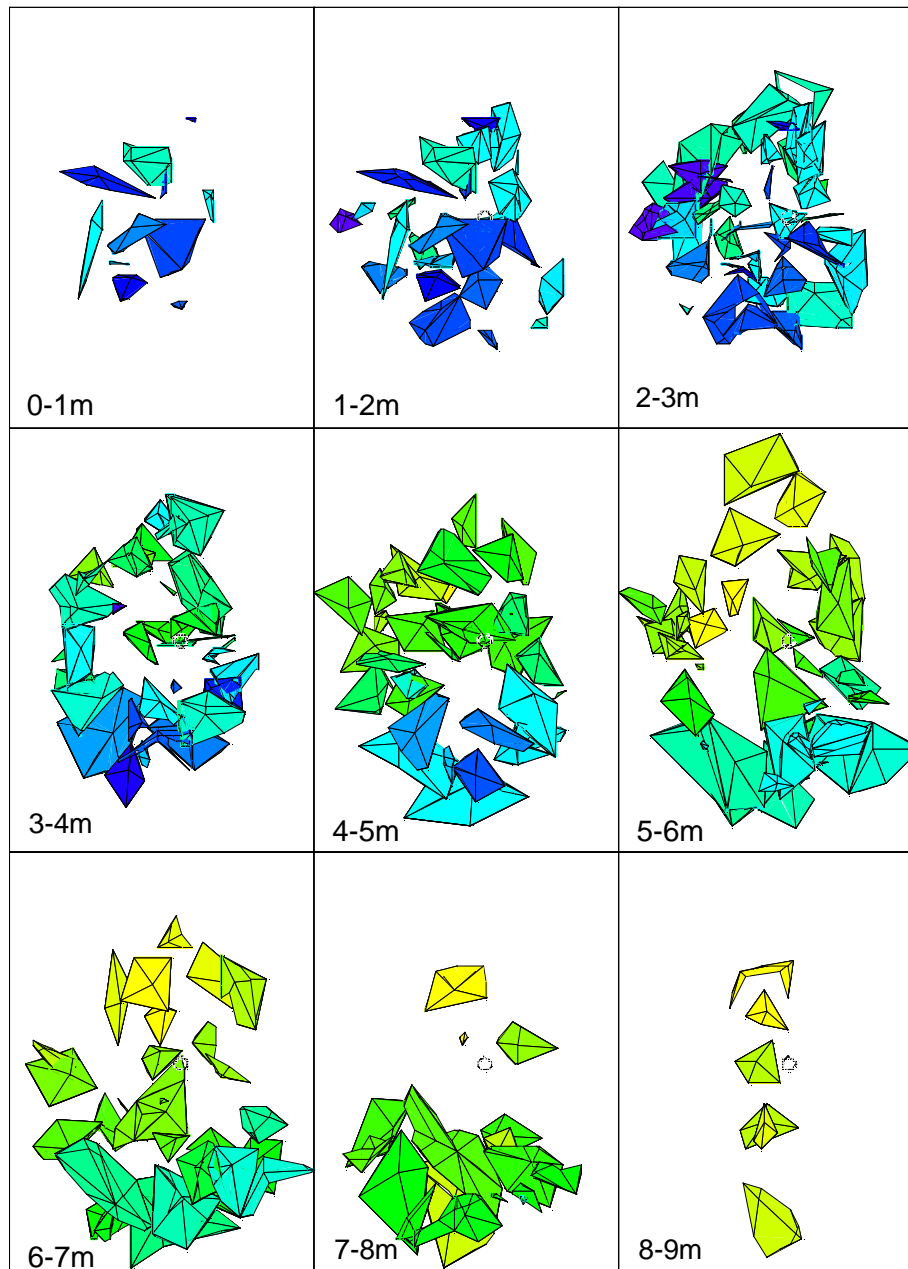


Fig. 111: $V_{c_{max}}$ of leaf clouds of beech Bu38 in horizontal layers (m below apex). The intensity of the colour is proportional to the average $V_{c_{max}}$ of the leaf cloud as calculated from the equation in Fig. 89. East and north co-ordinates (the east co-ordinate is on the abscissa, compare Figs. 19a,b) are evenly spaced.

with r denoting the radius of the cylinder, the intersection points have to be projected on a plane before the Delaunay triangulation may be used to construct a lid. The re-projection of the resulting triangles produces a lid of connected triangles that approximates the cylinder shaped intersection surface.

The CRISTO segmentation routine provides optical control of the segmentation process, so that also concave polyhedrons may be treated with these algorithms in a half-automated interactive way (Fig. 112) - single triangles of the Delaunay triangulation have to be removed manually, when they lie outside the intersection area.

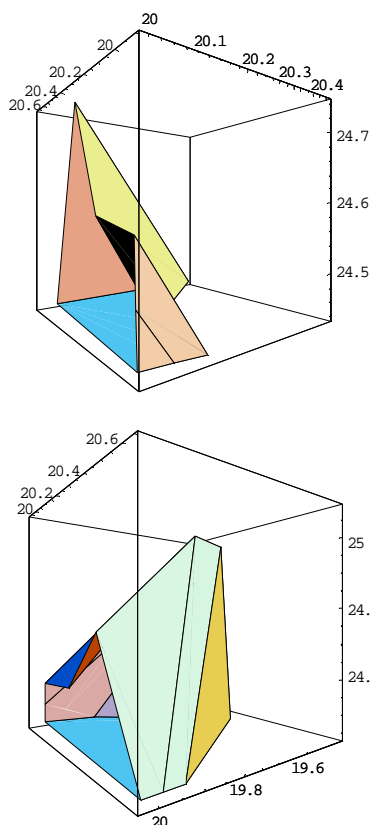
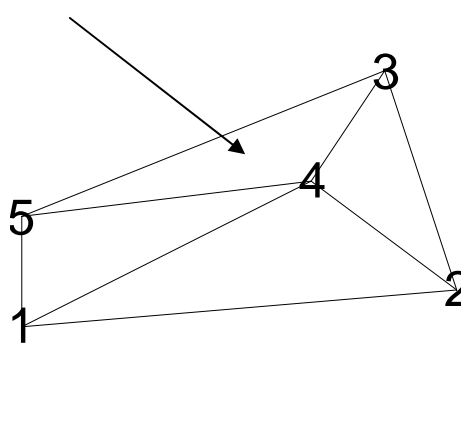


Fig. 112: The intersection of a concave polyhedron with a vertical plane produces two incomplete polyhedrons (left side, the incomplete polyhedron which was on the left side of the intersection plane is displayed below and has been turned around). The intersection area is concave. The Delaunay triangulation is based on the convex hull of the intersection points and therefore has to be corrected by removing the indicated triangle (below).



4.1.3 Parameterisation of STANDFLUX-SECTORS

4.1.3.1 Segmentation of leaf cloud enveloping polyhedrons

Boundaries of height layers, sectors, and sections as well as section height ranges have been chosen in order to construct compartments with as homogeneous conditions as possible, thereby explicitly representing larger gaps and inhomogeneity of the crown. This is best achieved, when the resulting compartments are either empty or densely filled with leaves. As less intersections as necessary were required on the other hand to reduce the number of compartments that have to be parameterised and calculated in the light-model.

Height layer boundaries for beech Gr12 have been chosen in an average vertical distance of around 1m with deviations due to canopy gaps. Figs. 113 a and b show the chosen sector boundaries in each height layer: 4-6 vertical intersection planes cut the polyhedrons in each layer into 3 - 12 filled sectors. The sector boundaries were chosen such that gaps in the crown may well be represented by additional cylinder shaped boundaries.

The 94 resulting sectors were cut into 410 sections using the optical representation of beech Gr12 in CRISTO (Fig. 114).

4.1.3.2 Segmentation of crown approximating polyhedrons in the stand *Großebene*

The convex shape and gradients of leaf area density or leaf angles in the crown could be represented by division of the homogeneous tree crown approximating polyhedrons into eight 45°-sectors in the main azimuth directions and four height layers per sector. The height layer boundaries of opposite sectors are the same due to the segmentation scheme (Fig. 115):

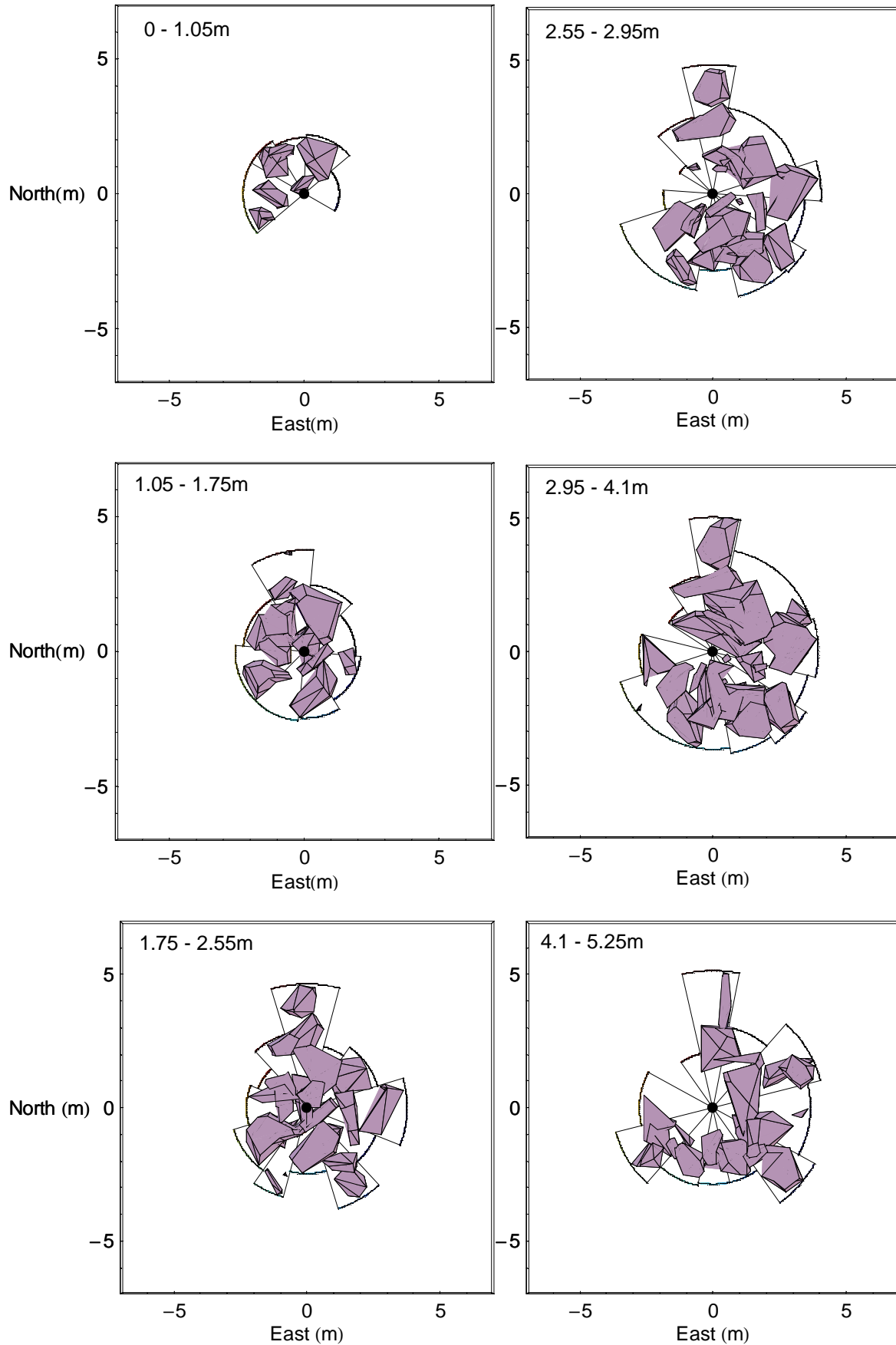


Fig. 113a: Segmentation of height layers of beech Gr12 into sectors of the light-model STANDFLUX-SECTORS. The height range of each layer is given in m below apex.

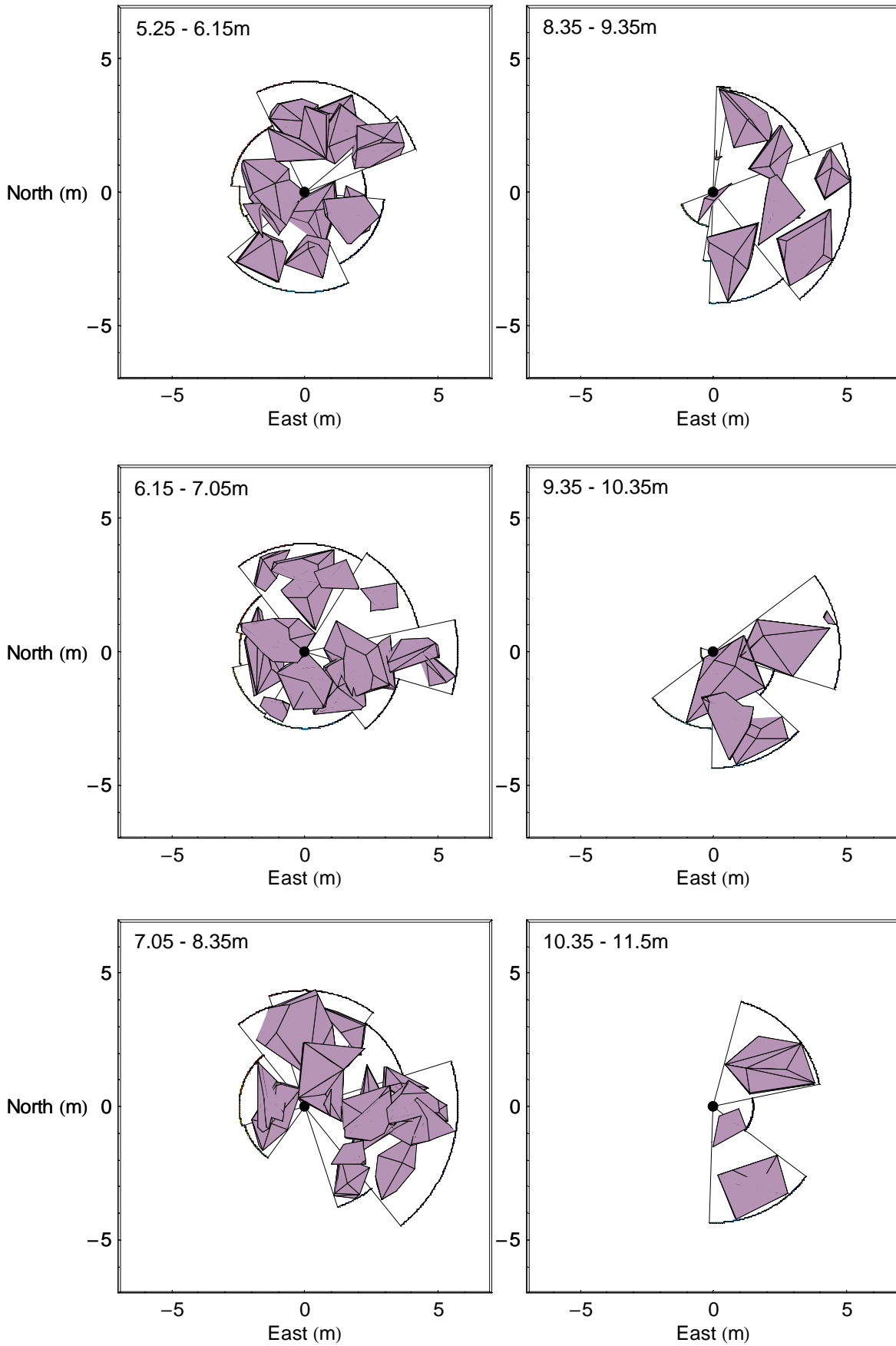


Fig. 113b: Segmentation of height layers of beech Gr12 into sectors of the light-model STANDFLUX-SECTORS. The height range of each layer is given in m below apex.

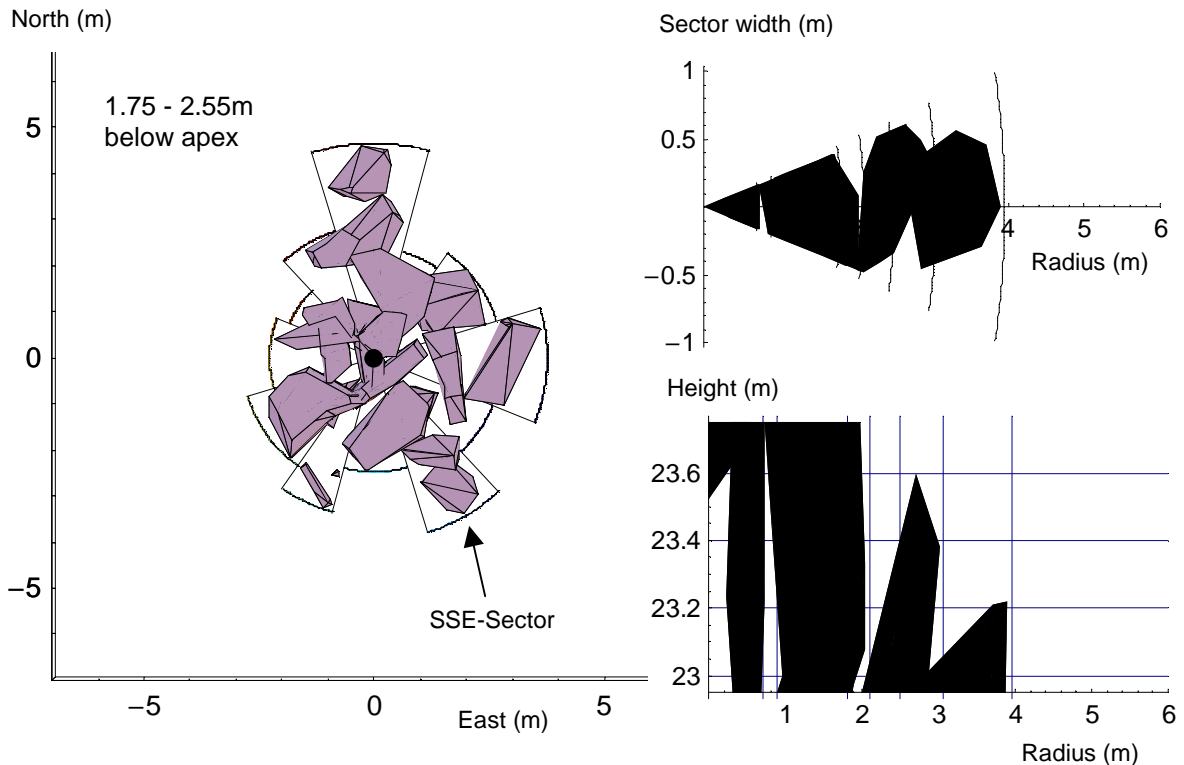


Fig. 114: Division of the South-South-East-sector of the third height layer of beech Gr12 into 7 sections, visually supported by an optical representation routine in CRISTO. The SSE-sector is shown from above with cylinder-shaped section boundaries (right side, above) and from the west side, where the cylinder shaped section boundaries occur as vertical lines (right side, below). The section boundaries were chosen in a way that allows to draw the height boundaries close to the border of leaf clouds, thereby enabling the representation of larger gaps.

Height boundaries for opposite sectors (east/west, south/north, north-east/south-west, north-west/south-east) were drawn in the middle between neighbours in height of 4 points: 2 measured outermost border points, crown-base and apex. The horizontal extension of 45°-sectors was given by the maximum extension of a linear approximation to the crown form (Fig. 115). This kind of segmentation results in cylinders, when tree crowns are symmetrical to the stem and may represent bigger cavities along the shape of the canopy.

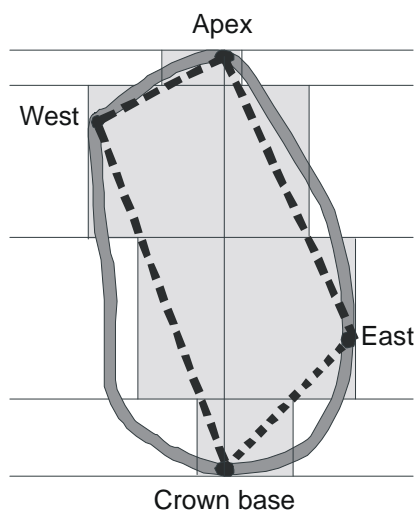


Fig. 115: Segmentation of tree crowns of the Großebene trees (vertical cross-section through the stem in west-east direction). The dotted line represents the cross-section of a tree crown approximating polyhedron with its corners at the western and eastern border points of the crown as explained above. The original crown form (thickest line) of most trees was more convex than the form of the polyhedron, which is considered in the segmentation. Height boundaries were set in the middle between the heights of measured points. The horizontal extensions of 45°-sectors (grey fields) are given by the maximum extension of the crown approximating polyhedron in each specific layer and direction.

4.1.3.3 Parameter determination for single compartments

Each compartment of beech Gr12 was automatically parameterised based on leaf area and volume share of included leaf cloud enveloping polyhedrons assuming volumetric homogeneity of leaf area density in the leaf clouds.

The relationship between projected wood area and leaf area of leaf clouds from Fig. 56 was employed to calculate wood area density of each compartment. The stem was considered as a cylinder with its diameter in 1.35m height, that reaches the middle height of the crown (19.75m above the floor, 5.75m below apex) and builds the central compartment of the simulated tree.

Average leaf angles of each compartment were calculated based on the average height of the compartment below apex using the relationships found for beech Bu38 (Figs. 61 and 62), which were recalculated to

$$\text{angle} = -2.63(\text{height below apex}) + 36.86 \quad (51)$$

in the upper part of the crown (range of 0 - 6.75m below apex) and to

$$\text{angle} = 4.162(\text{height below apex}) - 8.92 \quad (52)$$

in the lower part of the crown.

Branch angles in each compartment were calculated using the linear relationship from Fig. 64.

Transmissivity and reflectance were assumed to equal 10% and 6%, using the values of FALGE (1997).

The leaf area densities of tree sectors from the surrounding stand were derived from the height dependence of leaf area density as displayed in Fig. 24. All other parameters for the surrounding tree crowns were derived in the same manner as those of beech Gr12, because specific data for *Quercus petraea* trees were not available. From former studies it was expected that leaf and branch angles of neighbouring trees play a minor role for the light calculation and that the main impact of the different tree species is a result of their canopy form.

4.1.4 Validation of STANDFLUX-SECTORS

4.1.4.1 Light and LMA simulations

All light calculations are based on PPFD measurements with a Li-Cor quantum sensor above a clear-cut 1300m south-east of the investigated stand between 19.6.1998 and 2.7.1998 (measurements of M. SCHMIDT). The matrix points were placed in a 10cm grid spread over the volume of a vertical projection of 6 leaf cloud enveloping polyhedrons that represent leaf clouds whose sapflow was measured by M. SCHMIDT (DEPARTMENT OF PLANT ECOLOGY, UNPUBLISHED) - see Fig. 116. The volume of a vertical projection with the same height extension as the leaf cloud enveloping polyhedron was chosen because the segmentation in STANDFLUX-SECTORS allows only vertical borders. Direct and diffuse irradiation were calculated hourly (336 hours) for each of 125058 matrix points - 5460 points in the volume of leaf cloud E and 33670 points in the volume of leaf cloud B, for example. The maximum integrated value over 336 hours of diffuse plus direct irradiance of all matrix points from a leaf cloud was expressed relative to the measured irradiance above the clear-cut as maximum relative irradiance of each leaf cloud. Assuming that the site of maximum relative irradiance in the volume of a leaf cloud is

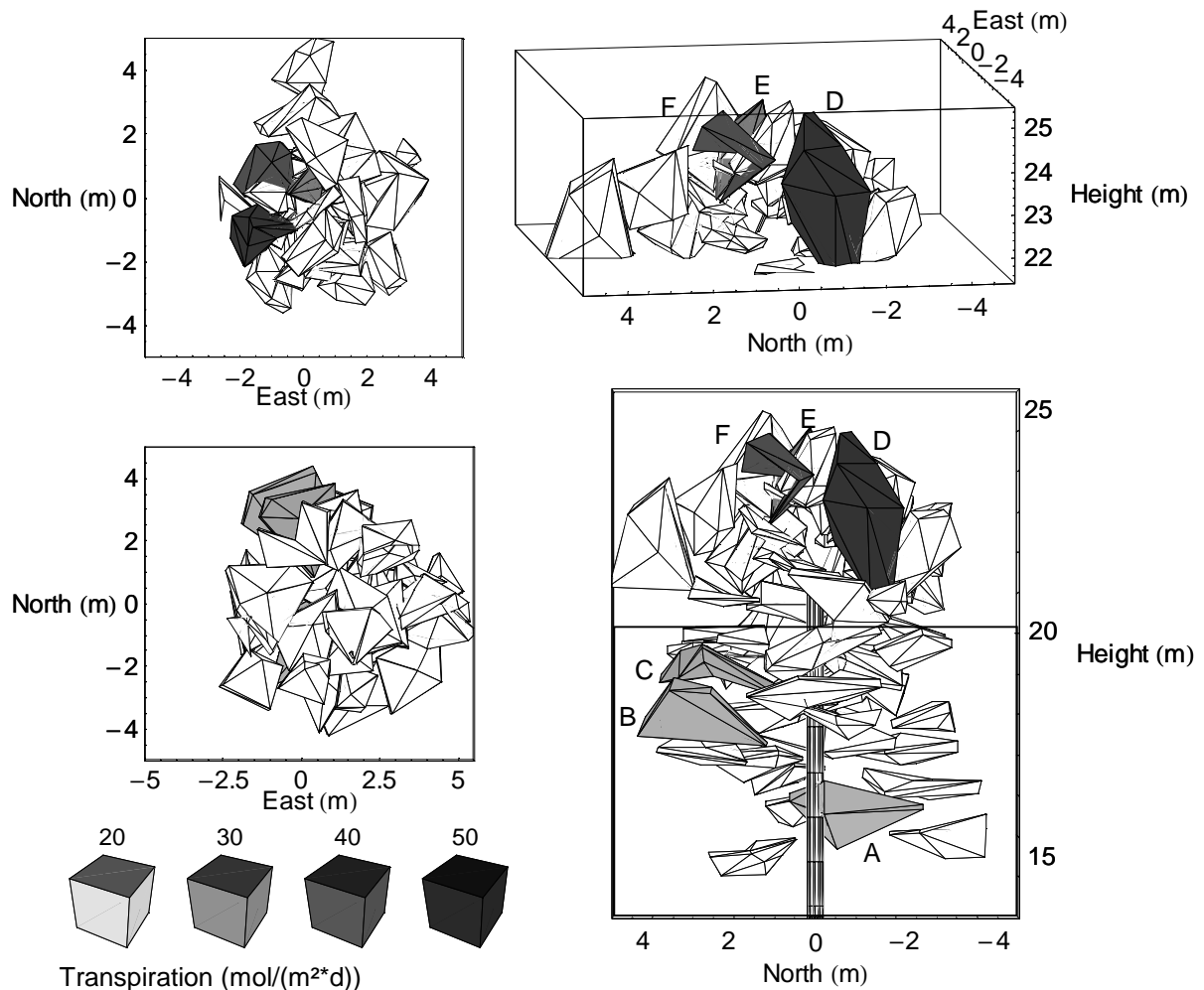


Fig. 116: Sapflow has been measured on 3 shade leaf clouds (A, B, C) and 3 sun leaf clouds (D, E, F) of beech Gr12 using the thermal dissipation method (GRANIER 1985, 1987, measurements of M. SCHMIDT, DEP. OF PLANT ECOLOGY). The measured average transpiration rates of the 6 leaf clouds during 19.6.98 - 2.7.98 are indicated by intensity of their colour. The left figures show a view from above the tree (above) and from above the shade crown in height 20.25m (below). One hidden sun-leaf cloud may only be seen from west side above (right above), while all other leaf clouds are visible from the west side of the tree (right side, below). Leaf cloud F was inserted as one of the two last branches directly below the apex leaf cloud that is visible between the letters E and F.

the location of its leaves with maximum LMA, maximum LMA was calculated from maximum relative irradiance based on the relationships in Fig. 75 adjusted to beech Gr12 (see below). The integrated average of all matrix points in the uppermost 10cm-layer of each leaf cloud projection was calculated as an estimation of the leaf cloud's light climate and expressed as average relative irradiance above the leaf cloud. Whole leaf mass divided by whole leaf area of each leaf cloud (leaf cloud LMA) was assumed to follow the same light dependence as that of single leaves and was calculated based on the equations in Fig. 75 and an adjustment to beech Gr12 (see below).

4.1.5 Validation data

Leaf clouds A,C,D,E, and F were harvested on 10th - 12th of August 1998 determining minimum and maximum LMA of each of their 1m branch segments with 5 leaves from the proximal part and 5 leaves from the distal part of the segment. Each of these leaf clouds consisted of 11-20

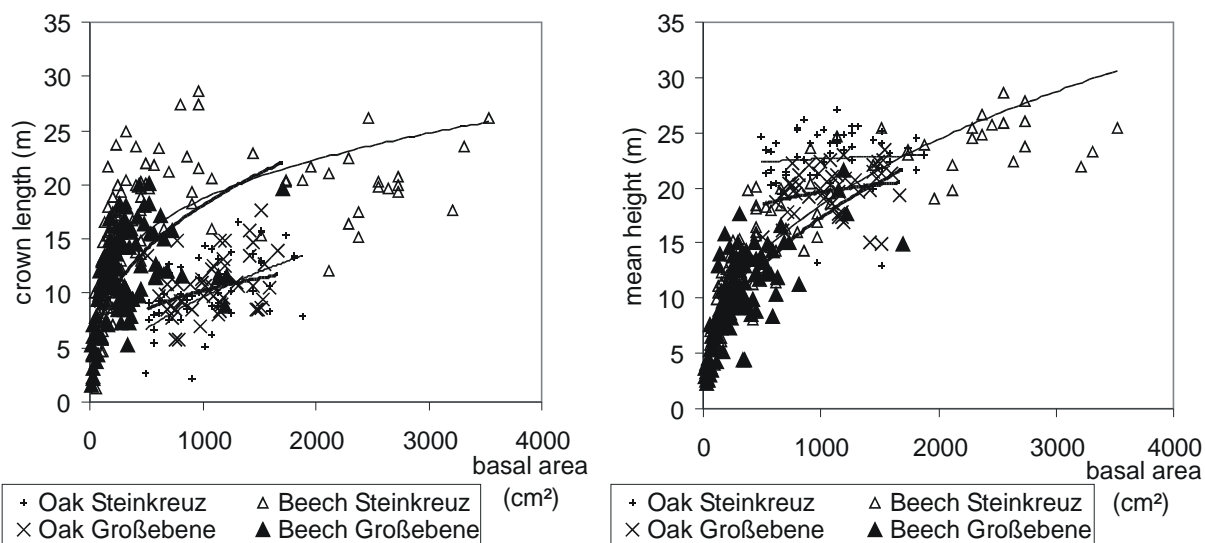


Fig. 117: Length of beech and oak canopies from the two mixed stands in the Steigerwald (left) and mean height (average of apex and crown base) of these canopies (right). The log-log-transformed data were approximated with linear functions to show the general trend for both species. The fits are indicated in the re-transformed data by fat (Großebene) and thin (Steinkreuz) lines.

1m branch segments. Leaf dry mass of the oven-dried samples was separately divided by the average LMA of each segment to calculate the leaf cloud's leaf area. Maximum LMA of the leaf clouds was the maximum LMA that was measured on any leaf sample from the leaf cloud. Leaf cloud B lost all its leaves during the vegetation period 1998 by itself and its leaf area during the measurement period could only be estimated by eye to equal 2.25m². Its leaf dry mass was calculated based on allometric relationships to 144.1 g. Maximum LMA of this leaf cloud was not determined.

4.2 Results

4.2.1 Stand Structure

4.2.1.1 Crown length and position of oak and beech trees in the Steigerwald stands

Oak and beech trees in the stands Großebene and Steinkreuz had different crown lengths with respect to their stems' basal area (Fig. 117): While crown length of beech trees in both stands increased with basal area to values between 15 and 20m (Großebene) or even 30m (Steinkreuz), oak trees had much shorter crowns (length around 10m) in both stands.

In contrast to this, mean heights (average of heights of apex and crown base) of the same crowns were higher for oaks than for beech trees in the same basal area class (Fig. 117, right). Therefore, oaks in both stands occupy spaces in the above part of the stand and are underrepresented in the lower parts (compare Figs. A1 and A2 in the appendix), which is confirmed by the observation of a high proportion of dead branches in the lower part of oak canopies (compare chapter 1). Beech crowns on the other hand often produced leaves rather close to the floor, sometimes even when the trees were large and old.

4.2.2 LMA-calculations

4.2.2.1 Validation of the light model with the LMA/irradiance relationship

The relationship between relative irradiance and LMA from the Buchenallee leaves leads to an underestimation of 14.3g/m² (mean absolute error), when combined with the maximum relative irradiance simulations of STANDFLUX-SECTORS to calculate maximum LMA-values of leaf clouds (Fig. 118). This underestimation equals 13.5% of the mean of measured values and is mainly due to the relatively high maximum LMA-values of the three sun leaf clouds (D, E, F). The root mean square error for this comparison was 17.5 g/m².

The main reason for this underestimation is the difference between maximum LMA- values of beech Gr12 (128 g/m²) and the beech trees from the Buchenallee stand (110 g/m²). Therefore, the equation of the approximation line from the Buchenallee produces LMA-values close to 110g/m² (104.6) at relative irradiance 1, which cannot be adequate for the GroÙebene beech. This individual or stand-specific difference may be considered by adjusting the equation for the LMA vs. relative irradiance (Q_{rel}) relationship to

$$LMA = 128 Q_{rel}^{0.377}, \quad (53)$$

thereby assuming the general shape of the curve to be conserved. Making this adjustment leads to a smaller overestimation (6.1g/m², = 5.9% of mean of measured values) with a root mean square error of 10.3 g/m², indicating that the corrected formula leads to relevant improvements. Thus, equation (55) should be preferred due to its adjustment to beech Gr12 LMA data.

4.2.2.2 Estimation of leaf cloud LMA

An additional indication of the validity of LMA calculation based on STANDFLUX-SECTORS and equation (55) was gained from the estimation of leaf cloud LMA (Fig. 119). When leaf cloud

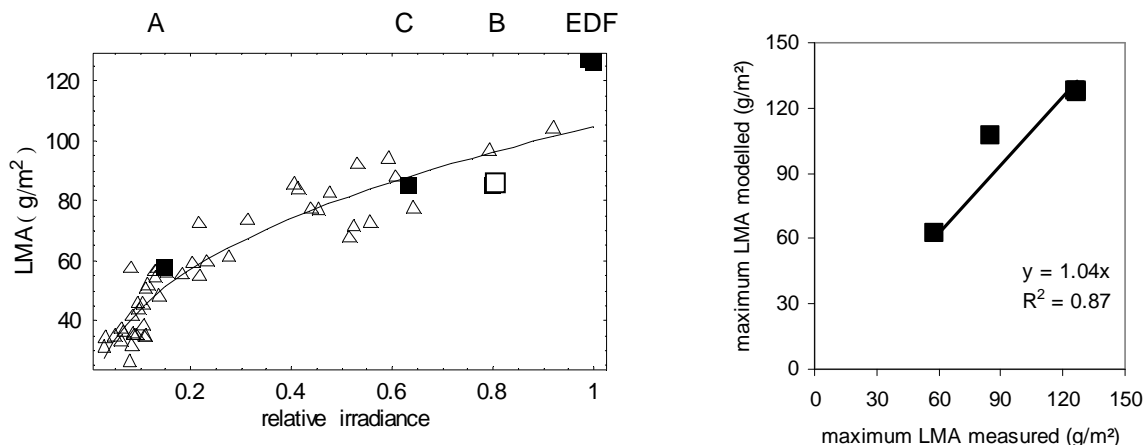


Fig. 118: The dependence of LMA on relative irradiance has been measured on leaves of Bu38 and Bu45 (left side, triangles) and the approximation line equals $y = 104.6 (\text{relative irradiance})^{0.377}$, $r^2 = 0.87$. The measured maximum LMA of five leaf clouds in relation to maximum simulated relative irradiance above each leaf cloud (filled squares) is compared for validation of STANDFLUX-SECTORS. The maximum LMA of leaf cloud B (open square) was not measured and may be estimated to equal approximately that of leaf cloud C.

When STANDFLUX-SECTORS and the adjusted equation (eq. 53) are used to model maximum LMA of each of the 5 leaf clouds, modelled vs. measured maximum LMA are compared with an r^2 of 0.87 (right side), a mean absolute error of -6.1 g/m² (-5.9% of mean of measured values), and a root mean square error of 10.3 g/m².

LMA was estimated from averaged relative irradiance above it, thereby treating the whole leaf cloud as a large leaf, the mean absolute error was $+1.5 \text{ g/m}^2$ (2% of mean of measured values) and the root mean square error equalled 10.28 g/m^2 . Thus, leaf cloud LMA could be modelled with a similar accuracy as that of single leaves using the same relationship. The effect of the used LMA vs. relative irradiance relationship has been shown to be rather big when applied to single leaf data and so is its effect in the leaf cloud LMA calculation: Using the original LMA vs. relative irradiance relationship from the Buchenallee trees (Fig. 75) turns the slight overestimation into a stronger underestimation (-9.9 g/m^2 mean absolute error) and increases the root mean square error to 13.1 g/m^2 . Both model comparisons (maximum LMA and leaf cloud LMA) show that the relative irradiance simulation with STANDFLUX-SECTORS may provide a reasonable basis for LMA calculations.

4.2.3 Comparison of climate and transpiration data

4.2.3.1 Daily courses

Absolute values of climate variables above a clear-cut near the BITÖK investigation site Steinkreuz were measured by G. LISCHIED, University of Bayreuth and are shown in Fig. 120. The days during the two weeks from 19.6. -2.7.1998 were mostly cloudy, though not very rainy: Only the days 21.6., 22.6., and 25.6. had permanently clear, sunny conditions. These days were also the warmest days, so that the first week was generally warmer than the second week. Main rain events occurred during the evening or night hours of 21.6., 26.6., and 27.6., while smaller rain events took place on 19.6., 23.6., 26.6., and 1.7.1998. The daily courses of VPD, PPFD, and temperature were more or less parallel on the three clear sunny days, on 24.6., and during

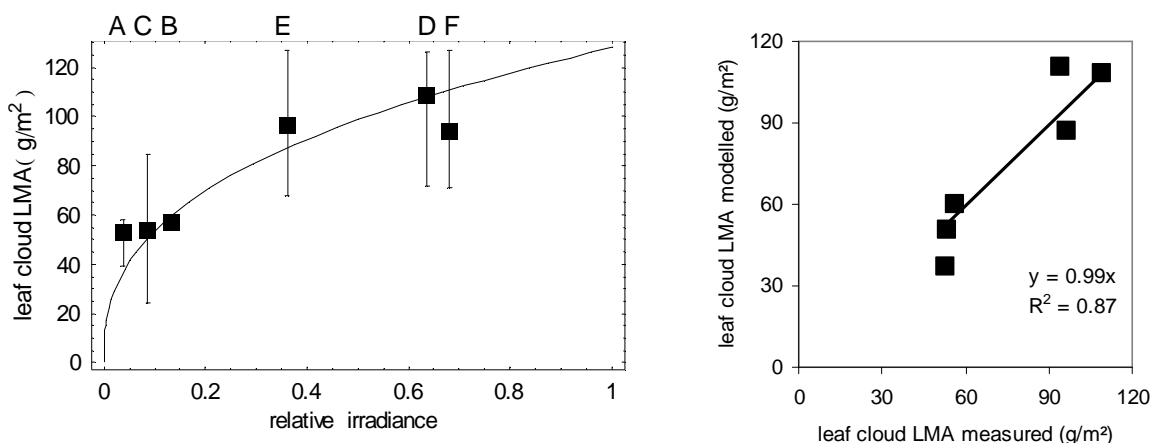


Fig. 119: The LMA of leaf clouds is given as their whole leaf mass divided by their leaf area and equals the average LMA of their leaves. Leaf cloud LMA has been set in relation to the average of simulated relative irradiance values in all matrix points directly above the leaf cloud (left side, filled squares). Equation (53) is plotted in the same graph for comparison. Error bars represent the range of LMA values occurring in each leaf cloud apart from leaf cloud B, where this was not measured. Modelled leaf cloud LMA on the base of averaged simulated relative irradiance and the corrected LMA vs. relative irradiance relationship is well correlated to the measured leaf cloud LMA values (right side, $r^2=0.87$). The model slightly overestimates leaf cloud LMA values by 1.5 g/m^2 (mean absolute error), equalling 2% of the mean of measured values. The root mean square error was 10.28 g/m^2 .

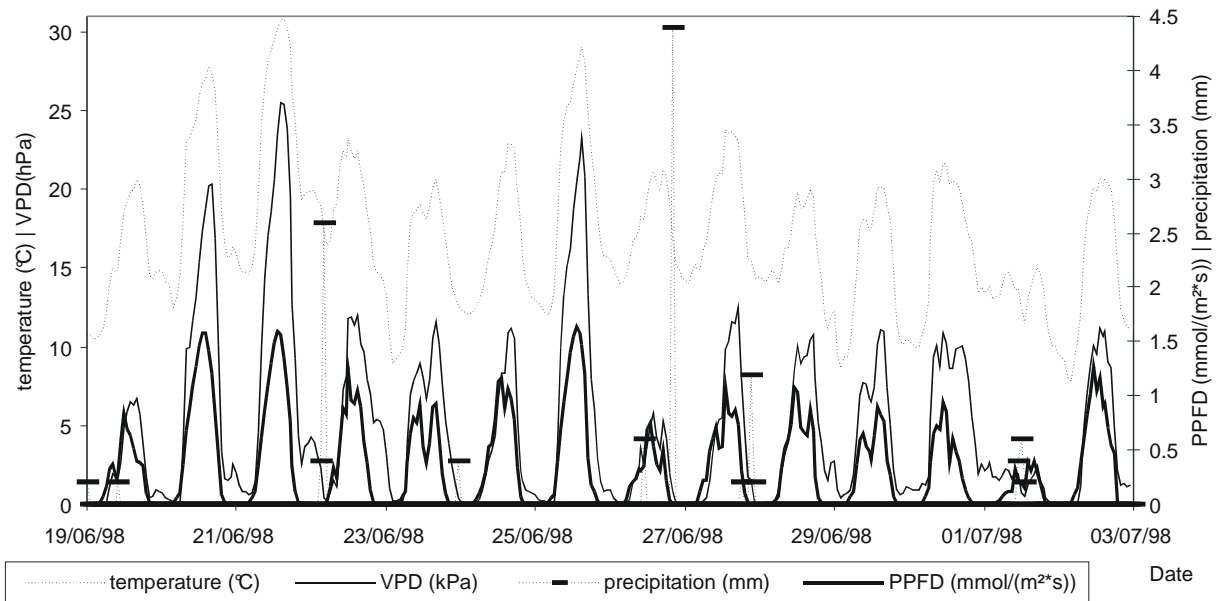


Fig. 120: Synopsis of climate variables during the investigation period 19.6.1998 - 2.7.1998. While temperature and VPD are scaled on the left y-axis, PPFD (in $\text{mmol}/(\text{m}^2\cdot\text{s})$) and precipitation are scaled on the right side. All measurements were performed at the BITÖK investigation site Steinkreuz, 5m above a clear-cut approximately 1300m in distance to the Großebene stand by G. LISCHIED, University of Bayreuth.

26.6. - 29.6.. Opposite tendencies in the courses of VPD and PPFD were due to temperature and were observed on 19.6., 24.6., 30.6., and 2.7..

Some observations may be summarised about the course of transpiration rates of sun and shade leaf clouds during the investigation period:

- The daily course of transpiration rates of sun leaf clouds was generally smoother than that of shade leaf clouds: while sun leaf clouds D, E, and F had wide and round daily peaks of transpiration (Fig. 122), the peaks in the course of transpiration rates from shade leaf clouds A, B, and C were more pointed (Fig. 121).
- When a continuous increase in irradiance was given, transpiration rates of leaf cloud D and the other sun leaf clouds steeply increased early in the morning and then approached to a maximum value at noon. Discontinuities in the irradiance increase with parallel discontinuities of the usual VPD increase in the morning - probably due to dew fall or smaller rain events - caused a decrease in transpiration rates even if irradiances just stayed constant, which may be observed on 19.6., 22.6., and 26.6. on all sun and shade leaf clouds.
- The shade leaf clouds often did not yet start to transpire on these days, when such a discontinuity occurred, which may indicate that a critical light or VPD level was not yet reached before that time. Their later start is one reason for the more pronounced peaks in transpiration.
- Another reason was that the course of PPFD above these leaf clouds consists also of pointed peaks, thereby inducing high irradiances for a short time.

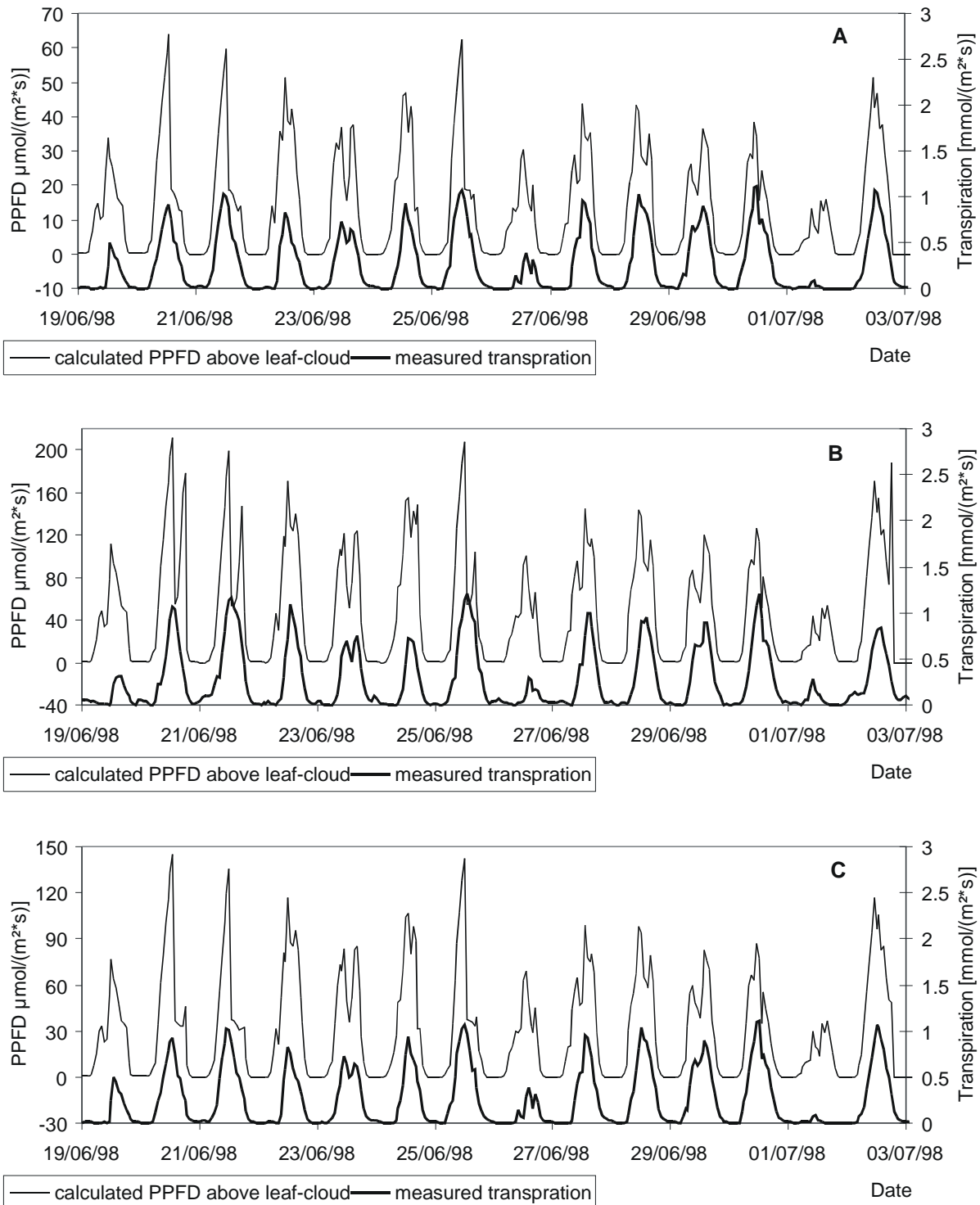


Fig. 121: Time course of measured transpiration rates and average of calculated PPFD of the matrix point layer directly above the investigated shade leaf clouds (clouds A, B, and C) during the investigation period. The time course of both variables is often parallel, but not strictly and not on every day.

- The decrease of irradiance after this maximum peak is often (leaf clouds A and C during 19.6.-26.6.) but not in all cases (leaf cloud B, 20.6., 21.6., and 25.6.) accompanied by a sharp decrease of transpiration rates. In opposite to the other shade leaf clouds, irradiance above leaf cloud B again increases in the afternoon and in opposite to A and C, the transpiration rates

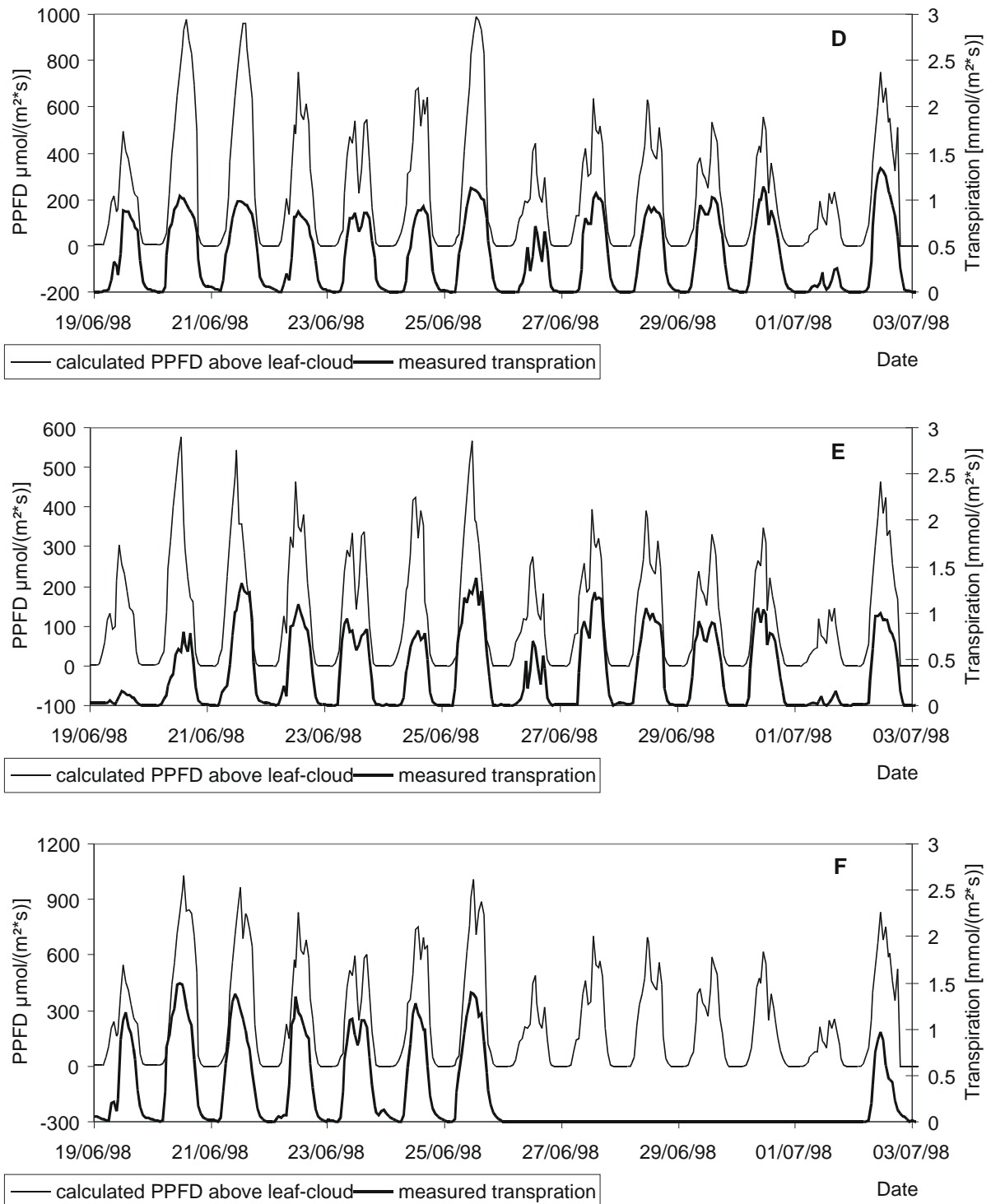


Fig. 122: Time course of measured transpiration rates and average of calculated PPFD directly above the investigated sun leaf clouds (clouds D, E, and F) during the investigation period. The time course of both variables is often parallel, but not strictly and not on every day. Transpiration “peaks” are generally wider than those of the shade leaf clouds. A gap exists in the sapflow measurements of leaf cloud F due to technical problems.

above leaf cloud B stay high or even increase (21.6., 25.6.) during the time of decreasing irradiance, thereby ignoring the sharp but short decrease in irradiance.

- In sun leaf clouds, a series of high transpiration rates was achieved on most days between 10:00 and 14:00, which was partly independent on light: The transpiration rates of leaf

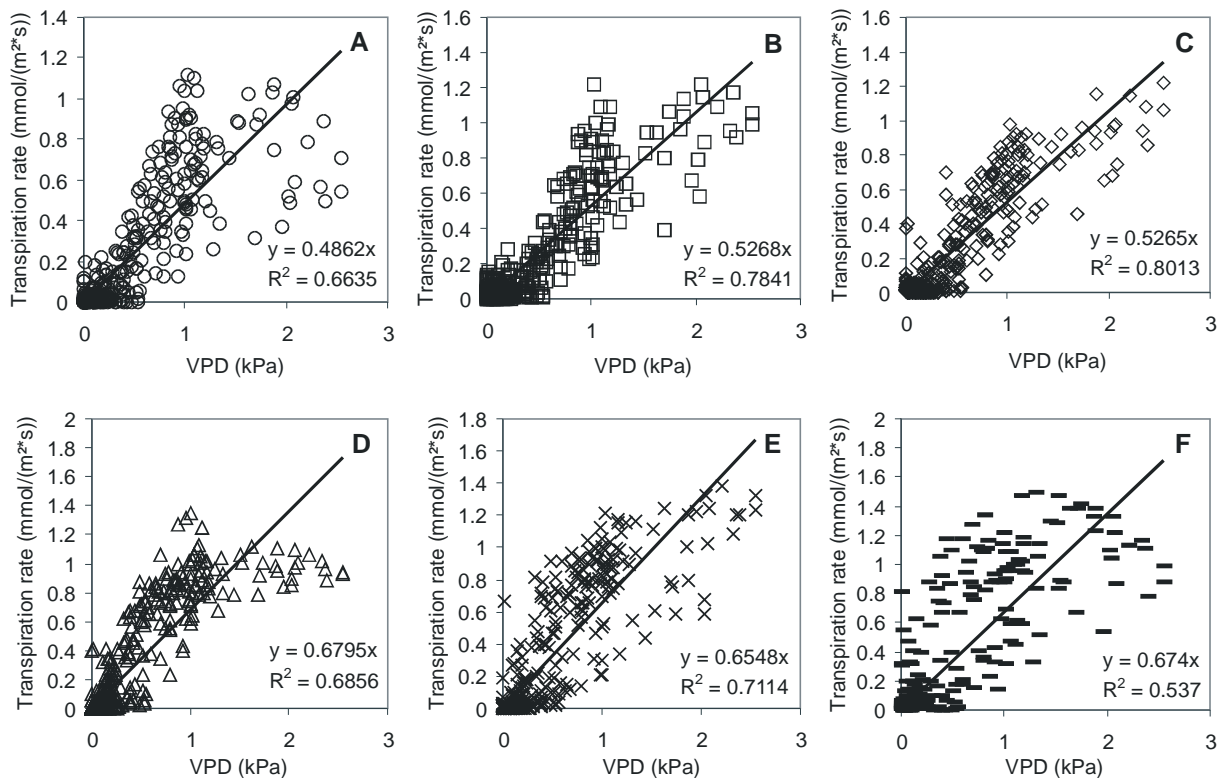


Fig. 123: Linearly approximated relationships between VPD above a nearby clear-cut and transpiration rates of leaf clouds A-F.

cloud D for example do not completely follow the course of irradiation on 22.6, 24.6., and 28.6.. More or less strong decreases in irradiance and VPD did not lead to reductions in transpiration on these days.

- If irradiance increases in the afternoon parallel to VPD, a reaction of transpiration rate is often visible in sun and shade clouds, which is best visible on 24.6. (all leaf clouds).

4.2.3.2 Dependence of leaf cloud transpiration on climate variables

VPD and PPFD belong to the main drivers of transpiration rates on tree, canopy and leaf scale (GRANIER ET AL. 2000), therefore it may be expected that leaf cloud transpiration is dependent on these variables, but it was not yet investigated, if differences between sun and shade leaf clouds concerning the VPD and PPFD dependence exist.

The average response of leaf cloud transpiration to VPD may be described with a linear approximation of this relationship (Fig. 123), which resulted in coefficients of determination between 0.54 and 0.8. The slope of the linear approximation may be termed sensitivity of transpiration to VPD, because it expresses the average increase of transpiration rates with VPD as observed in the investigation period. Sensitivity appears to be higher in sun leaf clouds than in shade leaf clouds as is expressed by the linear slope of the relationships (averaged 0.67 in sun leaf clouds and 0.51 in shade leaf clouds). But this effect may be a consequence of the VPD gradient in the canopy, which was not measured during the relevant period. Given that VPD differences of up to 2 kPa may principally occur in the canopy (Fig. 104), the effect may completely disappear, if the actual gradient in the canopy would be considered.

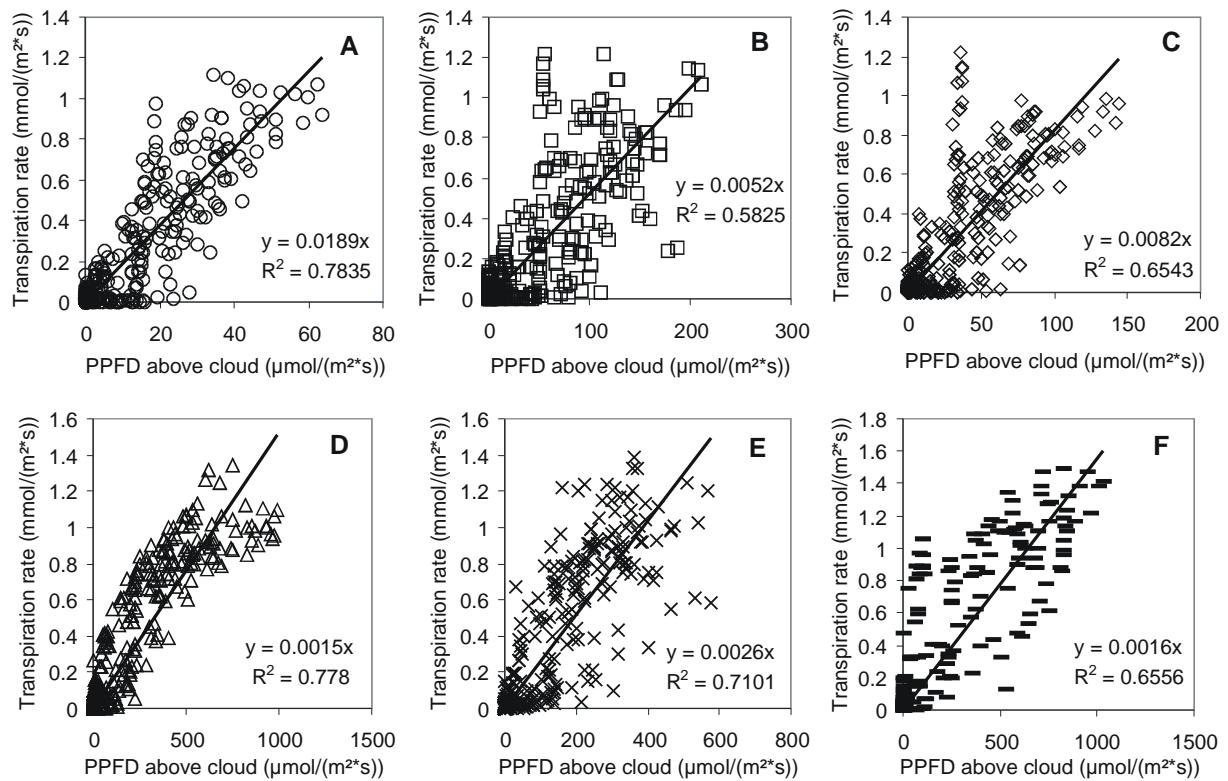


Fig. 124: A more or less strict linear light dependence of transpiration rates may be described for the investigation period from 19.6.1998 to 2.7.1998 for each leaf cloud (A-F). The graphs show measured transpiration rate relative to calculated PPFD in the matrix point layer directly above the leaf cloud

The consideration of canopy internal light gradients on the other hand is possible, due to their structure dependent calculation for defined parts of the whole crown by STANDFLUX-SECTORS. Coefficients of determination for the average response of leaf cloud transpiration rates to calculated PPFD above the leaf cloud (Fig. 124) lie between 0.58 and 0.78, thus in a similar range as those from the relationship to measured VPD. Shade leaf clouds had generally higher slopes in their light response than sun leaf clouds, indicating that lower light levels in the shade crown are sufficient to achieve the same transpiration rates as in the sun crown under higher light levels.

It may be supposed that differences in stomatal regulation between sun leaves and shade leaves are responsible for this effect: It is known that the photosynthetic light response of shade leaves is more sensitive to low light levels than that of sun leaves (RICHTER 1998) so that higher transpiration rates of shade leaf clouds than of sun leaf clouds would be expected under conditions of low light, given that stomatal coupling between assimilation and transpiration is relevant. Additionally, stomata of shade leaves of beech were allowed to transpire higher rates than sun leaves before stomatal closure

The physiological difference between sun and shade leaves of the investigated trees was associated with a change in nitrogen and LMA (Figs. 89 and 75). Figure 125 shows that also the different sensitivity of leaf cloud transpiration to PPFD is associated with a change of leaf cloud LMA, which supports the relevance of stomatal coupling of assimilation and transpiration as an explanatory scheme for leaf cloud transpiration.

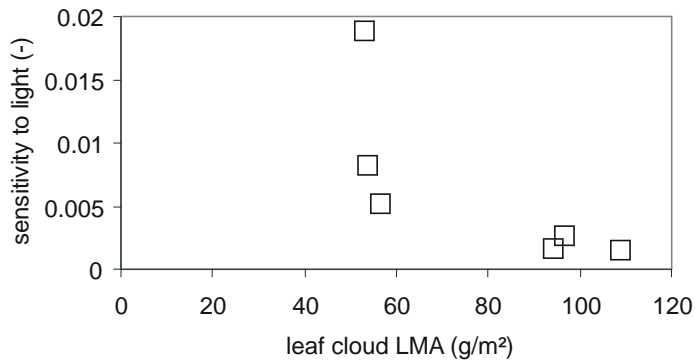


Fig. 125: Sensitivity of transpiration to PPFD versus leaf cloud LMA. PPFD was calculated for the matrix point layer above each leaf cloud

4.2.3.3 Summarising concepts

The 14-days period from 19.6. 1998 to 2.7. 1998 is only a short period with relatively constant weather conditions and is, therefore, not sufficient to derive general dependencies from it. Compared with the whole life of a tree it may be seen as a point in time with some typical qualities. Summing up the whole transpired water of each leaf cloud and expressing it either leaf area-related or not it was found that two concepts were relevant during this period (Fig. 126):

- Average transpiration rates over the whole period were very well correlated to the integrated sum of photosynthetically active quanta incident on a plane surface above each leaf cloud.
- The whole amount of transpired water was closely related to leaf weight of each leaf cloud.

4.3 Summary and discussion

Methods and results of this chapter show that the explicit consideration of the three-dimensional structure of forest stands and trees with the models STANDFLUX-SECTORS and CRISTO is possible and leads to reasonable results. The 3D-representation can help to elucidate important structural characteristics of investigated stands as was shown with the height positions of oak and beech crowns in the stands Steinkreuz and Großebene.

The relative irradiance values calculated with STANDFLUX-SECTORS provided a good basis for LMA estimations even when some insecurity concerning the LMA/relative irradiance relationship is considered. The validation was successful for single leaves and for leaf clouds of beech Gr12 (Figs. 118, 119). Better results were achieved, when the LMA/relative irradiance

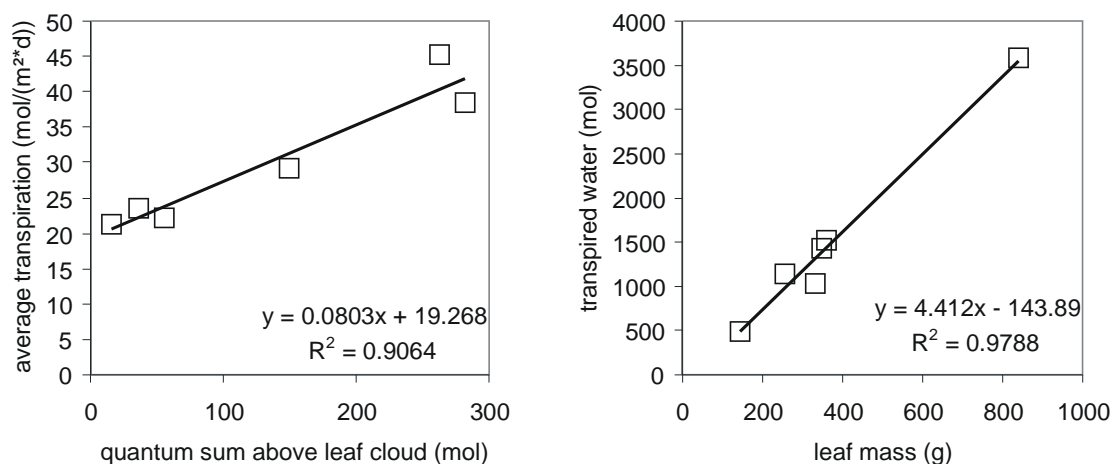


Fig. 126: The average transpiration rate over the whole investigation period and the sum of transpired water correlated best to quantum sum in the matrix point layer above the leaf cloud and leaf mass of the leaf clouds.

relationship was adjusted to the maximum LMA of the validation tree (beech Gr12), assuming the general shape of the functional relationship to be conserved.

The validation of such a complex model would be more satisfactory, when more validation data could be used and this is principally possible due to a vast amount of additional data from oak Gr13 and sapflow measurements on other trees in the stand (M. SCHMIDT, DEPARTMENT OF PLANT ECOLOGY, UNIVERSITY OF BAYREUTH) that were not evaluated for this project. Nevertheless the performed validation shows that the combination of STANDFLUX-SECTORS and CRISTO is able to function. Moreover, the calculated irradiance values are confirmed by reasonable relations to the course of transpiration during a 14-days investigation period:

- A coefficient of determination of 0.91 was found between the average measured transpiration rates of 6 leaf clouds during the whole investigation period and the calculated sum of photosynthetically active quanta incident on a plane surface above each of them (Fig. 126).
- Mostly parallel courses of irradiance and transpiration of leaf clouds were observed. Shade leaf clouds had for example very short periods of high transpiration which resulted in peak-like, pointed daily courses of transpiration, when compared to daily courses of sun leaf clouds (Figs. 121, 122). This was also found in the courses of calculated irradiance above shade leaf clouds. Peak-like courses of irradiance above shade leaf clouds were expected in advance due to smaller gaps in the canopy above them when compared to sun leaf clouds.
- Not parallel parts of the daily courses of calculated irradiance above leaf clouds and transpiration rates may be explained on the base of stomatal coupling between assimilation and transpiration. So was the initial increase of transpiration rates in the morning interrupted or even inverted, when irradiance and VPD did not further increase or stayed constant for a short time. An explanation for this overriding reaction may be found in feedforward responses of stomata (FARQUHAR 1978, SCHULZE 1994) that strengthen stomatal reactions to small environmental changes. Feedforward control means a directly environmentally induced closure of stomata that may close stomata to the extent that the rate of transpiration decreases despite of increases in VPD. Short-term variations of irradiance under conditions of high VPD led on the other hand not in all cases to variations in transpiration.

The transpiration of shade leaf cloud was more sensitive to changes in irradiance than that of sun leaf clouds. This may partly be explained by stomatal opening due to increasing irradiance, which is due to a photosynthesis induced reduction of leaf internal CO₂-concentration. This reduction is somewhat stronger in shade leaves than in sun leaves at very low irradiances. But since the sensitivity of leaf cloud transpiration to PPFD exponentially decreased with increasing LMA (Fig. 125) and the sensitivity of shade leaf clouds was not decreasing towards higher irradiances (Fig. 124), the main cause may be found in the parallel decrease of stomatal sensitivity (*g_{fac}*) with LMA or nitrogen per area of beech leaves (Fig. 98). The high *g_{fac}* - values at low nitrogen express the relatively high stomatal conductance that is generally allowed to shade leaves of beech even under less favourable conditions (low CO₂ use efficiency, mostly due to low light) and that increases stronger with increasing CO₂ use efficiency (or increasing light) than stomatal conductance of sun leaves of beech. Thus, the higher light sensitivity of shade leaf clouds may completely be due to differences in stomatal sensitivity (*g_{fac}*) between sun and shade leaves.

A very high coefficient of determination ($r^2=0.98$) was found between leaf mass and the sum of transpired water of each leaf cloud during the investigation period (Fig. 126). Further investigations are necessary to analyse, if this useful relationship is also valid for other conditions or even other trees and species. Further conclusions may be derived with this model combination and this data base since additional sapflow measurements on branches and stem of oak Gr13, as well as on stems of other trees in the stand were not yet evaluated.

5 Integrating discussion

5.1 Characteristics of oak and beech in the stand Großebeene

Many characteristics of oak and beech in the Großebeene stand have been collected on different levels of organisation and it seems worthwhile to compare these properties species-oriented to evaluate if they draw a reasonable picture of ecological specialization of the species in their stand, though general conclusions can not be drawn due to the low number of investigated trees. Table 9 summarises the clearest differences between the species found in this study.

Characteristics	<i>Fagus sylvatica</i>	<i>Quercus petraea</i>
Natural regrowth in the mixed stands	Yes (Fig. 3)	No (Fig. 3)
Height position of crowns in the stand	All height positions (Fig. 117)	Uppermost 8-12m of the stand (Figs. 19b, 117)
Crown length	Long (Fig. 117)	Short (Fig. 117)
Proportion of dead branches and boughs in the lower crown	Low (Figs. 7, 10)	High (Figs. 7, 10)
Growth pattern of branches	More deterministic (Figs. 9, 33, 34, 46)	Less deterministic (Figs. 9, 33, 34, 46)
Crown construction	Fan-shaped opening towards the surface (Figs. 16, 35, 37, 40, 41)	More irregular (Figs. 16, 35, 37)
Crown shape	Convex borders, greatest diameter in the lower part, long and pear-shaped (Figs. 18, 26)	Concave borders, greatest diameter in the upper part, short and strawberry-shaped (Figs. 18, 26)
Directions of strengthened development	One main direction, not towards a neighbouring tree (Figs. 43, 47, 51)	Several directions towards neighbouring trees (Figs. 43, 47, 51)
Total leaf area density	Lower (Table 5)	Higher (Table 5)
Leaf area densities in the crown	Highest leaf area density in the uppermost meter of the crown, continuously low densities in the lower half (Fig. 23)	Highest leaf area density 2-3m below the apex, decreasing towards the apex and the bottom (Fig. 23)
Self-shading	Less severe (Figs. 31, 32)	Stronger (Figs. 31, 32)
Leaf photosynthesis capacities	Low (Figs. 83-86, 89)	High (Figs. 83-86, 89)
Stomatal sensitivity (<i>g_{fac}</i>)	High in shade leaves, low in sun leaves (Fig. 98)	High in medium sun leaves, lower in uppermost sun leaves, low in shade leaves (Fig. 98)

Oak crowns in the stands Großebene and Steinkreuz occupy only the most sun-exposed positions in the stand, but are not able to reach this position by natural regrowth in the dense stand. This is in accordance with the forest management practice to save oaks from competition of neighbouring beeches by felling these beech trees. Once in the top of the canopy, the strategy of oak seems to be the occupation of high volumes in the upper region, producing a high overall leaf area density and thereby shading competing species below that region - and itself. The stronger self-shading of oak may be one reason for its short crown with several dead boughs in the lower part. This may also be seen as a specialization of oak in the use of only high light positions.

The occupation of high volumes in the upper part of the canopy is visible in the oak's crown shape. It is open to speculation if the concave (=rugged) and approximately strawberry-shaped crown form is a consequence of a general multi-directional development of oaks towards competing trees. Such a growth reaction to the spatial situation would require flexibility in the growth pattern of branches, which is apparently better achieved in oak than in beech. The investment into high photosynthesis capacities makes sense for a tree in a high-light environment. That stomatal sensitivity (*g_{fac}*) is high in medium sun leaves indicates that oak allowed high transpiration especially to these leaves, even when their CO₂ use efficiency (assimilation per CO₂-concentration) and relative humidity were not very high. The risk of high water losses in sun leaves is more reasonable when leaves have high photosynthesis capacities and may provide the resources for expansive growth in the region of these leaves. The lower transpiration support for shade leaves probably causes them to die earlier and again indicates the consequent adaptation of oak to high light environments.

Beech on the other hand was generally more carefully avoiding high water losses due to low coefficients of stomatal sensitivity. Only the lowest shade leaves were allowed to have high conductances when CO₂ use efficiency and relative humidity were not very high. This seems not as hazardous as allowing it to sun leaves, because relative humidity in the lowest part of the crown is usually higher than in the upper part. But it includes the possibility of useless transpiration due to the lower chance for sufficiently high assimilation gains of shade leaves. While beech, thus, seems to have supported shade leaves in allowing them high transpiration rates, oak mainly supported medium sun leaves in their water consumption.

The water support for the lowest shade leaves may help them to achieve a positive CO₂-balance and this could be one factor that allows beech to maintain high amounts of shade leaf biomass and to develop extensive shade crowns. The generally sparing equipment of beech leaves concerning photosynthesis capacities may additionally be advantageous in maintaining the high number of shade leaves. Another factor for the survival of shade leaves may be found in the fan-shaped formation of beech leaf clouds towards the canopy surface which probably improves the light situation of shade leaves. The more deterministic growth of branches of a beech tree, its unidirectional development, and the conserved convex crown projection may indicate that a pre-formed internal organisation scheme could be relevant for the CO₂-balance of shade leaves. A strengthened development towards several directions in order to compete with horizontal neighbours would hardly be possible, if a pre-formed pattern is to be conserved, while a general drift towards the most promising gap in the surrounding stand seems to be possible, especially since the fan-shaped formation of leaf clouds appears to be gap-oriented anyway. A generally and mainly in the shade crown lower leaf area density also improves the conditions for shade leaves due to less self-shading.

All these factors together with the rather low leaf photosynthesis capacities of beech may be seen as adaptations to shade conditions that are necessary for a tree with a large shade crown. The height distribution of leaf area densities in beech shows that it may on the other hand also be very competitive with regard to the most sunny positions in the stand. Its relative success in a mixed stand of oak and beech may, thus, be explained with two complementary, defensive and aggressive strategies: A light-oriented organisation of the shade crown can make the whole tree relatively insensible to shading by a neighbouring tree, which is supported by a growth pattern of the sun crown that avoids self-shading by occupying only small volumes. This could allow it to survive in the shade of other trees for years and even provide the resources for the growth of the sun crown. The concentration of highest amounts of leaf area in the uppermost layer of the sun crown on the other hand can assure high shading efficiency of this part of the crown, because shadow cast of this layer is relevant for the biggest possible part of the surrounding stand canopy. This may on the long run improve the conditions for the whole tree by effectively reducing growth rates of competitors (LEUSCHNER 2001). The double strategy of beech may also be expressed in its crown shape that is more clearly separated in sun crown and shade crown than that of the oak.

Thus, the characteristics found on single trees of both species fit into a reasonable description of their ecological specialization, though they can not prove the general validity of this concept.

5.2 Application of Beer's law

The description of light profiles in the stand with Beer's law was in a first approximation applicable to the beech crowns in the Buchenallee stand (Figs. 58, 59). However, two assumptions of Beer's law have been shown to be violated in these crowns:

- The leaf angle distribution was not constant throughout the canopies of beeches Bu45 and Bu38 (Figs. 62, 63). The frequency of steep inclinations that allow more light to penetrate a leaf layer decreased from the apex to a depth of around 6 m (Bu38) or 7 m (Bu45) in the crown, where horizontal inclinations were most abundant. The frequency of steep inclinations increased again from there towards deeper parts of the crown. The extinction coefficient of Beer's law was, therefore, variable along a vertical gradient through the crown.
- Leaf area density of crown layers was not constant and exhibited the general pattern of 2-3 "peak"-layers with higher leaf area density that were separated by layers with lower leaf area density (Figs. 21-23). The peak-layers of leaf area density of beech Bu38 were in a height of 3 m and 6 m below apex. The variation of leaf area density has to be included in the calculation of light profiles according to Beer's law.

The significance of the layer 6 - 7 m below apex of both crowns for the light profile is increased through the observed trend in width of leaf space and in angles of leaf cloud planes:

While width of leaf blade did not show a clear dependence on irradiance or height below apex, the effective width of leaf space was widest in this layer and decreased from there towards both ends of the crown (Fig. 66). This trend increases the effective leaf area density (based on projected leaf area instead of leaf area) of the layer 6 - 7 m below apex relative to the other layers.

The angles of leaf clouds were nearly horizontal in the layer 6 - 7m below apex and became negative below that layer, while they were positive above (Figs. 33 and 35). Thus, light extinction on a leaf cloud basis is maximum in this layer.

The consequence of the leaf angle variability for light profiles would be a stronger light gradient than calculated with Beer's law (using constant coefficients) in the upper 6 - 7 m of the crown and a less strong decrease in light intensity below that height. Leaf area density variability would strengthen this effect in the upper 3 m of the crown of beech Bu38 and in the lowest part below 7 m below apex, while it would damp the decrease of light intensity in the crown part between 3 m and 7 m below apex.

Thus, a stronger light gradient is to be expected in the upper 3 m of the beech crown Bu38 and a weaker light gradient in the lowest part below 7 m below the apex. This expectation is confirmed in a comparison with the measured relative irradiance in beech Bu38 (Fig. 58). Relative irradiance in the upper 3 m decreased stronger than an exponential fit based on the assumption of constant coefficients in Beer's law, though this approximation is for mathematical reasons stronger oriented on the relative high irradiance values than on the low irradiance values. This fit is not able to reproduce the "too high" relative irradiance values in the crown part below 6 m below the apex, indicating that no exponential function may adequately express both parts. The high coefficient of determination does not really consider the deviation in the lower crown part, which is big in relative units but small in absolute units. This might be the reason for it to be overlooked in comparable investigations. A "too high" relative irradiance in the lowest crown part was also observed on the data of beech Bu45 (Figs. 58, 59).

The "too high" relative irradiance values in the lowest crown part of these both trees may be interpreted as another adaptation of beech trees to the low light environment that they produce themselves for their shade crown. The light distribution inside the crowns becomes more homogeneous through the described variation in angles and density of foliage elements, which lowered relative irradiance in the above crown part and increased it in the lower shade crown.

5.3 Leaf mass per area (LMA)

The reported LMA-values of sun leaves of beech from different origins (Table 5, Fig. 108) show an increasing long-term trend since 1968, while it seemingly was lowest around 1943. Since the position of the investigated leaves is not mentioned in the study of BURGER (1945), the apparent relative decrease of average LMA between 1891 and 1943 could also be due to the different exposition and light situation of the investigated leaves (compare Figs. 68 and 69), though trees have been felled in the extensive studies of BURGER and a differentiation between sun and shade leaves was generally made. This could lead - apart from different stand conditions - to an artificial LMA-decrease, because this investigation is the only data point between 1891 and 1968.

But even the newer literature since 1970 shows an increasing long-term trend. The lowest LMA-values (40 - 60 g/m²) of sun leaves in this period were measured 1968 from a tower in 26m height on the outermost leaves of the sun crown of beech "B68" in the IBP stand Solling (international biological program, SCHULZE 1970). Though differences between stands like altitude, exposition, depositions, average temperature, or other differences may be influential, these differences would not necessarily lead to the compiled general increase of LMA of sun leaves. Stand-specific differences are not relevant in the case of beech B68 in the Solling project, whose sun leaves in 26m were investigated again in the period 1986 - 1988 and then had LMA-values of 80 to 110 g/m² (SCHULTE 1992).

Since the increase in LMA-values of beech B68 (Solling) goes along with the general trend found on data from various origin, it becomes likely that this difference shows a realistic

structural change in this crown that occurred apparently also on other beech trees in Europe. The newest compared values (those of this study) were also the highest LMA-values. This could mean that LMA of sun leaves of beech trees is still increasing and reasons as well as consequences of this trend need to be assessed, though additional LMA-data have to be evaluated to assure the validity of the LMA-trend.

Atmospheric CO₂, climate change, or nitrogen depositions come into question as potential causes for physiological changes that lead to an increase of LMA of sun leaves of beech. While effects of climate change are unlikely to be detectable in climate data between 1968 and 1987, nitrogen deposition to forests was increasing between 1968 and 1991 and decreasing in the latest years since 1991 (Level II - program, BML 1997). Yearly averages of atmospheric CO₂ concentration as measured at Mauna Loa (Hawaii) continuously and still exponentially increased from the years 1968 (323 µmol/mol) to 1987 (349 µmol/mol) and 1999 (368 µmol/mol) (KEELING & WHORF 2000), which was the strongest increase of this quantity since 1800 when it started to increase from a stable pre-industrial value of 270 ppm (SALISBURY & ROSS 1992). The time course of CO₂-concentrations corresponds best with that of the compiled LMA-increase, since the LMA-trend does not show a decrease.

A consequence of the LMA-increase in sun leaves of beech trees could be a higher sink strength of sun crowns of beech for CO₂ during the vegetation period, since more assimilates are needed to build up thicker leaves. This point needs further investigation due to a possible opposite trend in the allometric relationship between leaf area and basal area of trees, which was lower in all harvested trees than in the regressions based on former investigations (Fig. 14), so that trees eventually just organise the same leaf mass to a smaller area. Lower leaf area of beech trees and other forest species is also reported from public forestry studies in Germany (HMU 2000). The combination of both trends could potentially lead to a higher water use efficiency due to reduced transpiration rates (as a consequence of reduced leaf area) and increased light availability in the shade crown.

Though the deposition rates are decreasing since 1991, it can not be excluded that the LMA-increase is due to high nitrogen deposition, because nitrogen uptake by the trees might still be high. The observed nitrogen saturation of photosynthesis capacities of leaves of oak and beech indicates that the investigated sun leaves contained more nitrogen than they need for photosynthesis (Fig. 89).

5.4 Implications for gas-exchange modelling

It has been shown that homogeneity is not given on the level of tree crowns and, therefore, on the level of stands. Thus, the assumption of homogeneous conditions in smaller or bigger compartments (big leaves, layers, or 3D-compartments) is generally violated to some extent, though many effects of small scale inhomogeneity are probably neutralized on larger scales. The latter seemed also to be valid for the decrease of relative irradiance with depth in the canopy, since the general shape of the function of Beer's law was in a first approximation confirmed by fish-eye photos in beech canopies (Figs. 58, 59) and the found deviations were small in absolute units. Nevertheless these small deviations need consideration even in large scale models since gas-exchange models are very sensitive to changes in light profiles and the deviations are likely to represent a general phenomenon.

An indication of the relevance of these deviations is given by the application of layer-oriented gas-exchange models in net ecosystem exchange (NEE) calculations of beech stands: Such

models often use variations of Beer's law to describe the light gradient in stand canopies and then typically consider the leaves in the lower half of beech canopies as CO₂-sources on each day of the vegetation period due to light intensities below the light compensation point of these leaves (own simulations with the layer model GASFLUX (SALA & TENHUNEN 1996), data not shown). This is a consequence of the use of an exponential function that inevitably approaches zero in the lower part of the crown when it is fitted to represent the higher light values in the upper canopy. It is not impossible but unlikely that beech trees can afford this waste of resources.

The found deviations from Beer's law are likely to represent general properties of beech canopy structure that have an equalizing effect on the light profile, thereby inducing a steeper gradient in the upper canopy and a much lower gradient in the lower part of the crown. Thus, the height dependent leaf angle distributions and naturally layered leaf area density distributions (see 5.2.) should be considered in layered gas-exchange models.

Most gas-exchange models do not consider the leaves as bent and, therefore, probably consider about 20% too much leaf area in the crowns at least of beech, since projected leaf area is the relevant quantity for light transmission and absorption. Since bending has been found to be height dependent (Fig. 66), the area reduction may easily be included in gas-exchange models.

More complex evaluations would be necessary to investigate the effect of leaf cloud inclinations and their orientation towards the canopy surface, which probably improves the use of reflected and transmitted radiation in the shade crowns of beech due to a fan-shaped formation towards the canopy surface. Such an effect would again improve the light situation of shade leaves. This could affect gas-exchange calculations especially when leaves are wet and their reflectance may reach values above 50% (dependent on the angle of incident light, GATES 1980). Not all models of gas-exchange consider the changes in transmission and reflectance occurring on wet leaves.

A fine-scale 3D-representation of forest stands might be the most accurate way to represent inhomogeneity of stands and to evaluate small-scale effects, but it is not suitable for an application to large areas. This situation may change to some extent due to up-scaling relationships like those of the nitrogen dependent leaf gas exchange model, which may use the structure dependent light climate of leaves for the derivation of nitrogen per leaf area ($r^2 \geq 0.87$, Fig. 75) and thereby yields a completely parameterised leaf gas-exchange model that is valid for this spatial situation. Thus, an integrated and very detailed model of stand gas-exchange results from the combination of the nitrogen dependent leaf gas exchange model with STANDFLUX-SECTORS or any other 3D light model and estimations of soil and wood respiration (FLECK ET AL. 2001).

Such an integrated 3D model may be validated on many different scales using light measurements, LMA-distributions, leaf nitrogen contents, photosynthesis measurements on leaves and branches, sapflow measurements on branches and stems, or even eddy measurements, when extensive structure information has been gathered and soil respiration has been estimated. It thus may improve the reliability of stand gas exchange models in a way that allows up-scaling from sapflow measurements on trees to stand gas-exchange along canopy structures and could thereby be useful to provide reliable estimations of gas-exchange of stands, where eddy measurements can not be performed (for example stands in

mountainous regions). Reliable estimations of gas-exchange in these regions could be useful to validate regional NEE calculations.

The data set from the Großebene stand combines sapflow measurements on stems of beech Gr12, oak Gr13, other tree stems, and on branches from oak Gr13 with a detailed structure description that allows further testing of an integrated model. Automated methods of structure measurement are under development (KOCH & REIDELSTÜRZ 1998, LEFSKY ET AL. 2000, TANAKA ET AL. 1998) and might soon provide the necessary structure information for larger scale applications of a reliable integrated 3D model.

6 Summary

The gas exchange of mixed forest stands is - due to their high proportion within the forested area - an important quantity for the estimation of CO₂- and water balances on larger scales, but difficult to verify. This thesis assumes that a fundamentally new situation in terms of theory of cognition has emerged in this field of research due to the rapid development of computer-based data processing in recent years, since it allows for the first time the explicit consideration of spatial heterogeneity in process-oriented models. This provides the opportunity to validate models across spatial scales, thereby improving the reliability of forest stand gas-exchange calculations. The bottle-neck for this kind of evaluation is not data-processing or simulation, but rather the co-ordinated recording of all information relevant to the multiple verification of a process-oriented model of mixed stand gas-exchange.

The contribution of this investigation lies in the comprehensive representation and comparative fine-scale analysis of the spatially explicit description of trees in a 120 year old mixed stand of oak and beech in the Steigerwald. The 3-dimensional structure description is associated with the measured variability of photosynthesis parameters and validation data on different spatial scales. These data are discussed together with data from compared stands. Subroutines of an integrating up-scaling model were improved and verified with measurements.

The canopy structures of two beech trees and one oak were simulated in an optically controllable way based on branch-oriented harvests, branch-oriented geodetic measurements (Figs. 4, 5), and allometric relationships (Figs. 9, 14). The newly developed program CRISTO for spatial analysis is based on the representation of branches and their appending leaf biomass (leaf clouds) as polyhedrons and enables the calculation of height profiles of leaf area density in layers of 1m height (Fig. 23). A tendency to build single layers with very high leaf area densities was detectable. The canopies consisted of 2-3 natural layers of leaves, which contrasted with the optical impression of the trees (Figs. 20, 21). The proportion of gaps between leaf clouds was higher than 80% in most layers of all three trees (Fig. 25).

Measured species-specific differences between the crown shapes of 186 oak and beech trees were also found in the characteristic canopy shapes of the three investigated trees that were derived from maximum horizontal extensions of layers of 1m height (Fig. 26). Stronger self-shading of the oak tree was a consequence of its different canopy shape (Figs. 30 - 32).

Leaf clouds of both beech trees showed striking similarities in their main growth directions (Figs. 35, 37, 39 - 41), which affected light penetration into the canopy by the variation of leaf cloud angles towards the horizon (Fig. 33) and their orientation towards the canopy surface (Fig. 41). The leaf area density of leaf clouds was largely independent of any of 8 investigated crown structure parameters (Fig. 55).

The light profiles of beech crowns were measured using fish-eye-photos and were shown to differ from Beer's law (Fig. 58) in a way that may be explained by the variation of leaf area density and extinction coefficient, the latter of which was due to the variability of leaf angles. A height dependent variation of leaf angle frequency distributions of beech was found that could be described by single-parametric ellipsoidal distribution functions (Figs. 60, 62).

While the relationship between height or light and the width of leaf blades was scattered, the projected width of the beech leaves (which considers leaf bending) was shown to be height and light dependent (Fig. 66). Clear light dependencies were also established for leaf mass per area

(LMA, Fig. 69), leaf carbon concentration (Fig. 71), and area-related leaf nitrogen content (Fig. 75).

Occasionally very high LMA-values and area-related nitrogen contents have been measured. LMA-values from the Steigerwald were the highest when compared to literature data from 110 years and fit into a general tendency of increasing LMA-values of sun leaves of beech.

The program RACCIA has been developed for the automated derivation of photosynthesis capacities (J_{max} , $V_{C_{max}}$) from A/C_p -curves that were measured on oak and beech in the Steigerwald. The program is based on the HARLEY/TENHUNEN (1991) - model and was verified using chlorophyll fluorescence measurements (Fig. 78). J_{max} and $V_{C_{max}}$ were shown to increase with nitrogen per leaf area up to a certain nitrogen level, where leaf photosynthesis becomes apparently nitrogen saturated (Fig. 89). Nitrogen saturation of photosynthesis capacities and measured temperature dependencies were considered in the development of a nitrogen dependent model of leaf photosynthesis (Fig. 97) that reduces the number of necessary parameters by more than 50% (Table 7). The model validation was based on measured daily courses and provided evidence of the potential effects of stomatal patchiness (Figs. 106, 107).

The application of the highly resolving 3D light model STANDFLUX-SECTORS to the geometric representation of a beech tree and its surrounding stand in the Steigerwald was enabled by the development of a segmentation and parameterisation routine in the framework of CRISTO (Fig. 112 - 114). A beech crown was segmented into 410 parameterised homogeneous compartments. The light model was verified using the light dependence of LMA (Fig. 118, 119).

A stronger light sensitivity of transpiration was derived for shade leaf clouds of beech and was attributed to the higher sensitivity of stomata of shade leaves to CO_2 use efficiency and relative humidity (*gfac*) (Fig. 98, 125).

Totals of transpiration over 14 days of the investigated branches were well correlated to the calculated quantum sum above the leaf clouds and to their leaf biomass (Fig. 126).

The results provide a reasonable picture of the ecological specialization of oak and beech in a mixed stand: While beech has a strategy to cope with a shady environment that keeps a high amount of shade leaf biomass alive and reduces the tree's susceptibility to shadow cast from competing trees, oak secures a once achieved position in the upper canopy by expansive growth of the upper crown layers and is largely specialized in the more efficient photosynthesis of sun leaves.

Implications for gas-exchange models are derived from their high sensitivity to the used light profile. The use of exponential functions for the calculation of light profiles may lead to strong underestimations of CO_2 -uptake when the height dependence of leaf angle distributions and the multi-layered canopy structure are not adequately considered in the equation. Light absorbing leaf area is overestimated in most gas-exchange models by around 20%, because leaf bending is mostly not considered. The high reflectance of wet leaves should be considered due to the potentially higher irradiance in shade crowns under these conditions.

The model subroutines presented in this thesis may be combined to an integrated 3D model that may improve reliability of gas-exchange models, when further validation on different scales is performed. This is possible on additional data from the Großebene stand. The integrated model might be very useful in combination with automated structure measurements in future validation of NEE calculations in mountainous regions, where eddy measurements are more uncertain.

7 Zusammenfassung

Der Gaswechsel von Waldmischbeständen ist aufgrund ihres hohen Flächenanteils eine bedeutende, aber nur schwer zu verifizierende Größe in überregionalen Berechnungen von CO₂- und Wasseraustausch. Die vorliegende Arbeit geht davon aus, dass durch die rasche Entwicklung der computergestützten Datenverarbeitung der letzten Jahre eine neue erkenntnistheoretische Situation in diesem Forschungsgebiet eingetreten ist, die erstmals die explizite Berücksichtigung räumlicher Heterogenität in prozessorientierten Modellen ermöglicht. Hierdurch werden skalenübergreifende Validierungsmöglichkeiten eröffnet, die Gaswechselberechnungen auf Bestandesebene verlässlicher machen können. Engpässe bestehen durch diese Entwicklung weniger in der Datenverarbeitung und Simulation als in der koordinierten Erfassung aller relevanten Informationen, die zur mehrfachen Verifizierung eines prozessorientierten Modells des Mischbestandsgaswechsels notwendig sind.

Der Beitrag dieser Arbeit besteht in der umfassenden Darstellung und vergleichenden feinskaligen Analyse der räumlich expliziten Beschreibung von Bäumen eines 120-jährigen Eichen-Buchen-Mischbestands im Steigerwald. Die zu Simulationszwecken verwertbare 3-dimensionale Strukturbeschreibung ist mit der gemessenen räumlichen Variabilität von Photosyntheseparametern und mit Validierungsdaten auf verschiedenen räumlichen Ebenen verknüpft. Diese Daten werden zusammen mit Vergleichsbeständen diskutiert. Subroutinen eines skalenübergreifenden Modells wurden weiterentwickelt und anhand von Messdaten überprüft.

Der Kronenaufbau von zwei Buchen und einer Eiche wurde auf der Basis astbezogener Ernten, astbezogener geodätischer Messungen (Abb. 4, 5) und allometrischer Beziehungen (Abb. 9, 14) optisch verifizierbar simuliert. Die räumliche Analyse mit dem dafür entwickelten Programm CRISTO beruht auf der Repräsentation von Ästen mit ihrer anhängenden Blattmasse (Blattwolken) als Polyeder und ermöglicht durch Zerlegung der Kronen in 1m-Schichten die Berechnung von Höhenprofilen der Blattflächendichte (Abb. 23). Hieran war eine Tendenz zur Bildung einzelner sehr dichter Schichten erkennbar. Der Kronenaufbau erwies sich entgegen dem äußeren Anschein als natürlicherweise mehrschichtig hinsichtlich der Verteilung von Blattflächen (Abb. 20, 21). Der Anteil blattfreier Räume außerhalb der Blattwolken lag in den meisten Höhenschichten aller drei Bäume über 80% (Abb. 25).

Gemessene artspezifische Unterschiede in der Kronenform von 186 Buchen und Eichen spiegeln sich in den charakteristischen Kronenformen der drei Untersuchungs bäume wider, die aus der maximalen horizontalen Ausdehnung von Höhenschichten abgeleitet wurden (Abb. 26). Als Konsequenz der unterschiedlichen Kronenform wurde eine höhere Selbstbeschattung der Eichenkrone im Vergleich zu den Buchen ermittelt (Abb. 30-32).

Blattwolken in beiden Buchenkronen wiesen auffällige Übereinstimmungen hinsichtlich ihrer Wuchsrichtung auf (Abb. 35, 37, 39 - 41), die sich aufgrund des höhenabhängigen Blattwolkenwinkels (Abb. 33) und der Stellung zur Kronenoberfläche (Abb. 41) auf die Lichtverteilung in der Krone auswirken. Die Blattflächendichte von Blattwolken war weitgehend unabhängig von 8 untersuchten Strukturparametern (Abb. 55).

Die mittels Fish-eye-Fotografie erstellten Lichtprofile von Buchenkronen zeigten Abweichungen vom Lambert-Beer'schen Gesetz (Abb. 58), die sich aus der von Blattstellungswinkeln verursachten Variabilität des Extinktionskoeffizienten und der inhomogenen Blattflächendichtenverteilung erklären lassen. Es konnte eine höhenabhängige Variation der

Häufigkeitsverteilungen von Buchenblattwinkeln gezeigt werden, die durch einparametrische ellipsoide Verteilungsfunktionen beschreibbar war (Abb. 60, 62).

Im Unterschied zur Blattflächenbreite zeigte die projizierte Breite der gekrümmten Buchenblätter eine Licht- und Höhenabhängigkeit (Abb. 66). Deutliche Lichtabhängigkeiten konnten auch für die flächenbezogene Blatttrockenmasse (LMA, Abb. 69), die Blattkohlenstoffkonzentration (Abb. 71) und den flächenbezogenen Blattstickstoffgehalt (Abb. 75) festgestellt werden.

Es wurden sehr hohe maximale LMA-Werte und flächenbezogene Stickstoffgehalte festgestellt. Die LMA-Werte aus dem Steigerwald waren im Vergleich mit Literaturdaten aus 110 Jahren am höchsten und fügen sich in einen generellen überregionalen Trend zunehmender LMA-Werte von Buchen-Lichtblättern ein (Abb. 108).

Für die automatische Herleitung von Photosynthesekapazitäten (J_{max} , Vc_{max}) aus gemessenen A/C_p -Kurven an Eiche und Buche im Steigerwald wurde das Programm RACCIA auf der Basis des HARLEY/TENHUNEN (1991) -Modells entwickelt und mit Chlorophyllfluoreszenzmessungen überprüft (Abb. 78). J_{max} und Vc_{max} zeigten eine stickstoffabhängige Zunahme, die bei hohen Stickstoffgehalten in eine Sättigung übergeht (Abb. 89). Die Stickstoffsättigung der Photosynthesekapazitäten und die gemessenen Temperaturabhängigkeiten wurden in der Erstellung eines stickstoffabhängigen Blattphotosynthesemodells berücksichtigt (Abb. 97), durch das sich der Parametrisierungsbedarf für das Blattgaswechselmodell mehr als halbiert (Tabelle 7). Die Validierung des Modells anhand von Tagesgangmessungen weist auf Effekte von 'stomatal patchiness' in den Messungen hin (Abb. 106, 107).

Die Anwendung des beliebig hochauflösenden 3D-Lichtmodells STANDFLUX-SECTORS auf die polyedrisch repräsentierte Baum und Bestandesstruktur einer Buche im Bestand GroÙebene wurde durch die Entwicklung einer Kompartimentierungs- und Parametrisierungsroutine im Rahmen von CRISTO möglich (Abb. 112 -114), mit der eine Buchenkrone in 410 homogene Kompartimente zerlegt und kompartimentweise parametrisiert wurde. Das Lichtmodell wurde anhand der Lichtabhängigkeit der LMA validiert (Abb. 118, 119). Die stärkere Lichtsensitivität der Transpiration von Schattenästen ließ sich auf eine erhöhte Sensitivität gegenüber CO_2 -Nutzungseffizienz und relativer Luftfeuchte (g_{fac}) der Schattenblatt-Stomata zurückführen (Abb. 98, 125).

Transpirationssummen der untersuchten Äste über 2 Wochen korrelierten sehr gut mit der berechneten Strahlungssumme über jedem Ast bzw. zu ihrer Blattmasse (Abb. 126).

Die Ergebnisse fügen sich zu einer plausiblen Beschreibung der ökologischen Spezialisierung von Eichen und Buchen im Mischbestand zusammen: Während Buche eine Schattenstrategie verfolgt, die einer größeren Menge von Schattenblättern das Überleben sichert und zugleich die Empfindlichkeit des Baums für Beschattung durch Nachbarbäume reduziert, sichert Eiche einmal erworbene Positionen im oberen Kronendach durch expansives Wachstum der oberen Kronenschicht und spezialisiert sich dabei weitgehend auf die effektivere Photosynthese der Lichtblätter.

Schlussfolgerungen für die Gaswechselmodellierung ergeben sich aus der hohen Sensitivität von Bestandesgaswechselmodellen in Bezug auf das berechnete Lichtprofil. Exponentielle Funktionen zur Berechnung des Lichtprofils können die Ursache für eine deutliche Unterschätzung der CO_2 -Aufnahme sein, wenn die Höhenabhängigkeit von Blattwinkelverteilungen und die Mehrschichtigkeit des Kronendachs nicht angemessen repräsentiert sind. Die lichtabsorbierende Blattfläche dürfte in den meisten

Gaswechselmodellen um ca. 20% überschätzt werden, da die Krümmung der Blätter meistens nicht berücksichtigt wird. Die höhere Reflexion von nassen Blättern sollte wegen ihrer potenziellen Bedeutung für die die Schattenkrone erreichende Strahlung berücksichtigt werden.

Die in dieser Arbeit vorgestellten Modell-Subroutinen können zu einem integrierenden 3D-Modell kombiniert werden, das die Zuverlässigkeit von Gasaustauschberechnungen auf Bestandesebene erhöht, wenn weitere Validierungsschritte auf verschiedenen Skalen durchgeführt werden. Hierzu stehen weitere Daten aus dem Bestand Großebene zur Verfügung. Das integrierende Modell kann in Kombination mit automatisierten Methoden der Strukturbestimmung in der zukünftigen Validierung von NEE-Berechnungen in Gebirgsregionen sehr nützlich sein, da hier Eddy-Messungen zu Validierungszwecken noch nicht verlässlich sind.

8 Appendix

8.1 Parameter derivation for chapter 2.3.5

The vector of the main growth direction was found on the base of the equation for angles between vectors in cartesian co-ordinates (BRONSTEIN et al. 1995):

$$\text{Cos}(\varphi) = \frac{a_x b_x + a_y b_y + a_z b_z}{\sqrt{a_x^2 + a_y^2 + a_z^2} \times \sqrt{b_x^2 + b_y^2 + b_z^2}} \quad (\text{A1})$$

, with (a_x, a_y, a_z) , the known normal vector of the leaf cloud plane, and (b_x, b_y, b_z) denoting the 3-dimensional vector of the main growth direction in $(x,y,z) = (\text{east, north, height})$ direction. Because the x and y co-ordinates of (b_x, b_y, b_z) are known to be the leaf cloud centre's east and north co-ordinate (**E**, **N**) and in the case of $\varphi = 90^\circ$, i. e., when the vector lies in the leaf cloud plane, the equation simplifies to

$$0 = a_{\text{east}} E + a_{\text{north}} N + a_{\text{height}} b_{\text{height}} \quad (\text{A2})$$

, so that b_{height} may be determined. The equation for a straight line that represents the main growth direction in a two dimensional stem distance (Y) vs. height (X) co-ordinate system then is found as

$$Y = \frac{\sqrt{E^2 + N^2}}{b_{\text{height}}} \times (X - H_{\text{abs}}) + \sqrt{E^2 + N^2} \quad (\text{A3})$$

and the appertaining two dimensional vector is:

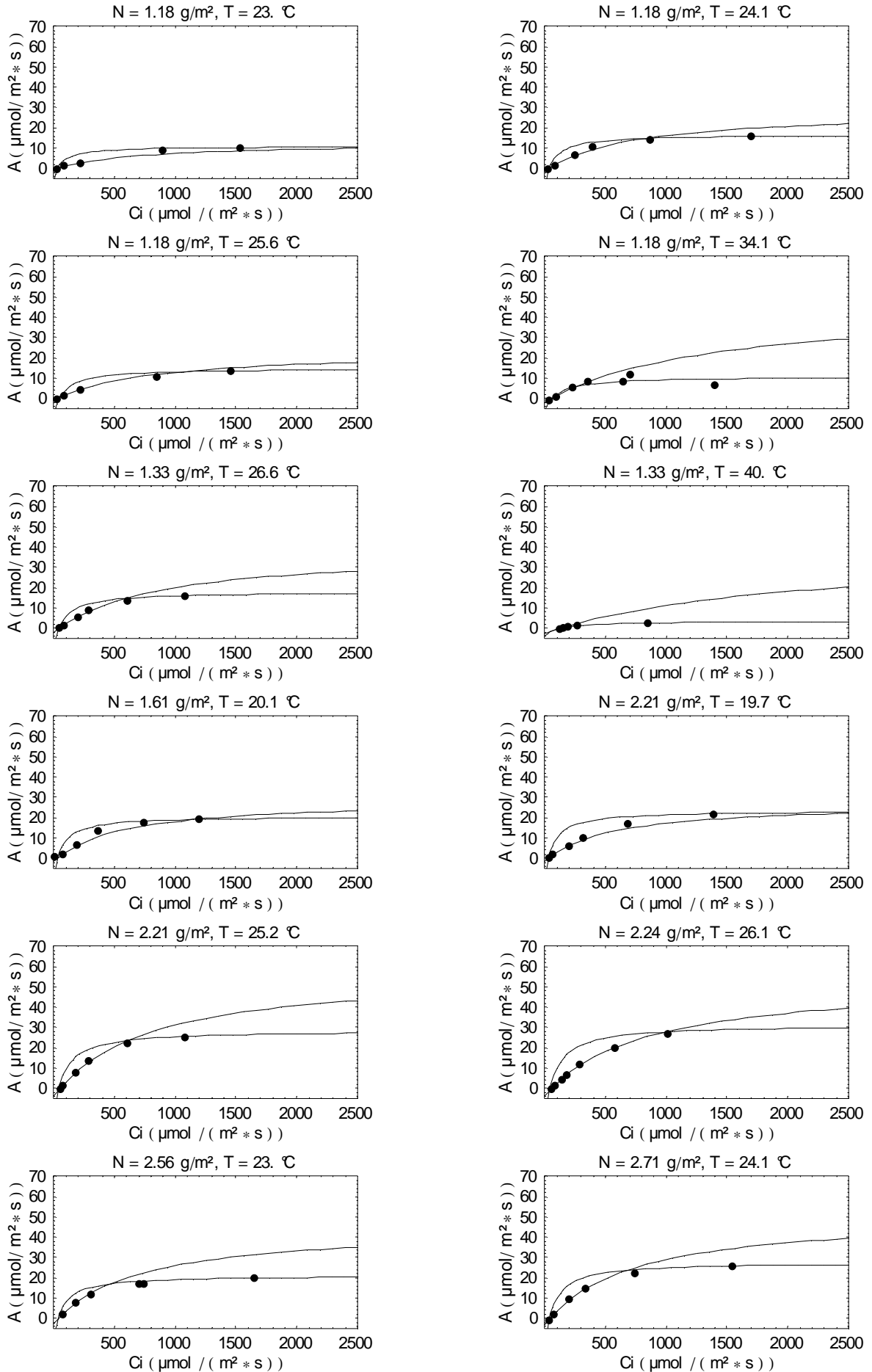
$$\vec{v} = (b_{\text{height}}, \sqrt{E^2 + N^2}) \quad (\text{A4})$$

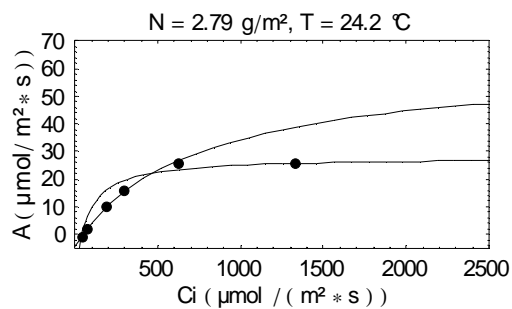
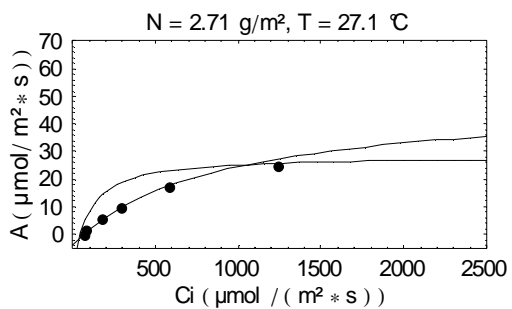
Finally equation (A3) and the shape function (Fig. 26) were equated to calculate x, which is the height co-ordinate of the intersection of both lines. Out of the resulting 5 solutions for the height of intersection that one was taken which was a real number and was between the upper and lower height limit of the investigated tree crown and closer to the height of the leaf cloud centre. D_s , the derivative of the shape function in this height was then transformed to a two-dimensional vector (along the tangent) and the angle to the two dimensional vector of the straight line (equation (A4)) was calculated according to equation (A1). The derivative of the canopy shape function gives the vector along the canopy surface towards positive x-direction ("above") and the main growth direction may be a vector towards negative or positive x-direction, so that angles up to 180° principally may occur.

8.2 Measured A/C_r-curves

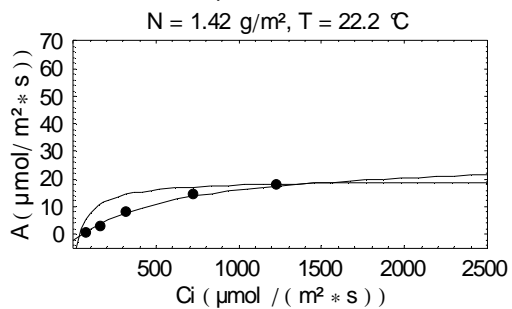
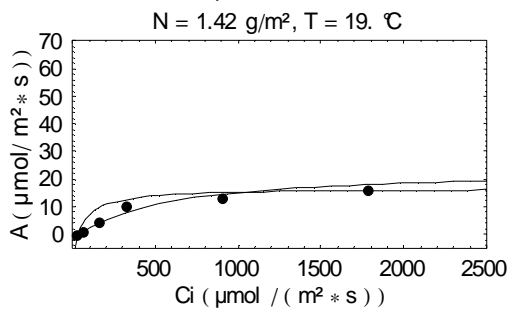
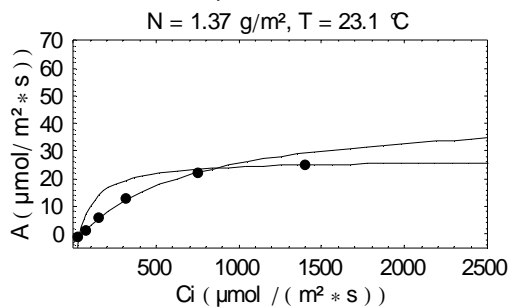
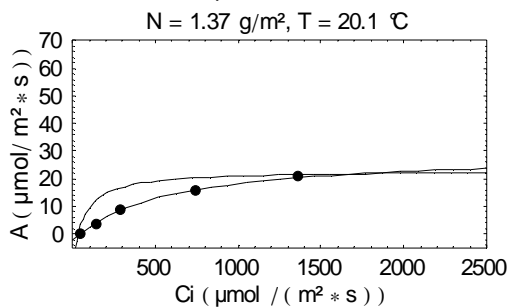
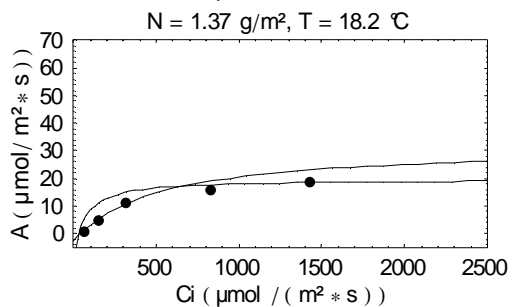
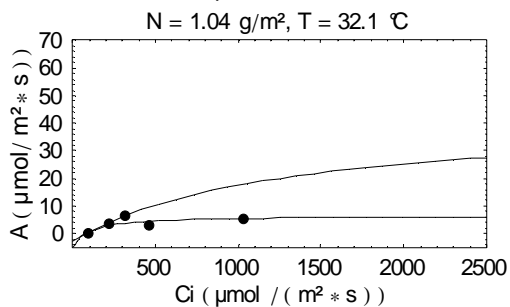
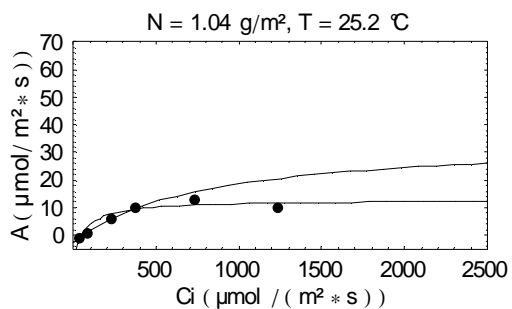
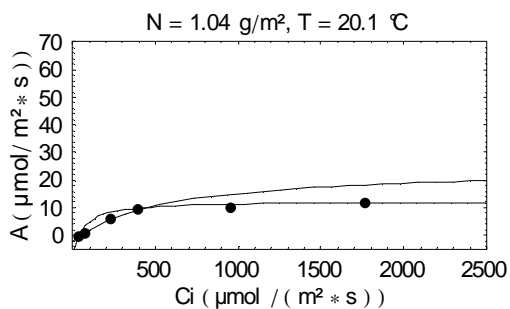
A/C_r-curves are sorted by nitrogen content of the measured leaves. Nitrogen per area and average leaf temperature during the measurement are indicated above each graph.

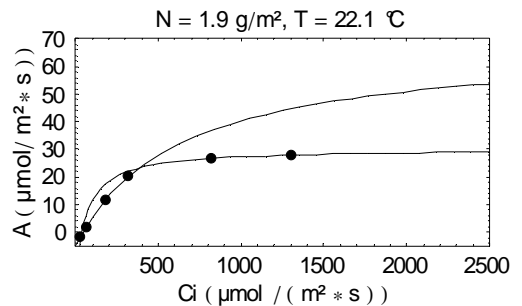
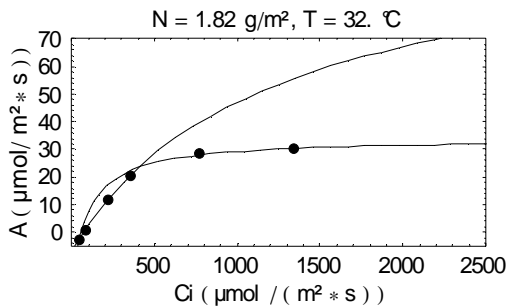
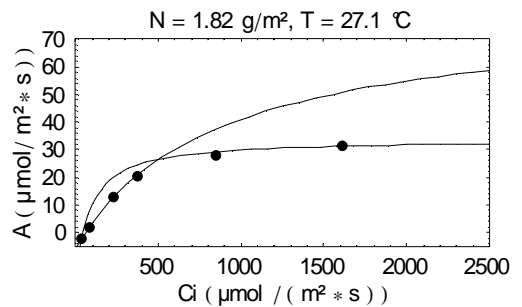
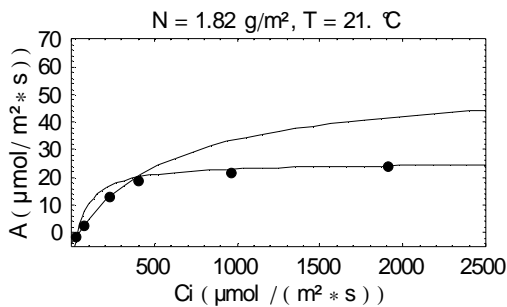
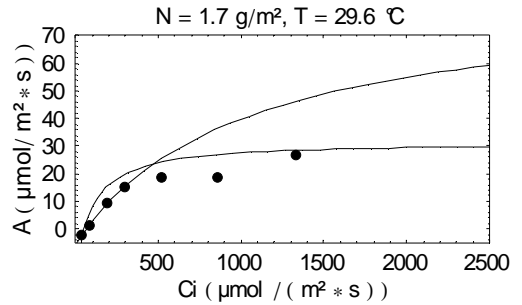
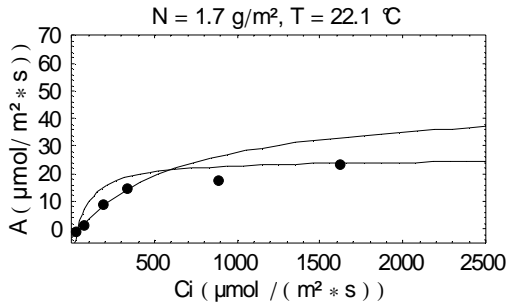
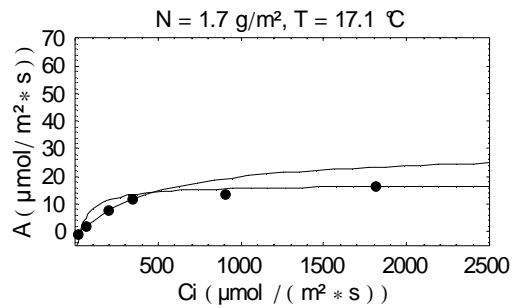
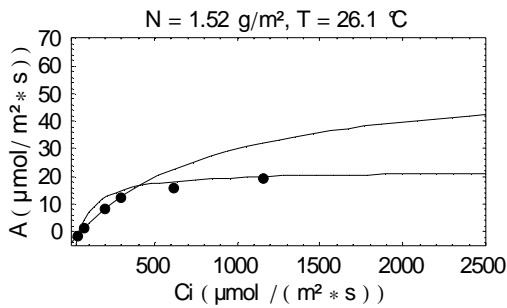
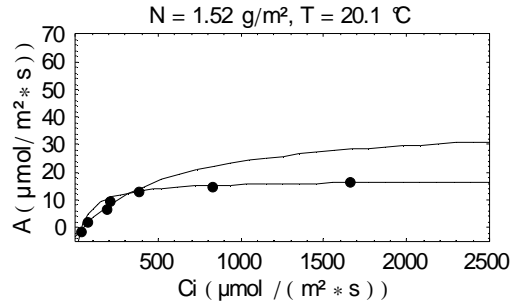
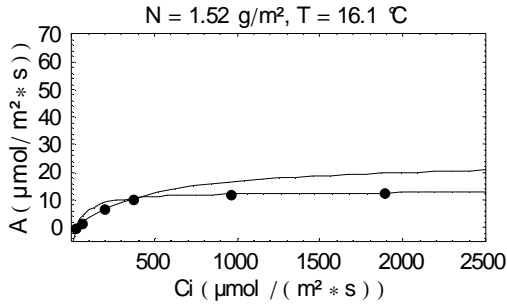
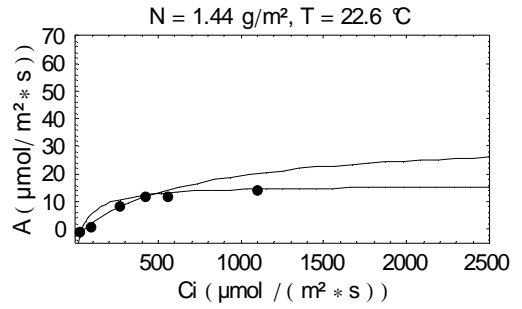
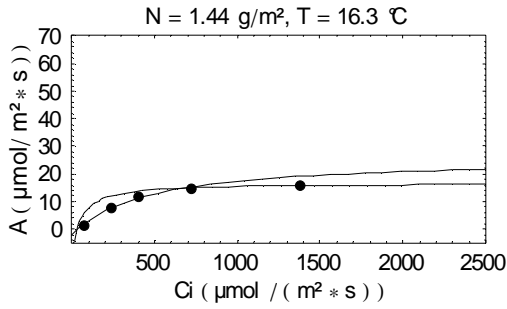
8.2.1 Leaves of beech Gr12

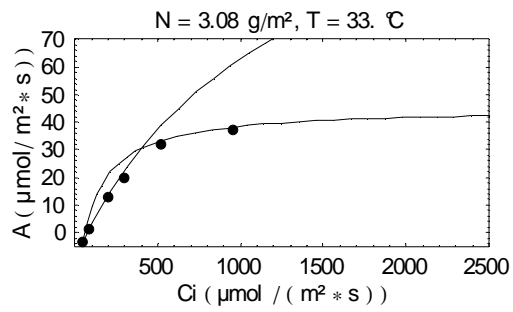




8.2.2 Leaves of oak Gr13







8.3 Figures

The following illustrations are side-products of the work with the optical representation routine of CRISTO and were included in the thesis because they may improve the imagination of structural traits of the investigated trees and the stand Großebene.

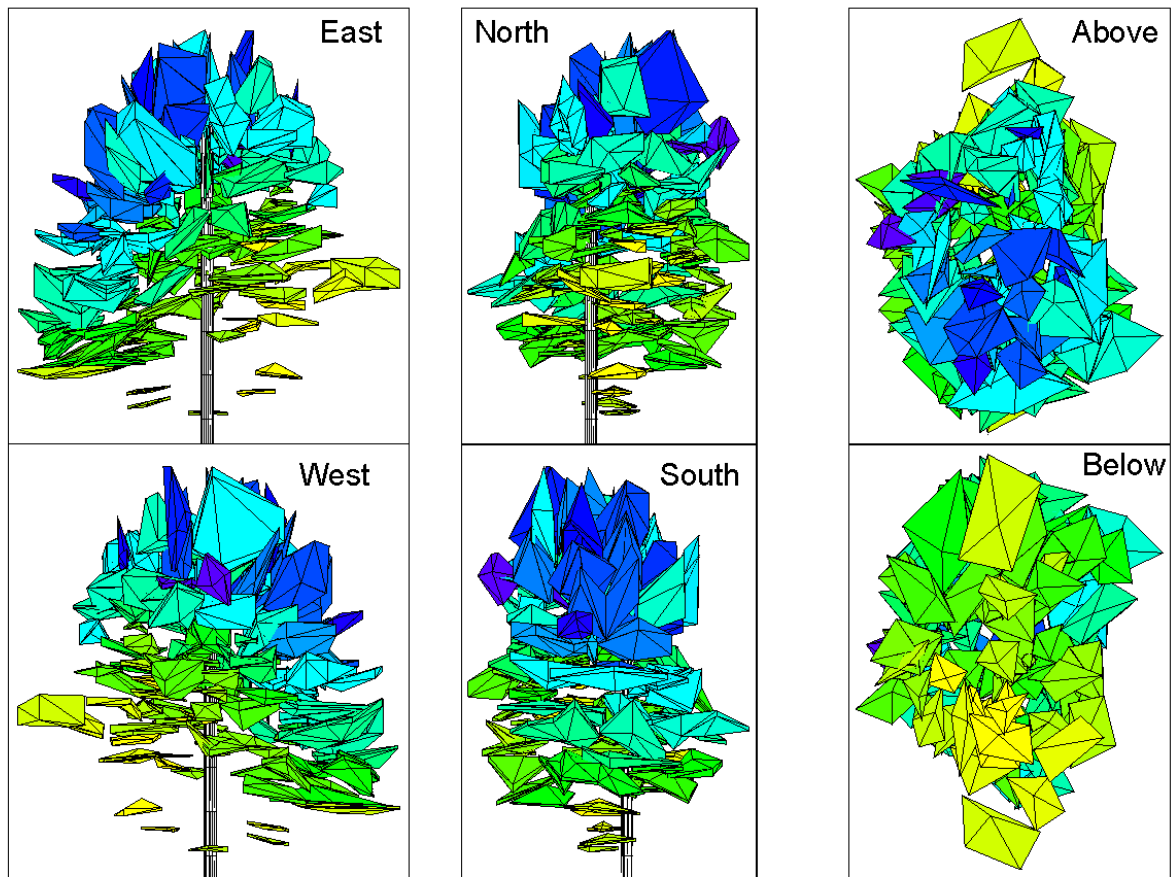


Fig. A1: View to the simulated crown of beech Bu38 from 6 view points. Different colours stand for different calculated average $V_{C_{max}}$ values as indicated in Fig. A2.

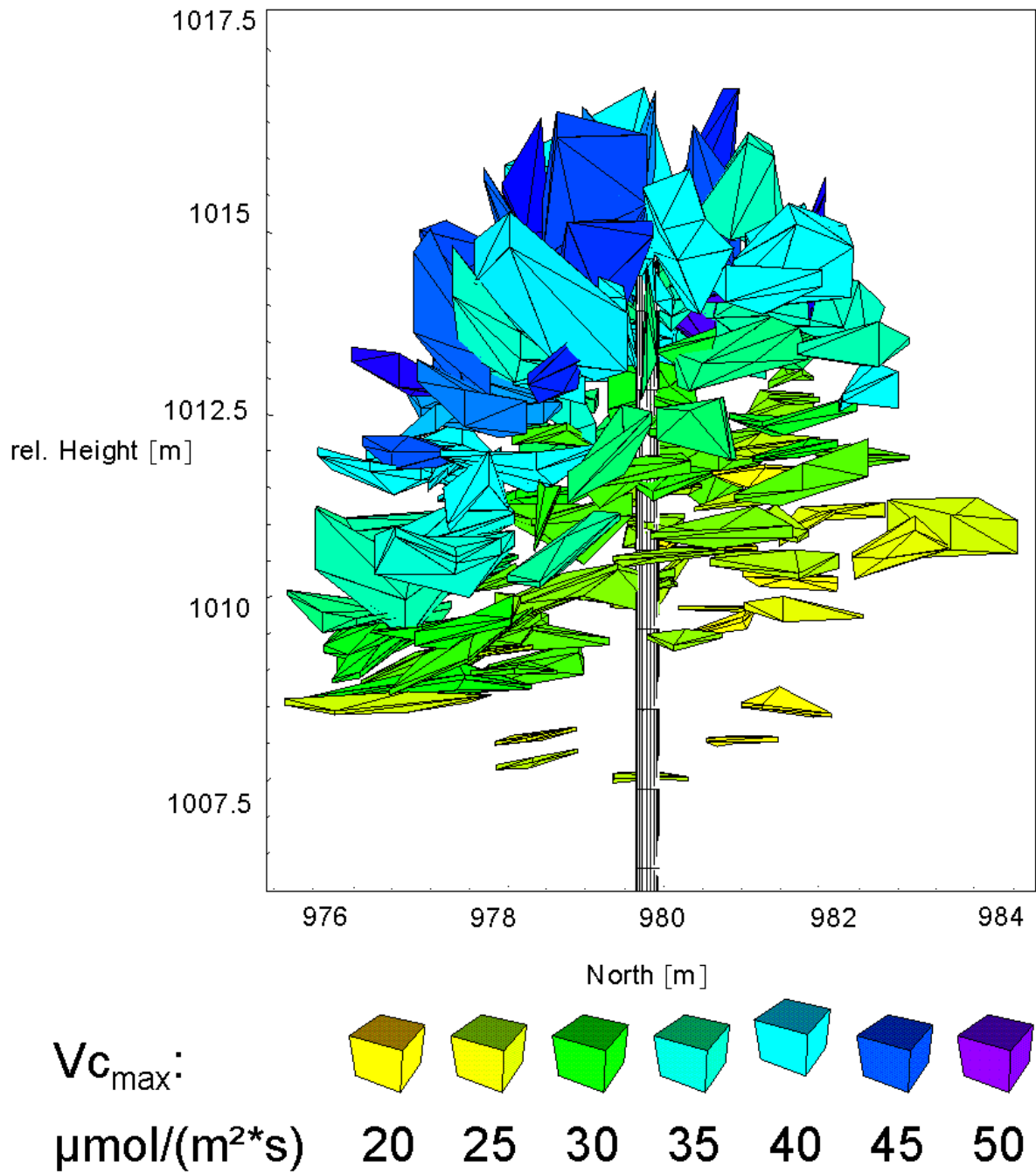
Fig. A2: Average $V_{c_{max}}$ of leaf clouds of beech Bu38

Fig. A3: Organisation of the stand Grossebene
View from above to the simulated stand Großebene

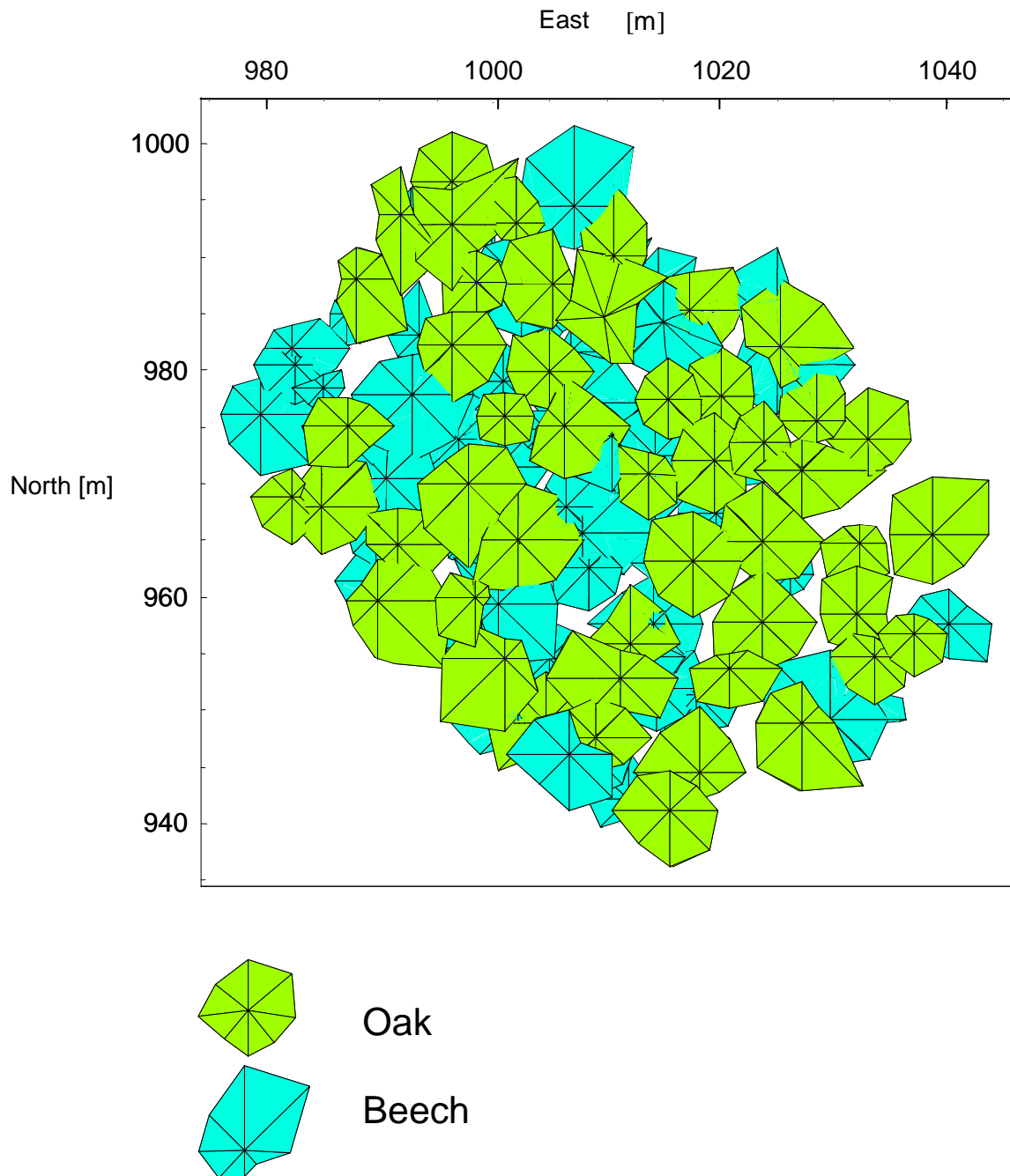


Fig. A4 Organisation of the stand Großebene
View towards below from 10m above the floor

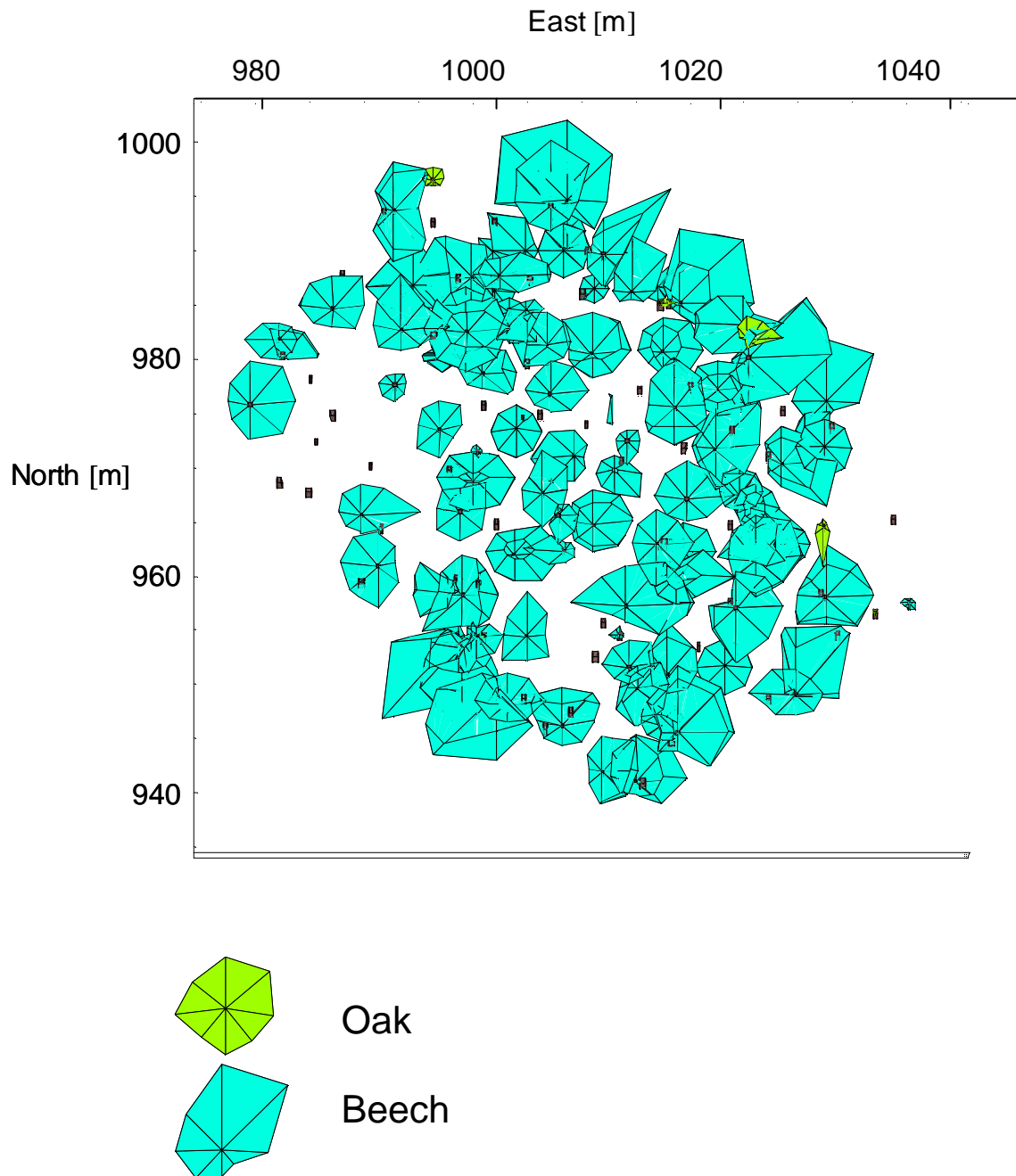


Fig. A5: Oak Gr13 (green and blue leaf clouds) and beech Gr12 (red leaf clouds) in the stand Grossebene. View from five different heights towards below

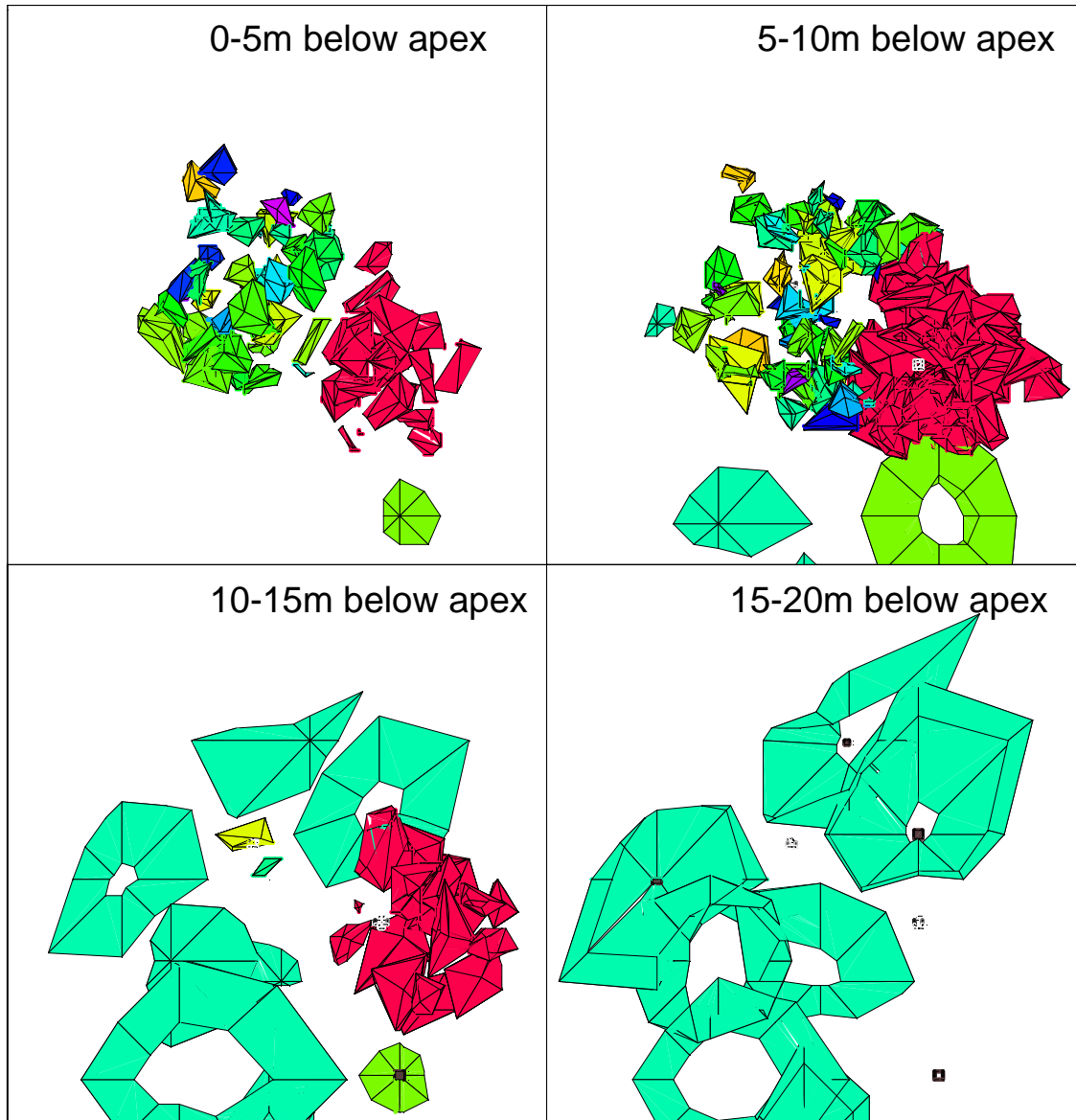


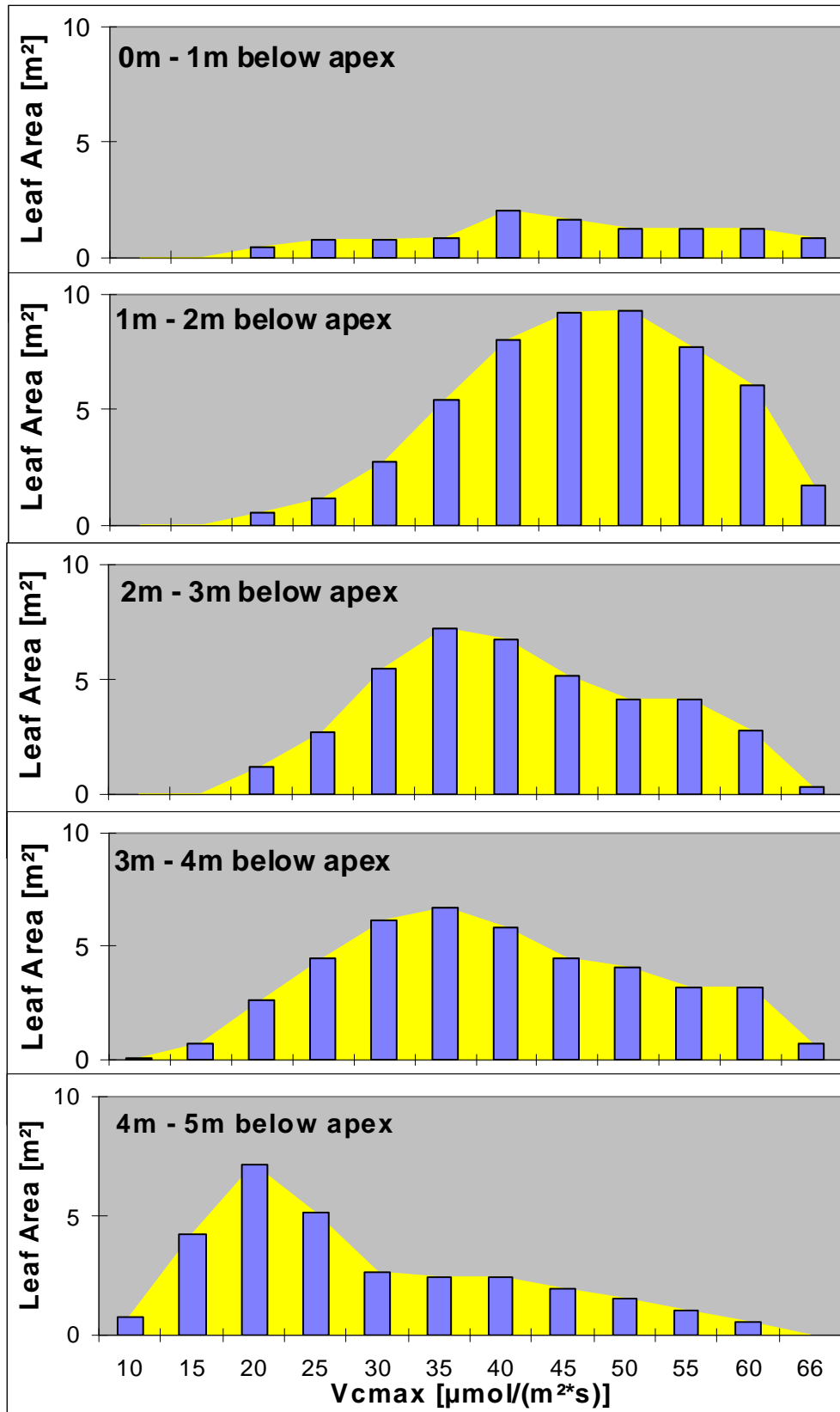
Fig. A6: $V_{c_{max}}$ frequency distributions in horizontal layers of beech Bu38

Fig. A7: $V_{c_{max}}$ frequency distributions in horizontal layers of beech Bu38 (shade crown)

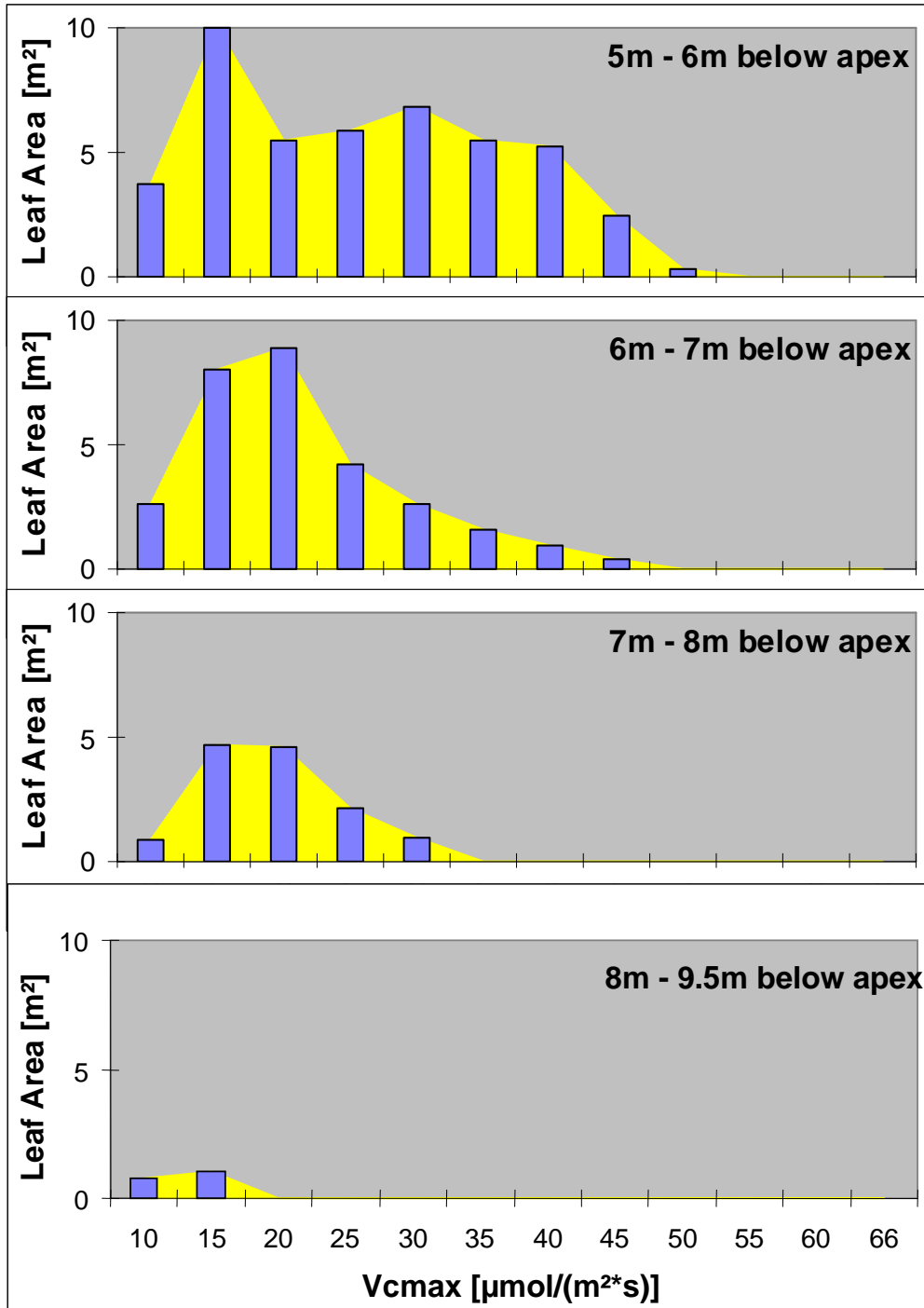
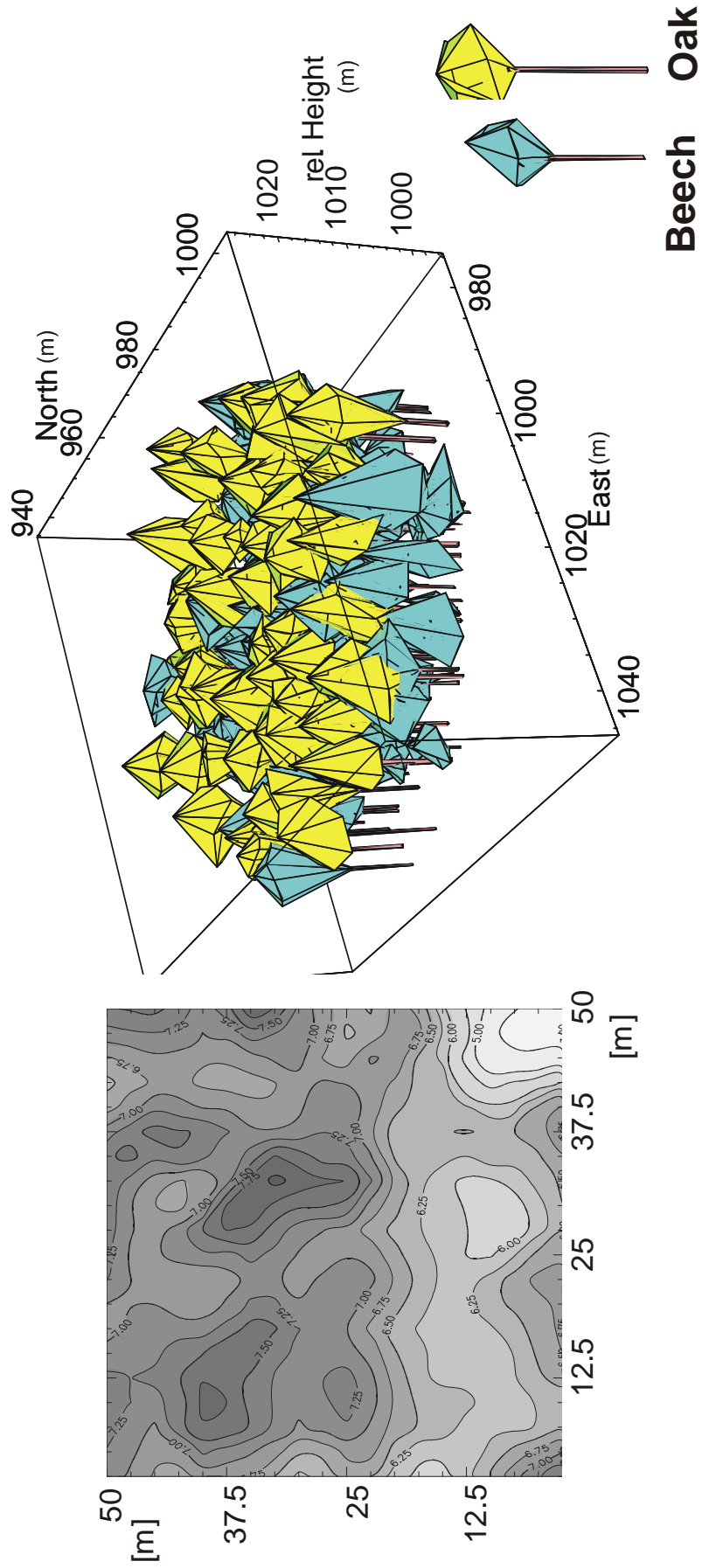


Fig. A8: Spatial distribution of plant area index and tree species in the stand Grosebene. The left picture was constructed from LAI-2000 measurements in July 1998 along a 5m * 5m grid on the floor of the stand Grosebene by interpolation between the grid points.



9 Literature

- Ali K, Nii N, Yamaguchi K, Nishimura M (1999) Levels of Nonstructural Carbohydrate in Leaves and Roots and Some Characteristics of Chloroplasts after Application of Different Amounts of Nitrogen Fertilizer to Peach Seedlings. *J Japan Soc Hort Sci* 68: 717-723
- Alsheimer M (1997) Charakterisierung räumlicher und zeitlicher Heterogenität der Transpiration unterschiedlicher montaner Fichtenbestände (*Picea abies* (L.) Karst.) durch Xylemflussmessungen. Ph.D. Dissertation, Universität Bayreuth.
- Anderson MC (1964) Studies of the woodland light climate. II. Seasonal variation in the light climate. *J Ecol* 52: 633-643
- Aphalo PJ, Ballaré CL, Scopel AL (1999) Plant-Plant signalling, the shade-avoidance response, and competition. *J Exp Bot* 50: 1629-1634
- Armond PA, Schreiber U, Björkman O (1978) Photosynthetic acclimation to temperature in the desert shrub, *Larrea divaricata*. II. Light harvesting efficiency and electron transport. *Plant Physiol* 61: 411-415
- Atkin OK, Westbeek MHK, Cambridge ML, Lambers H, Pons TL (1997) Leaf respiration in light and darkness. *Plant Physiol* 113: 961-965
- Atkin OK, Evans JR, Siebke K (1998) Relationship between the inhibition of leaf respiration by light and enhancement of leaf dark respiration following light treatment. *Aust J Plant Physiol* 25: 437-443
- Atkin OK, Evans JR, Ball MC, Lambers H, Pons TL (2000) Leaf Respiration of Snow Gum in the Light and Dark. Interactions between Temperature and Irradiance. *Plant Physiol* 122: 915-923
- Baldocchi D, Collineau S (1994) The physical nature of solar radiation in heterogeneous canopies: spatial and temporal attributes. In: Caldwell MM, Pearcy RW (eds) *Physiological ecology. A series of monographs, texts, and treatises: Exploitation of environmental heterogeneity by plants. Ecophysiological processes above- and belowground.* Academic Press, San Diego - New York - Boston - London - Sydney - Tokyo - Toronto
- Baldocchi DD, Harley PC (1995) Scaling carbon dioxide and water vapour exchange from leaf to canopy in a deciduous forest. II. Model testing and application. *Plant Cell Environ* 18: 1157-1173
- Ball JT, Woodrow IE, Berry JA (1987) A model predicting stomatal conductance and its contribution to the control of photosynthesis under different environmental conditions. In: Biggens J (ed) *Progress in photosynthesis research. Proc. VII Int. Photosynthesis congress, vol IV.* Martinus Nijhoff Publishers, Dordrecht
- Bamber RK, Fukazawa K (1985) Sapwood and heartwood: a review. *For Abstr* 46: 567-580
- Bartelink HH (1997) Allometric relationships for biomass and leaf area of beech (*Fagus sylvatica* L.). *Ann Sci For* 54: 39-50
- Battaglia LL, Sharitz RR, Minchin PR (1999) Patterns of seedling and overstory composition along a gradient of hurricane disturbance in an old-growth bottomland hardwood community. *Can J For Res* 29: 144-156
- Bauer G, Schulze E-D, Mund M (1997) Nutrient contents and concentrations in relation to growth of *Picea abies* and *Fagus sylvatica* along a European transect. *Tree Physiol* 17: 777-786
- Bayerischer Klimaforschungsverbund (1998): Klimakarte: Niederschläge 1961-1990. Bayerisches Landesamt für Wasserwirtschaft, München. Karten zur Wasserwirtschaft.
- Bens O (1999) Boden und Landschaft, Bd. 24: Grundwasser-Belastungspotentiale forstlich genutzter Sandböden in einem Wasserschutzgebiet bei Münster/Westfalen. Universität Giessen, Giessen
- Bernacchi CJ, Singsaas EL, Pimentel C, Portis jr AR, Long SP (2001) Improved temperature response functions for modelles of Rubisco-limited photosynthesis. *Plant Cell Environ* 24: 253-259
- Beyschlag W, Eckstein J (1997) Stomatal Patchiness. *Progress in Botany* 59: 283-298
- Beyschlag W, Pfanzen H, Ryel RJ (1992) Stomatal patchiness in Mediterranean evergreen sclerophylls. Phenomenology and consequences for the interpretation of the midday depression in photosynthesis and transpiration. *Planta* 187: 546-553
- Beyschlag W, Kresse F, Ryel RJ, Pfanzen H (1994) Stomatal patchiness in conifers: experiments with *Picea abies* (L.) Karst. and *Abies alba* Mill. *Trees* 8: 132-138
- BML (1997) Dauerbeobachtungsflächen zur Umweltkontrolle im Wald Level II, Erste Ergebnisse, Bundesministerium für Ernährung, Landwirtschaft und Forsten (BML), Bonn.

- BML (1998) Unser Wald - Natur und Wirtschaftsfaktor zugleich. Bundesministerium für Ernährung, Landwirtschaft und Forsten, Bonn
- Bohn U, Neuhäusl R (1999): Map of the natural vegetation of Europe, scale 1:2.5 million (reduced and generalized excerpt of the digital version). Bundesamt für Naturschutz. Germany.
- Bork HR, Dalchow C, Faust B, Piorr HP, Tousaint V, Werner A (2000) Future development of landscapes in marginal agrarian regions of Central Europe: Long-term effects of land use on the water balance. In: Tenhunen JD, Lenz R, Hantschel R (eds) Ecosystem approaches to landscape management in Central Europe. Springer, Berlin
- Bowes G (1993) Facing the inevitable: plants and increasing atmospheric CO₂. Ann Rev Plant Physiol Plant Mol Biol 44: 309-332
- Box GEP, Cox DR (1964) An Analysis of transformations. Journal of the royal statistical society B26: 211-252
- Brechtel HM (1989) Stoffeinträge in Waldökosysteme - Niederschlagsdeposition im Freiland und in Waldbeständen. DVWK 17: 27-52
- Bronstein IN, Semendjajew KA, Musiol G, Mühlig H (1995) Taschenbuch der Mathematik. Verlag Harri Deutsch, Frankfurt a. Main
- Brooks A, Farquhar GD (1985) Effects of temperature on the CO₂/O₂ specificity of ribulose-1,5-bisphosphate carboxylase/oxygenase and the rate of respiration in the light. Estimates from gas-exchange measurements on spinach. Planta 165: 397-406
- Brown K, Higginbotham KO (1986) Effects of carbon dioxide enrichment and nitrogen supply on growth of boreal tree seedlings. Tree Physiol 2: 223-232
- Buck-Sorlin GH, Bell AD (1998) A quantification of shoot shedding in pedunculate oak (*Quercus robur* L.). Bot J Linn Soc 127: 371-391
- Burger H (1945) Holz, Blattmenge und Zuwachs - Die Buche. Mitt Schweiz Anst Forstl Versuchswes 26: 419-468
- Burger H (1947) Die Eiche. Mitteilungen der schweizerischen Anstalt für das forstliche Versuchswesen 25: 211-279
- Burkhardt HE, Tham A (1992) Predictions from growth and yield models of the performance of mixed-species stands. In: Cannell MGR, Malcolm DC, Robertson PA (eds) The ecology of mixed-species stands of trees. Blackwell Scientific Publications, London
- Burschel P, Kürsten E, Larson BC (1993) Forstliche Forschungsberichte München, 126: Die Rolle von Wald und Forstwirtschaft im Kohlenstoffhaushalt - Eine Betrachtung für die Bundesrepublik Deutschland. Universität München, München
- Butin H (1983) Krankheiten der Wald- und Parkbäume. Thieme Verlag, Stuttgart
- Campbell GS (1986) Extinction coefficients for radiation in plant canopies calculated using an ellipsoidal inclination angle distribution. Agric For Meteorol 36: 317-321
- Campbell GS, Norman JM (1989) The description and measurement of plant canopy structure. In: Russell G, Marshall B, Jarvis PG (eds) Society for experimental biology seminar series, 31: Plant canopies: their growth, form and function. Cambridge University Press, Cambridge - New York - New Rochelle - Melbourne - Sydney
- Canham CD, Coates KD, Bartemucci P, Quaglia S (1999) Measurement and modeling of spatially explicit variation in light transmission through interior cedar-hemlock forests of British Columbia. Can J For Res 29: 1775-1783
- Cermak J, Cienciala E, Kucera J, Hällgren JE (1992) Radial velocity profiles of water flow in trunks of Norway spruce and oak and the response of spruce to severing. Tree Physiol 10: 367-380
- Cescatti A (1997) Modelling the radiative transfer in discontinuous canopies of asymmetric crowns I. model structure and algorithms. Ecol Modelling 101: 263-274
- Cescatti A (1998) Effects of needle clumping in shoots and crowns on the radiative regime of a Norway spruce canopy. Ann Sci For 55: 89-102
- Chang S-C (1999) The effect of stemflow on element fluxes and soil nitrogen transformations in a mixed beech oak stand in the Steigerwald, Germany. Ph.D. Dissertation, University of Bayreuth.

- Cheeseman JM (1991) PATCHY: Simulating and visualizing the effects of stomatal patchiness on photosynthetic CO₂ exchange studies. *Plant Cell Environ* 14: 593-599
- Chelle M, Andrieu B (1999) Radiative models for architectural modeling. *Agronomie* 19: 225-240
- Chen SG, Ceulemans R, Impens I (1994) A fractal-based *Populus* canopy structure model for the calculation of light interception. *For Ecol Manage* 69: 97-110
- Cobb DF, O'Hara KL, Oliver CD (1993) Effects of variations in stand structure on development of mixed-species stands in eastern Washington. *Can J For Res* 23: 545-553
- Collet C, Colin F, Bernier F (1997) Height growth, shoot elongation and branch development of young *Quercus petraea* grown under different levels of resource availability. *Ann Sci For* 54: 65-81
- Cumming SG, Burton PJ, Prahacs S, Garland MR (1994) Potential conflicts between timber supply and habitat protection in the boreal mixedwood of Alberta, Canada: a simulation study. *For Ecol Manage* 68: 281-302
- Davidson SR, Ashmore MR, Garretty C (1992) Effects of ozone and water deficit on the growth and physiology of *Fagus sylvatica*. *For Ecol Manage* 51: 187-193
- Day FP, Monk CD (1977) Seasonal nutrient dynamics in the vegetation on a Southern Appalachian watershed. *Amer J Bot* 64: 1126-1139
- DeJong TM, Doyle JF (1985) Seasonal relationships between leaf nitrogen content (photosynthetic capacity) and leaf canopy light exposure in peach (*Prunus persica*). *Plant Cell Environ* 8: 701-706
- Deleuze C, Hervé JC, Colin F, Ribeyrolles L (1996) Modelling crown shape of *Picea abies*: spacing effects. *Can J For Res* 26: 1957-1966
- Dobrowolska D (1998) Structure of silver fir (*Abies alba* Mill.) natural regeneration in the Jata reserve in Poland. *For Ecol Manage* 110: 237-247
- Dreyer E, Le Roux X, Montpied P, Daudet FA, Masson F (2001) Temperature response of leaf photosynthetic capacity in seedlings from seven temperate tree species. *Tree Physiol* 21: 223-232
- Ducrey M (1981) Etude bioclimatique d'une futaie feuillue (*Fagus sylvatica* L. et *Quercus sessiliflora* Salisb.) de l'est de la France III. - Potentialités photosynthétiques des feuilles à différentes hauteurs dans le peuplement *Ann Sci For* 38 (1): 71-86
- Düster H (1994) Geographica Bernensia, G44: Modellierung der räumlichen Variabilität seltener Hochwasser in der Schweiz. Arbeitsgemeinschaft Geographica Bernensia, Bern
- Duncan WG, Loomis RS, Williams WA, Hanau R (1967) A model for simulating photosynthesis in plant communities. *Hilgardia* 38: 181-205
- Eckstein J (1997) Heterogene Kohlenstoffassimilation in Blättern höherer Pflanzen als Folge der Variabilität stomatärer Öffnungsweiten. Charakterisierung und Kausalanalyse des Phänomens "stomatal patchiness". Ph.D. Dissertation, Universität Würzburg.
- Egli P, Maurer S, Günthard-Georg MS, Körner C (1998) Effects of elevated CO₂ and soil quality on leaf gas exchange and above-ground growth in beech-spruce model ecosystems. *New Phytol* 140: 185-196
- Ehleringer J, Björkman O (1977) Quantum yields for CO₂ uptake in C₃ and C₄ plants. Dependence on temperature, CO₂ and O₂ concentration. *Plant Physiol* 59: 86-90
- El Kohen A, Venet L, Mousseau M (1993) Growth and photosynthesis of two deciduous forest species at elevated carbon dioxide. *Funct Ecol* 7: 480-486
- Ellenberg H (1996) *Vegetation Mitteleuropas mit den Alpen*. Ulmer, Stuttgart
- Ellenberg H, Mayer, Schauer mann (1986) *Ökosystemforschung - Ergebnisse des Sollingprojekts, 1966-1986*. Ulmer, Stuttgart
- Eller BN, Glättli R, Flach B (1981) Optische Eigenschaften und Pigmente von Sonnen- und Schattenblättern der Rotbuche (*Fagus sylvatica* L.) und der Blutbuche (*Fagus sylvatica* cv. *Atropunicea*). *Flora* 171: 170-185
- Ellsworth DS, Reich PB (1993) Canopy structure and vertical patterns of photosynthesis and related leaf traits in a deciduous forest. *Oecol* 96: 169-178

- Emmert U (1985): Geologische Karte von Bayern, 1:25000, Blatt 6128, Ebrach. Bayerisches Geologisches Landesamt. München.
- Epron D, Dreyer E (1990) Stomatal and nonstomatal limitation of photosynthesis by leaf water deficits in three oak species: A comparison of gas exchange and chlorophyll a fluorescence. *Ann Sci For* 47: 435-450
- Epron D, Dreyer E (1993) Photosynthesis of oak leaves under water stress: maintenance of high photochemical efficiency of photosystem II and occurrence of non-uniform CO₂ assimilation. *Tree Physiol* 13: 107-117
- Epron D, Godard D, Cornic G, Genty B (1995) Limitation of net CO₂ assimilation rate by internal resistances to CO₂ transfer in the leaves of two tree species (*Fagus sylvatica* L. and *Castanea sativa* Mill.). *Plant Cell Environ* 18: 43-51
- Evans GC, Coombe DE (1959) Hemispherical and woodland canopy photography and the light climate. *J Ecol* 47: 103-113
- Evans JR (1989) Photosynthesis and nitrogen relationships in leaves of C₃ plants. *Oecol* 78: 9-19
- Falge E (1997) Die Modellierung der Kronendachtranspiration von Fichtenbeständen (*Picea abies* (L.) Karst.). Ph.D. Dissertation, BITÖK, Universität Bayreuth.
- Falge E, Graber W, Siegwolf R, Tenhunen JD (1996) A model of the gas exchange response of *Picea abies* to habitat conditions. *Trees* 10: 277-287
- Falge E, Tenhunen JD, Ryel R, Alsheimer M, Köstner B (2001) Modelling age- and density-related gas exchange of *Picea abies* canopies in the Fichtelgebirge, Germany. *Ann For Sci* 57: in press
- Faltin W (2001) Scaling up water and CO₂ fluxes of forested areas from stand to footprint level by means of an individual-based 3D model. Ph.D. Dissertation, University of Bayreuth, Bayreuth.
- Farquhar GD (1978) Feedforward responses of stomata to humidity. *Aust J Plant Physiol* 5: 787-800
- Farquhar GD, von Caemmerer S (1982) Modeling of photosynthetic response to environmental conditions. In: Lange OL, Nobel PS, Osmond CB, Ziegler H (eds) *Encyclopedia of plant physiology*, 12B: Physiological Plant Ecology, vol II. Springer-Verlag, Berlin
- Field CB (1991) Ecological scaling of carbon gain to stress and resource availability. In: Mooney HA, Winner WE, Pell EJ (eds) *Physiological ecology. A series of monographs, texts, and treatises: Response of plants to multiple stresses*. Academic Press, Inc., San Diego - New York - Boston - London - Sydney - Tokyo - Toronto
- Fleck S, Subke JA, Faltin W (2001) Entwicklung eines 3D-Mischbestandesmodelles des N-abhängigen CO₂- und Wasseraustausches von Buchenmischbeständen in Nordbayern. In: Gollan T, Gerstberger P (eds) *Bayreuther Forum Ökologie*, 84: BITÖK Forschungsbericht 2000. Bayreuther Institut für terrestrische Ökosystemforschung, Bayreuth
- Forstamt Ebrach (2000) Revierbuch des Forstamts Ebrach.,
- Forstamt Weissenstadt (1989): Standortskarte für das Forstamt Weissenstadt. Forstamt Weissenstadt. Standortskarten.
- Garcia S, Finch DM, Chavez Leon G (1998) Patterns of forest use and endemism in resident bird communities of north-central Michoacan, Mexico. *For Ecol Manage* 110: 151-171
- Gartner BL (1995) Patterns of xylem variation within a tree and their hydraulic and mechanical consequences. In: Gartner BL (ed) *Plant Stems: physiology and functional morphology*. Academic Press, San Diego
- Gates DM (1980) *Biophysical ecology*. Springer-Verlag, Berlin - Heidelberg - New York
- Gees A (1997) *Geographica Bernensia*, G53: Analyse historischer und seltener Hochwasser in der Schweiz - Bedeutung für das Bemessungshochwasser. Arbeitsgemeinschaft Geographica Bernensia, Bern
- Genty B, Briantais J-M, Baker NR (1989) The relationship between the quantum yield of photosynthetic electron transport and quenching of chlorophyll fluorescence. *Biochim Biophys Acta* 990: 87-92
- Gerstberger P (1997) The research sites of BITÖK. In: Gollan T, Gerstberger P (eds) *Bayreuther Forum Ökologie: BITÖK Forschungsbericht 1996*. Universität Bayreuth, Bayreuth
- Gezelius K (1975) Extraction and some characteristics of Ribulose-1,5-diphosphate. *PH* 9: 192-200
- Ghashghaie J, Cornic G (1994) Effect of temperature on partitioning of photosynthetic electron flow between CO₂ assimilation and O₂ reduction and on the CO₂/O₂ specificity of RubisCo. *J Plant Physiol* 143: 643-650

- Gilbert IR, Seavers GP, Jarvis PG, Smith H (1995) Photomorphogenesis and canopy dynamics. Phytochrome-mediated proximity perception accounts for the growth dynamics of canopies of *Populus trichocarpa* x *deltoides* 'Beaupré'. *Plant Cell Environ* 18: 475-497
- Givnish TJ (1995) Plant Stems: Biomechanical adaptation for energy capture and influence on species distributions. In: Gartner BL (ed) *Plant stems: Physiology and functional morphology*. Academic Press, San Diego
- Gond V, de Pury DGG, Veroustraete F, Ceulemans R (1999) Seasonal variation in leaf area index, leaf chlorophyll, and water content; scaling-up to estimate fAPAR and carbon balance in a multilayer, multispecies temperate forest. *Tree Physiol* 19: 673-679
- Grams TEE, Anegg S, Haeberle KH, Langebartels C, Matyssek R (1999) Interactions of chronic exposure to CO₂ and O₃ levels in the photosynthetic light and dark reactions of European beech (*Fagus sylvatica*). *New Phytol* 144: 95-107
- Granier A (1985) Une nouvelle methode pour la mesure du flux de seve brute dans le tronc des arbres. *Ann Sci For* 42: 193-200
- Granier A (1987) Evaluation of transpiration in a Douglas-fir stand by means of sap flow measurements. *Tree Physiol* 3: 309-320
- Granier A, Anfodillo T, Sabatti M, Cochard H, Dreyer E, Tomasi M, Valentini R, Breda N (1994) Axial and radial water flow in the trunks of oak trees: a quantitative and qualitative analysis. *Tree Physiol* 14: 1383-1396
- Granier A, Biron P, Lemoine D (2000a) Water balance, transpiration and canopy conductance in two beech stands. *Agric For Meteorol* 100: 291-308
- Granier A, Loustau D, Breda N (2000b) A generic model of forest canopy conductance dependent on climate, soil water availability and leaf area index. *Ann For Sci* 57: 755-765
- Gratani L, Fida C, Fiorentino E (1987) Ecophysiological features in leaves of a beech ecosystem during the growing period. *Bull soc R bot belg* 120: 81-88
- Grier CC, Waring RH (1974) Conifer foliage mass related to sapwood area. *For Sci* 20: 205-206
- Groninger JW, Zedaker SM, Barnes AD, Feret PP (2000) Pitch X loblolly pine hybrid response to competition control and associated ice damage. *For Ecol Manage* 127: 87-92
- Hättenschwiler S, Körner C (1998) Biomass allocation and canopy development in spruce model ecosystems under elevated CO₂ and increased N deposition. *Oecologia* 113: 104-114
- Hättenschwiler S, Miglietta F, Raschi A, Körner C (1997) Morphological adjustments of mature *Quercus ilex* trees to elevated CO₂. *Acta Oecol* 18: 361-365
- Häusler RE, Bailey KJ, Lea PJ, Leegood RC (1996) Control of photosynthesis in barley mutants with reduced activities of glutamine synthetase and glutamate synthase. *Planta* 200: 388-396
- Häusler RE, Kleines M, Uhrig H, Hirsch HJ, Smets H (1999) Overexpression of phosphoenolpyruvate carboxylase from *Corynebacterium glutamicum* lowers the CO₂ compensation point (Gamma*) and enhances dark and light respiration in transgenic potatoe. *J Exp Bot* 50: 1231-1242
- Hagemeyer M (1997) *Kronenstruktur und Schattenwurf verschiedener Pionier-und Schlusswald-Baumarten*. Dissertation, Universität Göttingen.
- Hallé F, Oldeman RAA, Tomlinson PB (1978) *Tropical trees and forests: an architectural analysis*. Springer-Verlag, Berlin
- Harley PC, Tenhunen JD (1991) Modeling the photosynthetic response of C₃ leaves to environmental factors. In: Boote KJ (ed) *CSSA Special Publication, No. 19.: Modeling crop photosynthesis - from biochemistry to canopy*. American Society of Agronomy and Crop Science Society of America, Madison
- Harley PC, Thomas RB, Reynolds JF, Strain BR (1992) Modelling photosynthesis of cotton in elevated CO₂. *Plant Cell Environ* 15: 271-282
- Hauhs M, Lange H, Kastner-Maresch A (2001) Complexity and simplicity in ecosystems: The case of forest management. *International Journal of Complex Systems* submitted
- Herppich WB, Herppich M, Tüffers A, von Willert DJ, Midgley GF, Veste M (1998) Photosynthetic responses to CO₂ concentration and photon fluence rates in the CAM-cycling plant *Delosperma tradescantioides*. *New Phytol* 138: 433-440

- Hertel D, Leuschner C (1998) Die Rhizosphäre in einem Eichen-Buchenmischwald: Feinwurzelproduktion und die Bedeutung der Wurzelkonkurrenz. *Verh d Gesell f Ökol (Bremen)* 28: 441-447
- Hikosaka K (1996) Effects of leaf age, nitrogen nutrition and photon flux density on the organization of the photosynthetic apparatus in leaves of a vine (*Ipomoea tricolor* Cav.) grown horizontally to avoid mutual shading of leaves. *Planta* 198: 144-150
- Hillis WE (1987) Heartwood and tree exudates. Springer, Berlin
- Hirose T, Werger WJA (1987) Nitrogen Use Efficiency in instantaneous and daily photosynthesis of leaves in the canopy of a *Solidago altissima* stand. *Physiol Plant* 70: 215-222
- Hirota O, Nakano Y (2000) Modeling of a soybean canopy structure by the approximation of a leaflet into an ellipsoid for estimating direct solar radiation. *Plant Production Science* 3: 67-74
- HMU (2001) Waldökosystemstudie Hessen: Waldzustandsbericht 2000. Hessisches Ministerium für Umwelt, Landwirtschaft und Forsten
- Holbrook NM (1995) Stem water storage. In: Gartner BL (ed) *Plant Stems: physiology and functional morphology*. Academic Press, San Diego
- Idso KE, Idso SB (1994) Plant responses to atmospheric CO₂ enrichment in the face of environmental constraints: a review of the past 10 years' research. *Agric For Meteorol* 69: 153-203
- Jacob J, Lawlor DW (1993) Extreme phosphate deficiency decreases the in vivo CO₂/O₂ specificity factor of Ribulose-1,5-Bisphosphate Carboxylase-Oxygenase in intact leaves of sunflower. *J Exp Bot* 44: 1635-1641
- Janssen PH, Heuberger PS (1995) Calibration of process-oriented models. *Ecol Modelling* 83: 55-66
- Jarvis PG (1995) The role of temperate trees and forests in CO₂ fixation. *Vegetatio* 121: 157-174
- Jayasekera R, Schleser GH (1988) Seasonal changes in potential net photosynthesis of sun and shade leaves of *Fagus sylvatica*. *J Plant Physiol* 133: 216-221
- Johansson T (1985) Estimating canopy density by the vertical tube method. *For Ecol Manage* 20: 139-144
- Johnson FH, Eyring H, Williams RW (1942) The nature of enzyme inhibitions in bacterial luminescence: sulfanilamide, urethane, temperature, and pressure. *J Cell Comp Physiol* 20: 247-268
- Jones HG (1992) *Plants and microclimate*. Cambridge University press, Cambridge
- Jose S, Gillespie AR (1997) Leaf area-productivity relationships among mixed-species hardwood forest communities of the central hardwood region. *For Sci* 43(1): 56-64
- Kakubari Y (1987) Analysis of dry matter production with an eco-physiological computer simulation model. In: Fujimori T, Kimura M (eds) *Human impacts and management of mountain forests*. Forestry and Forest Products Research Institute, Ibaraki, Japan
- Karlson P (1994) *Kurzes Lehrbuch der Biochemie für Mediziner und Naturwissenschaftler*. Thieme, Stuttgart
- Kaufmann MR, Troendle CA (1981) The relationship of leaf area and foliage biomass to sapwood conducting area in four subalpine forest tree species. *For Sci* 27: 477-482
- Kauppi PE, Mielikäinen K, Kuusela K (1992) Biomass and carbon budget of European forests, 1971 to 1990. *Science* 256: 70-74
- Kazda M, Salzer J, Reiter I (2000) Photosynthetic capacity in relation to nitrogen in the canopy of a *Quercus robur*, *Fraxinus angustifolia* and *Tilia cordata* flood plain forest. *Tree Physiol* 20: 1029-1037
- Keeling CD, Whorf TP (2000), Atmospheric CO₂ concentrations (ppmv) derived from in situ air samples collected at Mauna Loa Observatory, Hawaii Scripps Institution of Oceanography (SIO), University of California, La Jolla
- Kellogg EA, Juliano ND (1997) The structure and function of RuBisCO and their implications for systematic studies. *Amer J Bot* 84: 413-428
- Kelty MJ (1992) Comparative productivity of monocultures and mixed-species stands. In: Kelty MJ, Larson BC, Oliver CD (eds) *The ecology and silviculture of mixed-species forests*. Kluwer Academic Publishers, Dordrecht, Boston, London

- Kenk GK (1992) Silviculture of mixed-species stands in Germany. In: Cannell MGR, Malcolm DC, Robertson PA (eds) The ecology of mixed-species stands of trees. Blackwell, London
- Kikuzawa K, Koyama H, Umeki K, Lechowicz MJ (1996) Some evidence for an adaptive linkage between leaf phenology and shoot architecture in sapling trees. *Funct Ecol* 10: 252-257
- Klein I, De Jong TM, Weinbaum SA, Muraoka TT (1991) Specific Leaf Weight and Nitrogen Allocation Responses to Light Exposure within Walnut Trees. *HortSci* 26: 183-185
- Kloppel BD, Abrams MD, Kubiske ME (1993) Seasonal ecophysiology and leaf morphology of 4 successional Pennsylvania barrens species in open versus understory environments. *Can J For Res* 23: 181-189
- Knyazikhin Y, Miessen G, Panfyorov O, Gravenhorst G (1997) Small-scale study of three-dimensional distribution of photosynthetically active radiation in a forest. *Agric For Meteorol* 88: 215-239
- Koch B, Reidelstürz P (1998) Terrestrische Stereophotogrammetrie für forstliche Anwendungen. *Allgemeine Forst Zeitschrift* 24: 1464-1467
- Köstner B, Granier A, Cermak J (1998) Sapflow measurements in forest stands - methods and uncertainties. *Ann Sci For* 55: 13-27
- Küppers M (1994) Canopy gaps: competitive light interception and economic space filling - a matter of whole-plant allocation. In: Exploitation of environmental heterogeneity by plants. Ecophysiological processes above- and belowground. (Eds: Caldwell, Martyn M; Pearcy, Robert W) (Series Ed: Mooney, Harold A. Physiological ecology. A series of monographs, texts, and treatises) Academic Press, San Diego - New York - Boston - London - Sydney - Tokyo - Toronto: 111-144
- Küppers M, Küppers BIL, Godkin C (1993) Kohlenstoff-Akquisition und Wachstumsstrategien zweier konkurrierender *Eucalyptus*-Arten auf einem hochmontanen Standort in Australien. In: Pfadenhauer J (ed) Verhandlungen der Gesellschaft für Ökologie, vol 22. Gesellschaft für Ökologie, Freising-Weißenstephan
- Küppers M, Heiland I, Schneider H, Neugebauer PJ (1999) Light-flecks cause non-uniform stomatal opening - studies with special emphasis on *Fagus sylvatica* L. *Trees* 14: 130-144
- Kull O, Niinemets Ü (1993) Variation in leaf morphometry and nitrogen concentration in *Betula pendula* Roth., *Corylus avellana* L. and *Lonicera xylosteum* L. *Tree Physiol* 12: 311-318
- Kull O, Broadmeadow M, Kruijt B, Meir P (1999) Light distribution and foliage structure in an oak canopy. *Trees* 14: 55-64
- Kurth W (1994) Berichte des Forschungszentrums Waldökosysteme Göttingen, B38: Growth Grammar interpreter GROGRA 2.4 - A software tool for the 3-dimensional interpretation of stochastic, sensitive growth grammars in the context of plant modelling. Introduction and reference manual. Universität Göttingen,
- Kurth W (1998) Some new formalisms for modelling the interactions between plant architecture, competition and carbon allocation. In: Kastner-Maresch A, Kurth W, Sonntag M, Breckling B (eds) Bayreuther Forum Ökologie, Bd. 52: Individual-based structural and functional models in ecology. Bayreuther Institut für Terrestrische Ökosystemforschung, Bayreuth
- Kurth W, Sloboda B (1999) Tree and stand architecture and growth described by formal grammars - I. Non-sensitive trees. *Science* 45: 16-30
- Kuuluvainen T (1992) Tree architectures adapted to efficient light utilization - is there a basis for latitudinal gradients? *Oikos* 65: 275-284
- Laik A (1977) Kinetika fotosinteza i fotodihaniya C₃-rastenii. (Kinetics of photosynthesis and photorespiration in C₃-plants). Nauka, Moscow (In Russian)
- Laik A, Loreto F (1996) Determining photosynthetic parameters from leaf CO₂ exchange and chlorophyll fluorescence. *Plant Physiol* 110: 903-912
- Lange H (1999) Are ecosystems dynamical systems? *Int J of computing anticipatory systems* 3: 169-186
- Larsen DR, Kershaw JA (1996) Influence of canopy structure assumptions on prediction from Beer's law: A comparison of deterministic and stochastic simulations. *Agric For Meteorol* 81: 61-77
- Larson BC (1992) Pathways of development in a mixed-species stand. In: Kelty MJ, Larson BC, Oliver CD (eds) the ecology and silviculture of mixed-species forests. Kluwer Academic Publishers, Dordrecht, Boston, London

- Lauri PE, Terouanne E (1998) The influence of shoot growth on the pattern of axillary development on the long shoots of young apple trees (*Malus domestica* Borkh.). *Int J Plant Sci* 159: 283-296
- Lebaube S, Le Goff N, Ottorini J-M, Granier A (2000) Carbon balance and tree growth in a *Fagus sylvatica* stand. *Ann For Sci* 57: 49-61
- Lefsky M, Cohen WB, Acker SA, Parker GG, Spies TA, Harding D (1999) Lidar remote sensing of the canopy structure and biophysical properties of Douglas-fir western hemlock forests. *Remote Sens Environ* 70: 339-361
- Le Roux X, Grand S, Dreyer E, Daudet F (1999) Parameterization and testing of a biochemically based photosynthesis model for walnut (*Juglans regia*) trees and seedlings. *Tree Physiol* 19: 481-492
- Leuning R (1997) Scaling to a common temperature improves the correlation between the photosynthesis parameters J_{max} and $V_{C_{max}}$. *J Exp Bot* 48: 345-347
- Leuning R, Kelliher FM, de Pury DGG, Schulze E-D (1995) Leaf nitrogen, photosynthesis, conductance and transpiration: scaling from leaves to canopies. *Plant Cell Environ* 18: 1183-1200
- Leuschner C (1994) Walddynamik in der Lüneburger Heide: Ursachen, Mechanismen und die Rolle der Ressourcen. *Habil. Dissertation, Universität Göttingen.*
- Leuschner C, Rode MW, Heinken T (1993) Gibt es eine Nährstoffmangel-Grenze der Buche im nordwestdeutschen Flachland? (Does soil nutrient availability limit the distribution of European beech in North-west Germany?). *Flora* 188: 239-249
- Leuschner D (2000) Changes in forest ecosystem function with succession in the Lüneburger Heide. In: Tenhunen JD, Lenz R, Hantschel R (eds) *Ecosystem approaches to landscape management in Central Europe*. Springer, Heidelberg
- Lichtenthaler HK (1981) Adaptation of leaves and chloroplasts to high quanta fluence rates. In: Akoyunoglou G (ed) *Photosynthesis, VI: Photosynthesis and productivity, photosynthesis and environment*. Balaban International Science Services, Philadelphia
- Lichtenthaler HK, Buschmann C, Döll M, Fietz H-J, Bach T, Kozel U, Meier D, Rahmsdorf U (1981) Photosynthetic activity, chloroplast ultrastructure, and leaf characteristics of high-light and low-light plants and of sun and shade leaves. *Photosynth Res* 2: 115-141
- Linacre E (1992) *Climate, data and resources - a reference and guide*. Routledge, London
- Lischeid G, Gerstberger P (1997) The Steinkreuz Catchment as a main investigation site of BITÖK in the Steigerwald region: experimental setup and first results. In: Gollan T, Gerstberger P (eds) *Bayreuther Forum Ökologie*, 41: BITÖK Forschungsbericht 1996. Bayreuther Institut für terrestrische Ökosystemforschung, Bayreuth
- List R, Küppers M (1997) Kohlenstoffwerb und Kronenarchitektur von Holzgewächsen in Konkurrenzsituationen - Messung an Einzelzweigen, Modellierung für Pflanzengruppen. *EcoSys* 20: 89-99
- List R, Küppers M (1998) Light climate and assimilate distribution within segment-oriented woody plants growth in the simulation program MADEIRA. In: Kastner-Maresch A, Kurth W, Sonntag M, Breckling B (eds) *Bayreuther Forum Ökologie*, 52: Individual-based structural and functional models in ecology. Bayreuther Institut für terrestrische Ökosystemforschung, Bayreuth
- Little CHA, Pharis RP (1995) Hormonal control of radial and longitudinal growth in the tree stem. In: Gartner BL (ed) *Plant Stems: physiology and functional morphology*. Academic Press, San Diego
- Mäkelä A (1986) Implications of the pipe model theory on dry matter partitioning and height growth of trees. *J Theor Biol* 123: 103-120
- Mäkelä A (1997) A carbon balance model of growth and self-pruning in trees based on structural relationships. *For Sci* 43: 7-23
- Mäkinen H (1996) Effects of intertree competition on branch characteristics of *Pinus sylvestris* families. *Scand J For Res* 11: 129-136
- Maherali H, DeLucia EH, Sipe TW (1997) Hydraulic adjustment of maple saplings to canopy gap formation. *Oecologia* 112: 472-480
- Makino A, Mae T, Ohira K (1988) Differences between wheat and rice in the enzymatic properties of ribulose-1,5-bisphosphate carboxylase/oxygenase and the relationship to photosynthetic gas exchange. *Planta* 174: 30-38

- Manderscheid B, Alewell C (2000) Die Wasser- und Stoffflüsse im Lehstenbach-Einzugsgebiet. In: Bayreuther Institut für terrestrische Ökosystemforschung (BITÖK) (ed) Exkursionsführer: Das Lehstenbach-Wassereinzugsgebiet am Waldstein: die BITÖK-Intensivmessflächen im Fichtelgebirge (Nordost-Bayern), Bayreuth
- Martin JG, Kloeppel BD, Schaefer TL, Kimbler DL, McNulty SG (1998) Aboveground biomass and nitrogen allocation of ten deciduous southern Appalachian tree species. *Can J For Res* 28: 1648-1659
- Mattheck C (1995) Biomechanical optimum in woody stems. In: Gartner BL (ed) *Plant Stems: Physiology and functional morphology*. Academic Press, San Diego
- Mattheck C, Bethge K (1998) The mechanical survival strategy of trees. *Arb J* 22: 369-386
- Matyssek R, Günthardt-Goerg MS, Saurer M, Keller T (1992) Seasonal growth, $\delta^{13}\text{C}$ in leaves and stem, and phloem structure of birch (*Betula pendula*) under low ozone concentrations. *Trees* 6: 69-76
- Matyssek R, Keller T, Koike T (1993) Branch growth and leaf gas exchange of *Populus tremula* exposed to low ozone concentrations throughout two growing seasons. *Environ Pollut* 79: 1-7
- Matyssek R, Günthardt-Goerg MS, Maurer S, Keller T (1995) Nighttime exposure to ozone reduces whole-plant production in *Betula pendula*. *Tree Physiol* 15: 159-165
- Mayer DG, Butler DG (1993) Statistical validation. *Ecol Modelling* 68: 21-32
- Medlyn BE, Badeck FW, De Pury DGG, Barton CVM, Broadmeadow M, Ceulemans R, De Angelis P, Forstreuter M, Jach ME, Kellomäki ME, Laitat E, Marek M, Philippot S, Rey A, Strassmeyer J, Laitinen K, Liozon R, Portier B, Wang K, Jarvis PG (1999) Effects of elevated CO_2 on photosynthesis in European forest species: a meta-analysis of model parameters. *Plant Cell Environ* 22: 1475-1495
- Michalsky JJ (1988) The Astronomical Almanac's algorithm for approximate solar position (1950-2050). *Solar Energy* 40: 227-235
- Miller RE, Reukema DL, Max TA (1993) Size of douglas-fir trees in relation to distance from a mixed red alder - douglas-fir stand. *Can J For Res* 23: 2413-2418
- Monsi M, Saeki T (1953) Über den Lichtfaktor in den Pflanzengesellschaften und seine Bedeutung für die Stoffproduktion. *Jap Journ Bot* 14: 22-52
- Mortensen LM (1994) The influence of carbon dioxide or ozone concentration on growth and assimilate partitioning in seedlings of nine conifers. *Acta Agric Scand Sect B Soil and Plant Sci* 44: 157-163
- Myneni RB, Keeling CD, Tucker CJ, Asrar G, Nemani RR (1997) Increased plant growth in the northern high latitudes from 1981 to 1991. *Nature* 386: 698-702
- Naidu SL, DeLucia EH, Thomas RB (1998) Contrasting patterns of biomass allocation in dominant and suppressed loblolly pine. *Can J For Res* 28: 1116-1124
- Nair MNB (1995) Sapwood and Heartwood. In: Braun HJ (ed) *Handbuch der Pflanzenanatomie*. Gebrüder Bornträger, Berlin, Stuttgart
- Newton PF, Joliffe PA (1998) Aboveground modular component responses to intraspecific competition within density-stressed black spruce stands. *Can J For Res* 28: 1587-1610
- Nicolai V (1993) The arthropod fauna on the bark of deciduous and coniferous trees in a mixed forest of the Itasca state Park, MN, USA. *Spixiana* 16: 61-69
- Niinemets Ü (1997) Distribution patterns of foliar carbon and nitrogen as affected by tree dimensions and relative light conditions in the canopy of *Picea abies*. *Trees* 11: 144-154
- Niinemets Ü, Tenhunen JD (1997) A model separating leaf structural and physiological effects on carbon gain along light gradients for the shade-tolerant species *Acer saccharum*. *Plant Cell Environ* 20: 845-866
- Niinemets Ü, Bilger W, Kull O, Tenhunen JD (1998) Acclimation to high irradiance in temperate deciduous trees in the field: changes in xanthophyll cycle pool size and in photosynthetic capacity along a canopy light gradient. *Plant Cell Environ* 21: 1205-1218
- Niinemets Ü, Kull O (1998) Stoichiometry of foliar carbon constituents varies along light gradients in temperate woody canopies: implications for foliage morphological plasticity. *Tree Physiol* 18: 467-497

- Niinemets Ü, Oja V, Kull O (1999a) Shape of leaf photosynthetic electron transport versus temperature response curve is not constant along canopy light gradients in temperate deciduous trees. *Plant Cell Environ* 22: 1497-1513
- Niinemets Ü, Tenhunen J, Canta N, Chaves M, Faria T, Pereira J, Reynolds J (1999b) Interactive effects of nitrogen and phosphorus on the acclimation potential of foliage photosynthetic properties of oak, *Quercus suber*, to elevated atmospheric CO₂ concentrations. *GCB* 5: 455-470
- Niklas KJ (1994) *Plant allometry: the scaling of form and process*. The University of Chicago Press, Chicago - London
- Nolan WG, Smillie RM (1976) Multi-temperature effects on Hill reaction activity of barley chloroplasts. *Biochim Biophys Acta* 440: 461-475
- Norby RJ, Gunderson CA, Wullschlegel SD, O'Neill EG, McCracken MK (1992) Productivity and compensatory responses of yellow-poplar trees in elevated CO₂. *Nature* 357: 322-324
- Norman J (1979) Modeling the complete crop canopy. In: Barfield BJ, Gerber JF (eds) *Modification of the aerial environment of crops*. Amer Soc Agricultural Engineers, St. Joseph, Michigan
- O'Neill EG, Luxmoore RJ, Norby RJ (1987) Elevated atmospheric CO₂ effects on seedling growth, nutrient uptake, and rhizosphere bacterial populations of *Liriodendron tulipifera*. *Plant Soil* 104: 3-11
- Parker GG (1995) Structure and microclimate of forest canopies. In: Lowman MD, Nadkarni NM (eds) *Forest canopies*. Academic Press, London
- Parry MAJ, Schmidt CNG, Cornelius MJ, Millard BN, Burton S, Gutteridge S, Dyer TA, Keys AJ (1987) Variations in properties of ribulose-1,5-bisphosphate carboxylase from various species related to differences in amino acid sequences. *J Exp Bot* 38: 1260-1271
- Pearson M, Mansfield TA (1994) Effects of exposure to ozone and water stress on the following season's growth of beech (*Fagus sylvatica* L.). *New Phytol* 126: 511-515
- Peck AK (1995) Verdunstung von Wäldern in Abhängigkeit von Bestandesparametern. Dissertation, Meteor. Inst. Uni Freiburg.
- Peck A, Mayer H (1996) Einfluss von Bestandesparametern auf die Verdunstung von Wäldern. *Forstwiss Cbl* 115: 1-9
- Pellinen P (1986) Biomasseuntersuchungen im Kalkbuchenwald. Ph.D. Dissertation, Universität Göttingen.
- Peterson AG, Ball JT, Luo Y, Field CB, Curtis PS, Griffin KL, Gunderson CA, Norby RJ, Tissue DT, Forstreuter M, Rey A, Vogel CS, CMEAL Participants (1999) Quantifying the response of photosynthesis to changes in leaf nitrogen content and leaf mass per area in plants grown under atmospheric CO₂ enrichment. *Plant Cell Environ* 22: 1109-1119
- Phong BT (1975) Illumination for Computer generated pictures. *CACM* 18: 253-318
- Porte A, Loustau D (1998) Variability of the photosynthetics of mature needles within the crown of a 25-year-old *Pinus pinaster*. *Tree Physiol* 18: 223-232
- Pretzsch H (1996) Growth trends in forests in Southern Germany. In: Spiecker H, Mielikäinen K, Köhl M, Skovsgaard JP (eds) *European Forest Institute Report, No.5: Growth trends in European forests*. Springer, Berlin
- Pretzsch H, Kahn M, Grote R (1998) Die Fichten-Buchen-Mischbestände des Sonderforschungsbereiches "Wachstum oder Parasitenabwehr?" im Kranzberger Forst. *Forstwiss Cbl* 117: 241-257
- Protz CG, Silins U, Lieffers VJ (2000) Reduction in branch sapwood hydraulic permeability as a factor limiting survival of lower branches of lodgepole pine. *Can J For Res* 30: 1088-1095
- Rackham O (1992) Mixtures, mosaics and clones: the distribution of trees within European woods and forests. In: Cannell MGR, Malcolm DC, Robertson PA (eds) *The ecology of mixed-species stands of trees*. Blackwell, London
- Ramann, E (1911) Blättergewicht und Blattflächen einiger Buchen. *Zeitschrift für Forst- und Jagdwesen* 43: 916-919
- Rasulov BK, Laisk AK, Asrorov KA (1984) Photosynthesis and photorespiration during ontogenesis of several species of cotton. *Soviet Plant Physiology* 75: 95-101
- Reekie EG (1996) The effect of elevated CO₂ on developmental processes and its implications for plant-plant interactions. In: Körner C, Bazzaz FA (eds) *Physiological ecology. A series of monographs texts and treatises: Carbon dioxide, populations, and communities*. Academic Press, Inc., San Diego

- de Reffye P, Houllier F, Blaise F, Barthelemy D, Dauzat J, Auclair D (1995) A model simulating above- and below-ground tree architecture with agroforestry applications. *Agroforestry Systems* 30: 175-197
- de Reffye P, Fourcaud T, Blaise F, Barthélémy D, Houllier F (1997) A functional model of tree growth and tree architecture. *Silva Fenn* 31: 297-311
- Reynolds JF, Hilbert DW, Chen J-L, Harley PC, Kemp PR, Leadley PW (1992) TR, 054: Modeling the response of plants and ecosystems to elevated CO₂ and climate change. United States Department of Energy, Washington, DOE/ER-60490T-H1, Dist. Category UC-402
- Richter G (1998) *Stoffwechselfysiologie der Pflanzen*. Thieme, Stuttgart
- Rogers R, Hinckley TM (1979) Foliar weight and area related to current sapwood area in oak. *For Sci* 25: 298-303
- Rohrig M, Stutzel H, Alt C (1999) A three-dimensional approach to modeling light interception in heterogeneous canopies. *Agron J* 91: 1024-1032
- Roloff A (1986) Morphologie der Kronenentwicklung von *Fagus sylvatica* L. (Rotbuche) unter besonderer Berücksichtigung möglicherweise neuartiger Veränderungen. Ph.D. Dissertation, Universität Göttingen.
- Rothe A, Kreutzer K (1998) Wechselwirkungen zwischen Fichte und Buche im Mischbestand. *Allgemeine Forst Zeitschrift* 15: 784-787
- Ryel RJ (1993) Light relations in tussock grasses as assessed with a new three-dimensional canopy photosynthesis model. Structure and function of foliage organization of a growth form prevalent in environments characterized by stress. Ph.D. Dissertation, University Würzburg.
- Ryel RJ, Beyschlag W, Caldwell MM (1993) Foliage orientation and carbon gain in two tussock grasses as assessed with a new whole-plant gas-exchange model. *Funct Ecol* 7: 115-124
- Saito H, Kakubari Y (1999) Spatial and seasonal variations in photosynthetic properties within a beech (*Fagus crenata* Blume) crown. *J For Res* 4: 27-34
- Sala A, Tenhunen JD (1996) Simulations of canopy net photosynthesis and transpiration in *Quercus ilex* L. under the influence of seasonal drought. *Agr For Met* 78: 203-222
- Sales Luis JF, Do Loreto Monteiro M (1998) Dynamics of a broadleaved (*Castanea sativa*) conifer (*Pseudotsuga menziesii*) mixed stand in Northern Portugal. *For Ecol Manage* 107: 183-190
- Salisbury FB, Ross CW (1992) *Plant Physiology*, Wardsworth, Belmont, California
- Sallanon H, Dimon B, Carrier P, Chagvardieff P (1995) Effects of CO₂ concentration and irradiance on growth and photosynthesis of *Juglans regia* plantlets grown in vitro. *PH* 31: 241-249
- Schäfer KVR (1997) Wassernutzung von *Fagus sylvatica* L. und *Quercus petraea* (MATT.) Liebl. im Wassereinzugsgebiet Steinkreuz im Steigerwald, Bayern. Diplomarbeit, Universität Bayreuth.
- Scheffer F, Schachtschabel P (1998) *Lehrbuch der Bodenkunde*. Enke, Stuttgart
- Schreiber U, Bilger W, Neubauer C (1994) Chlorophyll fluorescence as a noninvasive indicator for rapid assessment of in vivo photosynthesis. In: Schulze E-D, Caldwell MM (eds) *Ecological studies*, 100: Ecophysiology of photosynthesis. Springer Verlag, Berlin - Heidelberg - New York - London - Paris - Tokyo - Hong Kong - Barcelona - Budapest
- Schulte M (1991) Saisonale und interannuelle Variabilität des CO₂-Gaswechsels von Buchen (*Fagus sylvatica* L.) - Bestimmung von C-Bilanzen mit Hilfe eines empirischen Modells. Ph.D. Dissertation, Universität Göttingen.
- Schulze ED (1970) Der CO₂-Gaswechsel der Buche (*Fagus sylvatica* L.) in Abhängigkeit von den Klimafaktoren im Freiland. *Flora* 159: 177-232
- Schulze E-D (1994) The regulation of plant transpiration: interactions of feedforward, feedback, and futile cycles. In: Schulze E-D (ed) *Flux control in biological systems. From enzymes to populations and ecosystems*. Academic Press, Inc., San Diego
- Schweingruber FH (1978) *Mikroskopische Holzanatomie*. Kommissionsverlag Zürcher AG, Zug
- Seiler J (1995) Bodenkundliche Charakterisierung der Einzugsgebiete "Steinkreuz/Erlensumpf" bei Ebrach und "Runderbusch" bei Schrapbach im nördlichen Steigerwald.
- Sharpe PJH, DeMichele DW (1977) Reaction kinetics of poikilotherm development. *J Theor Biol* 64: 649-670

- Shinozaki K, Yoda K, Hozumi K, Kira T (1964) A quantitative analysis of plant form - the pipe model theory I. Basic analyses. *Jap J Ecol* 14(3): 97-105
- Sievänen R, Nikinmaa E, Perttunen J (1997) Evaluation of Importance of Sapwood Senescence on Tree Growth Using the Model Lignum. *Silva Fenn* 31: 329-340
- Sinoquet H, Mouliat B, Bonhomme R (1991) Estimating the three-dimensional geometry of a maize crop as an input of radiation models: Comparison between three-dimensional digitizing and plant profiles. *Agric For Meteorol* 55: 233-250
- Sionit N, Strain BR, Hellmers H, Riechers GH, Jaeger CH (1985) Long-term atmospheric CO₂ enrichment affects growth and development of *Liquidambar styraciflua* and *Pinus taeda* seedlings. *Can J For Res* 15: 468-471
- Skaar C (1988) Springer series in wood science: Wood-water relations. Springer-Verlag, Berlin - Heidelberg - New York - London - Paris - Tokyo
- Smaltschinski T (1990) Mischbestände in der Bundesrepublik Deutschland. *Forstarchiv* 61(4): 137-140
- Smith WR (1994) An empirical evaluation of a three-dimensional crown model for predicting volume growth. *For Ecol Manage* 69: 199-209
- Sprugel DG, Hinckley TM, Schaap W (1991) The theory and practice of branch autonomy. *Ann Rev Ecol Syst* 22: 309-334
- Stafstrom JP (1995) Developmental potential of shoot buds. In: Gartner BL (ed) *Plant Stems: physiology and functional morphology*. Academic Press, San Diego
- Strasburger E, Sitte P (1991) *Lehrbuch der Botanik für Hochschulen*. Fischer, Stuttgart
- Sumberg A, Laisk A (1995) Measurements of the CO₂/O₂ specificity of ribulose-1,5-bisphosphate carboxylase-oxygenase. In: Mathis P (ed) *Photosynthesis: from light to biosphere*, vol V. Kluwer academic publishers, Dordrecht
- Sumida A, Komiyama A (1997) Crown spread patterns for five deciduous broad-leaved woody species: ecological significance of the retention patterns of larger branches. *Ann Bot* 80: 759-766
- Tanaka T, Yamaguchi J, Takeda Y (1998) Measurement of forest canopy structure with a laser plane range-finding method - development of a measurement system and applications to real forests. *Agric For Meteorol* 91: 149-160
- Tanner V, Eller BM (1986) Veränderungen der spektralen Eigenschaften der Blätter der Buche (*Fagus sylvatica* L.) von Laubaustrieb bis Laubfall. *AFJZ* 157(6): 108-117
- Taylor G, Dobson MC (1989) Photosynthetic characteristics, stomatal responses and water relations of *Fagus sylvatica*: impact of air quality at a site in southern Britain. *New Phytol* 113: 265-273
- Thomas FM, Büttner G (1998) Nutrient relations in healthy and damaged stands of mature oaks on clayey soils: two case studies in northwestern Germany. *For Ecol Manage* 108: 301-319
- Tjoelker MG, Volin JC, Oleksyn J, Reich PB (1993) Light environment alters response to ozone stress in seedlings of *Acer saccharum* Marsh. and hybrid *Populus* L. I. *In situ* net photosynthesis, dark respiration and growth. *New Phytol* 124: 627-636
- Triboulot MB, Fauveau ML, Breda N, Label P, Dreyer E (1996) Stomatal conductance and xylem-sap abscisic acid (ABA) in adult oak trees during a gradually imposed drought. *Ann Sci For* 53: 207-220
- Turnbull MH, Tissue DT, Griffin KL, Rogers GND, Whitehead D (1998) Photosynthetic acclimation to long-term exposure to elevated CO₂ concentration in *Pinus radiata* D. Don is related to age of needles. *Plant Cell Environ* 21: 1019-1028
- UNO (1998) Kyoto Protocol to the united nations framework convention on climate change.
- UNO (2000) Report of the conference of the parties on its fifth session, held at Bonn from 25 October to 5 November 1999, part two: action taken by the conference of the parties at its fifth session.
- Valentini R, Matteucci G, Dolman AJ, Schulze ED, Rebmann C, Moors EJ, Granier A, Gross P, Jensen NO, Pilegaard K, Lindroth A, Grelle A, Bernhofer C, Grünwald T, Aubinet M, Ceulemans R, Kowalski AS, Vesala T, Rannik Ü, Berbigier P, Loustau D, Gudmundsson J, Thorgeirsson H, Ibrom A, Morgenstern K, Clement R, Moncrieff J, Montagnani L, Minerbi S, Jarvis PG (2000) Respiration as the main determinant of European Forests Carbon balance. *Nature* 404: 861-865
- Valladeres (1999) Architecture, ecology, and evolution of plant crowns. In: Pugnaire FI, Valladeres F (eds) *Handbook of functional plant ecology*. Marcel Dekker Inc., New York

- Van den Burg J (1990) Foliar analysis for determination of tree nutrient status - a complication of literature data. "De Dorschkamp", Institute for Forestry and Urban Ecology, Wageningen, Netherlands
- Van Oosten J-J, Besford RT (1995) Some relationships between the gas exchange, biochemistry and molecular biology of photosynthesis during leaf development of tomato plants after transfer to different carbon dioxide concentrations. *Plant Cell Environ* 18: 1253-1266
- von Caemmerer S, Farquhar GD (1981) Some relationships between the biochemistry of photosynthesis and the gas exchange of leaves. *Planta* 153: 376-387
- von Caemmerer S, Evans JR, Hudson GS, Andrews TJ (1994) The kinetics of ribulose-1,5-bisphosphate carboxylase/oxygenase *in vivo* inferred from measurements of photosynthesis in leaves of transgenic tobacco. *Planta* 195: 88-97
- von Willert DJ, Matyssek R, Herppich W (1995) *Experimentelle Pflanzenökologie - Grundlagen und Anwendungen*. Thieme Verlag, Stuttgart
- Walter H, Breckle S-W (1999) *Vegetation und Klimazonen*. Ulmer, Stuttgart
- Wang KY, Kellomäki S, Laitinen K (1996) Acclimation of photosynthetic parameters in Scots pine after three years exposure to elevated temperature and CO₂. *Agric For Meteorol* 82: 195-217
- Wang Y-P, Jarvis PG (1990) Description and validation of an array model - MAESTRO. *Agric For Meteorol* 47: 257-280
- Waring RH, Gholz HL, Grier CC, Plummer ML (1977) Evaluating stem conducting tissue as an estimator of leaf area in four woody angiosperms. *Can J Bot* 55: 1474-1477
- Weber JA, Grulke NE (1995) Response of stem growth and function to air pollution. In: Gartner BL (ed) *Plant Stems: physiology and functional morphology*. Academic Press, San Diego
- Welss W (1985) *Waldgesellschaften im nördlichen Steigerwald*. Ph.D. Dissertation, Universität Erlangen-Nürnberg.
- Weyer T (ed) (1993) *Bonner bodenkundliche Abhandlungen, Bd. 12: Kalkungsversuche mit carbonatisch und silikatisch gebundenen Kalk- und Magnesiumdüngern - Initialeffekte auf versauerte Waldböden Nordrhein-Westfalens.*, Bonn
- Williams M (1996) A three-dimensional model of forest development and competition. *Ecol Modelling* 89: 73-98
- Wrzesinsky T, Klemm O (2000) Summertime fog chemistry at a mountaineous site in Central Europe. *Atmospheric Environment* 34: 1487-1496
- Wullschleger SD (1993) Biochemical limitations to carbon assimilation in C₃ plants - a retrospective analysis of the A/C_i curves from 109 species. *J Exp Bot* 44: 907-920
- Wullschleger SD, Norby RJ, Hanson PJ (1995) Growth and maintenance respiration in stems of *Quercus alba* after four years of CO₂ enrichment. *Physiol Plant* 93: 47-54
- Zhang H, Sharifi MR, Nobel PS (1995) Photosynthetic characteristics of sun versus shade plants of *Encelia farinosa* as affected by photosynthetic photon flux density, intercellular CO₂ concentration, leaf water potential, and leaf temperature. *Aust J Plant Physiol* 22: 833-841
- Zimmermann MH (1983) *Xylem structure and the ascent of the sap*. Springer-Verlag, Berlin
- Zingg A (1996) Diameter and basal area increment in permanent growth and yield plots in Switzerland. In: Spiecker H, Mielikäinen K, Köhl M, Skovsgaard JP (eds) *European Forest Institute Report, No. 5: Growth trends in European forests*. Springer, Heidelberg
- Zipse A, Mattheck C, Gräbe D, Gardiner B (1998) The effect of wind on the mechanical properties of the wood of beech (*Fagus sylvatica* L.) growing on the borders of Scotland. *Arb J* 22: 247-257

10 Abbreviations

Abbreviations and symbols are listed in the following table together with their meaning and unit. Symbols were mostly not changed from their usual names as they are used in publications to avoid the introduction of unusual names, which led partly to similar variable names. In this cases, differentiations were made using italic fonts or upper and minor case letters to indicate the different meaning. All variables that are used in the text are also explained at the place where they occur, thereby giving orientation to the reader. The table is sorted by the latin alphabet, upper case letters coming before lower case letters and greek symbols.

Symbol	Meaning	Unit
A	Net photosynthesis	$\mu\text{mol}/(\text{m}^2\cdot\text{s})$
A_v	Rubisco limited assimilation rate	$\mu\text{mol}/(\text{m}^2\cdot\text{s})$
A_J	Electron transport limited assimilation rate	$\mu\text{mol}/(\text{m}^2\cdot\text{s})$
ar	Area of a leaf	m^2
area	Projected area of a leaf cloud	m^2
AZ _P	Azimuth of the leaf clouds exposition	$^\circ$
AZ _S	Azimuth of the horizontal vector from stem to leaf cloud centre	$^\circ$
α	Initial slope of the CO ₂ -saturated photosynthesis vs. irradiance relationship	mol/mol
α_{AZ}	Inclination of the main growth direction of a leaf cloud	$^\circ$
α_{h}	Leaf cloud angle	$^\circ$
α_{S}	Angle between main growth direction and idealised canopy surface	$^\circ$
$\beta_1, \beta_2, \text{etc.}$	Model coefficients	-
CLA	Sum of leaf area above a leaf cloud (belonging to the same tree)	m^2
CLAD	Average leaf area density above a leaf cloud (related to the same tree)	m^2/m^3
CVOL	Tree canopy volume above one of its leaf clouds	m^3
c	Generally: a constant	
C_a	CO ₂ concentration outside the leaf	$\mu\text{mol CO}_2/\text{mol air}$
C _i	Incoming mole fraction of carbon dioxide	$\mu\text{mol CO}_2/\text{mol air}$
C_i	Leaf internal CO ₂ concentration	$\mu\text{mol CO}_2/\text{mol air}$
C _o	Outgoing mole fraction of carbon dioxide	$\mu\text{mol CO}_2/\text{mol air}$
C _s	Mole fraction of CO ₂ in the sample air stream	$\mu\text{mol CO}_2/\text{mol air}$
C_S	CO ₂ concentration on the leaf surface	$\mu\text{mol CO}_2/\text{mol air}$
D _S	Derivative of the idealised canopy shape at the point of intersection with the main growth direction vector	m / m
d	Distance that a beam of light travelled in a medium	(m)
E	Transpiration	$\text{mmol}/(\text{m}^2\cdot\text{s})$
E	East co-ordinate of the leaf cloud centre relative to the stem	m
e _i	Model error	-
F ₀	Minimum fluorescence	relative units
F _M	Maximum fluorescence	relative units
F _B	Relative proportion of direct quantum flux density to the integrated sum of irradiance over a given period	-

Abbreviations

Symbol	Meaning	Unit
F_D	Relative proportion of diffuse quantum flux density to the integrated sum of irradiance over a given period	-
$f_1, f_2, \text{ etc.}$	A variable	-
Gap	Volumetric gap fraction of layers	-
g_{fac}	Stomatal sensitivity to CO_2 use efficiency and relative humidity	-
g_{min}	Cuticular conductance for water vapour	$\text{mol H}_2\text{O}/(\text{m}^2\text{s})$
g_{SW}	Stomatal conductance to water vapour	$\text{mol H}_2\text{O}/(\text{m}^2\text{s})$
g_{tC}	Total leaf conductance to CO_2	$\text{mol CO}_2/(\text{m}^2\text{s})$
g_{tW}	Total leaf conductance to water vapour	$\text{mol H}_2\text{O}/(\text{m}^2\text{s})$
g_{SW}	Boundary layer conductance to water vapour	$\text{mol H}_2\text{O}/(\text{m}^2\text{s})$
Γ^*	Rubisco-specific CO_2 -compensation point	$\mu\text{mol CO}_2/\text{mol air}$
H	Relative height of the leaf cloud centre in the canopy	-
H_{abs}	Absolute height of the leaf cloud centre above the floor	m above the floor
H_{apex}	Height co-ordinate of the apex of a tree	m above the floor
H_{Ca}, H_{Cb}	Height limit above and below a leaf cloud	m above the floor
H_{La}, H_{Lb}	Height limit above (a) and below (b) a height layer	m above the floor
H_{range}	Height range of a leaf cloud	m
H_A	Activation energy for temperature dependent reactions	J/mol
H_d	Deactivation energy for temperature dependent reactions	J/mol
H_s	Height of intersection of the main growth direction vector with the idealised canopy surface	m above the floor
h_s	Relative humidity on the leaf surface	-
i	Generally: an iterator	-
I	Quantum flux density (in a compartment)	$\mu\text{mol}/(\text{m}^2\text{s})$
I_0	Radiation flux density reaching the surface of a compartment	$\mu\text{mol}/(\text{m}^2\text{s})$
I_B	Direct site factor	-
I_D	Diffuse site factor	-
J	Electron transport rate	$\mu\text{mol}/(\text{m}^2\text{s})$
J_{max}	Maximum electron transport rate across the thylakoid membrane	$\mu\text{mol}/(\text{m}^2\text{s})$
k	Generally: a coefficient	-
k_f	Correction factor	-
K	Fraction of stomatal conductance on one side of a leaf towards the other side	-
$K_{M,C}$	Rubisco Michaelis-Menten constant for carboxylation	$\mu\text{mol}/\text{mol}$
$K_{M,O}$	Rubisco Michaelis-Menten constant for oxygenation	mmol/mol
LA_C	Leaf area of a leaf cloud	m^2
$LA_{L,dm}$	Leaf area of layers of 1dm height	m^2
LAD	Leaf area density of a leaf cloud	m^2/m^3
LAD_{Crown}	Leaf area density of a crown	m^2/m^3
LAD_L	Leaf are density of a layer	m^2/m^3
$LAD_{L,m}$	Leaf area density of layers of 1 m height	m^2/m^3
$LAD_{p\wedge}$	Leaf area density in the volume of all polyhedrons of a layer	m^2/m^3
LMA	leaf mass per area	g/m^2

Abbreviations

Symbol	Meaning	Unit
<i>N</i>	Leaf nitrogen content	g/m ²
N	North co-ordinate of the leaf cloud centre relative to the stem	m
<i>P_m</i>	CO ₂ -saturated rate of photosynthesis	μmol/(m ² *s)
<i>P_{ml}</i>	Light- and CO ₂ -saturated rate of photosynthesis	μmol/(m ² *s)
Q_{rel}	Relative irradiance	-
<i>R</i>	Gas constant	8.314 J/(K*mol)
<i>R_d</i>	Day respiration, i.e. respiration continuing in the light	μmol/(m ² *s)
<i>rh</i>	External relative humidity	-
<i>S</i>	Entropy term in the description of temperature dependent processes	J/(K*mol)
stemd	Horizontal distance of the leaf cloud centre to the stem	m
<i>T</i>	Temperature	K
TLAI, TLAI_g	Tree leaf area index, g = gap corrected	m ² /m ²
<i>τ</i>	Rubisco specificity factor	-
u_i	Incoming flow rate	mol/s
volume, V_C	Volume of a whole polyhedron (=leaf cloud volume)	m ³
V_L	Volume of a layer	m ³
V_P	Volume of a polyhedron segment	m ³
<i>V_c</i>	Carboxylation rate	μmol/(m ² *s)
<i>V_o</i>	Oxygenation rate	μmol/(m ² *s)
<i>V_{cmax}</i>	Maximum carboxylation velocity	μmol/(m ² *s)
<i>V_{cmax, 298}</i>	Maximum carboxylation velocity at a temperature of 298 K	μmol/(m ² *s)
WAD	Wood area density	m ² /m ³
<i>W_C</i>	Rubisco limited carboxylation rate	μmol/(m ² *s)
<i>W_J</i>	Calvin-cycle dependent carboxylation rate	μmol/(m ² *s)
<i>W_P</i>	Phosphate limited carboxylation rate	μmol/(m ² *s)
W_i	Molar concentration of water vapour in a leaf	mmol H ₂ O/mol air
W_s	Sample water mole fraction	mmol H ₂ O/mol air
w_i	Incoming water mole fraction	mol H ₂ O/mol air
w_o	Outgoing water mole fraction	mol H ₂ O/mol air
x, y, z	Variables	-
Y	Quantum yield of a leaf	-